BIOLOGICAL NITROGEN FIXATION IN THE SOUTHEASTERN AMAZON: THE EFFECTS OF MOLYBDENUM, PHOSPHORUS, AND FOREST FIRES

A Dissertation

Presented to the Faculty of the Graduate School

of Cornell University

In Partial Fulfillment of the Requirements for the Degree of

Doctor of Philosophy

by

Michelle Yeelin Wong

August 2019

BIOLOGICAL NITROGEN FIXATION IN THE SOUTHEASTERN AMAZON: THE EFFECTS OF MOLYBDENUM, PHOSPHORUS, AND FOREST FIRES

Michelle Yeelin Wong, Ph. D.

Cornell University 2019

Biological nitrogen fixation (BNF) is the main pathway for new nitrogen (N) to enter ecosystems. The highest rates of BNF are found in tropical forests, but the majority of studies on BNF in tropical forests have been conducted along coastal regions, which receive high rates of sea-salt aerosols likely rich in molybdenum (Mo). Much evidence suggests that the low availability of Mo, a co-factor in the nitrogenase enzyme, can constrain BNF, even in forests that receive large inputs of Mo. Thus, Mo could be even more limiting to BNF in tropical forests isolated from atmospheric inputs. In Chapter 1, I modeled how sea-salt aerosols, mineral dust, and volcanoes distribute atmospheric Mo to terrestrial ecosystems. I then identified the southern Amazon basin as a region where atmospheric inputs and parent material weathering is low, and hypothesized that 1) Mo limitation of BNF is prevalent in this region, further exacerbated by low soil pH, and that 2) BNF rates would be low compared to other tropical forests. In Chapter 2, I conducted two long-term experiments where I added Mo, phosphorus (P), and lime (to raise soil pH) separately and together. I found that, free-living BNF did not respond strongly to Mo and P additions, likely because of high soil N availability that suppresses BNF.

In the southeastern Amazon, interactions of drought, deforestation, and agricultural have led to increased forest fires. Early in forest succession after large N losses, BNF has been found to increase in many tropical forests to support secondary

forest recovery. In Chapters 3 and 4, I asked if trees capable of hosting symbiotic BNF (N-fixing) in the *Fabaceae* family and associated symbiotic BNF, as well as free-living BNF, increase to support forest recovery post-fires. I found low rates of free-living and symbiotic BNF despite 1) large aboveground losses of N post-fire and 2) a large increase in the abundance of N-fixing trees. The low rates of BNF in the southeastern Amazon have important implications for understanding the role of BNF in tropical forests more generally, because large areas of tropical forest occur in lowland, interior basins on highly weathered oxisols.

BIOGRAPHICAL SKETCH

Michelle Yeelin Wong (王穎菱) was born in Sacramento, CA to Agnes Wong (王新润）and Keng Wong (王敬之), who emigrated from China to the United States. Michelle grew up alongside her younger brother Anthony Wong (王颂然) with her grandmother (郑娉嬋) and other extended family members nearby. Michelle attended Genevieve Didion K-8 and John F. Kennedy High School, where her passion for environmental issues began. During her sophomore year at the University of California, Berkeley, she enrolled in Environmental Issues with Ronald Amundson, who sparked her fascination in soils. Her interest in soil biogeochemistry grew as she took courses such as Soil Characteristics, Soil Microbial Ecology, Tropical Forest Ecology, and Ecosystem Ecology. In 2009, Michelle worked through the work-study program as an assistant in Dr. Garrison Sposito's laboratory, and later moved on to conduct independent research on selenium reduction in the laboratory of Dr. Céline Pallud. In 2010, she graduated with a B.A. in Sociology and a B.S. in Molecular Environmental Biology and began working as technician in Dr. Whendee Silver's group, studying novel pathways of the nitrogen cycle, carbon sequestration in soils, and iron redox cycling. This experience was profoundly influential, and the option to study biogeochemistry stayed on the back of her mind as she began working as an Environmental Scientist at the California Environmental Protection Agency, Department of Pesticide Regulation in 2011. There, she learned more about the socio-environmental consequences of agricultural nitrogen on groundwater and decided to continue pursuing research. In 2013, Michelle joined the Department of Ecology and Evolutionary Biology at Cornell University to study nitrogen biogeochemistry under Dr. Robert W. Howarth. She became an active member of Cornell's biogeochemistry program, the Prison Education Program, and Diversity Preview Weekend.

To Agnes and Keng

ACKNOWLEDGMENTS

I am deeply grateful for the scientific community at Cornell University, Instituto de Pesquisa Ambiental da Amazônia (IPAM), Woods Hole Research Center (WHRC), Marine Biological Station (MBL), and the University of Brasilia. Without the support, comradery, and commitment of everyone that I have met, I would not have been able to carry out this work.

This work would not have been possible without the guidance and support of my committee. I am grateful to my major advisor, Bob Howarth for the ideas, mentorship, generosity, and care he has given me over the past six years. Bob has thought about molybdenum and nitrogen fixation for decades, and I am honored to be able to work on the culmination of those years of thought. Bob has taught me much about scientific integrity and thoroughness, communication, and team-building, and I would not be the scientist I am today without him. To Christopher Neill, for his unwavering enthusiasm, encouragement, and positivity; I am unbelievably grateful to Chris for bringing me into the Tanguro family and having the upmost confidence in me to carry out the work. I thank him for making science fun. To Natalie Mahowald, who treated me with the upmost respect—more as a scientific colleague than a student. Natalie opened scientific doors and collaborations, and has always given me her time and steadfast support. To Tim Fahey, who has always been a rich source of knowledge. Tim has always shared his vast amount expertise and helped me decide where to go when I found forks in the road.

I am deeply grateful to the Howarth-Marino lab for being my academic family. Without Roxanne Marino's laboratory and field guidance, this work would not have

been possible. Roxanne, more than anyone, has helped me learn how to design and think about experimental design and analyses with rigor. She has also been the best lab manager—directing me where to go, teaching me all the tricks of the trade with gases, and allowing me to feel confident about my experimental design and methods (and safely getting all my equipment to Brazil). I also want to thank Dennis Swaney for his unfaltering reliability, calm demeanor, and wisdom beyond his years—I always knew I would survive if he was there; Tom Butler, for always being a source of humor and dependability in times of crisis; Melanie Hayn, for her friendship, advice, and extremely inspiring organization; Liz Duskey, for her attitude and peace, and Katie Haviland, for her positivity and fun energy.

The interdepartmental Biogeochemistry, Environmental Science, and Sustainability (BESS) group has been the best part of being at Cornell. To Fiona Soper, for without whom I would not have funding nor a dissertation. I am deeply grateful for Fiona's generosity with her friendship and mentorship. Fiona's worldview led me to adjust my own attitude and lens in which to value what is important. I am also so grateful to have met Alex Flecker, who made me learn how fun it is to teach a large undergraduate course with the right group of people, and always made us feel welcome at his home with Sunny Power; Joe Yavitt, for all the enjoyable and exciting conversations about tropical forests; Murray McBride for his kind and sage presence at BESS seminars on Friday afternoons; and Christy Goodale for being so welcoming and for administering the IGERT program.

I want to extend the thanks to the many people who have helped with the technical aspects of my research. To Lou Derry and the rest of his group, I thank for

being my other lab group at Cornell—Lou always brought jolly energy; to Greg McElwee for his expertise and responsiveness; Mary Reinthal for her comradery during the late nights and weekends; and Alida Perez Fodich and Arnulfo Aguirre for the friendship and technical help. I am also grateful for all the help from Kim Sparks at the Cornell Stable Isotope Laboratory, Richard McHorney from the Marine Biological Laboratory, Debra Driscoll from the State University of New York College of Environmental Science and Forestry; Pat Sullivan from Natural Resources; and Stephen Parry at the Cornell Statistical Consulting Unit.

To my other academic families in Brazil, at IPAM-Tanguro and at the University of Brasilia; I am deeply indebted to all the scientists and staff at IPAM—Paulo Brando and Divino Silvéiro for their thoughtful scientific support; Darlisson Nunes, Maria Lucia Nascimento, Raimundo Mota Quintino, Sandro Rocha, Leonardo Maracahipes, Leandro Maracahipes, Sebastião Nascimento, Ebis Nascimento, Adilson Coelho, and Meri Maestri for the unwavering help, for inviting me into their homes and feeding me when I was thousands of miles away from own home. It takes more than a village to conduct research at Tanguro, and I am so grateful for the friendship, laughter, and stories with all the other scientists at Tanguro. To Marcia Macedo for her magnanimity and being cognizant of everyone's needs, Alex Huddell for her inspiring independence, KathiJo Jankowski for her warmth and her sunshine, Hillary Sullivan for her friendship and competence, and Paul Lefebvre for his wisdom and for sharing the stories of everyone's lives before I could speak Portuguese. To Rafaella Silveira, I thank for sharing with me her world. To Giovanna Gomes, Ray Pinheiro, Nubia Marques, Regina Satori, Thiago DeRoure Bandeirade Mello, I thank for sharing with

me how science can be done.

I am deeply grateful to the Department of Ecology and Evolutionary Biology for the administrative support and the sense of community: Monica Geber as a Director of Graduate Studies, Jeremy Searle for being a kind chair, and to the past and present EEB staff: Luanne Kenjerska, Scott Williams, Patty Jordan, Carol Damm, Ashley Pendell, Jennifer Robinson, Brian Mlodzinski, Janeen Orr, John Howell, and Gary Oltz for the help with getting equipment and supplies prepared for the field. I am also deeply grateful to the graduate students in EEB for instilling in me a courageousness and compass of justice.

I am grateful to the Cross Scale Biogeochemistry and Climate NSF IGERT program for providing fellowship funding and grant opportunities that largely supported the research in this dissertation; the National Science Foundation for dissertation support and fellowship support; Mario Eunadi Center for International Studies, Paul P. Feeny Graduate Student Research grant, Orenstein Endowment Fund, the Andrew W. Mellon Student Research Grant, Sigma Xi, and Cornell University for travel and conference support.

I want to thank NextGen for opening up my world at Cornell, especially to Colleen McLinn and Sara Hernandez, and the rest of the cohort of NextGen scholars. I am also grateful for Nicole Peppin and Kyri Murdough at Cornell Prison Education Program.

To Katie Grant, my family; you have been there for the highest highs and the lowest lows and all the adventures in between. Thank you for taking care of me. I would not have survived without your humor and your lens of reality; your loyalty. To

Sue Pierre, my soul food, I thank for sharing with me the whole spectrum of being a human. To Erin Larson, my inspiration, I look up to you for almost everything. You have made serving on EEB committees and teaching BioEE 1610 and CPEP such a blast. Thank you for infusing fun, feeling, and hard work everywhere you go. To Jay Falk, you remind me of the good in the world; to Cait McDonald, for your sense of justice and equity; Lizzie Lombardi for being so sensitive, aware, and deeply kind. Thank you all those years ago for saying yes to joining our Ragnar team across the tubs of beer at SNEEB. To Emily Funk for bringing me on your adventures; Lina Arcila Hernández for your warmth and kindness; Nick Fletcher for your infectious energy; Irene del Real for your love of life; and to many more friends that I have made in Ithaca: Charlotte Levy, Gregor Siegmund, John Mason, Ellie Goud, Lindsay Schaffner, Angela Possinger, Rachel Hestrin, Bridget Darby, Aubrie James, Rachel Wilkins, Henry Kunerth, Young Na Suh, Nancy Chen, David Chang van Oordt, Kelsey Jensen, Jake Berv, Tram Nguyen, Valeria Dani, Cinnamon Mittan, and Katie Holmes.

To my family and friends far away, but not so far away—Maya Almaraz for being my remote co-worker. Thank you for being by my side during this journey. To Elaine, Ellyse, Emily, Eunice, Sumita, Leah, Liz, and Michelle, who have shaped me to be the person I am today. To Terence, for always being my rock. And most of all, to Mom and Dad, you sacrificed your own hopes and dreams to give me and Anthony the opportunities that we have today. This is for you.

TABLE OF CONTENTS

LIST OF FIGURES

LIST OF TABLES

CHAPTER 1 . INTRODUCTION

1.1. Background

Biological nitrogen fixation (BNF) is an essential process that provides the primary input of new nitrogen (N) into ecosystems. There are two main pathways for BNF—symbiotic and free-living. The largest source of symbiotic BNF occurs when specific bacteria live in association with specific leguminous plants in the *Fabaceae* family and fix N in root nodules. Free-living BNF is catalyzed by bacteria and archaea that live freely in soils, and is ubiquitous. Despite the importance of BNF for ecosystem function and for predicting future responses to global change, we still know little about the rates of and the controls on BNF, particularly in tropical forests where BNF is thought to be potentially high, but where measurements are rare. While P is thought to ultimately limit net primary productivity in tropical forests on old, highly weathered soils, N often limits secondary forest regrowth until forests mature (Davidson et al. 2007, Wright et al. 2018). Thus, BNF rates are often high after disturbances and in forest gaps (Barron et al. 2011, Batterman et al. 2013). In contrast to temperate forests, BNF rates are estimated to be 5-10 times higher in tropical forests (Sullivan et al. 2014). The high abundance of *Fabaceae* across the Neotropics (~10% basal area) (ter Steege et al. 2006), and the potential for relatively high rates of free-living BNF associated with the warm and moist soil and litter suggest that tropical forests can fix large quantities of N rapidly.

The highest rates of primary production and measured rates of BNF occur in tropical forests (Cleveland et al. 1999), but most studies have been conducted in coastal regions that receive large inputs of sea-salt aerosols likely rich in molybdenum

(Mo). Aerosol inputs can be important to tropical forests situated on ancient, highly weathered soils, since high temperatures and precipitation lead rock-derived nutrients, such as P (Porder and Hilley 2011) and likely Mo to be in short supply. Molybdenum is the most prevalent and efficient co-factor in the nitrogenase enzyme (Eady 2003), and experimental Mo additions have shown that the low concentrations of Mo can limit BNF rates in tropical forests (Barron et al. 2009, Wurzburger et al. 2012). Molybdenum is rare in soils, with an average crustal abundance of 1-2 $\mu g\ g^{-1}$ (Taylor and McLennan 1995). In addition, when present as the oxidized anion molybdate (MoO_4^{2-}), Mo is highly soluble and easily leached (Wichard et al. 2009). While plants and bacteria have highly specialized mechanisms to take up molybdate (Grunden and Shanmugam 1997, Tomatsu et al. 2007), in highly acidic tropical soils (pH < 5) Mo forms biologically-inaccessible protonated compounds such as molybdic acid (Anbar 2004). How then can Mo be sustained in highly weathered, acidic, tropical systems that account for roughly 70% of global terrestrial BNF (Wang and Houlton 2009, Cleveland et al. 2013)?

1.2. Chapter 2

Highly weathered soils of tropical forests are generally regarded as being in delicate nutrient balance, so the influx of new nutrients through atmospheric input can be crucial to tropical forest productivity (Swap et al. 1992, Mahowald et al. 2008b, Yu et al. 2015). While atmospheric sources may be important contributors of Mo to weathered tropical systems, atmospheric Mo deposition had not yet been studied spatially (Nriagu 1989). Despite being a trace constituent of the crust, Mo is relatively unreactive in oxygenated, aqueous solution and is removed so slowly from seawater

that it is the most abundant transition metal in the oceans, with a concentration of about 106 nmol kg^{-1} (Nakagawa et al. 2012). In contrast to P, Mo is highly-concentrated in sea-water, making sea-salt inputs to terrestrial ecosystems much more important for Mo than for P. I hypothesized that atmospheric inputs of Mo, such as sea-salt aerosol spray, contribute to the Mo supply in the tropics and sustain some of the previously measured high BNF rates.

In Chapter 2, I examined the global distribution of potential inputs of Mo to terrestrial ecosystems, modifying the model that Mahowald et al. (2008) used for P and iron (Fe). In the model, I focused on the primary long-term natural inputs that redistribute Mo: mineral dust, redistributed from deserts across far distances; sea-salt aerosols, which can be large inputs along coasts; and volcanoes, which are highly localized sources. While the concentrations of Mo concentrations in seawater are highly conserved and well-known (Emerson and Huested 1991, Nakagawa et al. 2012), Mo in dust had not yet been quantified. A large global source of mineral dust is the Bodélé Depression in North Africa, which makes its way westward annually from North Africa across the Atlantic Ocean, to the Caribbean, Central America, and parts of the Amazon Basin. We quantified Mo in dust and sediments from the Bodélé Depression to constrain our global model. Our group used the same samples as Abouchami et al. (2013) in their study characterizing dust and sediments from the Bodélé Depression to assess accumulation of dust in the Amazon Basin.

I found higher Mo deposition to terrestrial ecosystems along coasts downwind of trade winds, near active volcanoes, and in areas that receive transatlantic dust deposition from North Africa, such as the northern Amazon Basin, the Caribbean, and

Central America. Mineral dust is the largest natural source of Mo deposition (70%), while sea-salt follows (26%), and volcanoes are the lowest (4%). Sea-salt spray deposition of Mo is likely well-constrained since seawater Mo is a conservative constituent of seawater globally. Again, we noted that most studies that have directly measured BNF rates in the tropics are conducted in coastal regions, and therefore subject to inputs of Mo in sea-salt aerosol spray. The lowest Mo deposition rates were in the high latitudes, the northern parts of North America, Western Australia, Southern Africa, and much of central South America, including the southern Amazon basin. This leads to the question: is Mo is short supply where there is little to no parent material contribution and where atmospheric inputs of Mo are low?

1.3. Chapter 3

Based on our model findings, I hypothesized that the southern Amazon, which receives relatively little dust, sea-salt aerosol, or volcanic inputs would be low in Mo and P availability. Phosphorus availability is also important for BNF since it is the element that has been found to most frequently limit tropical BNF (Reed et al. 2011). Many N fixers (free-living and symbiotic) increase in both abundance and fixation rates when P supply is high. This can be explained by one of three mechanisms: (1) most systems are limited by P supply, with the supply of N adjusting to P; when P is added, the system shifts to N-limitation and induces a higher demand for BNF; (2) because N fixers systematically require more P for cell growth; or (3) N fixers are less competitive in acquiring P than non-fixers (Vitousek and Howarth 1991, Crews 1993, Vitousek et al. 2002, Benner and Vitousek 2007). However, teasing apart Mo and P limitation in previous research is complicated because in many P addition

experiments, Mo may have been present as a contaminant not actively controlled for (Charter et al. 1995, Barron et al. 2009). This calls into question the results of historical P addition experiments in which Mo could represent an incidental nutrient addition (Reed et al. 2011). Molybdenum could be more important in limiting BNF than previously thought, but because Mo is rarely measured in soils due methodological issues, we do not yet have a grasp on Mo abundance in tropical systems.

Furthermore, I hypothesized 1) that the southeastern Amazon may have low rates of symbiotic and free-living BNF in contrast to empirical studies of other tropical forests, and 2) that Mo limitation of free-living BNF is widespread in the southern Amazon. Even in areas where atmospheric Mo inputs are high to tropical forests that are P- and not N-limited, Mo often limits BNF (Barron et al. 2009, Wurzburger et al. 2012, Reed et al. 2013, Winbourne et al. 2017). Thus in areas of low atmospheric Mo inputs, such as the southeastern Amazon, Mo limitation of BNF is likely even stronger than in other tropical forests. In addition, the high soil acidity of the Amazon may further make Mo unavailable for microbial uptake. The forest soils in the southeastern Amazon are highly acidic with an average pH of 3.9 (Riskin et al. 2013), which affects Mo and P formation of chemical complexes and sorption to soils (Haynes 1982, Anbar 2004). Currently, the five studies that have assessed Mo and P limitation on free-living BNF rates in the tropics have not examined Mo and P limitation alone in the field; they have either looked at short-term Mo and P limitation in the lab, or combined long-term Mo and P limitation in the field without Mo and P alone.

For Chapters 3-5, I conducted my dissertation fieldwork at Fazenda Tanguro in Mato Grosso, Brazil in the southeastern Amazon, one of Brazil's (Long-Term Ecological Research) LTER field stations run by Instituto de Pesquisa Ambiental da Amazônia (IPAM), where research has been ongoing since 2004. For Chapter 3, I conducted two block-design field experiments during the wet and dry seasons by adding Mo, P, and lime alone and in combination. I measured free-living BNF in the soil and litter immediately, and then weeks and months after the applications. To verify that my experiment altered soil conditions, I measured total and resin-extractable Mo and P along with soil pH one day and one month after the applications.

I found that as I hypothesized, soil Mo and P concentrations were low in the southeastern Amazon. My measurements verified that additions of Mo, P, and lime resulted in higher concentrations of resin-extractable Mo and P and higher pH. However, the additions did not strongly and consistently increase BNF over time as I originally hypothesized. BNF increased in the soil one day after applications in response to Mo and P in the dry season (17-fold on average, $p = 0.049$), and in response to Mo and P in combination with lime one month after applications in the soil in the wet season five-fold on average, $p = 0.045$). Three months after the applications in the dry season, Mo and P in combination with lime increased BNF rates in the litter layer four-fold, but variation was high and the effect, if real, was statistically weak ($p = 0.11$). BNF rates varied widely depending on seasonality and precipitation. The high variability in the field, compared to previous short-term laboratory experiments, may have precluded the detection of significant responses in the litter layer.

I postulate that while Mo and P may be important for regulating BNF during periodic N limitation, N richness ultimately downregulates free-living BNF at this site. Indirect indicators, such as the stoichiometric ratios of soil N:P and soil and foliar C:N (the average foliar C:N was 23.8, compared to a tropical forest average of 36 (McGroddy et al. 2004)) and the high soil concentrations of nitrate and ammonium (1.35 µg NO_3^- and 14.58 µg NH_4^+ g^{-1} in the wet season; 6.17 µg NO_3^- g^{-1} and 23.03 µg NH_4^+ g^{-1} in the dry season) in the southeastern Amazon indicate that N availability is high, especially when compared to many other tropical forests on younger soils. The higher N availability could explain the overall low rates of BNF, and the lack of strong responses to Mo or P.

1.4. Chapter 4

Deforestation and greater drought intensity are increasing the susceptibility of tropical forests to fire over large areas of the Amazon. Although tropical forests on old soils are not typically limited by N, after forest fires, N is lost to the atmosphere preferentially to P (Kauffman et al. 1995), potentially inducing N limitation relative to P during early succession. In areas isolated from atmospheric N deposition, BNF is the primary mechanism to support N acquisition and the recovery of the N cycle (Batterman et al. 2013). In wet tropical forests of Panama, symbiotic BNF can increase to high rates in disturbed forests, but generally stays low in high-N soils in mature forests (Barron et al. 2011). I hypothesized in the southeastern Amazon, N-fixing species downregulate symbiotic N fixation when N is available in mature forests, and that after fires, aboveground losses of N would facilitate higher rates of free-living and symbiotic BNF.

I hypothesized that BNF would increase post-fire for two reasons: 1) aboveground losses of N relative to P would induce temporal N limitation; and 2) fires would release biomass Mo and P, as well as cations, to the forest floor. Thereby the increase in availability of Mo and P for microbial uptake would reduce potential Mo and P limitation on BNF while increasing soil pH. I investigated the role of BNF by free-living and symbiotic microbes seven years after experimental burns in the southeastern Amazon. At Fazenda Tanguro, a large-scale experiment (150-ha) compared control forests with forests that were burned three years apart (triennially) in 2004, 2007 and 2010, and annually from 2004 to 2010 (except 2008). I measured the changes in aboveground biomass N using tree inventories and monthly leaf area index measurements as a proxy for aboveground N recovery. I quantified free-living BNF in the dry and wet seasons and symbiotic BNF in the wet season to test the hypothesis that BNF is elevated after a fire to support forest regrowth.

After forest fires, about half the aboveground N was lost (~280 kg ha^{-1}), and post-fire average aboveground regrowth assimilated a gross between 5 and 6 kg N ha^{-1} yr^{-1}. However, symbiotic and free-living BNF rates did not increase as expected, especially relative to other secondary forests, where mean rates have ranged from 4 to 29 kg N ha^{-1} yr^{-1} (Batterman et al. 2013, Sullivan et al. 2014, Winbourne et al. 2018, Taylor et al. 2019). Seven years after the last fires, free-living and symbiotic BNF rates (0.16-0.69 kg N ha^{-1} yr^{-1} across all plots) were eight-fold lower than estimates for all tropical forests (5.7 kg N ha^{-1} y^{-1}) (Sullivan et al. 2014). I conclude that BNF in the burned forests in the southeastern Amazon behaves more like mature forests than secondary forests found elsewhere, probably due to high N availability in surface soils

as well as high nitrate availability stored deeper in soils from 1-4 m (Jankowski et al. 2018). Although we found slightly decreased nitrate and ammonium in the burned plots, the surface soil nitrate and ammonium concentrations in the southeastern Amazon were much higher than many other succession studies across the tropics, averaging a total of 16.0 μg NO_3^- + NH_4^+ g^{-1} in the dry season and 4.8 μg NO_3^- + NH_4^+ g^{-1} in the wet season across both burned treatments. In another study at Fazenda Tanguro, Jankowski et al. (2018) found substantial deep nitrate pools in forest soils, 228 kg N-NO_3^- + NH_4^+ ha^{-1} from 0-4 m deep, indicating a buildup of N. The large nitrate pools were indicative of potential anion exchange in the highly weathered, topographically stable tropical forests. The high availability of N likely suppresses BNF, even in secondary forests where N has been lost. Previous BNF studies have mostly been conducted on much younger and more topographically variable parent material, where there is likely less accumulation of inorganic N.

1.5. Chapter 5

Tropical forests are characterized by a high abundance of trees and lianas in the family *Fabaceae*, which are capable of supporting symbiotic BNF. They are thought to play an important role in the carbon cycle, particularly in recovering tropical forests, when N can be limiting (Davidson et al. 2007, Wright et al. 2018). *Fabaceae* are more abundant in dry tropical forests than in wet tropical forests, which likely is related to their reduced leaflet size and thus drought tolerance, as well as their ability to fix N (Gei et al. 2018). While successional patterns have been documented for these trees capable of supporting symbiotic BNF in wet tropical forests after logging, fewer patterns have been studied in dry tropical forests post-fire.

In Chapter 5, I tested the hypothesis that tree species that are often associated with symbiotic BNF (potential N fixers) would be more competitive than tree species that do not support symbiotic BNF (non-fixers) in growth, recruitment, and mortality post-fire, but not in the mature forest. Using a tree inventory census from the large-scale fire experiment at Fazenda Tanguro in the southeastern Amazon (2004-2016), I investigated the successional patterns of non-fixers and potential N fixers post-fire. Post-fire, potential N-fixer stem percentage and basal area percentage increased relative to the mature control forest, particularly in the smaller size classes. This pattern was driven by a higher recruitment rate of N fixers in the burned forests, lower mortality of N fixers in the burned relative to the mature forest, and faster growth rates of potential N fixers compared to non-fixers. These patterns were consistent with previous studies in wet and dry tropical forests. However, in the southeastern Amazon, most of the demographic processes were driven by one potential N-fixing species, *Tachigali vulgaris*, common to the Cerrado and southern Amazon biomes. However, nodule surveys and indirect isotopic evidence suggests that *T. vulgaris* was not supporting N-fixing symbionts. It is surprising that species with the capability of fixing N are still successful even when they are not actively fixing N. This may be explained by potential N fixers having other ecological advantages, such as higher water-use efficiency or higher leaf N (Adams et al. 2016).

1.6. Conclusion

In conclusion, I found that atmospheric sources of Mo could potentially produce a spatial gradient of Mo availability, and I identified the southern Amazon as a region that receives very low Mo deposition. The southern Amazon is a region

where BNF has not yet been quantified, and where parent material weathering contribution is low. I then focused the field work and experimentation of my dissertation in the southeastern Amazon. There, I found surprisingly low rates of symbiotic and free-living BNF (eight-fold lower than the tropical forest estimated average), even in response to Mo and P additions, perhaps because of high N availability suppressing BNF. In response to disturbance, when BNF has been shown to increase in other tropical forests, BNF did not increase after fires in the southeastern Amazon. I also found that potential N-fixing species in the *Fabaceae* family are still dominant early in succession in tropical forests, but perhaps not because of BNF, but rather because of drought tolerance.

These patterns likely represent large areas of tropical forest that occur in lowland, interior basins on highly weathered oxisols. The low rates of BNF in southeastern Amazon forests have important implications for understanding and predicting the role of BNF in tropical forests more generally, because about 30% of tropical forests globally (the majority of the Amazon and Congo Basins) occur in lowland, interior basins on highly weathered soils that likely behave similarly, where N stocks have built up in soils over time from increasing anion exchange capacity. Currently our knowledge of tropical forest function and biogeochemistry is geographically-biased, and sampling across lowland, interior tropical forests reveals more variation in the biogeochemical cycling across tropical forests than previously thought.

1.7. References

Abouchami, W., K. Näthe, A. Kumar, S. J. G. Galer, K. P. Jochum, E. Williams, A. M. C. Horbe, J. W. C. Rosa, W. Balsam, D. Adams, K. Mezger, and M. O. Andreae. 2013. Geochemical and isotopic characterization of the Bodélé Depression dust source and implications for transatlantic dust transport to the Amazon Basin. Earth and Planetary Science Letters 380:112–123.

Adams, M. A., T. L. Turnbull, J. I. Sprent, and N. Buchmann. 2016. Legumes are different: Leaf nitrogen, photosynthesis, and water use efficiency. Proceedings of the National Academy of Sciences 113:4098–4103.

Anbar, A. 2004. Molybdenum stable isotopes: observations, interpretations and directions. Reviews in Mineralogy and Geochemistry 55:429–454.

Barron, A. R., D. W. Purves, and L. O. Hedin. 2011. Facultative nitrogen fixation by canopy legumes in a lowland tropical forest. Oecologia 165:511–20.

Barron, A. R., N. Wurzburger, J. P. Bellenger, S. J. Wright, A. M. L. Kraepiel, and L. O. Hedin. 2009. Molybdenum limitation of asymbiotic nitrogen fixation in tropical forest soils. Nature Geoscience 2:42–45.

Batterman, S. A., L. O. Hedin, M. Van Breugel, J. Ransijn, D. J. Craven, and J. S. Hall. 2013. Key role of symbiotic dinitrogen fixation in tropical forest secondary succession. Nature 502:224–227.

Benner, J. W., and P. M. Vitousek. 2007. Development of a diverse epiphyte community in response to phosphorus fertilization. Ecology letters 10:628–636.

Charter, R. A., M. A. Tabatabai, and J. W. Schafer. 1995. Arsenic, molybdenum, selenium, and tungsten contents of distinct fertilizers and phosphate rocks. Communications in Soil Science and Plant Analysis 26:3051–3062.

Cleveland, C. C., A. R. Townsend, D. S. Schimel, H. Fisher, R. W. Howarth, L. O. Hedin, S. Perakis, E. F. Latty, C. Von Fischer, A. Elseroad, and M. F. Wasson. 1999. Global patterns of terrestrial biological nitrogen (N_2) fixation in natural ecosystems. Global Biogeochemical Cycles 13:623–645.

Crews, T. E. 1993. Phosphorus regulation of nitrogen fixation in a traditional Mexican agroecosystem. Biogeochemistry 21:141–166.

Davidson, E. A., C. J. R. de Carvalho, A. M. Figueira, F. Y. Ishida, J. P. H. B. Ometto, G. B. Nardoto, R. T. Sába, S. N. Hayashi, E. C. Leal, I. C. G. Vieira, and L. A. Martinelli. 2007. Recuperation of nitrogen cycling in Amazonian forests following agricultural abandonment. Nature 447:995–998.

Eady, R. R. 2003. Current status of structure function relationships of vanadium

nitrogenase. Coordination Chemistry Reviews 237:23–30.

Emerson, S. R., and S. S. Huested. 1991. Ocean anoxia and the concentrations of molybdenum and vanadium in seawater. Marine Chemistry 34:177–196.

Gei, M., D. M. A. Rozendaal, L. Poorter, F. Bongers, J. I. Sprent, M. D. Garner, T. M. Aide, J. L. Andrade, P. Balvanera, J. M. Becknell, P. H. S. Brancalion, G. A. L. Cabral, R. G. César, R. L. Chazdon, R. J. Cole, G. D. Colletta, B. De Jong, J. S. Denslow, D. H. Dent, S. J. Dewalt, J. M. Dupuy, S. M. Durán, M. M. Do Espírito Santo, G. W. Fernandes, Y. R. F. Nunes, B. Finegan, V. G. Moser, J. S. Hall, J. L. Hernández-Stefanoni, A. B. Junqueira, D. Kennard, E. Lebrija-Trejos, S. G. Letcher, M. Lohbeck, E. Marín-Spiotta, M. Martínez-Ramos, J. A. Meave, D. N. L. Menge, F. Mora, R. Muñoz, R. Muscarella, S. Ochoa-Gaona, E. Orihuela-Belmonte, R. Ostertag, M. Peña-Claros, E. A. Pérez-García, D. Piotto, P. B. Reich, C. Reyes-García, J. Rodríguez-Velázquez, I. E. Romero-Pérez, L. Sanaphre-Villanueva, A. Sanchez-Azofeifa, N. B. Schwartz, A. S. De Almeida, J. S. Almeida-Cortez, W. Silver, V. De Souza Moreno, B. W. Sullivan, N. G. Swenson, M. Uriarte, M. Van Breugel, H. Van Der Wal, M. D. D. M. Veloso, H. F. M. Vester, I. C. G. Vieira, J. K. Zimmerman, and J. S. Powers. 2018. Legume abundance along successional and rainfall gradients in Neotropical forests. Nature Ecology and Evolution 2:1104–1111.

Grunden, A. M., and K. T. Shanmugam. 1997. Molybdate transport and regulation in bacteria. Archives of Microbiology 168:345–354.

Haynes, R. J. 1982. Effects of liming on phosphate availability in acid soils - A critical review. Plant and Soil 68:289–308.

Jankowski, K. J., C. Neill, E. A. Davidson, M. N. Macedo, C. Costa, G. L. Galford, L. Maracahipes Santos, P. Lefebvre, D. Nunes, C. E. P. Cerri, R. McHorney, C. O'Connell, and M. T. Coe. 2018. Deep soils modify environmental consequences of increased nitrogen fertilizer use in intensifying Amazon agriculture. Scientific Reports 8:1–11.

Kauffman, J. B., D. L. Cummings, D. E. Ward, and R. Babbitt. 1995. Fire in the Brazilian Amazon: 1. Biomass, nutrient pools, and losses in slashed primary forests. Oecologia 104:397–408.

Mahowald, N., T. D. Jickells, A. R. Baker, P. Artaxo, C. R. Benitez-Nelson, G. Bergametti, T. C. Bond, Y. Chen, D. D. Cohen, B. Herut, N. Kubilay, R. Losno, C. Luo, W. Maenhaut, K. A. McGee, G. S. Okin, R. L. Siefert, and S. Tsukuda. 2008. Global distribution of atmospheric phosphorus sources, concentrations and deposition rates, and anthropogenic impacts. Global Biogeochemical Cycles 22:1–19.

McGroddy, M. E., T. Daufresne, and L. O. Hedin. 2004. Scaling of C:N:P stoichiometry in forests worldwide: implications of terrestrial redfield-type ratios. Ecology 85:2390–2401.

Nakagawa, Y., S. Takano, and M. Firdaus. 2012. The molybdenum isotopic composition of the modern ocean. Geochemical Journal 46:131–141.

Nriagu, J. 1989. A global assessment of natural sources of atmospheric trace metals. Nature 338:47–49.

Porder, S., and G. E. Hilley. 2011. Linking chronosequences with the rest of the world: Predicting soil phosphorus content in denuding landscapes. Biogeochemistry 102:153–166.

Reed, S. C., C. C. Cleveland, and A. R. Townsend. 2011. Functional Ecology of Free-Living Nitrogen Fixation: A Contemporary Perspective. Annual Review of Ecology, Evolution, and Systematics 42:489–512.

Reed, S. C., C. C. Cleveland, and A. R. Townsend. 2013. Relationships among phosphorus, molybdenum and free-living nitrogen fixation in tropical rain forests: results from observational and experimental analyses. Biogeochemistry 114:135–147.

Riskin, S. H., S. Porder, C. Neill, A. M. e Silva Figueira, C. Tubbesing, and N. Mahowald. 2013. The fate of phosphorus fertilizer in Amazon soya bean fields. Philosophical Transactions of the Royal Society B: Biological Sciences 368:1–10.

ter Steege, H., N. C. A Pitman, O. L. Phillips, J. Chave, D. Sabatier, A. Duque, J.-F. Molino, M.-F. Prévost, R. Spichiger, H. Castellanos, P. von Hildebrand, and R. Vásquez. 2006. Continental-scale patterns of canopy tree composition and function across Amazonia. Nature 443:444–447.

Sullivan, B. W., W. K. Smith, A. R. Townsend, M. K. Nasto, S. C. Reed, R. L. Chazdon, and C. C. Cleveland. 2014. Spatially robust estimates of biological nitrogen (N) fixation imply substantial human alteration of the tropical N cycle. Proceedings of the National Academy of Sciences of the United States of America 111:8101–6.

Swap, R., M. Garstang, S. Greco, R. Talbot, and P. Kållberg. 1992. Saharan dust in the Amazon Basin. Tellus B 44B:133–149.

Taylor, B. N., R. L. Chazdon, and D. N. L. Menge. 2019. Successional dynamics of nitrogen fixation and forest growth in regenerating Costa Rican rainforests. Ecology, in press e02637.

Taylor, S. R., and S. M. McLennan. 1995. The geochemical evolution of the continental crust. Reviews of Geophysics 33: 241-256.

Tomatsu, H., J. Takano, H. Takahashi, A. Watanabe-Takahashi, N. Shibagaki, and T. Fujiwara. 2007. An Arabidopsis thaliana high-affinity molybdate transporter required for efficient uptake of molybdate from soil. Proceedings of the

National Academy of Sciences of the United States of America 104:18807–12.

Vitousek, P. M., K. E. N. Cassman, C. Cleveland, C. B. Field, N. B. Grimm, and W. Hole. 2002. Towards an ecological understanding of biological nitrogen fixation. Biogeochemistry 57/58:1–45.

Vitousek, P. M., and R. W. Howarth. 1991. Nitrogen limitation on land and in the sea: how can it occur? Biogeochemistry 13:87–115.

Wichard, T., B. Mishra, S. C. B. Myneni, J. P. Bellenger, and A. M. L. Kraepiel. 2009. Storage and bioavailability of molybdenum in soils increased by organic matter complexation. Nature Geoscience 2:625–629.

Winbourne, J. B., S. W. Brewer, and B. Z. Houlton. 2017. Iron controls over di-nitrogen fixation in karst tropical forest. Ecology 98:773–781.

Winbourne, J. B., A. Feng, L. Reynolds, D. Piotto, M. G. Hastings, and S. Porder. 2018. Nitrogen cycling during secondary succession in Atlantic Forest of Bahia, Brazil. Scientific Reports 8:1–9.

Wright, S. J., B. L. Turner, J. B. Yavitt, K. E. Harms, M. Kaspari, E. V. J. Tanner, J. Bujan, E. A. Griffin, J. R. Mayor, S. C. Pasquini, M. Sheldrake, and M. N. Garcia. 2018. Plant responses to fertilization experiments in lowland, species-rich, tropical forests. Ecology 99:1129–1138.

Wurzburger, N., J. P. Bellenger, A. M. L. Kraepiel, and L. O. Hedin. 2012. Molybdenum and phosphorus interact to constrain asymbiotic nitrogen fixation in tropical forests. PloS one 7:1–7.

Yu, H., M. Chin, T. Yuan, H. Bian, L. A. Remer, J. M. Prospero, A. Omar, D. Winker, Y. Yang, Y. Zhang, Z. Zhang, and C. Zhao. 2015. The fertilizing role of African dust in the Amazon rainforest: A first multiyear assessment based on data from Cloud-Aerosol Lidar and Infrared Pathfinder Satellite Observations. Geophysical Research Letters:1–8.

CHAPTER 2 . MODELED GLOBAL ATMOSPHERIC DEPOSITION OF MOLYBDENUM FROM MINERAL DUST, VOLCANOES, AND SEA-SALT AEROSOLS AND POTENTIAL CONSEQUENCES FOR NITROGEN FIXATION IN TROPICAL FORESTS

Authors

Wong, Michelle Y.[1*], Natalie M. Mahowald[2], Roxanne Marino[1], Earle Williams[3], Robert W. Howarth[1].

[1]Department of Ecology and Evolutionary Biology, Cornell University, Ithaca, NY 14853, U.S.A.
[2]Department of Earth and Atmospheric Sciences, Cornell University, Ithaca, NY 14853, U.S.A.
[3]Massachusetts Institute of Technology, Cambridge, MA 02139-4307, USA

2.1. Summary

Molybdenum (Mo) is an essential trace metal that plays a central role in biological nitrogen fixation (BNF) as the cofactor of the nitrogenase enzyme. The low availability of Mo in soils often constrains BNF rates in many terrestrial ecosystems. Atmospheric sources may supply a critical source of exogenous Mo to regions with highly weathered soils likely low in Mo, particularly in tropical forests where BNF rates are thought to be high. Here, we present results of a global model of Mo deposition that considers the principal natural sources that redistribute Mo—windborne mineral dust, sea-salt aerosols, and volcanic sources, which operate over geologic time. The largest source of mineral dust globally is from North Africa. We quantified Mo concentrations in dust and sediments from the Bodélé Depression, a large source of dust within North Africa, to constrain our model. Because the Mo concentration of seawater is relatively high, we also hypothesized that sea-salt aerosols would contribute atmospheric Mo. Our model predicted higher Mo deposition

to terrestrial ecosystems along coasts downstream in trade winds, near active volcanoes, and in areas that receive dust deposition from North Africa, such as the northern Amazon Basin, the Caribbean, and Central America. Regions with higher Mo deposition tend to also be areas where BNF has previously been measured. The lowest Mo deposition rates were in the high latitudes, northern parts of North America, Western Australia, Southern Africa, and much of central South America. Atmospheric Mo could play an important role in supplying Mo across geologic time, particularly in tropical regions with highly weathered soils.

2.2. Introduction

The distribution of molybdenum (Mo) deposition to terrestrial ecosystems from the atmosphere is important because Mo plays a critical role in nitrogen (N) fixation, the reaction that transforms atmospheric N into plant-available forms. Molybdenum is the most prevalent and efficient co-factor of the nitrogenase enzyme (Eady 1996), and the availability of Mo constrains biological nitrogen fixation (BNF) rates across many terrestrial ecosystems (e.g. Barron et al. 2009). Despite the key biological role of Mo, it is rare in most soils, with an average crustal abundance of 1-2 $\mu g\ g^{-1}$ (Taylor and McLennan 1995). Molybdenum availability is likely even lower across many acidic and highly weathered tropical soils remote from atmospheric inputs, where leaching over geologic time removes Mo and other soluble elements. There has been little study on Mo availability in tropical regions, but it may be particularly low in remote regions such as the interior Amazon, where BNF rates are thought to be high (Wang and Houlton 2009), but where BNF has not yet been quantified. Our current understanding of tropical BNF is geographically-limited,

particularly for areas remote from the mineral dust, sea-salt aerosol, or volcanic inputs that provide the dominant sources for Mo deposition.

While weathering of parent material is the major contributor of rock-derived elements to soils, atmospheric sources can be an important source of new nutrients to highly weathered soils (Chadwick et al. 1999). Sea-salt aerosols are carried inland varying distances by prevailing winds, and the largest rates of deposition occur in coastal regions. Because of sea-salt aerosol deposition, sodium (Na) concentrations in rainfall can drop up to 700-fold from coastal to inland regions across 3000 km (Stallard and Edmond 1981). Molybdenum eventually leaches from soils into rivers and accumulates in the ocean because of its high solubility when oxidized in the form of molybdate (MoO_4^{2-}). Because Mo is relatively unreactive in oxygenated, aqueous solution and is only very slowly removed from seawater by organisms or by most common mineral phases (Helz and Vorlicek 2019), Mo is the most abundant transition metal in the oceans with a concentration of about 106 nmol kg^{-1} (Nakagawa et al. 2012). We hypothesize that Mo likely follows a similar deposition pattern as Na, with highest deposition in coastal regions.

Away from coastal regions, mineral dust is the major source of aerosols globally, and annual estimates of dust production range from 1000-2150 Tg yr^{-1} (Zender et al. 2004). Dust aerosols are produced by wind erosion in arid and semi-arid regions, and the main source regions globally include the edges of the Sahara desert and Sahel region in North Africa (50-70% of global dust sources), the Arabian Peninsula, the Gobi and Taklamakan deserts in Asia (10-25%), and the Australian and South American deserts (Tegen and Schepanski 2009). The westward movement of

North African dust across the Atlantic Ocean, and the presence of this dust in the Caribbean and the Amazon Basin are well-known (e.g. Artaxo et al. 1990), and thought to help maintain long-term productivity of vegetation in the Amazon Basin (Swap et al. 1992, Okin et al. 2004, Yu et al. 2015) by supplying phosphorus (P). Although dust transport is highly variable from year to year, these dust emissions have likely occurred over tens of thousands of years (Albani et al. 2015), and were possibly even higher before the Last Glacial Maximum (Mahowald et al. 1999) because of high aridity and wind speeds. A major source of dust from the Sahara and Sahel regions comes from the Bodélé Depression in Chad (Koren et al. 2006), where the easily-eroded, diatomite-rich sediments are located between two mountain chains that direct and accelerate the strong and frequent surface winds (Bristow et al. 2009). While the annual rates of atmospheric deposition are typically low for most ecosystems when distributed over large areas, deposition can be important on geologic timescales (Swap et al. 1992, Chadwick et al. 1999). Empirical measurements and models have demonstrated that dust from the Sahara and Sahel regions are an important source of P and iron (Fe) in regions with P and Fe limitation (Mahowald et al. 2005b; Yu et al. 2015).

Volcanoes can also be a source of trace elements to the atmosphere when episodic events release volcanic ash composed of gases, aerosols, and metal salts. Even when not erupting, small amounts of sulfur dioxide gas leak from non-erupting degassing volcanoes, which act as carrier phases for trace elements. In volcanic aerosols from Kilauea volcano in Hawaii, Mo was relatively enriched compared with other trace elements (Sansone et al. 2002), indicating that volcanoes could also be a

source for atmospheric Mo (King et al. 2016). Nriagu (1989) previously synthesized estimates of total sources of Mo to the atmosphere, but Mo deposition has not yet been evaluated spatially, and differential deposition rates could influence ecosystem structure over geologic time. While model-based maps of deposition of Fe (Mahowald et al. 2005b) and P (Mahowald et al. 2008b) from different sources have been constructed, Mo deposition has not yet been evaluated in a similar manner.

Here, we quantify for the first time Mo concentrations in mineral dust, and present the first model-based global deposition map for Mo. We focused on pre-industrial, natural source emissions since the end of the Last Glacial Maximum, with a particular emphasis on the fate of dust from the Sahara and Sahel regions and the potential impact of deposition on tropical regions such as the Amazon Basin. Anthropogenic activity has increased Mo deposition since the 19th century (Hong et al. 2004), and biogenic particles and biomass burning could also be important sources of the atmospheric Mo cycle, redistributing local sources of Mo. However, natural sources of sea-salt aerosols, mineral dust, and volcanoes likely dominated the atmospheric cycles during the past 12,000 years. Previous studies based on precipitation concentrations and Mo isotopes indicate an important role of atmospheric Mo in contributing to soil Mo (Marks et al. 2015; Siebert et al. 2015; King et al. 2016). Our objectives were to quantify Mo in dust, develop a model that depicts atmospheric Mo deposition worldwide, and determine if atmospheric Mo could be an important source of Mo to highly weathered soils of the world. We hypothesized that: (1) dust inputs from North Africa are important in the northern Amazon, (2) sea-salt deposition is important only near coastal regions, and (3) that volcanoes could be

locally-important sources of Mo.

2.3. Methods

2.3.1. Sample collection

We collected dried samples of dust and sediment from the Bodélé Depression in September 2010 along the main trajectory of the wintertime Harmattan wind system, a dusty West African trade wind that moves westward from North Africa (Abouchami et al 2013). The sediment samples consist of dry lake-bed sediments collected from eight locations in the Bodélé Depression, located about 200 km south of Faya Largeau, a town north of the Bodélé Depression. These dry lake sediments consist of mostly diatomites, the dominant material in the central lake bed of former Lake Megachad, which now is the Bodélé Depression. Here, we use the same sample names as described by Abouchami et al. (2013). The five dust samples were collected from Chad and Niger from high ledges inside abandoned buildings in which dust had collected over a period of many decades. Sample locations and collections as well as data on many elements (but not Mo) in these same dust samples are further described in Abouchami et al. (2013) (Table 2.1).

Table 2.1. Bodélé Depression dust and sediment total Mo concentrations and sample locations. Sample identification parameters correspond to those from Abouchami et al. (2013).

Sample	Sample Description	Latitude	Longitude	Mo (μg g^{-1})
Bodélé Dust				
#1 Faya Largeau (Chad)		17° 56.113' N	19° 06.743'E	1.1
#1 Harmattan (Niamey, Niger)		13° 29.492' N	02° 10.189' E	1.2
#1 Radome (Niamey, Niger)		13° 29.492' N	02° 10.189' E	1.2
#2 Mao (rafters, Chad)		14° 07.704' N	15° 18.753' E	1.3
#2 Nguimi (police station, Chad)		14° 15.175' N	13° 06.878' E	1.0
Bodélé Sediment				
Bodéle soil 43.5 (Chad)	gray flakes and highly localized red plates	16° 06.120' N	18° 33.000' E	0.9
Bodéle soil 44 (Chad)	mixture of gray and white flakes of diatomite and surrounding sand	16 °08.139' N	18 °35.930' E	1.1
Bodéle soil 44B (Chad)	mixture of gray and white flakes of diatomite and surrounding sand	16 °08.139' N	18 °35.930' E	2.4
Bodéle soil 44C (Chad)	gray flakes and highly localized red plates	16 °12.273' N	18 °36.397' E	0.7
Bodéle soil 44D (Chad)	gray flakes and highly localized red plates	16 °12.273' N	18 °36.397' E	0.7
Bodéle soil 51 (Chad)	gray flakes and highly localized red plates	17 °13.777' N	19 °02.149' E	3.6
Bodéle soil 54A (Chad)	gray flakes and highly localized red plates	16 °09.190' N	18 °35.464' E	0.7
Bodéle soil 54B (Chad)	gray flakes and highly localized red plates	16 °09.190' N	18 °35.464' E	1.3

2.3.2. Sample analysis

Molybdenum concentrations in the dust and sediment samples were measured at the W.M. Keck Foundation Laboratory for Environmental Biogeochemistry, School of Earth & Space Exploration, Arizona State University (ASU). The dust and sediment samples were re-dried at 105°C, sieved at 2 mm and powdered, and ashed at 550°C overnight to remove organic matter. Samples were digested in HNO_3, HF, and HCl depending on sample solubility in a closed Savillex reactor on a hot plate. After digestion, samples were then diluted in 2% HNO_3 and Mo concentrations were determined by quadrupole ICP-MS (ThermoFisher Scientific iCAP Q, with CCT

option). All samples were run in conjunction with SDO-1, a Devonian Ohio shale available from the USGS, and SCo-1, a grey shale low in Mo concentration available from the USGS, and yielded values of 142 ± 5.4 and 1.12 ± 0.2 μg g^{-1} (1 s.d.; n = 9).

2.3.3. Atmospheric Modeling

To estimate Mo deposition from mineral dust, sea-salt aerosols, and volcanoes, we used an atmospheric transport model to simulate atmospheric Mo deposition from source areas through emission processes (Figure 2.1), transport, and deposition mechanisms, using the parameterizations from (Brahney et al. 2015). Because Mo in the atmosphere is present almost exclusively in the solid aerosol phase, we simulated Mo using an aerosol transport and deposition scheme within the Community Atmosphere Model, version 4 (CAM4), the atmospheric component of the Community Earth System Model (CESM) developed at the National Center for Atmospheric Research (NCAR). We ran the model using climate model-derived winds with the slab ocean model. Simulations were conducted for 5 years, with the last 4 years used for analysis. The model simulates three-dimensional transport and wet and dry deposition for gases and aerosols. Model spatial resolution was 1.9° by 2.5°. For each grid box, we obtained an estimate of deposition fluxes for every day of the year which were summed into annual estimates.

For Mo in dust, we assumed a constant fraction of the dust was Mo using concentrations measured in this study, described above. In the model, mineral dust was entrained in unvegetated dry, arid regions with easily erodible soils during strong wind events. The dominant source regions of mineral aerosols were the arid regions of North Africa, the Arabian Peninsula, Central Asia, China, Australia, North America,

and South Africa, most of which contain basins that drain from highlands that collect small particles (Figure 2.1a). The entrainment process to the atmosphere was proportional to the wind friction velocity, a measure of wind shear stress on soil surfaces and a function of planetary boundary layer winds, surface roughness, and atmospheric stability, further described by Mahowald et al. (2005b). The dust model included four particle size bins (0.1–1, 1–2.5, 2.5–5, and 5–10 μm) which were transported and deposited separately using the size fractionation by Albani et al. (2014). The regional source strengths of the mineral dusts were tuned to best match available aerosol optical depth, concentration and deposition data as described by Albani et al. (2014).

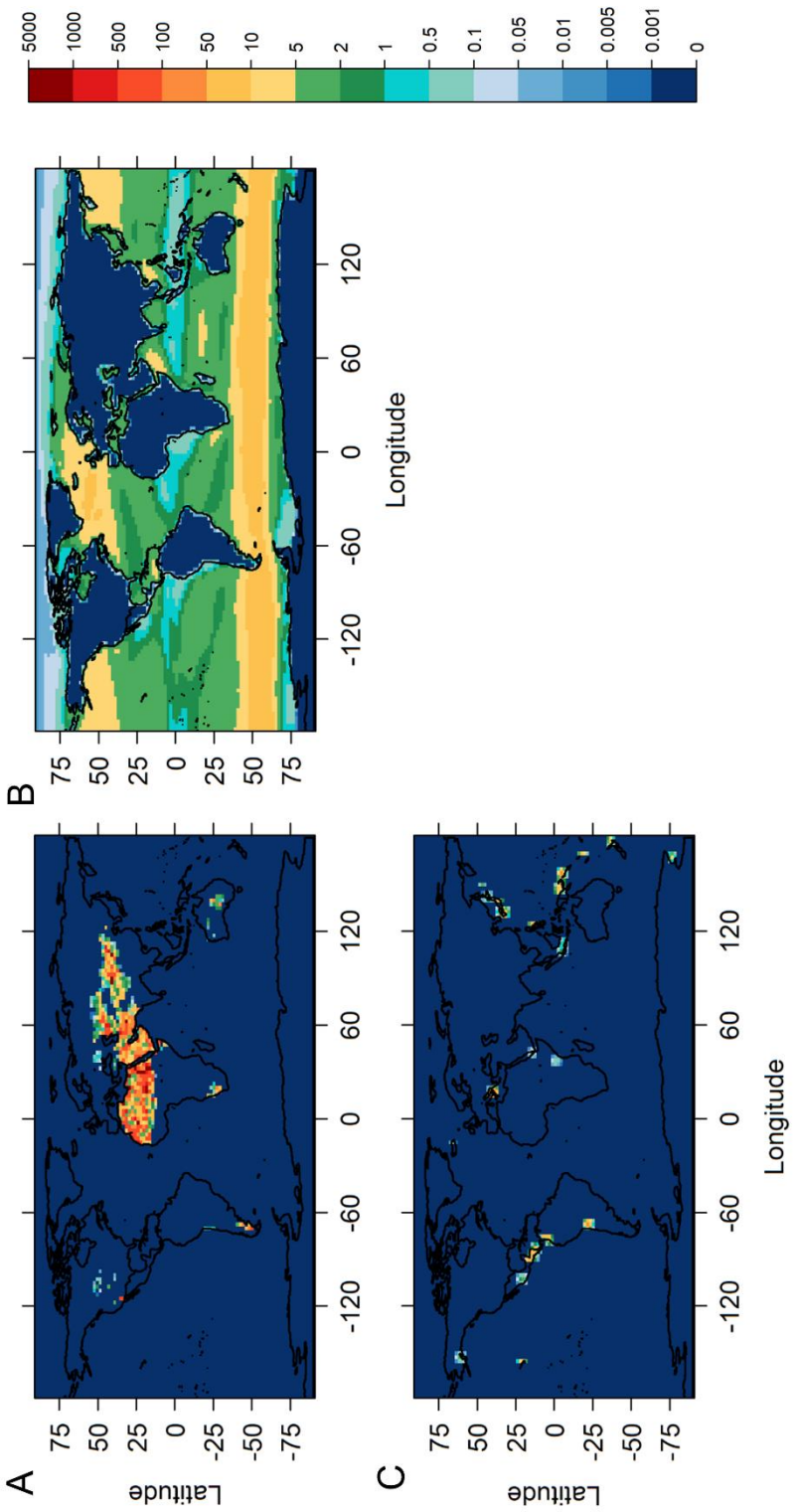

Figure 2.1. Annual sources of sea-salt Mo (μg m^{-2} yr^{-1}) (A), Annual dust Mo sources (μg m^{-2} yr^{-1}) (B), Annual volcano Mo sources from degassing volcanoes (μg m^{-2} yr^{-1}) (C).

Similarly, to model the Mo in sea-salt aerosols, we used a constant concentration of Mo in seawater and used the sea-salt module (Mahowald et al. 2006) with parameterizations from Gong et al. (1997). Because Mo, unlike any other trace element, is a conservative element in seawater with a constant ratio with salinity, we could assume that the concentration of Mo in sea-salt aerosols reflected that of surface seawater (Collier 1985). In the oxic seawater surface, Mo occurs as the stable molybdate oxyanion (Smedley and Kinniburgh 2017), slowly removed by organisms and most minerals (Helz and Vorlicek 2019). Therefore, the average Mo atom circulates the oceans about 300 times, resulting in a homogenous distribution across oceans, with the largest variations in the Mo concentration ~5% when normalized to salinity (Tuit 2003). We derived the Mo sea-salt aerosol concentration from an average ocean concentration of 106 nM Mo (Nakagawa et al. 2012) normalized to average seawater salinity of 35 g kg^{-1}, resulting in a value of 0.29 μg Mo g^{-1} salt. The source of the sea-salt aerosols was the open ocean under high wind speed conditions (Figure 2.1b). Distribution into each size bin (0.1-1, 1-3, 3-10, and 10-20 μm) was independent of wind speed or relative humidity.

We used the Mo to sulfur (S) ratio to approximate volcanic Mo deposition, normalized to estimates of S emissions from volcanoes from gridded global data sets (Spiro et al. 1992) of non-erupting volcanoes (Figure 2.1c). Sulfur is used as a parameter for volcanic activity because of the ability to easily measure S with ground and satellite-based remote sensing (Carn et al. 2017). We simulated S emission as continuous release from active volcanoes. While volcanic ash from episodic events can contribute significant elements, we focused here on average estimated background

volcanic activity only for the steady-state spatial model because of the difficulty in capturing historical episodic events, but include eruptive events in the total budget. We assumed that the volcanic Mo is in fine aerosols because it is formed at high temperatures, and used a mass-based ratio of 4×10^{-4} of Mo/S from Nriagu (1989), estimate Mo emissions as a fraction of S emissions. Volcanic aerosols were simulated in the size same bins as dust and sea salt for this study following (Brahney et al. 2015). Once the aerosols were entrained into the atmosphere, they underwent transport, wet and turbulent dry depositions and gravitational settling appropriate for their assumed composition and size.

2.4. Results

2.4.1 Dust Mo concentrations

The Bodélé Depression sediment Mo concentrations ranged from 0.7 to 3.6 µg g^{-1} and the Bodélé Depression dust Mo concentrations ranged from 1.0 to 1.3 µg g^{-1} (Table 2.1). The dust samples averaged a total Mo concentration of 1.15 ± 0.14 µg g^{-1} (standard error) while the sediment samples averaged 1.42 ± 1.04 µg g^{-1}. The dust samples had a much smaller range, likely due to filtering of particles that are entrained in the atmosphere and the downstream mixing that occurs in the atmosphere. We used the dust concentrations here to parameterize the model because up to half the dust from the Sahara, the main mineral source to the Amazon Basin, is thought to be emitted from the Bodélé Depression (Koren et al. 2006).

The average sediment and dust concentrations of 1.4 and 1.1 ug g^{-1} are within the range of the crustal abundance estimates of Mo at 1-2 µg g^{-1} (Taylor and McLennan 1995). Often models use the concentrations from crustal abundance when

dust concentrations are not available (Chadwick et al. 1999, Okin et al. 2004). Using the crustal abundance tends to be a conservative estimate for trace elements, since dusts is typically enriched in trace elements (Lawrence and Neff 2009). Although we did not sample dust from other desert sources, the average concentration of dust measured from the Bodélé falls within the crustal abundance range; thus, we assume conservatively that the concentration of 1.1 μg g^{-1} represents other mineral dust sources.

2.4.2. Modeled sea-salt deposition

Our model predicted higher Mo deposition from sea-salt aerosols in coastal regions facing trade winds (Figure 2.2a). Because of prevailing wind patterns in the equatorial regions where the northeast and southeast trade winds converge, the Caribbean and the northeast coast of South America received relatively high Mo deposition compared to islands situated between the Indian and Pacific Oceans. Deposition rates were higher and extended farther inland to terrestrial ecosystems in the coastal regions of western North America, Western Europe, southern Asia, eastern South America, eastern and southern Australia, Hawaiian Islands, and Central America. The East Indies, eastern North America, western South America, northwestern Australia, which do not have onshore trade winds, received less sea-salt-derived Mo deposition. Because of higher wind speeds in the latitudinal regions, sea-salt sources and subsequent deposition rates were generally higher across the oceans farther from the equator. In South America, for example, moving westward, there was a drop-off of sea-salt aerosol deposition rates. Near Maceio, Brazil at 10.4°S and 35°W, sea-salt deposition rates abruptly decline from 6 μg Mo m^{-2} yr^{-1} to 2.4 times

lower across 270 km, 10 times lower at 820 km, and 18 times lower at 1400 km (Figure 2.2a).

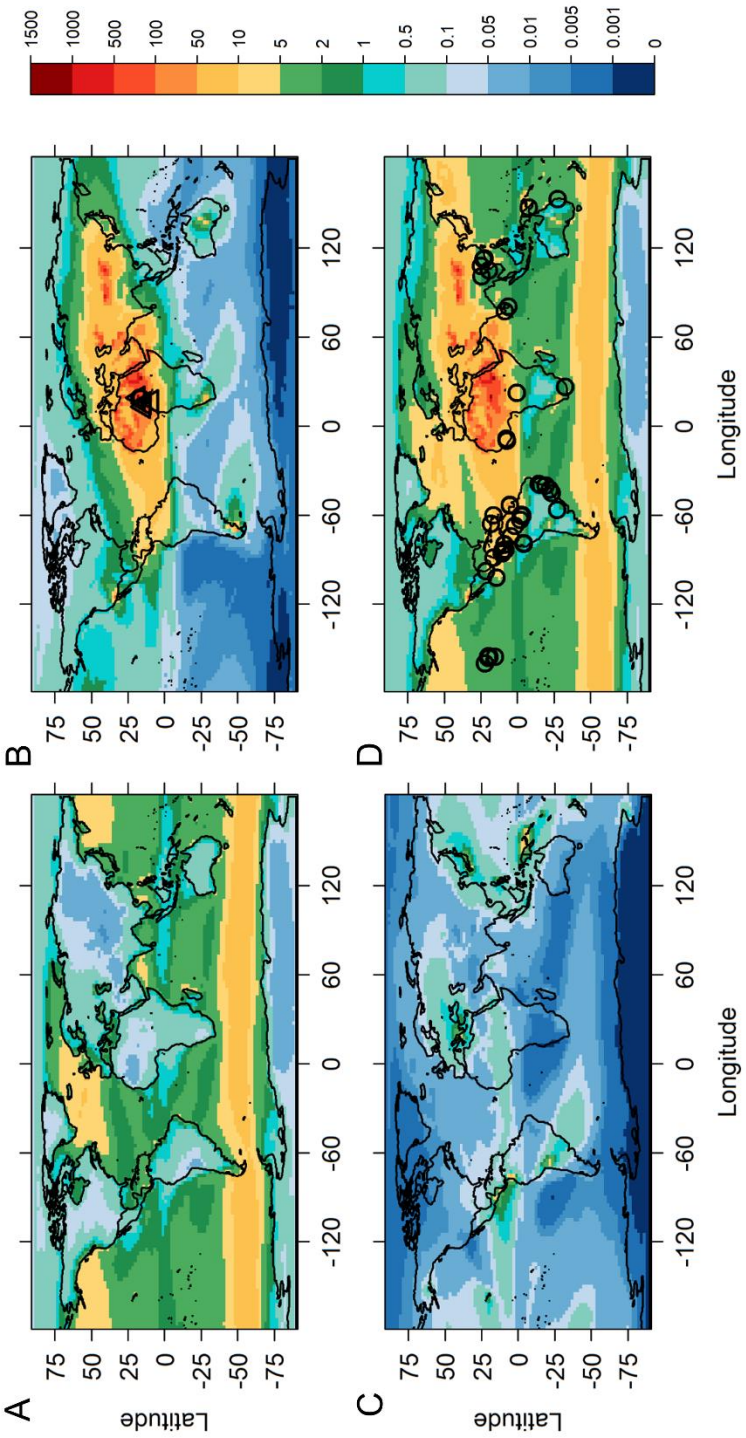

Figure 2.2. Annual sea-salt Mo deposition (μg m^{-2} yr^{-1}) (A), Annual dust Mo deposition (μg m^{-2} yr^{-1}) with triangles indicating Bodélé dust samples and circles indicating Bodélé sediment samples (B), Annual volcano Mo deposition from degassing volcanoes (μg m^{-2} yr^{-1}) (C), and combined annual sea-salt, dust, and volcano Mo deposition (μg m^{-2} yr^{-1}) with circles indicating where BNF studies have previously been conducted in the tropics, summarized in Appendix Table 1 (D).

2.4.3. Modeled Mo dust deposition

The regions that received the most Mo from mineral dust were proximal to the dust sources with onshore winds, such as North Africa, the Arabian Peninsula, the Gobi and Taklamakan deserts in Asia, deserts in central and southern Australia, the Patagonian desert on the southern part of South America, and the southwestern U.S. For example, following the westerly winds, dust moved eastward from the Gobi and Taklamakan deserts in Asia. Exogenous deposition rates were highest, similar to sea-salt spray, in the direction following trade wind movement. Globally, the highest rates decreased moving westward from North Africa, as dust from that source is deposited in the Caribbean, Central America, and the northern Amazon Basin. We found a particularly steep gradient in Mo dust deposition from northern South America to central South America (Figure 2.2b). For example, moving south from Trindad and Tobago in the Caribbean, dust deposition rates decreased from a peak at 8.5°N and 60°W from 30 μg Mo m^{-2} yr^{-1} to 0.042 μg Mo m^{-2} yr^{-1} at 2.38°S and 60°W near Manaus, Brazil in the Amazon, decreasing about 800-fold as precipitation scavenges the atmospheric dust. This pattern held relatively constant from the northern to southern Amazon Basin, and did not correlate with the amount of annual precipitation.

2.4.4. Modeled Mo volcano deposition

The major volcanic sources of Mo were located near the major degassing volcanic regions, such as active volcanoes in Italy, Papua New Guinea, Colombia, Japan, Hawaii, Chile, Guatemala, and Nicaragua (Carn et al. 2017). Deposition patterns of volcanic Mo also followed the direction trade winds, with higher and more extensive deposition moving in the direction of the trade winds relative to the source.

We found the highest deposition rates in Papua New Guinea at 16 µg Mo m^{-2} yr^{-1}. Within the Hawaiian Islands, the highest deposition rates were 1.5 µg Mo m^{-2} yr^{-1} near Hawai'i, Hawaii, and values dropped off three-fold to nearby Hawaiian Islands from scavenging by precipitation, such as Kauai, Hawaii 500 km away. Deposition of Mo associated with volcanic activity ranged between 0.1 to 10 µg Mo m^{-2} yr^{-1} across Central America and the Andean region, and between from 0.1 to 5 µg Mo m^{-2} yr^{-1} from Chile to the southern parts of South America (Figure 2.2c).

2.4.5. Total modeled Mo deposition

When combining sea-salt, dust, and volcanic aerosol deposition, we found the lowest rates of total natural deposition in the high latitudes, the northern parts of North America, the Indian Ocean, Western Australia, Southern Africa, and much of central South America and the southern tip of South America (Figure 2.2d). In total, in the central part of South America, for example, at 65°W and 29.4°S, total deposition rates were 0.16 µg Mo m^{-2} yr^{-1}. The total deposition patterns followed the dust and sea-salt deposition patterns closely, with the highest deposition rates near dust sources and downwind of dust sources, coastal regions facing trade winds, and near active degassing volcanoes (Figure 2.2d).

Mineral dust inputs to the atmosphere dominated natural sources (70%), while sea-salt deposition followed (26%), while the smallest source were degassing and eruptive volcanoes (4%) (Table 2.2). Dust deposition had a far-reaching influence on terrestrial land surfaces within the same continent as the source regions, but also across oceans. In contrast, sea-salt deposition had a stronger influence within oceans and a relatively small influence on terrestrial landscapes, with the exception of coastal

regions facing trade winds. Volcanoes were the smallest source globally, and had predominantly local influences near active, degassing volcanoes. In tropical regions with low dust and sea-salt deposition such as Indonesia, volcanic sources dominated. Across most tropical regions, either dust, sea-salt aerosols, or volcanic activity contributed notable amounts of atmospheric Mo deposition, except for the central region of South America. For example, Hawaii and Central America receive between 2 to 5 μg Mo m^{-2} yr^{-1}, the northern Amazon receives between 5 to 0.010 μg Mo m^{-2} yr^{-1}, and the southern Amazon receives between 0.1 to 1 μg Mo m^{-2} yr^{-1}. Notably, many of the regions where BNF has been measured in the tropics are located in areas with higher rates of sea-salt Mo deposition (Figure 2.2d), such as the Hawaiian Islands, Central America, and coastal South America.

Table 2.2. Global sources of natural atmospheric Mo (Gg/yr)

Source	**Our Model**	**Ngiaru (1989)**	**Relative Uncertainty**
Dust	4.3	1.3	Medium
Sea salts	1.6	0.22	Low
Volcanoes	0.22*	0.4	High

*Includes both degassing and eruptive volcanoes: 0.07 Gg/yr for degassing, and 0.15 Gg/yr for erupting volcanoes

2.5. Discussion

Our model results suggest that globally, mineral dust inputs dominate the natural atmospheric cycle (Table 2.2). Our estimates are some three-fold higher for dust, 8-fold higher for sea-salt aerosols, and roughly half as much for volcanoes compared to previous estimates (Nriagu 1989). Nriagu's sea-salt aerosol estimates were lower and dust estimates were higher because they normalized their sea-salt production to 0.1-1 x 10^{16} g of sea-salt spray, their dust production to 0.6 to 5 x 10^{14} g

of dust derived from (Prospero et al. 1983), while our estimates are derived from simulated sea-salt aerosol and dust entrainment into the atmosphere that were previously tuned to observational data (Mahowald et al. 2006, 2008b). Our modeled sea-salt aerosol Mo deposition estimates are relatively robust because model estimates were tuned to empirical measurements of Na and chloride for sea-salt aerosols (Mahowald et al. 2008b), and the conservative nature of Mo leads to a consistent ratio with sea salts. Our mineral dust model is relatively robust as well, because the dust model has been tuned to observational data from aerosols, as well as satellite data (Mahowald et al. 2003). Although we parameterized the model only with dust samples from the Bodélé Depression, the concentrations from this region fit within the crustal abundance range and represents the largest global source relative to its size. The least well-constrained estimates are the volcano sources because we used a Mo/S ratio, and Mo is rarely measured in volcano plumes or in volcanic ash (Crowe et al. 1987), and often not together with S (e.g. Mather et al. 2012). Our estimates of volcanic emissions from active, degassing volcanoes are likely on the higher end, since Mo is much less volatile than S. While trace metals are often thought to be abundant in degassing volcano plumes because of fractionation processes that concentrate trace metals (Hinkley et al. 1994), a study conducted in Iceland demonstrated relatively low levels of Mo in degassing materials (Arnórsson and Óskarsson 2007). Though volatilization of Mo from degassing volcanoes still needs to be investigated, eruptive volcanoes are still likely to be a source of Mo, as in Hawaii, where Mo in soils was isotopically traced to volcanic emissions (King et al. 2016).

Our modeled Mo deposition rates agreed relatively well with estimates from

the two existing empirical estimates of atmospheric Mo deposition based on precipitation fluxes. In Iceland, a total atmospheric input of 2 to 9 μg Mo m^{-2} yr^{-1} was estimated (Siebert et al. 2015), which is within the range of our model predictions of 3.5 and 6.1 μg Mo m^{-2} yr^{-1} for that region. The Pacific Northwest of the U.S. is also a region for which our model predicted relatively high sea-salt deposition of 4 to 7 μg Mo m^{-2} yr^{-1}. In the same region, Marks et al. (2015), estimated atmospheric Mo deposition rates of 19 μg Mo m^{-2} yr^{-1}, within one order of magnitude of our model estimates. Both of these regions are relatively pristine with little anthropogenic influence but with a higher importance of sea-salt aerosols and in the case of Iceland, volcanic inputs relative to dust.

Across long timescales, atmospheric Mo deposition could support Mo cycling in particular ecosystems that receive relatively high Mo atmospheric deposition with low parent material weathering. For example, in Iceland where deposition rates from sea-salt aerosols are relatively high, Siebert et al. (2015) suggested that atmospheric deposition contributed to between 5 and 9% of the Mo soil pool relative to the basaltic bedrock. They found the strongest sea-salt influence (9%) in the more weathered soils where Mo pools were lower (Siebert et al. 2015). These results suggest that atmospheric Mo inputs can be particularly important on older highly weathered soils in regions of high precipitation where soluble Mo has been lost to leaching. Strong evidence that soil age affects rock-derived nutrient availability also comes from Hawaiian Islands, which vary widely in ecosystem age, ranging from 300 years to 4,100,000 years old. Atmospheric P and calcium (Ca) inputs are particularly important for the fertility of the older islands, where the basaltic parent material is highly

weathered. On islands older than 20,000 years, atmospheric inputs of Ca are the dominant source of Ca (Chadwick et al. 1999). Hawaii is a region where sea-salt deposition of Mo and volcanic deposition of Mo are relatively high, and where BNF rates have also been found to be high (Vitousek and Walker 1989, Ley and D'Antonio 1998, Pearson and Vitousek 2002), indicating that atmospheric Mo may also be important on the older islands, potentially overcoming any potential Mo limitation of BNF.

Tropical forests are thought to be major global sites of BNF rates and important to global BNF totals (Cleveland et al. 1999, Wang and Houlton 2009) for a few reasons. First, tropical forests have a higher abundance of leguminous trees capable of forming symbiotic relationships with bacteria compared to other biomes. Second, the warm, wet conditions of the litter layer facilitate higher rates of heterotrophic, free-living BNF associated with bacteria and archaea. In addition, higher BNF rates in the tropics have been associated with the canopy, epiphytes, decaying wood, bryophytes, and lichens compared to other ecosystems (Cleveland et al. 1999, Matzek and Vitousek 2003). The nitrogenase enzyme, which catalyzes BNF, can be synthesized by all N-fixing bacteria and archaea in its conventional form, of which Mo is the most efficient and prevalent co-factor (Eady 1996).

Evidence of Mo limitation on BNF in tropical forests and other biomes has been increasing (Dynarski and Houlton 2018). Phosphorus was previously thought to be the dominant nutrient control on BNF, but teasing apart the effects of Mo and P in previous research is complicated. In many P addition experiments, Mo may have been present as a contaminant, calling into question the results of historical P addition

experiments where Mo could have been incidentally added (Barron et al. 2009). Almost all previous addition experiments in different biomes have demonstrated Mo limitation on BNF to some extent. However, much of the previous research on Mo and its control on BNF, measured through Mo fertilization experiments, has been conducted in regions where atmospheric deposition of Mo may supply sufficient Mo to support high BNF rates. Even where atmospheric Mo deposition is relatively high in tropical forests in Panama, previous addition experiments have demonstrated an experimental response of BNF to Mo at rates of 39 $\mu g\ m^{-2}\ yr^{-1}$ (Barron et al. 2009). These rates could be supplied by atmospheric deposition over decades to hundreds of years at our modeled rates in some tropical regions (Figure 2.2d).

Thus, if Mo constrains BNF widely across tropical forests, then this constraint is likely more prominent in N-limited regions of low Mo deposition, where parent material weathering is low. For example, the eastern, central and southeastern Amazon are some of the oldest geologic surfaces exposed in South America, with maximum geological ages ranging from 1500 to 3600 million years (Quesada et al. 2011). In the Amazon, the lack of recent geologic activity has suggested the link of atmospheric inputs of P with the long-term productivity of the forests (Swap et al. 1992). Okin et al. (2004) speculated that in the Amazon and Congo Basins, dust P from the Sahara are large enough relative to soil P concentrations to have replenished the soil P many times since the evolution of these ecosystems. From isotopic analysis, the lack of strong dust accumulation from the Bodélé in the Amazon Basin suggests that the dust is consumed, contributing nutrients to stimulate plant growth (Abouchami et al. 2013). While we do not have the soil Mo measurements across the Amazon and Congo

Basins to make the same conclusion as Okin et al. (2004), their results suggests that Mo availability could be relatively low across the lower Amazon and could constrain BNF, compared to other regions like Hawaii where BNF rates have been measured to be relatively high, and Mo deposition is relatively high (Figure 2.2d). Because regions like the Amazon and Congo are not where the majority of BNF studies have previously been conducted (Figure 2.2d), the consequence may be that BNF in interior basins is underrepresented in tropical forest estimates, and we need more studies in these to test whether or not the patterns found in the tropical forests are representative of forests where atmospheric deposition of Mo is low. Atmospheric Mo is likely highly tied to N cycling in N-limited systems with older soils, and more BNF measurements should be conducted to study how BNF behaves there compared to areas that receive relatively high atmospheric inputs of Mo.

Here, we demonstrate the large range in deposition rates of atmospheric Mo globally, which could impact the structure of ecosystems, particular in N-limited ecosystems. To predict the future importance of atmospheric Mo on ecosystem function, we need to further understand the retention and loss of Mo within ecosystems, collect more empirical observations of Mo in soils and in aerosol measurements, and study the impacts of human activity and land-use change on the atmospheric Mo cycle. This will help further understand how tightly coupled Mo availability will be to atmospheric Mo transport in the future, and what the ultimate impact of atmospheric Mo on N-cycling is. Ultimately, BNF should be measured in more remote tropical forests, many of which receive little to no atmospheric Mo inputs and could be limited by Mo.

Acknowledgements

We thank G.D. Gordon and A.D. Anbar at ASU for help with the analysis of the dust and sediment samples. This work was funded by a grant from the David R. Atkinson Center for a Sustainable Future to R.W.H, R.M.M., N.M.M., and Murray McBride (M.M.)

2.6. References

Abouchami, W., K. Näthe, A. Kumar, S. J. G. Galer, K. P. Jochum, E. Williams, A. M. C. Horbe, J. W. C. Rosa, W. Balsam, D. Adams, K. Mezger, and M. O. Andreae. 2013. Geochemical and isotopic characterization of the Bodélé Depression dust source and implications for transatlantic dust transport to the Amazon Basin. Earth and Planetary Science Letters 380:112–123.

Albani, S., N. M. Mahowald, G. Winckler, R. F. Anderson, L. I. Bradtmiller, B. Delmonte, R. François, M. Goman, N. G. Heavens, P. P. Hesse, S. A. Hovan, S. G. Kang, K. E. Kohfeld, H. Lu, V. Maggi, J. A. Mason, P. A. Mayewski, D. McGee, X. Miao, B. L. Otto-Bliesner, A. T. T. Perry, A. Pourmand, H. M. Roberts, N. Rosenbloom, T. Stevens, and J. Sun. 2015. Twelve thousand years of dust: The Holocene global dust cycle constrained by natural archives. Climate of the Past 11:869–903.

Albani, S., N. Mahowald, A. Perry, R. Scanza, C. Zender, and M. G. Flanner. 2014. Improved representation of dust size and optics in the CESM. Journal of Advances in Modeling of Earth Systems 6.

Arnórsson, S., and N. Óskarsson. 2007. Molybdenum and tungsten in volcanic rocks and in surface and <100 °C ground waters in Iceland. Geochimica et Cosmochimica Acta 71:284–304.

Artaxo, P., W. Maenhaut, H. Storms, and R. Van Grieken. 1990. Aerosol characteristics and sources for the Amazon Basin during the wet season. Journal of Geophysical Research 95:16971–16985.

Barron, A. R., N. Wurzburger, J. P. Bellenger, S. J. Wright, A. M. L. Kraepiel, and L. O. Hedin. 2009. Molybdenum limitation of asymbiotic nitrogen fixation in tropical forest soils. Nature Geoscience 2:42–45.

Brahney, J., N. Mahowald, D. S. Ward, A. P. Ballantyne, and J. C. Neff. 2015. Is atmospheric phosphorus pollution altering global alpine Lake stoichiometry? Global Biogeochemical Cycles 29:1369–1383.

Bristow, C. S., N. Drake, and S. Armitage. 2009. Deflation in the dustiest place on Earth: The Bodélé Depression, Chad. Geomorphology 105:50–58.

Carn, S. A., V. E. Fioletov, C. A. Mclinden, C. Li, and N. A. Krotkov. 2017. A decade of global volcanic SO2emissions measured from space. Scientific Reports 7:1–12.

Chadwick, O. A., L. A. Derry, P. M. Vitousek, B. J. Huebert, and L. O. Hedin. 1999. Changing sources of nutrients during four million years of ecosystem development. Nature 397:491–497.

Cleveland, C. C., A. R. Townsend, D. S. Schimel, H. Fisher, R. W. Howarth, L. O.

Hedin, S. Perakis, E. F. Latty, C. Von Fischer, A. Elseroad, and M. F. Wasson. 1999. Global patterns of terrestrial biological nitrogen (N_2) fixation in natural ecosystems. Global Biogeochemical Cycles 13:623–645.

Collier, R. W. 1985. Molybdenum in the Northeast Pacific Ocean. Limnology and Oceanography 30:1351–1354.

Crowe, B. M., D. L. Finnegan, W. H. Zoller, and W. V. Boynton. 1987. Trace element geochemistry of volcanic gases and particles from 1983-1984 eruptive episodes of Kilauea Volcano. Journal of Geophysical Research: Solid Earth 92:13708–13714.

Dynarski, K. A., and B. Z. Houlton. 2018. Nutrient limitation of terrestrial free-living nitrogen fixation. New Phytologist 217:1050–1061.

Eady, R. R. 1996. Structure−Function Relationships of Alternative Nitrogenases. Chemical Reviews 96:3013–3030.

Emerson, S. R., and S. S. Huested. 1991. Ocean anoxia and the concentrations of molybdenum and vanadium in seawater. Marine Chemistry 34:177–196.

Gong, S. L., L. A. Barrie, and J.-P. Blanchet. 1997. Modeling sea-salt aerosols in the atmosphere: 1. Model development.

Helz, G. R., and T. P. Vorlicek. 2019. Precipitation of molybdenum from euxinic waters and the role of organic matter. Chemical Geology 509:178–193.

Hinkley, T. K., M. F. Le Cloarec, and G. Lambert. 1994. Fractionation of families of major, minor, and trace metals across the melt-vapor interface in volcanic exhalations. Geochimica et Cosmochimica Acta 58:3255–3263.

Hong, S., C. Barbante, C. Boutron, P. Gabrielli, V. Gaspari, P. Cescon, L. Thompson, C. Ferrari, B. Francou, and L. Maurice-Bourgoin. 2004. Atmospheric heavy metals in tropical South America during the past 22,000 years recorded in a high altitude ice core from Sajama, Bolivia. Journal of Environmental Monitoring 6:322–326.

King, E. K., A. Thompson, O. A. Chadwick, and J. C. Pett-Ridge. 2016. Molybdenum sources and isotopic composition during early stages of pedogenesis along a basaltic climate transect. Chemical Geology 445:54–67.

Koren, I., Y. J. Kaufman, R. Washington, M. C. Todd, Y. Rudich, J. V. Martins, and D. Rosenfeld. 2006. The Bodélé depression-a single spot in the Sahara that provides most of the mineral dust to the Amazon forest. Environmental Research Letters 1:1–5.

Lawrence, C. R., and J. C. Neff. 2009. The contemporary physical and chemical flux of aeolian dust: A synthesis of direct measurements of dust deposition.

Chemical Geology 267:46–63.

Ley, R. E., and C. M. D'Antonio. 1998. Exotic grass invasion alters potential rates of N fixation in Hawaiian woodlands. Oecologia 113:179–187.

Mahowald, N., T. D. Jickells, A. R. Baker, P. Artaxo, C. R. Benitez-Nelson, G. Bergametti, T. C. Bond, Y. Chen, D. D. Cohen, B. Herut, N. Kubilay, R. Losno, C. Luo, W. Maenhaut, K. A. McGee, G. S. Okin, R. L. Siefert, and S. Tsukuda. 2008. Global distribution of atmospheric phosphorus sources, concentrations and deposition rates, and anthropogenic impacts. Global Biogeochemical Cycles 22:1–19.

Mahowald, N., K. Kohfeld, M. Hansson, Y. Balkanski, S. P. Harrison, I. C. Prentice, M. Schulz, and H. Rodhe. 1999. Dust sources and deposition during the last glacial maximum and current climate: A comparison of model results with paleodata from ice cores and marine sediments. Journal of Geophysical Research 104: 15895-15916

Mahowald, N., C. Luo, and J. de Corral. 2003. Interannual variability in atmospheric mineral aerosols from a 22-year model simulation and observational data. Journal of Geophysical Research 108:4352.

Mahowald, N. M., A. R. Baker, G. Bergametti, N. Brooks, R. A. Duce, T. D. Jickells, N. Kubilay, J. M. Prospero, and I. Tegen. 2005. Atmospheric global dust cycle and iron inputs to the ocean. Global Biogeochemical Cycles 19: 4025.

Mahowald, N. M., J. F. Lamarque, X. X. Tie, and E. Wolff. 2006. Sea-salt aerosol response to climate change: Last Glacial Maximum, preindustrial, and doubled carbon dioxide climates. Journal of Geophysical Research: Atmospheres 111:1–11.

Marks, J. A., S. S. Perakis, E. K. King, and J. Pett-Ridge. 2015. Soil organic matter regulates molybdenum storage and mobility in forests. Biogeochemistry 125:167–183.

Mather, T. A., M. L. I. Witt, D. M. Pyle, B. M. Quayle, A. Aiuppa, E. Bagnato, R. S. Martin, K. W. W. Sims, M. Edmonds, A. J. Sutton, and E. Ilyinskaya. 2012. Halogens and trace metal emissions from the ongoing 2008 summit eruption of Kilauea volcano, Hawai'i. Geochimica et Cosmochimica Acta 83:292–323.

Matzek, V., and P. Vitousek. 2003. Nitrogen fixation in bryophytes, lichens, and decaying wood along a soil-age gradient in Hawaiian montane rain forest. Biotropica 35:12–19.

Nakagawa, Y., S. Takano, and M. Firdaus. 2012. The molybdenum isotopic composition of the modern ocean. Geochemical Journal 46:131–141.

Nriagu, J. 1989. A global assessment of natural sources of atmospheric trace metals.

Nature 338:47–49.

Okin, G. S., N. Mahowald, O. A. Chadwick, and P. Artaxo. 2004. Impact of desert dust on the biogeochemistry of phosphorus in terrestrial ecosystems. Global Biogeochemical Cycles 18.

Pearson, H. L., and P. M. Vitousek. 2002. Soil phosphorus fractions and symbiotic nitrogen fixation across a substrate-age gradient in Hawaii. Ecosystems 5:587–596.

Prospero, J. M., R. J. Charlson, V. Mohnen, R. Jaenicke, A. C. Delany, W. Zoller, and K. Rahn. 1983. The Atmospheric Aerosol System: An Overview. Reviews of Geophysics and Space Physics 21:1607–1629.

Quesada, C. A., J. Lloyd, L. O. Anderson, N. M. Fyllas, M. Schwarz, and C. I. Czimczik. 2011. Soils of Amazonia with particular reference to the RAINFOR sites. Biogeosciences 8:1415–1440.

Sansone, F., C. Benitez-Nelson, J. Resing, E. DeCarlo, S. Vink, J. Heath, and B. Huebert. 2002. Geochemistry of atmospheric aerosols generated from lava-seawater interations. Geophysical Research Letters 29.

Siebert, C., J. C. Pett-Ridge, S. Opfergelt, R. A. Guicharnaud, A. N. Halliday, and K. W. Burton. 2015. Molybdenum isotope fractionation in soils: Influence of redox conditions, organic matter, and atmospheric inputs. Geochimica et Cosmochimica Acta 162:1–24.

Smedley, P. L., and D. G. Kinniburgh. 2017. Molybdenum in natural waters: A review of occurrence, distributions and controls. Applied Geochemistry 84:387–432.

Spiro, P. A., D. J. Jacob, and J. A. Logan. 1992. Global inventory of sulfur emissions with 1° × 1° resolution. Journal of Geophysical Research 97:6023–6036.

Stallard, R. F., and J. M. Edmond. 1981. Geochemistry of the Amazon: 1. Precipitation chemistry and the marine contribution to the dissolved load at the time of peak discharge. Journal of Geophysical Research 86:9844–9858.

Swap, R., M. Garstang, S. Greco, R. Talbot, and P. Kållberg. 1992. Saharan dust in the Amazon Basin. Tellus B 44B:133–149.

Taylor, S. R., and S. M. McLennan. 1995. The geochemical evolution of the continental crust. Reviews of Geophysics 33: 241-256.

Tegen, I., and K. Schepanski. 2009. The global distribution of mineral dust. IOP Conference Series: Earth and Environmental Science 7:012001.

Tuit, C. 2003. The marine biogeochemistry of molybdenum, Massachussets Institute of Technology and Woods Hole Oceanographic Institution. PhD thesis.

Vitousek, P. M., and L. R. Walker. 1989. Biological invasion by Myrica Faya in Hawai'i: Plant demography, nitrogen fixation, ecosystem effects. Ecological Monographs 59:247–265.

Wang, Y.-P., and B. Houlton. 2009. Nitrogen constraints on terrestrial carbon uptake: implications for the global carbon-climate feedback. Geophysical Research Letters 36:1-5.

Yu, H., M. Chin, T. Yuan, H. Bian, L. A. Remer, J. M. Prospero, A. Omar, D. Winker, Y. Yang, Y. Zhang, Z. Zhang, and C. Zhao. 2015. The fertilizing role of African dust in the Amazon rainforest: A first multiyear assessment based on data from Cloud-Aerosol Lidar and Infrared Pathfinder Satellite Observations. Geophysical Research Letters:1–8.

Zender, C., R. Miller, and I. Tegen. 2004. Quantifying Mineral Dust Mass Budgets: Terminology, Constraints, and Current Estimates. Eos 85:509–512.

CHAPTER 3 . MOLYBDENUM, PHOSPHORUS, AND PH EFFECTS ON FREE-LIVING NITROGEN FIXATION IN A TROPICAL FOREST IN THE SOUTHEASTERN AMAZON

Authors

Wong, Michelle Y.[1*], Christopher Neill[2], Roxanne Marino[1], Paulo M. Brando[2,3], Divino Silvéiro, Robert W. Howarth[1,2].

[1]Department of Ecology and Evolutionary Biology, Cornell University, Ithaca, NY 14853, U.S.A.
[2]Woods Hole Research Center, Falmouth, MA 02450, U.S.A.
[3]Instituto de Pesquisa Ambiental da Amazônia, Brasília-DF, Brazil

3.1. Summary

High rates of biological nitrogen fixation (BNF) are commonly reported for tropical forests, but most studies have been conducted in regions that receive substantial inputs of Mo from atmospheric dust and sea-salt aerosols. Even in these regions, the low availability of molybdenum (Mo) can constrain free-living BNF. We hypothesized that in regions where atmospheric inputs of Mo are low and soils are highly weathered, such as the southeastern Amazon, Mo would constrain BNF. We also hypothesized that the high soil acidity, characteristic of the Amazon Basin, would further constrain Mo availability and therefore BNF. We conducted two field experiments across the wet and dry seasons, adding Mo, phosphorus (P), and lime alone and in combination to the forest floor in the southeastern Amazon. We sampled soils and litter immediately, and then weeks and months after the applications, measuring Mo and P availability through resin extractions and measuring BNF by the acetylene reduction assay. The experimental additions of Mo and P increased their availability and the lime increased soil pH. BNF rates varied widely as a function of

precipitation. While the combination of Mo and P increased BNF at some time points, BNF did not increase rates strongly or consistently across the study as a whole, suggesting that Mo, P, and soil pH are not the dominant controls over BNF at this site. Instead, we postulate that high nitrogen (N) availability, revealed by stoichiometry relative to other tropical forests, may suppress BNF at this site. These patterns may also extend across many oxisols in topographically stable regions of the tropics.

3.2. Introduction

Tropical forests are highly productive ecosystems, where the greatest rates of terrestrial biological nitrogen fixation (BNF) rates have been measured and modeled (Cleveland et al. 1999, Wang and Houlton 2009). BNF is the main source of N input to tropical forests, and is mediated either by free-living bacteria and archaea that reside in litter or soil, or by bacteria in symbiotic associations with specific tree species. Even in the tropics, where there are abundant leguminous N-fixing plants in the *Fabaceae* family, free-living BNF can often be more dominant than symbiotic BNF (e.g. Nardoto *et al.*, 2014; Taylor *et al.*, 2019). Molybdenum (Mo), a co-factor in the nitrogenase enzyme, and phosphorus (P), required for the BNF process, often limit free-living BNF in many well-studied tropical forests (such as those in Central America or Hawaii (Crews et al. 2000, Barron et al. 2009, Wurzburger et al. 2012, Winbourne et al. 2017)). However, less is known about the occurrence of Mo and P limitation in tropical forests further from major sources of atmospheric input of Mo (Chapter 2; Dynarski and Houlton 2018). In the tropics, higher temperatures and precipitation facilitate more chemical and physical weathering (Stallard 1988, Porder and Hilley 2011), leading to lower rock-derived nutrient availability. Tropical forests

situated on older parent material, with maximum geological ages ranging between 1500 to 3600 million years (Quesada et al. 2011) are characteristic of many tropical regions such as central Africa and much of the Amazon Basin. These regions are likely characterized by even lower P (Sanchez 1977, Vitousek et al. 2010) and Mo availability.

Phosphorus and Mo limitation to both symbiotic and free-living BNF has been observed across multiple tropical forests (e.g. Vitousek and Hobbie 2000, Barron et al. 2009, Wurzburger et al. 2012, Winbourne et al. 2017), as well as temperate and boreal forest biomes (e.g. Silvester 1989, Jean et al. 2013, Rousk et al. 2016, Pérez et al. 2017). Phosphorus is the element that is found to most frequently limit tropical BNF (Reed et al. 2011), with BNF often increasing when P supply is high. This can happen for one of two reasons: (1) most tropical forest ecosystems are limited by P supply, with the supply of N adjusting to P; when P is added, the system shifts to N limitation to be more favorable for BNF; or (2) N fixers systematically require more P than non-fixers for cell growth (Vitousek and Howarth 1991, Crews 1993, Vitousek et al. 2002b, Benner and Vitousek 2007). Molybdenum is the most common and most efficient co-factor for the nitrogenase enzyme (Eady 1996). However, teasing apart Mo and P limitation based upon previous research is complicated because in many P addition experiments, Mo may have been present as a contaminant in the fertilizer (Charter et al. 1995, Barron et al. 2009). Thus, Mo limitation of BNF could be more prevalent than previously thought.

While high rates of BNF are commonly reported for tropical forests (Cleveland et al. 1999, Sullivan et al. 2014), most studies have been conducted in regions that

receive substantial inputs of molybdenum (Mo) from atmospheric dust and sea salt (Chapter 2), and P from dust. Even in regions that receive relatively high atmospheric inputs of Mo, the low availability of Mo may still constrain free-living BNF. We hypothesized that in regions such as the southeastern Amazon where atmospheric inputs of Mo are low and soils are highly weathered, Mo may be especially limiting to BNF. Molybdenum is already rare in soils, with an average crustal abundance of 1-2 $\mu g\ g^{-1}$ (Taylor and McLennan 1995). Moreover, because lower soil pH ($pH < 5$) affects the chemical speciation of Mo (Anbar 2004), increases adsorption of Mo to soils (Reddy et al. 1997), and likely reduces biological uptake (Wanner and Soppa 1999, Zahalak et al. 2004, Tomatsu et al. 2007), Mo limitation is likely even more prevalent in the acidic soils of the Amazon Basin that range from pH 4.17 to 4.94 (Negreios and Nepstad 1994, Laurance et al. 1999). Phosphorus behaves similarly in acidic soils, and to combat this, agricultural liming is often used in the tropics to increase to P availability to plants (Haynes 1982). The same prevalence of soil acidity is likely true in forests, where the low pH effects on Mo and P further exacerbate the already low soil concentrations.

The southeastern Amazon is a region where Mo and P limitation might be pronounced, because soils are developed from old, stable surfaces with little to no parent material contribution (Quesada et al. 2011), and atmospheric inputs are low (Mahowald *et al.*, 2008, Chapter 2). Currently, five studies have assessed the simultaneous effects of Mo and P on free-living BNF rates in the tropics. These studies were located in Hawaii, Panama, Costa Rica, and Belize (Vitousek and Hobbie 2000, Barron et al. 2009, Wurzburger et al. 2012, Reed et al. 2013, Winbourne et al.

2017), all of which receive higher weathering and atmospheric inputs, particularly from sea-salt aerosols (Chapter 2). In addition, these five studies have either been short-term experiments, or longer-term studies with Mo added as a nutrient "cocktail" where responses to Mo alone have not been examined (Vitousek and Hobbie 2000, Barron et al. 2009). In contrast, we know less about controls on free-living BNF across the Amazon, the world's largest tropical forest facing transitions in deforestation and recovery (Aguiar et al. 2016), which may drive the need for BNF in forest recovery (Batterman et al. 2013).

In this study, we tested the hypothesis that absolute Mo and P availability, or low effective availability as a function of low soil pH, limit free-living BNF across old, highly weathered tropical soils receiving minimal atmospheric inputs. We conducted a multi-factorial Mo, P and lime addition experiment in a dominantly evergreen forest in the southeastern Amazon, and measured BNF responses across days, weeks, and months across both the wet and dry seasons.

3.3. Methods

3.3.1. Site description

The study was conducted at Fazenda Tanguro, an 800 km^2 working farm in eastern Mato Grosso State, Brazil (13°04' S, 52°23' W). Forest tree species composition in this predominantly evergreen forest represents a transition between the central Amazon forest and the more seasonal Cerrado, which lies 30 km south of the study site (Ivanauskas et al. 2003). The soils in this region are classified as red-yellow alic dystrophic latosols (Brazilian soil classification), relatively infertile sandy ferralsols (FAO classification), or oxisols (Haplustox; USDA classification), and are

among the oldest in Amazonia (Quesada et al. 2011), with Tertiary and Quaternary fluvial deposits over Precambrian gneisses of the Xingu Complex (Projeto Radambrasil 1981). Further site characteristics are described in Chapter 4.

3.3.2. Fertilization experiment and sample collection

In the dry season beginning in October 2016 and the wet season beginning in February 2017, we conducted two separate fertilization experiments to test Mo, P, and pH controls on free-living BNF. Five plots per treatment received either no addition (control), Mo (as $Na_2MoO_4 \cdot 2H_2O$), P ($Na_3PO_4 \cdot 12H_2O$), Mo and P together, lime ($9CaCO_3 \bullet 1MgCO_3$), or lime with Mo and P, for a total of 30 plots. Prior to the experiment, we dissolved the P and lime in nitric acid (HNO_3) and quantified Mo contamination in the P additions, and both Mo and P contamination in the lime additions using the analytical methods described below, because Mo has been found in phosphate fertilizers at 2.4-18.5 μg^{-1} Mo g^{-1} fertilizer (Charter et al. 1995). The lime contained no quantifiable Mo or P (< 33.4 ng Mo g^{-1} and < 1.3 µg P g^{-1}) and the $Na_3PO_4 \cdot 12H_2O$ added had an average concentration of 52.1 ng Mo g^{-1}, which are much lower than for standard fertilizers.

In the dry season, plots (2 x 2 m) were set up in a randomized block design 2 m apart, unless physically obstructed by a large standing or fallen tree, with each block separated by 50 m distance (Appendix C Supplementary Figure 1). For the lime treatments, the litter layer was removed by hand, and lime was sprinkled by hand at a rate of about 1.2 kg lime per plot to raise the pH of the soil to about pH 5. Litter was returned back on the forest floor. The Mo, P, and Mo plus P treatments were added by hand-broadcast sprayer with 1.5 L of distilled water over the leaf litter layer, and

separate sprayers were used for Mo and P to avoid cross-contamination. Control and lime-only treatments received only distilled water on the leaf litter layer. The same fertilization experiment was repeated in the following wet season on a separate set of plots in a randomized block design for a total of 60 plots (Appendix B Supplementary Figure 1).

We determined background soil Mo and P concentrations from a nearby forest (Chapter 4) and added Mo with a target to double the concentration in the top 10 cm of surface soil and P to raise soil concentrations by 10 percent; this is equivalent to a Mo addition rate of 348 g Mo ha^{-1} and a P addition rate of 18.1 kg P ha^{-1}. To compare our addition rates on a mass basis to prior short-term lab experiments, we assume that the additions were contained in the top 10 cm of soil with a bulk density of 1.09 g cm^{-2} (Riskin et al. 2013) and in the litter layer with an average of 8000 kg litter ha^{-1} (Chapter 4). The addition rates would then be equivalent to 317 µg Mo kg^{-1} sample and 16.5 mg P kg^{-1} sample in our study. Thus these Mo and P addition rates were mostly in between the low and high range added by other bottle addition studies (Table 3.1).

Table 3.1. Addition rates of other studies testing Mo and P limitation on BNF.

Forest type	Site	Study	Reference	Addition rate by area	Addition rate by mass
Tropical Forest	Costa Rica	Incubation	Reed et al. 2013		297 µg Mo kg^{-1}
	Panama	Field, Incubation	Barron et al. 2009	10 g Mo ha^{-1}, 50 kg P ha^{-1}	42 to 504 µg Mo kg^{-1}, 2.8 to 283 mg P kg^{-1}
	Panama	Incubation	Wurzburger et al. 2012		667 µg Mo kg^{-1}, 283 mg P kg^{-1}
	Belize	Incubation	Winbourne et al. 2017		667 µg Mo kg^{-1}, 283 mg P kg^{-1}
	southeastern Amazon	Field	This study	348 g Mo ha^{-1}, 18.1 kg P ha^{-1}	317 µg Mo kg^{-1}, 16.5 mg P kg^{-1}
Temperate forest	Chile	Incubation	Pérez et al. 2017		2000 µg Mo kg^{-1}, 1000 mg P kg^{-1}
	Oregon, USA	Incubation	Perakis et al. 2017		80 µg Mo kg^{-1}, 800 mg P kg^{-1}
	Pacific Northwest, USA	Incubation	Silvester et al. 1989		250 µg Mo kg^{-1}
	Canada	Incubation	Jean et al. 2013		144 µg Mo kg^{-1}, 4.8 mg P kg^{-1}
Boreal forest	Sweden	Field	Rousk et al. 2016	7 to 70 g Mo ha^{-1}, 40 to 400 kg P ha^{-1}	

For the October dry season addition experiment, we collected separate soil and litter samples two days prior to treatment applications, and one day, 11 days, or four months after treatment. For the February wet season additions, we collected soil and litter samples one week before and one day, one week, four weeks, and 11 months after treatment. For each sampling, we weighed soils on the day of collection and incubated them overnight using the acetylene reduction assay (described below), and weighed litter the next morning and incubated the litter across the following day. In each plot, we composited three individual soil cores (0-2 cm) for each replicate within the plot. We collected a total of three replicates per plot, or 90 soil incubations per time point. The litter was collected by hand, with two replicates per plot for a total of 60 litter incubations per time point, except for the last sampling day where there were 90 litter incubations.

3.3.3. Short-term lab addition experiment

To aid comparison with previous short-term studies, we conducted a separate lab experiment with ten replicates of soil and litter each for the following treatments: control, lime (~0.2 g), Mo, double (2x) Mo, P, Mo+P, Mo+P+lime for a total of 70 incubations, at the same estimated mass-basis rates as the field experiment described above. After additions, we incubated samples for 12 hours before ARA incubations were initiated, the time expected for microbes to respond to Mo based upon previous studies (Bellenger et al. 2011). Treatments were added in 5 mL solutions (control: distilled water; Mo: 0.83 µg Mo mL^{-1}; high Mo: 1.65 µg Mo mL^{-1}; P: 80.3 µg P mL^{-1}) to about 15 grams of litter or 25 grams of fresh surface soil as Mo ($Na_2MoO_4 \cdot 2H_2O$) and P (trace metal grade NaH_2PO_4). The NaH_2PO_4 added had an average concentration of 80.7 ng Mo g^{-1}.

3.3.4. Free-living BNF by acetylene reduction

We measured free-living BNF in soil and litter using the acetylene reduction assay (ARA) method (Hardy et al. 1968, Barron et al. 2009). For each incubation, we added about 15 grams of litter or 25 grams of fresh surface soil to 125 mL gas tight jars with lids fitted with septa (Fisher Scientific 501215190), sealed these, and added a 10% atmosphere of acetylene generated from calcium carbide. We incubated litter samples for 8-10 hours and soil samples for 14-18 hours at ambient temperature in an open-air greenhouse environment.

After incubations, we collected 30 mL headspace into pre-evacuated gas tight vials (Teledyne Tekmar 22mL) fitted with thick butyl septa (Geo-Microbial Technologies, Inc.). After the ARA was terminated, we weighed litter and soil before

and after drying for two days at 65°C or 105°C, respectively. We measured the ethylene concentrations from the field-collected samples at Cornell University using a Shimadzu 8-A gas chromatograph equipped with a flame ionization detector (330°C) and a Porapak-N 80/100 column at 70°C with two standard curves and check standards every ten samples. For the short-term laboratory experiment, we analyzed samples at Brown University using a Shimadzu GC-2014 gas chromatograph equipped with a flame ionization detector (330°C) and a Poropak-T column at 80°C. To measure background ethylene production from litter without exposure to acetylene, we incubated six additional litter samples per sampling. Acetylene blanks were made following the same methods as discussed in Chapter 4. Ethylene production rates from litter averaged 17% of the total ethylene concentrations, but varied widely, with a relative standard deviation of 107%. Ethylene production from soil without exposure to acetylene was insignificant. Ethylene blanks averaged 12% of the ethylene production in litter incubations but 50% in soil incubations, due to the low rates measured.

We measured the soil pH using a 1:2 soil (field moisture) to distilled water ratio by weight, stirred and equilibrated for 30 minutes with a pH meter standardized at pH 7 and 4 daily using single junction, epoxy body, sealed electrode (Cole-Parmer).

3.3.5. Resin-extractable and total soil Mo and P

To confirm the addition of fertilizers and track their fate, we collected soil samples from nine randomized locations within the plots. Soil from 0-2 cm depth was collected into a bag, shaken, dried, and subsampled. Because our export permit

precluded us from exporting litter samples, we were unable to analyze leaf litter for Mo or P.

We extracted available Mo and P from soils using anion-exchange beads following the same procedures as Wurzburger *et al.* (2012) for mineral soils. We conducted extractions with a bead:soil:water ratio of 1:5:50 where the beads (Dowex 1x4-200) were loaded into acid-washed tubing capped at both ends with Nitex bolting cloth (243 µm) held by plastic clamps to expose the beads to the solution in 50 mL vials. The soil solution was shaken for 16 hrs at 80 rpm, and we rinsed the resins with DI to remove excess soil particles, eluted the resins with 10% HNO_3 on the shaker for another hour in a separate 50 mL vial, and then filtered the final solution. Procedural blanks and spiked check standards in DI were also run with each set.

To measure total soil Mo and P, samples were ground in an alumina ceramic ring and puck shatterbox, oven-dried at 105°C, ashed at 550°C for four hours, and digested in concentrated nitric acid (HNO_3) using the 3052 EPA microwave-assisted acid digestion of siliceous and organically based matrices. The digests were centrifuged, filtered, and diluted. A procedural blank and a certified natural sample were digested and run in parallel with each set of microwave digestions: SCO-1, USGS Geochemical Reference Standard, Cody Shale.

Resin Mo, total Mo, and resin P concentrations were measured on an Elan DRC-e quadrople Inductively Coupled Plasma Mass Spectrometer at the State University of New York College of Environmental Science and Forestry (SUNY ESF), and total P concentrations were measured on a Perkin Elmer Optima 3300DV Inductively Coupled Plasma-Optical Emission Spectrometry (ICP-OES).

Concentrations of Mo and P in procedural blanks were subtracted from final sample concentrations, and accounted for less than 7% of the Mo and 15% of the P concentrations in the resin samples, and less than 1% of the Mo and P concentrations in the nitric acid digestions.

3.3.6. Statistical analyses

For the field experiments, we used linear mixed-effects model (LMM) to examine the ln-transformed rate (ln(+0.0001) for soils and ln(+0.001) for litter) with random effects for the block and plot with interactions with the time point. The time point and treatment were treated as factors in the LMM. Analyses were conducted for each substrate (litter and soil) for each set of plots (additions in October, additions in February). Substrates were analyzed separately because the ARA rates found within the litter layer and the soil differed by an order of magnitude or more. For analysis, we dropped one control plot due to continuously high rates from an ant waste mound located on the plot (Pinto-Tomás et al. 2009). We also followed the approach of (Rousk et al. 2016, Perakis et al. 2017) and analyzed the effects of Mo, P, and lime on ARA rates as response ratios (nutrient additions relative to the average of the control treatment) in the Supplementary Information (Appendix B). If values found in the control plot were zero, then the rate was estimated as half the lowest rate found within the group. The relationship between ARA rates and sample moisture content was tested using linear regression analysis with ln-transformed rate (ln(+0.0001) for soils and ln(+0.001) for litter), while the relationship between season and ARA rates were tested with a Wilcoxon rank sum test. In the lab experiments, we used a one-way ANOVA with the treatment as the factor with an ln-transformed rate. For total soil Mo

and P and resin Mo and P, we used a LMM with random effects for the block with the treatment as a factor. Multiple comparisons within the LMM were analyzed using a Tukey post-hoc test, both between treatments and grouped treatments (P, Mo and P, and Mo and P with lime, for example). Residuals were visually inspected by examining the QQ plots to see whether the distribution was relatively normal, and heteroscedasticity was investigated. Statistical analyses were performed using R software v.3.0.3 (R Development Core Team).

3.4. Results

3.4.1. Study site chemistry

In the control plots, surface soil (0-2 cm) total Mo concentrations averaged 89 ± 9.7 ng g^{-1} and P concentrations averaged 84 ± 9.6 µg g^{-1} for all time points (Figure 3.1, Appendix B Supplementary Table 1). The resin-extractable Mo averaged 1.3 ng g^{-1}, while the resin-extractable P averaged 0.97 µg g^{-1} in the control plots for all time points. The soil pH averaged 4.2 ± 0.02 (Table 3.2).

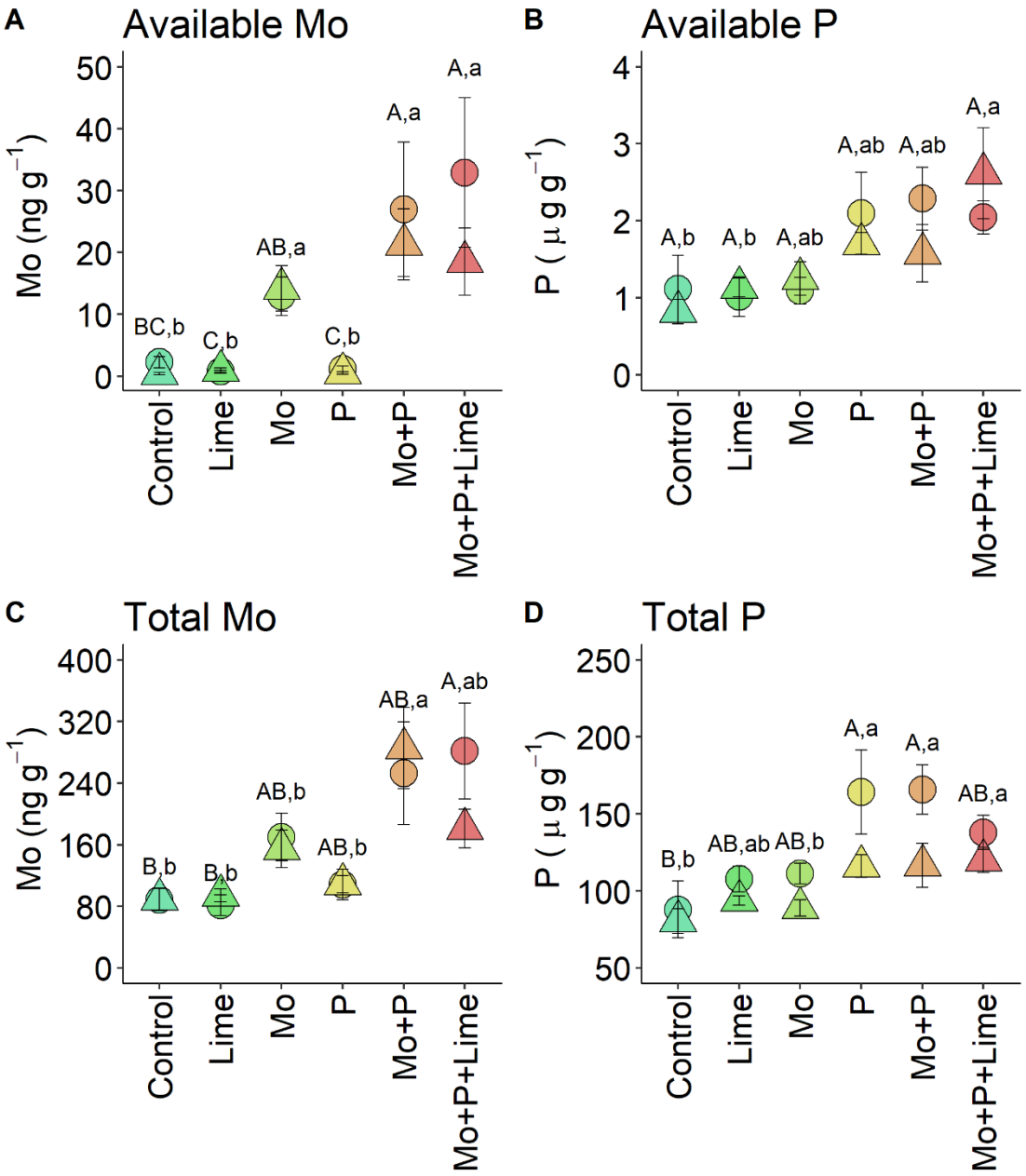

Figure 3.1. Field-based resin-extractable available molybdenum (Mo) (A), phosphorus (P) (B), and total Mo (C), and P (D) one day and one month after applications in the wet season (February additions) in the southeastern Amazon. The circles (●) represent the means one day after and the triangles (▲) represent the means one month after applications. The error bars represent ± standard error. Capital letters signify statistically significant differences between treatments one day after applications, and lower-case letters signify differences one month after ($p < 0.05$) (Tukey post-hoc test).

Table 3.2. Surface soil (0-2 cm) pH of soils before and after liming across the wet and dry seasons in field fertilization experiments in the southeastern Amazon. Data are means ± 1 standard error. Letters signify statistically significant differences ($p < 0.05$) (Tukey post-hoc test).

	October Application				February Application				
	Dry Season			Wet season					
	Pre-addition	1 Day	10 Days	3 Months	Pre-addition	1 Day	1 Week	1 Month	11 Months
Control	4.01 (0.05)^{a}	4.16 (0.05)^{a}	3.97 (0.06)^{b}	4.46 (0.04)^{ab}	4.23 (0.02)^{a}	4.24 (0.04)^{b}	4.12 (0.06)^{c}	3.95 (0.03)^{b}	4.15 (0.03)^{b}
Lime	3.95 (0.07)^{a}	4.31 (0.18)^{a}	5.19 (0.20)^{a}	4.99 (0.15)^{ab}	4.20 (0.05)^{a}	5.34 (0.14)^{a}	5.11 (0.16)^{a}	5.25 (0.22)^{a}	5.38 (0.15)^{a}
Mo	3.82 (0.05)^{a}	4.02 (0.08)^{a}	3.85 (0.06)^{b}	4.37 (0.03)^{b}	4.23 (0.03)^{a}	4.21 (0.05)^{b}	4.25 (0.05)^{c}	4.01 (0.04)^{b}	4.34 (0.14)^{b}
P	3.99 (0.08)^{a}	4.57 (0.17)^{a}	4.44 (0.12)^{b}	4.68 (0.06)^{ab}	4.16 (0.04)^{a}	4.40 (0.05)^{b}	4.38 (0.05)^{bc}	4.01 (0.03)^{b}	4.19 (0.02)^{b}
Mo + P	4.04 (0.09)^{a}	4.44 (0.11)^{a}	4.21 (0.12)^{b}	4.54 (0.05)^{ab}	4.14 (0.05)^{a}	4.46 (0.07)^{b}	4.38 (0.04)^{bc}	4.09 (0.06)^{b}	4.19 (0.02)^{b}
Mo + P + lime	4.00 (0.10)^{a}	4.38 (0.16)^{a}	5.25 (0.22)^{a}	5.04 (0.12)^{a}	4.17 (0.03)^{a}	5.10 (0.11)^{a}	4.96 (0.10)^{ab}	5.00 (0.15)^{a}	5.04 (0.09)^{a}

The treatments increased soil pH, total Mo and P, and resin-extractable "available" Mo and P both one week and one month after applications during the wet season. One day after applications, the P additions increased resin-extractable P concentrations two-fold ($p = 0.0001$) and total P concentrations two-fold ($p = 0.0004$), and the Mo additions increased resin-extractable Mo 11-fold ($p = 0.0004$), and total Mo concentrations three-fold ($p = 0.0002$). Despite precipitation during the wet season, we observed treatment effects in the surface soils one month after applications. One month after applications, the P additions increased resin-extractable P concentrations two-fold ($p = 0.0032$) and total P concentrations by half ($p < 0.0001$), and the Mo additions increased resin-extractable Mo 46-fold ($p < 0.0001$) and total Mo concentrations two-fold ($p = 0.0002$) (Figure 1). The lime additions increased the soil pH (Table 1) across all time points, on average, to 5.02 ± 0.05 ($p < 0.0001$). Available Mo and P typically represented 0.5 to 2.5% of total Mo and P in the control

plots. The Mo additions increased resin-extractable Mo relatively more than P additions increased resin-extractable P.

3.4.2. Dry and wet season free-living BNF in the field experiment

In the long-term field experiment, additions of lime, Mo, and P alone and in combination did not strongly or consistently increase free-living BNF in the litter layer or the soil. The only exceptions were increased BNF one day after applications in the surface soil in the dry season in response to Mo and P, three months after dry season applications in the litter layer in response to Mo and P in combination with lime, and one month after applications in the wet season in the surface soil in reponse to Mo and P in combination with lime (Figures 3.2, 3.3).

Before the applications in the dry season, mean free-living BNF rates were similar across plots. One day after the applications in the dry season, on average, Mo and P increased BNF rates in the soil by 17-fold ($p = 0.049$), driven by one sample where rates were 0.59 nmol C_2H_4 g^{-1} hr^{-1}; similarly, Mo and P in combination with lime increased BNF rates on this date by four-fold, although the high variation precluded a statistically-significant response ($p = 0.15$). In the dry season no effects were seen in the surface soil ten days after additions ($p > 0.97$ for all treatments), although there was one hotspot in the P addition, where BNF rates were 0.67 nmol C_2H_4 g^{-1} hr^{-1}. Three months after applications, which was at the onset of the wet season, the additions also had no significant effect on BNF in the surface soil ($p > 0.58$ for all treatments) (Figure 3.2, Appendix B Supplementary Table 2).

In the litter layer, one day and eleven days after applications in the dry season, the additions had no effect on BNF rates ($p > 0.99$ for all treatments). Three months

after dry season applications, P increased BNF in the litter layer by four-fold (p = 0.16), and Mo and P in combination with lime increased BNF rates four-fold (p = 0.11), but the high variation precluded detection of a statistically-significant response (Figure 3.2, Appendix B Supplementary Table 3).

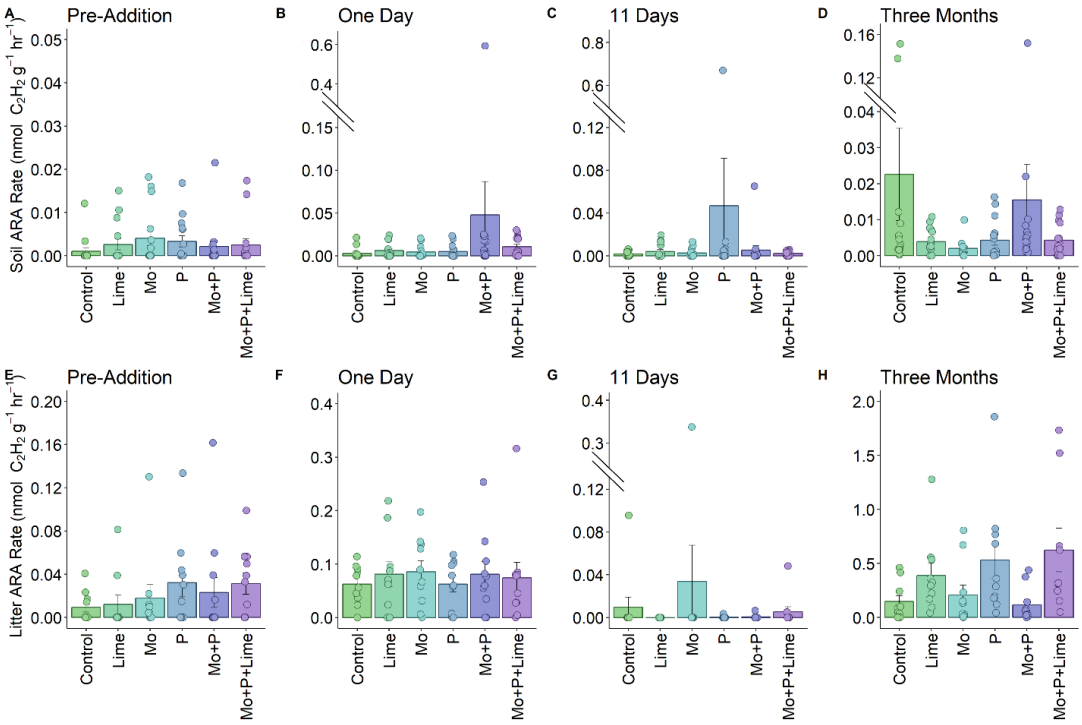

Figure 3.2. Field-based free-living BNF by acetylene reduction (nmol C_2H_4 g^{-1} hr^{-1}) in surface soils in response to fertilizations before applications (A), one day after (B), eleven days after (C), and four months after (D) applications, and free-living BNF in the litter layer before applications (E), one day after (F), eleven days after (G), and four months after (H) applications that began during the dry season in October in the southeastern Amazon. The boxes represent the mean and the error bars represent ± standard error.

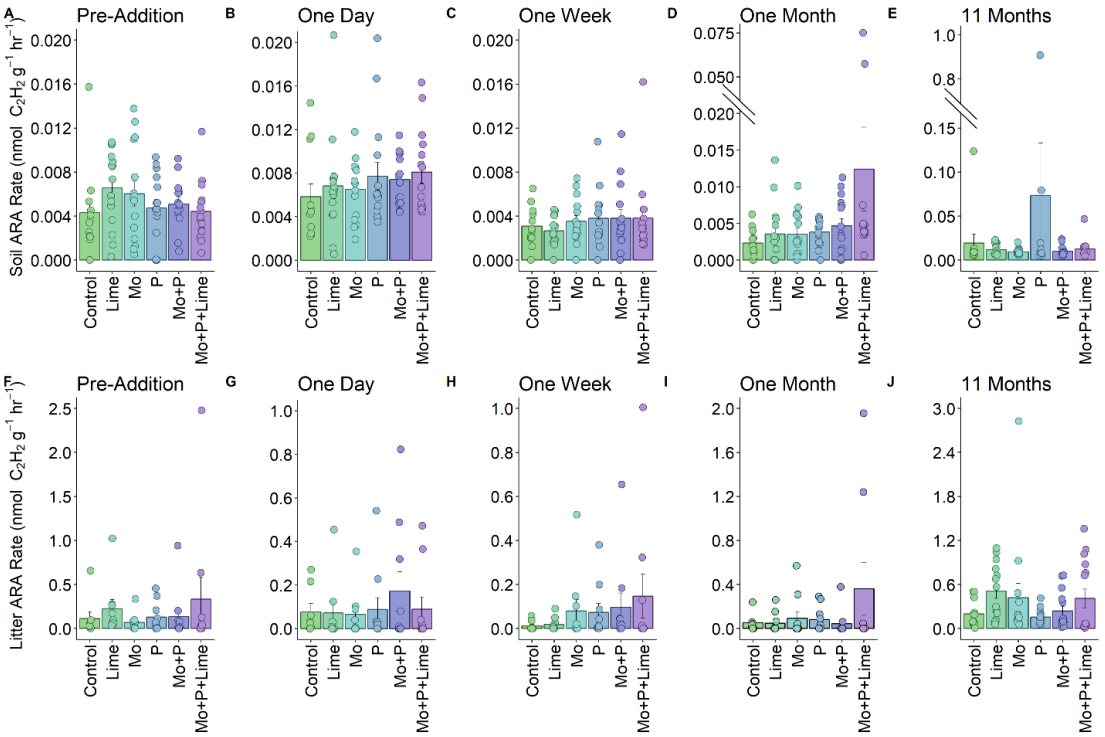

Figure 3.3. Field-based free-living BNF rates by acetylene reduction (nmol C_2H_4 g^{-1} hr^{-1}) in surface soils in response to fertilization before applications (A), one day after (B), one week after (C), one month after (D), and eleven months after (E) applications, and free-living BNF rates found in the litter layer before additions (F), one day after (G), one week after (H), one month after (I), and eleven months after (J) applications that began in the wet season in February in the southeastern Amazon. The boxes represent the mean and the error bars represent ± standard error.

Before the applications in the wet season, mean free-living BNF rates in the surface soil were similar across plots. One day and one week after applications during the wet season, there were no effects of the treatments on BNF in the soil ($p > 0.93$ for all treatments). One month after applications in the wet season, Mo and P in combination with lime increased BNF rates in the soil by five-fold ($p = 0.045$), driven by two hotspots of 0.057 and 0.075 nmol C_2H_4 g^{-1} hr^{-1}. There were no effects again eleven months after applications ($p > 0.97$ for all treatments) (Figure 3.3, Appendix B Supplementary Table 2). One day, one week, one month, and eleven months after

applications in the wet season, the treatments had no effect in the litter layer ($p > 0.90$, $p > 0.65$, $p > 0.92$, $p = 1.0$ for all treatments, respectively) (Figure 3.3, Appendix B Supplementary Table 3).

Many of these patterns were not statistically significant despite the apparent increase in mean BNF rates in response to additions because they were driven by single samples of high value, or hotspots (Appendix B Supplementary Information). When we calculated differences based on response ratios, similar results were found where most additions did not significantly increase BNF. The variation among the individual plots (2 x 2 m) and the individual blocks in the block design experiment (50 m) were relatively similar (Appendix B Supplementary Table 4), which illustrates the high amount of variation associated with BNF in the field, irrespective of spatial proximity.

3.4.3. Short-term lab experiment

In the bottle addition experiment, the lime and 2x Mo treatments slightly increased BNF rates in soil, although most of these differences were not statistically significant (Figure 3.4). In the litter layer, the additions had no significant effect ($p > 0.63$ for all treatments). In the surface soil, lime increased BNF rates by 1.8 fold ($p = 0.095$), Mo increased BNF rates by a third ($p = 0.82$) and 2x Mo increased BNF rates by two-fold ($p = 0.21$); however, the high variation precluded the detection of significant differences. The 2x Mo and lime treatments were significantly higher than the Mo and P in the combination lime treatments ($p = 0.025$, $p = 0.0088$, respectively).

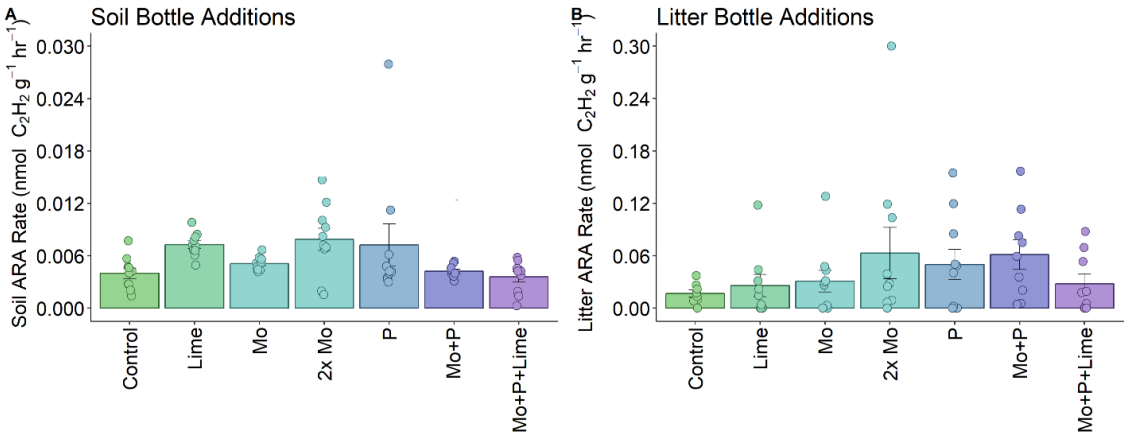

Figure 3.4. Free-living BNF by acetylene reduction in a lab-based addition experiment (nmol C_2H_4 g^{-1} hr^{-1}) in surface soil (A) and the litter layer (B) (n = 10). The control represents distilled water added alone.

3.4.4. Seasonal patterns in BNF

Across the fertilizations, BNF rates in the litter layer and surface soil varied greatly, depending on the seasonality and often were higher if there was recent precipitation (Figure 3.5). BNF rates in the litter layer and soil were both affected by seasonality (wet vs. dry season), and moisture. In the litter layer and surface soil, there were significant relationships between the seasonality (wet vs. dry) ($p < 0.0001$, Wilcoxon rank sum test) and moisture with BNF rates (litter, $F_{1,434} = 48.13$, ANOVA, $p < 0.0001$, $R^2 = 0.10$) (soil, $F_{1,613} = 43.8$, ANOVA, $p < 0.0001$, $R^2 = 0.067$).

Mean free-living BNF rates in the soil and litter closely followed precipitation patterns, measured from rain gauges at Tanguro (Figure 3.5). For example, before the applications in the dry season, mean free-living BNF rates in the control plots were relatively low, averaging 0.001 nmol C_2H_4 g^{-1} hr^{-1} in the soil and 0.010 nmol C_2H_4 g^{-1} hr^{-1} in the litter (Figure 3.5) after no precipitation fell for the five days prior. However, after the applications, mean free-living BNF rates in the control plots increased to

0.003 nmol C_2H_4 g^{-1} hr^{-1} in the soil and 0.063 nmol C_2H_4 g^{-1} hr^{-1} in the litter, when 16 mm of precipitation fell the day before (Figure 3.5).

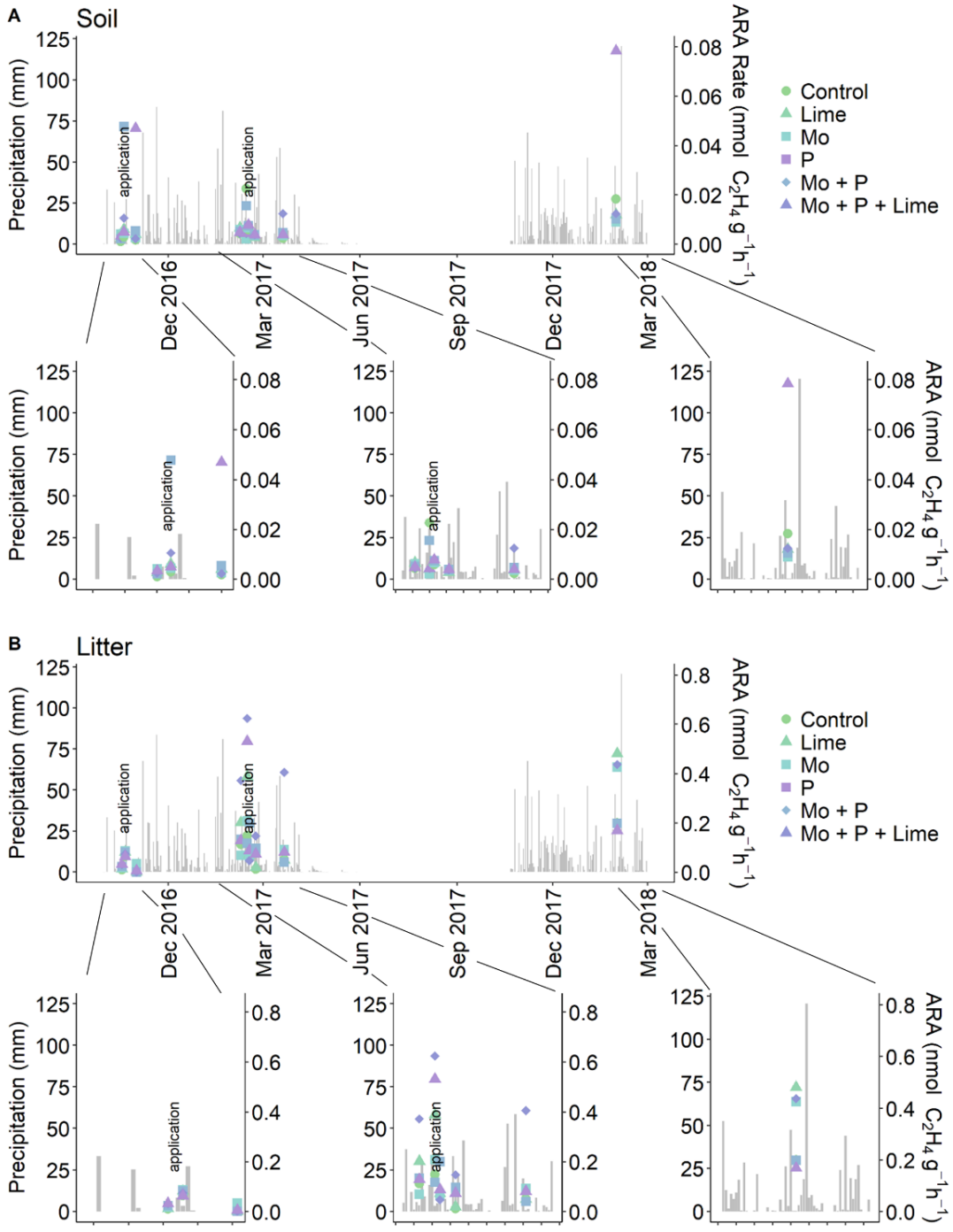

Figure 3.5. Temporal pattern in precipitation (grey bars) and mean field-based free-living BNF acetylene reduction rates (nmol C_2H_4 g^{-1} hr^{-1}) (points) in the surface soil (A) and in the litter layer (B) in response to fertilizations between October 2016 and March 2018 in the southeastern Amazon. Application dates are indicated on the figure.

3.5. Discussion

3.5.1. Low concentrations of Mo and P in the southeastern Amazon

As we hypothesized from the high degree of weathering and low atmospheric inputs, Mo and P concentrations in soils were low at this dry tropical forest site in southeastern Amazon compared with other regions of the tropics. Total Mo (89 ± 9.7 ng g^{-1}) and P (84 ± 9.6 µg g^{-1}) concentrations are at the low end of the range reported for other tropical forest sites where BNF limitation by soil Mo and P had been found, such as Costa Rica and Belize. In Costa Rica, for example, surface soil Mo and P concentrations exceed those measured here by around an order of magnitude, while this number varies between two-fold and 30-fold for Belize and Panama (Barron et al. 2009, Wurzburger et al. 2012, Reed et al. 2013, Winbourne et al. 2017) (Table 3.3).

Table 3.3. Soil and litter Mo and P concentrations and their respective quantification methods in unmanaged tropical and temperate forests.

Forest type	Site	Substrate	Reference	P method	Mo method	P (ug g^{-1})	Mo (ug g^{-1})
Tropical forest	Costa Rica	Litter	Reed et al. 2013	sulfuric acid/hydrogen peroxide digest, colorimetric analysis	35% nitric acid, ICP-MS	844 (131)	0.297 (0.045)
	Panama		Barron et al. 2009	70% nitric acid, ICP-MS		397 (28)	0.053 (0.007)
	Panama		Wurzburger et al. 2012	70% nitric acid, ICP-MS		377 to 629	0.07 to 0.157
	Belize	Soil	Winbourne et al. 2017	mixed acid digest and ICP-MS	aqua regia digest and ICP-MS	157, 2354	1.73, 1.79
	Costa Rica		Reed et al. 2013	sulfuric acid/hydrogen peroxide digest, colorimetric analysis	35% nitric acid and ICP-MS	557 (45)	7.2 (4.64)
	Panama		Wurzburger et al. 2012	70% nitric acid, ICP-MS		170 to 700	
	southeastern Amazon		This study	70% nitric and ICP-OES	70% nitric and ICP-MS	36 to 138	0.032 to 0.124
Temperate forest	Chile	Litter	Perez et al. 2017	concentrated sulfuric acid/water peroxide solution, colorimetric	nitric acid/water peroxide and graphite furnace AAS	168.5 to 512.1	1.32 to 1.78
	Oregon, USA		Perakis et al. 2017	nitric/hydrochloric/hydrofluoric acid, ICP-OES	nitric/hydrochloric/hydrofluoric acid, ICP-MS	870 to 1580	0.018 to 0.68
	Canada	Soil	Jean et al. 2013	70% nitric acid, ICP-MS		367 to 1557	0.535 to 2.42
	Chile		Perez et al. 2017	concentrated sulfuric acid/water peroxide solution, colorimetric	nitric acid/water peroxide and graphite furnace AAS	71.8 to 356.6	1.37 to 1.98

Available Mo and P typically represented 0.5 to 2.5% of total Mo and P in our control plots, similar to what Jean et al. (2013) found for soils (0.4 to 14.4%) in temperate forests in Canada. Contrary to expectations, lime additions did not affect resin-extractable "available" Mo and P, perhaps due to smaller pH shift (4.15 to 5.05) induced by our lime addition relative to other studies. Relationships between soil pH and resin-extractable Mo (Bhella and Dawson 1972) and ammonium-acetate extractable Mo (Evans et al. 1951) have been demonstrated before, although over a much wider pH range, in the range of 5-7 and 5-9 in the aforementioned studies. However, in other cases, studies have been unable to demonstrate a relationship between resin-extractable Mo and Mo limitation (Wurzburger et al. 2012, Jean et al. 2013). This could be due to the fact that extractants may not always be good predictors of biologically-accessible Mo, since bacteria may have separate metallophores to obtain Mo that resins may not predict availability (Bellenger et al. 2008).

3.5.2. Mo or P limitation did not strongly limit BNF

We tested whether Mo and P availability limit free-living BNF in the southeastern Amazon, a region where we predicted strong limitation due to ancient, highly weathered soils and isolation from atmospheric inputs. Contrary to our hypothesis, and despite the relatively low Mo and P concentrations and availability in the southeastern Amazon, we did not find strong responses of free-living BNF in the surface soil or litter layer to Mo and P additions both immediately and across time, with few exceptions. Where we did see responses, they occurred one day after Mo and P applications to soil during the dry season, three months after Mo and P in combination with lime during the onset of the wet season, and one month after

applications of Mo, P and lime combined in the wet season. These results were unexpected, given that all previous studies that tested Mo or P limitation on BNF in the tropics have demonstrated more prominent responses to Mo (Barron et al. 2009, Winbourne et al. 2017), to P (Vitousek and Hobbie 2000, Reed et al. 2013), or to both (Wurzburger et al. 2012). This is particularly surprising considering that Mo limitation is seemingly widespread in temperate and boreal ecosystems (Horstmann et al. 1982, Silvester 1989, Jean et al. 2013, Rousk et al. 2016, Perakis et al. 2017, Pérez et al. 2017), spanning from temperate regions of relatively high Mo richness and deposition (Marks et al. 2015) to boreal systems with relatively low Mo deposition (Rousk et al. 2016). Granted, long-term limitation by Mo and P is still unknown for many of these sites, since only three of the studies that have monitored limitation on longer timescales have looked at Mo and P together in the tropics (Barron et al. 2009) and in temperate and boreal systems (Jean et al. 2013, Rousk et al. 2016). Thus, to further our understanding of the extent to which Mo and P limit free-living BNF, longer-term field fertilization studies should be conducted more widely.

3.5.3. Experimental variation

The high variability exhibited in the field fertilization experiment may have precluded detection of significant differences of free-living BNF in response to fertilizations. Our short-term laboratory fertilization experiment resembled the methodology most comparable to other studies, and the variation was much smaller than compared to the field experiment. At the field level, the variation increased, and there was as much variation within a 2 x 2m plot as there was across the blocks, which were 50 m apart (Appendix B Supplementary Table 4). The wide variation in ethylene

production from litter and the low soil ARA rates may have also contributed more variation and thus difficultly in detecting responses. Studies at this site or in other locations likely require more replication to detect significant responses to additions.

The difficulty in detecting consistent responses to Mo and P could also because nutrient limitation can be seasonal and spatially variable. Of studies that have examined Mo and P limitation to BNF across multiple time points, all studies have found variation as to when and where Mo and P are limiting (Jean et al. 2013, Rousk et al. 2016, Winbourne et al. 2017). The responses after one day (both in response to 2x Mo in the short-term lab experiment, as well as to Mo and P additions in the dry season soil), and well as after one month in the surface soil and three months in litter layer could reflect two separate phenomena. The short-term responses to Mo, as found in the current tropical studies, reflect the ability of bacteria and to utilize the added Mo rapidly and increase nitrogenase synthesis and activity (Bellinger et al. 2011), while the longer-term effects integrate nutrient recycling from decomposition (Rousk et al. 2016).

3.5.4. High N availability may control free-living BNF

Even in tropical forests where Mo and P limitation on free-living BNF has been demonstrated, BNF may still be suppressed by high N availability, as evidenced by decreases in response to N, Mo, and P additions in combination (Winbourne et al. 2017). While Winbourne et al. (2017) found that Mo suppressed BNF in their volcanic sites, when they combined N with Mo and P additions, the additions in combination suppressed BNF, indicating that N exerts a greater control on BNF rather than Mo and P availability. The same pattern was found in Hawaii, where Crews et al. (2000) added

P and other micronutrients to the litter layer, free-living BNF generally increased, but when N and P and micronutrients were added together, BNF decreased. Thus, even when Mo and P are limiting to BNF, if N availability is high, BNF is downregulated and will not respond to Mo and P additions because BNF is an energetically-expensive process (Gutschick 1981).

Previous work at our Tanguro site demonstrated high concentrations of inorganic N in surface soils, averaging a total of 37 µg and 7.5 µg $N\text{-}NO_3^- + NH_4^+$ g^{-1} in the dry and wet seasons respectively (Chapter 4), values that are four to nine-fold higher than other previously measured tropical forests where BNF has been quantified (e.g. Sullivan et al. 2014, Winbourne et al. 2018) (Chapter 4). Concentrations at depth are even greater, and the top 4 m of soil contains 230 kg $N\text{-}NO_3^- + NH_4^+$ ha^{-1} (Jankowski et al., 2018). These large pools of inorganic N have only been found in other regions where oxisols dominate, such as the central Amazon (Schroth et al. 1999) and in Kenya (Tully et al. 2016). The buildup of inorganic N suggests that deep oxisols could have anion exchange capacity to hold onto large quantities of nitrate, in contrast to other tropical soils, such as forests measured in Costa Rica, where nitrate is highly mobile (Newbold et al. 1995). These deeper pools of inorganic N are likely accessible to plants, where trees in the seasonally-dry evergreen forest have deep roots that allow them to access water during a several months-long dry season (Nepstad et al. 1994), thus accessing and recycling inorganic N back to the soil surface.

The ranges in BNF rates I found in the Tanguro site are much closer to rates found in response to experimental N additions in tropical forests. The free-living BNF rates in the litter layer on a mass basis (0.10 nmol C_2H_4 g^{-1} hr^{-1} in the wet season) fall

in the range of rates measured by other studies in the tropics following N additions (Cusack et al. 2009, Barron et al. 2009, Wurzburger et al. 2012), and are at least an order of magnitude lower than rates found in many other tropical forests (Vitousek and Hobbie 2000, Reed et al. 2013, Winbourne et al. 2017) (Figure 3.6). The similarity in rates measured in the southeastern Amazon to rates found in response to N fertilization at other sites is consistent with the hypothesis that the low rates may due to a level of high N richness in the southeastern Amazon.

The C:N ratios in the canopy and soil in the southeastern Amazon are much higher than other sites where BNF has been measured, while the BNF rates are much lower than other sites (Figure 3.6), suggesting a relationship between C:N ratios and BNF (Figure 3.6). The foliar C:N ratio measured at our site in the southeastern Amazon (23.8) (Chapter 4), is on the low end of the tropical forest average (C:N = 36; (McGroddy et al. 2004)). Even within specific sites, such as a tropical forest in southern China, stoichiometry explained 13-53% of the variation in BNF (Zheng et al. 2018), and as both litter and foliar C:N increased from 12.5 to 45, BNF in the litter and canopy also increased. Cusack et al. (2009) found the same pattern in Puerto Rico, where BNF increased as foliar C:N increased from 40 to 85. In Panama, the site with the lowest litter C:N, or highest N availability, also had the lowest BNF rates that did not response to Mo or P additions. In contrast, at the sites in Panama with higher C:N ratios, BNF rates were the highest and responded to Mo and P (Wurzburger et al. 2012), which suggests that Mo and P availability are more important for BNF when N is more limiting.

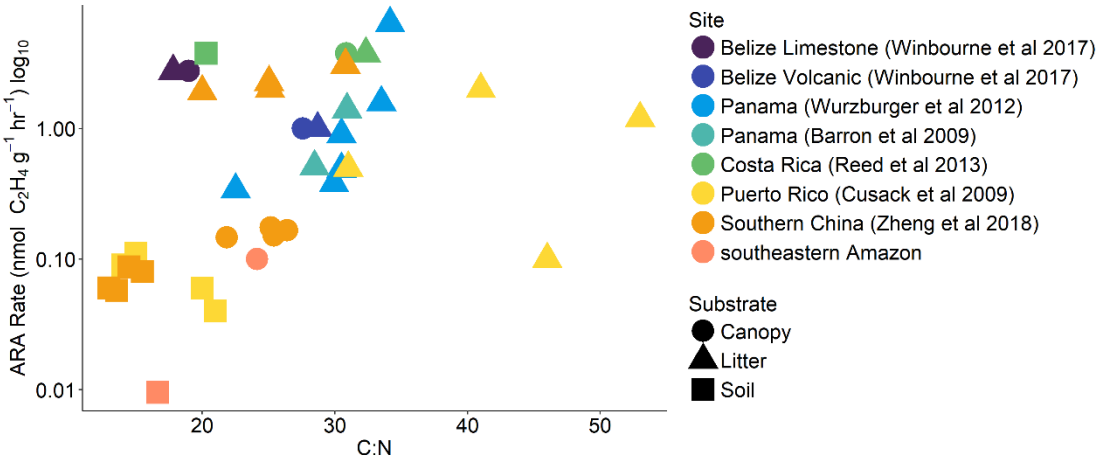

Figure 3.6. Relationship between substrate stoichiometry (soil, litter, or canopy C:N) stoichiometry and ARA rates (log_{10} scale) in substrate. For the southeastern Amazon and Belize, we plot the average wet season ARA rates in the litter with the canopy C:N ratio instead of litter C:N. All other ARA rates are associated with the specified substrate: (●) canopy, (▲) litter, and (■) soil.

The mean soil N:P (33.3), derived from values measured in Chapter 4 , indicates relative N richness to P in the southeastern Amazon. While the soil % N in this region falls within ranges found in other tropical forests (Batterman et al. 2013), the soil P concentrations were much lower, explaining the high soil N:P ratio (Chapter 4). However, the soil N:P in the southeastern Amazon is much higher than compared to other tropical forests where BNF rates are higher (in the range of 6-16, (Batterman et al. 2013, Reed et al. 2013, Sullivan et al. 2014, Winbourne et al. 2017). When adding P fertilizer to soils in the southeastern Amazon, the soil N:P ratio theoretically shifted to 18, a value still outside the typical range of N:P ratios which might be considered favorable for BNF based on observations from other sites. The negative relationship between soil N:P and BNF was demonstrated clearly in a tropical forest in southern China, as soil N:P ratios increased from 4 to 21, soil BNF declined (Zheng et al. 2018).

In the southeastern Amazon, P:Mo in the soil ratios averaged 950, which were not close to the ranges in sites where there were strong responses to P or Mo alone. This potentially explains why there were responses of BNF to Mo and P together at Tanguro, but not to Mo or P alone. In previous studies, litter P:Mo ratios also explained BNF responses to Mo and to P additions for both (Wurzburger et al. 2012, Perakis et al. 2017). In Panama, P:Mo ranged between 2600 to 6300, and when the P:Mo ratios were higher, there was a response of BNF to Mo but not to P (Wurzburger et al. 2012). Similarly, in temperate forests in the Pacific Northwest, the high P:Mo ratios ranging from 14,000 to 61,000 likely explained the strong response of BNF to Mo but not P (Perakis et al. 2017). In contrast, Vitousek & Hobbie (2000) found litter P:Mo values of 100 and 670 which could perhaps partially explain the response to P, but not Mo.

3.6. Conclusion

We found little support for the hyphothesis that Mo and P availability prominently limit BNF at the Tanguro site, and instead propose that N availability exerts stronger controls that manifest to the generally low BNF rates we observed. We currently lack any measurements from similar forests on oxisols with flat topography, characterized by large inorganic N pools and low C:N stoichiometric ratios, despite the fact such these forests may represent a large proportion of forests across the Amazon and Congo. To reach broader generalizations, it would be crucial to know whether Mo and P limitation are similarly absent, and if BNF rates are consistently low across the lowland Amazon. BNF is an important parameter in many Earth System models, and given that nutrient availability is a key constraint on tropical

forest responses to rising carbon dioxide in the atmosphere, understanding hierarchical controls on BNF and their geographical patterns will be important to resolve. This is especially true as it becomes increasingly clear that no "one" nutrient is sufficient to explain controls on BNF across diverse ecosystems.

Acknowledgements

We thank Debra Driscoll at SUNY ESF and Louis Derry at Cornell University (Earth and Atmospheric Sciences) for analytical help with Mo and P analysis; Joy Winbourne and Kelsey Fenn for help and logistics for gas chromatograph use at Brown University; Stephen Parry at the Cornell Statistical Consulting Unit; Darlisson Nunes, Maria Lucia Nascimento, Raimundo Mota Quintino, Sandro Rocha, Leonardo Maracahipes, Sebastião Nascimento, Ebis Nascimento, Adilson Coelho, and Meri Maestri for the field and logistical help from the Instituto de Pesquisa Ambiental da Amazônia; and KathiJo Jankowski, Hillary Sullivan, and Paul Lefebvre from the Woods Hole Research Center. Access to field site provided by Grupo André Maggi. Funding for this study was provided by NSF Grant DGE-1069193, NSF DDIG-1701092, Mario Einaudi and Cornell University travel grants, Sigma Xi (Cornell Chapter), Paul P. Feeny Graduate Student Research, and the Andrew W. Mellon Student Research Grant.

3.7. References

Aguiar, A. P. D., I. C. G. Vieira, T. O. Assis, E. L. Dalla-Nora, P. M. Toledo, R. A. Oliveira Santos-Junior, M. Batistella, A. S. Coelho, E. K. Savaget, L. E. O. C. Aragão, C. A. Nobre, and J. P. H. Ometto. 2016. Land use change emission scenarios: Anticipating a forest transition process in the Brazilian Amazon. Global Change Biology 22:1821–1840.

Anbar, A. 2004. Molybdenum stable isotopes: observations, interpretations and directions. Reviews in Mineralogy and Geochemistry 55:429–454.

Barron, A. R., N. Wurzburger, J. P. Bellenger, S. J. Wright, A. M. L. Kraepiel, and L. O. Hedin. 2009. Molybdenum limitation of asymbiotic nitrogen fixation in tropical forest soils. Nature Geoscience 2:42–45.

Batterman, S. A., L. O. Hedin, M. Van Breugel, J. Ransijn, D. J. Craven, and J. S. Hall. 2013. Key role of symbiotic dinitrogen fixation in tropical forest secondary succession. Nature 502:224–227.

Bellenger, J.-P., T. Wichard, A. B. Kustka, and A. M. L. Kraepiel. 2008. Uptake of molybdenum and vanadium by a nitrogen-fixing soil bacterium using siderophores. Nature Geoscience 11:243–246.

Bellenger, J.-P., T. Wichard, Y. Xu, and A. M. L. Kraepiel. 2011. Essential metals for nitrogen fixation in a free-living N-fixing bacterium: chelation, homeostasis and high use efficiency. Environmental Microbiology 13:1395–1411.

Benner, J. W., and P. M. Vitousek. 2007. Development of a diverse epiphyte community in response to phosphorus fertilization. Ecology letters 10:628–636.

Bhella, H. S., and M. D. Dawson. 1972. The use of anion exchange resin for determining available soil molybdenum. Soil Science Society of America Journal 36:177–179.

Charter, R. A., M. A. Tabatabai, and J. W. Schafer. 1995. Arsenic, molybdenum, selenium, and tungsten contents of distinct fertilizers and phosphate rocks. Communications in Soil Science and Plant Analysis 26:3051–3062.

Cleveland, C. C., A. R. Townsend, D. S. Schimel, H. Fisher, R. W. Howarth, L. O. Hedin, S. S. Perakis, E. F. Latty, J. C. Von Fischer, A. Elseroad, and M. F. Wasson. 1999. Global patterns of terrestrial biological nitrogen (N_2) fixation in natural ecosystems. Global Biogeochemical Cycles 13:623–645.

Crews, T. E. 1993. Phosphorus regulation of nitrogen fixation in a traditional Mexican agroecosystem. Biogeochemistry 21:141–166.

Crews, T. E., H. Farrington, and P. M. Vitousek. 2000. Changes in asymbiotic,

heterotrophic nitrogen fixation on leaf litter of metrosideros polymorpha with long-term ecosystem development in Hawaii. Ecosystems 3:386–395.

Cusack, D., W. Silver, and W. McDowell. 2009. Biological nitrogen fixation in two tropical forests: ecosystem-level patterns and effects of nitrogen fertilization. Ecosystems 12:1299–1315.

Dynarski, K. A., and B. Z. Houlton. 2018. Nutrient limitation of terrestrial free-living nitrogen fixation. New Phytologist 217:1050–1061.

Eady, R. R. 1996. Structure−Function Relationships of Alternative Nitrogenases. Chemical Reviews 96:3013–3030.

Evans, H. J., E. R. Purvis, and F. E. Bear. 1951. Effect of soil reaction on availability of molybdenum. Soil Science 71:117–124.

Gutschick, V. 1981. Evolved strategies in nitrogen acquisition by plants. American Naturalist 118:607–637.

Hardy, R. W. F., R. D. Holsten, E. K. Jackson, and R. C. Burns. 1968. The Acetylene - Ethylene Assay for N_2 Fixation: Laboratory and Field Evaluation. Plant Physiology 43:1185–1207.

Haynes, R. J. 1982. Effects of liming on phosphate availability in acid soils - A critical review. Plant and Soil 68:289–308.

Horstmann, J. L., W. C. Denison, and W. B. Silvester. 1982. 15N2 fixation and molybdenum enhancement of acetylene reduction by Lobaria spp. New Phytologist:235–241.

Ivanauskas, N. M., R. Monteiro, and R. R. Rodrigues. 2003. Alterations following a fire in a forest community of Alto Rio Xingu. Forest Ecology and Management 184:239–250.

Jankowski, K. J., C. Neill, E. A. Davidson, M. N. Macedo, C. Costa, G. L. Galford, L. Maracahipes Santos, P. Lefebvre, D. Nunes, C. E. P. Cerri, R. McHorney, C. O'Connell, and M. T. Coe. 2018. Deep soils modify environmental consequences of increased nitrogen fertilizer use in intensifying Amazon agriculture. Scientific Reports 8:1–11.

Jean, M. E., K. Phalyvong, J. Forest-Drolet, and J. P. Bellenger. 2013. Molybdenum and phosphorus limitation of asymbiotic nitrogen fixation in forests of Eastern Canada: Influence of vegetative cover and seasonal variability. Soil Biology and Biochemistry 67:140–146.

Laurance, W. F., P. M. Fearnside, S. G. Laurance, P. Delamonica, T. E. Lovejoy, J. M. Rankin-De Merona, J. Q. Chambers, and C. Gascon. 1999. Relationship between soils and Amazon forest biomass: A landscape-scale study. Forest

Ecology and Management 118:127–138.

Mahowald, N., T. D. Jickells, A. R. Baker, P. Artaxo, C. R. Benitez-Nelson, G. Bergametti, T. C. Bond, Y. Chen, D. D. Cohen, B. Herut, N. Kubilay, R. Losno, C. Luo, W. Maenhaut, K. a. McGee, G. S. Okin, R. L. Siefert, and S. Tsukuda. 2008. Global distribution of atmospheric phosphorus sources, concentrations and deposition rates, and anthropogenic impacts. Global Biogeochemical Cycles 22: 1-19.

Marks, J. A., S. S. Perakis, E. K. King, and J. Pett-Ridge. 2015. Soil organic matter regulates molybdenum storage and mobility in forests. Biogeochemistry 125:167–183.

McGroddy, M. E., T. Daufresne, and L. O. Hedin. 2004. Scaling of C:N:P stoichiometry in forests worldwide: implications of terrestrial redfield-type ratios. Ecology 85:2390–2401.

Nardoto, G. B., C. A. Quesada, S. Patiño, G. Saiz, T. R. Baker, M. Schwarz, F. Schrodt, T. R. Feldpausch, T. F. Domingues, B. S. Marimon, B.-H. Marimon Junior, I. C. G. Vieira, M. Silveira, M. I. Bird, O. L. Phillips, J. Lloyd, and L. A. Martinelli. 2014. Basin-wide variations in Amazon forest nitrogen-cycling characteristics as inferred from plant and soil 15N:14N measurements. Plant Ecology & Diversity 7:173–187.

Negreios, G., and D. C. Nepstad. 1994. Mapping deeply rooting forests of Brazilian Amazonia with GIS. Pages 334–338 Proceedings of ISPRS Commission VII Symposium - Resource and Environmental Monitoring, Rio de Janeiro 7(a).

Nepstad, D. C., C. R. de Carvalho, E. A. Davidson, P. H. Jipp, P. A. Lefebvre, G. H. Negreiros, E. D. da Silva, T. A. Stone, S. E. Trumbore, and S. Vieira. 1994. The role of deep roots in the hydrological and carbon cycles of Amazonian forests and pastures. Nature 372:666–669.

Newbold, J. D., B. W. Sweeney, J. K. Jackson, and L. A. Kaplan. 1995. Concentrations and export of solutes from six mountain streams in northwestern Costa Rica. Journal of the North American Benthological Society 14:21–37.

Perakis, S. S., J. C. Pett-Ridge, and C. E. Catricala. 2017. Nutrient feedbacks to soil heterotrophic nitrogen fixation in forests. Biogeochemistry 134:41–55.

Pérez, C. A., F. M. Thomas, W. A. Silva, R. Aguilera, and J. J. Armesto. 2017. Biological nitrogen fixation in a post-volcanic chronosequence from south-central Chile. Biogeochemistry 132:23–36.

Pinto-Tomás, A. A., M. A. Anderson, G. Suen, D. M. Stevenson, F. S. T. Chu, W. W. Cleland, P. J. Weimer, and C. R. Currie. 2009. Symbiotic Nitrogen Fixation in the Fungus Gardens of Leaf-Cutter Ants. Science 326:1120–1123.

Porder, S., and G. E. Hilley. 2011. Linking chronosequences with the rest of the world: Predicting soil phosphorus content in denuding landscapes. Biogeochemistry 102:153–166.

Projeto, R. 1981. Folha SD.22 Goiàs. Page Geologia, geomorphologia, pedologia, vegetaçao, uso potencial da terra. Rio de Janeiro: Ministério das Minas e Energia, Departamento Nacional de Mineral, Fundução, Rio de Janeiro, Brasil.

Quesada, C. A., J. Lloyd, L. O. Anderson, N. M. Fyllas, M. Schwarz, and C. I. Czimczik. 2011. Soils of Amazonia with particular reference to the RAINFOR sites. Biogeosciences 8:1415–1440.

Reddy, K. J., L. C. Munn, and L. Wang. 1997. Chemistry and Mineralogy of Molybdenum in Soils. Pages 4–22 in U. C. Gupta, editor. Molybdenum in Agriculture. Cambridge University Press, Cambridge, United Kingdom.

Reed, S. C., C. C. Cleveland, and A. R. Townsend. 2011. Functional Ecology of Free-Living Nitrogen Fixation: A Contemporary Perspective. Annual Review of Ecology, Evolution, and Systematics 42:489–512.

Reed, S. C., C. C. Cleveland, and A. R. Townsend. 2013. Relationships among phosphorus, molybdenum and free-living nitrogen fixation in tropical rain forests: results from observational and experimental analyses. Biogeochemistry 114:135–147.

Reed, S. C., A. R. Townsend, C. C. Cleveland, and D. R. Nemergut. 2010. Microbial community shifts influence patterns in tropical forest nitrogen fixation. Oecologia 164:521–31.

Riskin, S. H., S. Porder, C. Neill, A. M. e Silva Figueira, C. Tubbesing, and N. Mahowald. 2013. The fate of phosphorus fertilizer in Amazon soya bean fields. Philosophical Transactions of the Royal Society B: Biological Sciences 368:1–10.

Rousk, K., J. Degboe, A. Michelsen, R. Bradley, and J. Bellenger. 2016. Molybdenum and phosphorus limitation of moss-associated nitrogen fixation in boreal ecosystems. New Phytologist 214:97–107.

Sanchez, P. A. 1977. Properties and Management of Soils in the Tropics.

Schroth, G., L. F. da Silva, R. Seixas, W. Geraldes, J. L. V. Macêdo, and W. Zech. 1999. Subsoil accumulation of mineral nitrogen under polyculture and monoculture plantations, fallow and primary forest in a ferralitic Amazonian upland soil. Agriculture, Ecosystems and Environment 75:109–120.

Silvester, W. B. 1989. Molybdenum Limitiation of Asymbiotic Nitrogen Fixation in Forests of Pacific Northwest America. Soil Biology and Biochemistry 21:283–289.

Stallard, R. F. 1988. Weathering and Erosion in the Humid Tropics. Pages 225–246 in A. Lerman and M. Meybeck, editors. Physical and Chemical Weathering in Geochemical Cycles.

Sullivan, B. W., W. K. Smith, A. R. Townsend, M. K. Nasto, S. C. Reed, R. L. Chazdon, and C. C. Cleveland. 2014. Spatially robust estimates of biological nitrogen (N) fixation imply substantial human alteration of the tropical N cycle. Proceedings of the National Academy of Sciences of the United States of America 111:8101–6.

Taylor, B. N., R. L. Chazdon, and D. N. L. Menge. 2019. Successional dynamics of nitrogen fixation and forest growth in regenerating Costa Rican rainforests. Ecology, in press e02637.

Taylor, S. R., and S. M. McLennan. 1995. The geochemical evolution of the continental crust. Reviews of Geophysics 33: 241-256.

Tomatsu, H., J. Takano, H. Takahashi, A. Watanabe-Takahashi, N. Shibagaki, and T. Fujiwara. 2007. An Arabidopsis thaliana high-affinity molybdate transporter required for efficient uptake of molybdate from soil. Proceedings of the National Academy of Sciences of the United States of America 104:18807–12.

Tully, K. L., J. Hickman, M. McKenna, C. Neill, and C. A. Palm. 2016. Effects of fertilizer on inorganic soil N in East Africa maize systems: vertical distributions and temporal dynamics. Ecological Applications 26:1907–1919.

Vitousek, P., and S. Hobbie. 2000. Heterotrophic nitrogen fixation in decomposing litter: patterns and regulation. Ecology 81:2366–2376.

Vitousek, P. M., K. E. N. Cassman, C. Cleveland, C. B. Field, N. B. Grimm, and W. Hole. 2002. Towards an ecological understanding of biological nitrogen fixation. Biogeochemistry 57/58:1–45.

Vitousek, P. M., and R. W. Howarth. 1991. Nitrogen limitation on land and in the sea: how can it occur? Biogeochemistry 13:87–115.

Vitousek, P. M., D. N. L. Menge, S. C. Reed, C. C. Cleveland, and P. T. R. S. B. 2013. Biological nitrogen fixation : rates , patterns and ecological controls in terrestrial ecosystems Biological nitrogen fixation : rates , patterns and ecological controls in terrestrial ecosystems.

Vitousek, P. M., S. Porder, B. Z. Houlton, and O. A. Chadwick. 2010. Terrestrial phosphorus limitation: mechanisms, implications, and nitrogen-phosphorus interactions. Ecological Applications 20:5–15.

Wang, Y. P., and B. Z. Houlton. 2009. Nitrogen constraints on terrestrial carbon uptake: Implications for the global carbon-climate feedback. Geophysical Research Letters 36.

Wanner, C., and J. Soppa. 1999. Genetic identification of three ABC transporters as essential elements for nitrate respiration in Haloferax volcanii. Genetics 152:1417–1428.

Winbourne, J. B., S. W. Brewer, and B. Z. Houlton. 2017. Iron controls over di-nitrogen fixation in karst tropical forest. Ecology 98:773–781.

Winbourne, J. B., A. Feng, L. Reynolds, D. Piotto, M. G. Hastings, and S. Porder. 2018. Nitrogen cycling during secondary succession in Atlantic Forest of Bahia, Brazil. Scientific Reports 8:1–9.

Wurzburger, N., J. P. Bellenger, A. M. L. Kraepiel, and L. O. Hedin. 2012. Molybdenum and phosphorus interact to constrain asymbiotic nitrogen fixation in tropical forests. PloS one 7:1–7.

Zahalak, M., B. Pratte, K. J. Werth, and T. Thiel. 2004. Molybdate transport and its effect on nitrogen utilization in the cyanobacterium Anabaena variabilis ATCC 29413. Molecular Microbiology 51:539–549.

Zheng, M., W. Zhang, Y. Luo, D. Li, S. Wang, J. Huang, X. Lu, and J. Mo. 2018. Stoichiometry controls asymbiotic nitrogen fixation and its response to nitrogen inputs in a nitrogen-saturated forest. Ecology 99:2037–2046.

CHAPTER 4 . BIOLOGICAL NITROGEN FIXATION AND FOREST RECOVERY AFTER FIRES IN THE SOUTHEASTERN AMAZON

Authors

Wong, Michelle Y.[1*], Christopher Neill[2], Roxanne Marino[1], Divino V. Silvério[3], Paulo M. Brando[2,3], Robert W. Howarth[1,2].

[1]Department of Ecology and Evolutionary Biology, Cornell University, Ithaca, NY 14853, U.S.A.
[2]Woods Hole Research Center, Falmouth, MA 02450, U.S.A.
[3]Instituto de Pesquisa Ambiental da Amazônia, Brasília-DF, Brazil.

4.1. Summary

Tropical forest fires have become more common due to interactions between deforestation, land clearing, and drought. Recovery of these forests may be constrained by nitrogen. Biological nitrogen fixation (BNF) is the main pathway for new nitrogen (N) to enter most tropical forests, but this process may be constrained by other elements, such as molybdenum and phosphorus, which are required for BNF. We studied the role of BNF seven years into the recovery of southeastern Amazon tropical forests that were burned experimentally either annually or every three years between 2004 and 2010. We hypothesized that, compared with unburned primary forests, BNF in burned forests would increase due to the depletion of N in the aboveground biomass pool post-fire, and that soil concentrations of molybdenum and phosphorus from ash inputs would increase, reducing their potential constraints on BNF. Despite the fires depleting about half the aboveground N pool and rapid rates of recovery in the leaf N pool, we found low rates of both free-living and symbiotic BNF. Higher concentrations of molybdenum and phosphorus in the surface soils of the burned forests indicated that these elements were likely not limiting BNF post-fire.

Our results suggest that despite the N demand for regrowth post-fire, substantial N stored in soils likely downregulates BNF. Overall, we found surprisingly low BNF rates (<1 kg N ha^{-1} yr^{-1}) in this region of the Amazon, which contrasts with the traditional paradigm that, 1) tropical forests fix large quantities of N, and 2), that BNF increases after forest disturbance.

4.2. Introduction

Interactions between deforestation, expansion of agriculture, and droughts now increase the occurrence of fires across large areas of seasonally dry Amazon forest that historically were relatively unaffected by fires (Uhl and Kauffman 1990, Cochrane 2001). Even low-intensity Amazon forest fires increase tree mortality and create conditions that increase the likelihood of future fires, particularly during severe droughts (Cochrane and Schulze 1999, Brando et al. 2014). Despite the decreasing rates of deforestation in the tropics during the past decade, a greater incidence of fires now account for about a third of carbon emissions from deforestation (Aragão et al. 2018). Most Earth System Models predict longer dry seasons and more droughts in the future, which will likely increase fire frequency and severity in the Amazon (Cox et al. 2000, Aragão et al. 2014).

Because of the widespread change in fire regimes, understanding controls on the recovery of burned forests in the tropics is increasingly important. Worldwide, secondary tropical forests that regrow after disturbances such as fires are found to recover rapidly (Poorter et al. 2016) and often serve as a large carbon sink (Pan et al. 2011). Twenty-one percent of the Brazilian Amazon has been cleared (INPE), but about 20% of this cleared land is in now in some stage of secondary forest succession.

By 2030, secondary forests are predicted to make up a third of cleared land (Aguiar et al. 2016). Thus, increasingly large areas of recovering tropical forests in the Amazon have the potential to serve as a large carbon sink.

Little is known about the mechanisms that control the recovery of Amazon forests after fires and whether nutrients such as nitrogen (N) and phosphorus (P) will limit secondary forest recovery. While P ultimately limits net primary productivity in most tropical forests (e.g. Vitousek 1984; Hedin et al. 2003), recovery and regrowth in young forests following disturbance are typically constrained by N (Davidson et al. 2007, Wright et al. 2018). Nitrogen is selectively lost during fires owing to its low temperature of volatilization in comparison with other macronutrients (Neary et al. 1999). Nitrogen can be lost in gaseous forms through both high-temperature flaming combustion (as NO, NO_2, N_2O, and N_2) and even in low-temperature smoldering combustion (as NH_3, amines, and nitriles) (Andreae and Merlet 2001). During severe fires in slashed Amazon forest, ecosystem losses of aboveground biomass N ranged from 51 to 62%, while only 7 to 32% of biomass P was lost through volatilization (Kauffman et al. 1995). Compared to N and P, which are particularly abundant in leaf biomass that combusts more readily, the base cations (Ca, Mg, and K) are notably concentrated in woody biomass, which is mostly conserved as ash and redistributed to the soil following fires (McGrath et al. 2001). Though intact and relatively undisturbed tropical forests are not typically N limited, forests could be temporarily N limited during the critical period of recovery and regrowth that occurs after fires due to the preferential loss of N relative to P and other elements.

Tropical forests are thought to rebuild ecosystem N stocks relatively rapidly post-disturbance through two distinct mechanisms that contribute new N—symbiotic and free-living biological nitrogen fixation (BNF). First, tropical forests have a high abundance of leguminous trees (ter Steege et al. 2006a) which can form root nodules that harbor N-fixing bacterial symbionts. Symbiotic N-fixing plants theoretically have a competitive advantage in low N, post-fire conditions, and higher abundances of leguminous plants with associated higher rates of symbiotic BNF can thereby enable ecosystems to recover from fire-induced N losses (Batterman et al. 2013). Second, the warm and generally wet conditions of tropical forests and the relatively steady input of litter, even after fires (Rocha et al. 2014), to the forest floor create the potential for high rates of heterotrophic free-living BNF associated with litter decomposition.

No studies we are aware of have examined the role of BNF in forest recovery after forest fires in the tropics. In addition, few studies have directly measured BNF in secondary forests in the Amazon, despite its vast geographical range. In temperate forests and grasslands, BNF typically increases following fires (Casals et al. 2005, Yelenik et al. 2013). Most studies that have measured BNF during tropical forest recovery following disturbance have been conducted in wet tropical forests after logging outside of the Amazon (Batterman et al. 2013, Sullivan et al. 2014, Winbourne et al. 2018a), or have measured BNF indirectly in the Amazon (Gehring et al. 2005, Davidson et al. 2007, 2018) with mixed results. Secondary forests usually contain a higher proportion of putatively N-fixing trees, but this does not always lead to increased N inputs through BNF. It remains unclear how BNF will respond to fire disturbance in seasonally dry tropical forests. While a greater role of BNF could be

expected following fires in seasonally dry tropical forests where N-fixers are often more abundant (Gei et al. 2018), water can be seasonally limiting, thereby reducing BNF.

Symbiotic and free-living BNF are often constrained by P (Vitousek et al. 2002a) and free-living BNF also by the trace metals molybdenum (Mo) and vanadium (V). Phosphorus can constrain BNF either because N-fixers have a higher P demand, or because greater P availability can shift a system towards N limitation, thus inducing BNF (Vitousek and Howarth 1991). Mo is a major co-factor in the nitrogenase enzyme, while V can substitute for Mo in 'alternative' nitrogenases, a much less commonly identified class of nitrogenase enzymes in natural systems (Bellenger et al. 2014). Mo and P can constrain free-living BNF (Crews et al. 2000, Barron et al. 2009, Winbourne et al. 2017), and in highly Mo-depleted environments, V could be important (Darnajoux et al. 2017). The availability of Mo and P are likely low across large areas of the lowland Amazon for two reasons. First, large interior regions of the Amazon are located far from sources of ocean-derived aerosols and long-distance transport of Saharan dust that are the main new sources of Mo, P, and V inputs to many other tropical forests with low rates of parent material weathering. The southeastern Amazon has been shown to receive low inputs of exogenous P in atmospheric deposition (Mahowald et al. 2005a), and likely Mo. Second, this region of the Amazon is situated on some of the oldest surfaces in South America (Quesada et al. 2011), and highly weathered soils are likely to be depleted in these rock-derived nutrients.

We hypothesized that Mo and P limitation of BNF may be stronger in the southeastern Amazon where soils are depleted in rock-derived nutrients and forests are subject to frequent fires. Earlier studies on BNF in the tropics have been conducted in regions with younger soils, or with higher atmospheric inputs of Mo and P. We hypothesized that Mo, P, and V released from aboveground biomass and the litter layer would be redeposited on the soil surface post-fire, and thus more available for uptake by N-fixing bacteria; and that both free-living and symbiotic BNF rates would be higher several years after fires. To test these hypotheses, we compared a suite of burning manipulations in the southeastern Amazon to evaluate how fire affects the availability of Mo, P, and V required for BNF, and measured rates of BNF during post-fire forest recovery. Lastly, given that the dearth of BNF estimates from many remote regions, such as the southeastern Amazon, limits our understanding of global patterns, controls, and rates of BNF, we quantified biome-specific BNF rates for this region.

4.3. Methods

4.3.1. Location

The study was conducted at Fazenda Tanguro, an 800 km^2 working farm in eastern Mato Grosso State, Brazil. Fazenda Tanguro contains 400 km^2 of primary predominantly evergreen tropical forest 30 km north of the southern boundary of the Amazon forest (13°04’ S, 52°23’ W). The average annual air temperature is 27°C with <5°C seasonal variation. Annual rainfall is 1700 mm, with an intense dry season between May and September. Forest tree species composition represents a transition

between the central Amazon forest and the more seasonal Cerrado (Ivanauskas et al. 2003).

The soil is classified as a red-yellow alic dystrophic latosol (Brazilian soil classification), a relatively infertile sandy ferralsol (FAO classification), or an oxisol (Haplustox; USDA classification). These soils located on the crystalline Brazilian Shield are among the oldest in Amazonia (Quesada et al. 2011), with Tertiary and Quaternary fluvial deposits over Precambrian gneisses of the Xingu Complex (Projeto Radambrasil 1981).

4.3.2. Fire treatments

To test tropical forest susceptibility to fire, a prescribed fire experiment was initiated at Fazenda Tanguro in 2004. Three 0.5 x 1 km (50 ha) plots were established with three treatments: (1) an unburned control, (2) a plot burned three years apart, or triennially, in 2004, 2007, and 2010 (Burn 3yr), and a plot burned annually from 2004 to 2010 (except 2008) (Burn 1yr). Experimental fires were ignited at the end of the dry season when forests of the region are most susceptible to fire. Initial fires were low-intensity and slow-moving (Balch et al. 2008), typical of tropical understory forest fires (Cochrane and Schulze 1999). For the initial fires, mean flame height was 31 (±1) cm, with a mean initial temperature that ranged from 128°C belowground (2 cm) to 273°C at the surface to 87°C aboveground (100 cm). The fire in the Burn 3yr treatment during 2007 was more severe than the Burn 1yr treatment because of extreme dry conditions due to drought and increased fuel load from accumulated litterfall (Brando et al. 2014). By 2009, the cumulative tree mortality was 63% in the Burn 3yr treatment and 50% in the Burn 1yr treatment (Brando et al. 2014). Balch et

al. (2008) provide a further description of the site, experimental design, and fire behavior.

4.3.3. Symbiotic BNF

We estimated symbiotic BNF in the wet season of 2017 (between February and April), seven years after the last fires, when we expected to find higher rates of symbiotic BNF after time had passed from the immediate post-fire period when mineral N from ash would likely suppress BNF. In an earlier chronosequence study in Panama, Batterman et al. (2013) found the highest recruitment of putatively N-fixing trees and the highest symbiotic BNF rates between 5 and 12 years after logging. Using a stratified adaptive cluster sampling approach to capture the irregular distribution of root nodules (Sullivan et al. 2014), we placed four 10 x 50 m survey grids randomly within each 50 ha fire treatment plot for a total of 12 survey grids. In each survey grid, we collected a minimum of 55 square soil cores (225 cm^2) hammered into the soil 15 cm deep for a minimum of 660 total cores per 50 ha treatment plot. If nodules were found in a specific core, we then sampled in all the neighboring cores until no more adjacent cores contained nodules.

Following collection of individual nodules from the survey grids, we conducted an acetylene reduction assay (ARA) (Hardy 1968) incubated for one hour in the field (Sullivan et al. 2014) in 125 mL gas tight jars with lids fitted with septa (Fisher Scientific 501215190) and exposed to a 10% atmosphere of acetylene generated from calcium carbide. We took three sets of ethylene blanks for each batch of acetylene. We also tested for abiotic ethylene production, and ethylene lost due to photodegradation during transport, but found undetectable effects.

After incubations, we collected 30 ml headspace samples and stored them in pre-evacuated 22 mL gas-tight vials (Teledyne Tekmar) fitted with thick butyl septa (Geo-Microbial Technologies, Inc.). We then dried nodules in a 65°C oven overnight to determine moisture content and dry weight. Gas samples were returned to Cornell University where we measured ethylene concentrations using a Shimadzu 8-A gas chromatograph equipped with a flame ionization detector and a Porapak-N 80/100 column at 70°C with two standard curves daily and check standards every ten samples. Ethylene blanks from the acetylene were subtracted from sample ethylene values. For nodule samples, ethylene blanks averaged 0.1% of total ethylene production. We calculated ARA rates in units of micromoles of ethylene produced per gram dry mass of sample per hour of incubation. To convert nodule ARA rates into BNF rates, we used a theoretical ratio of 3:1 (mol acetylene reduced:mol N_2 fixed) (Hardy et al. 1968).

4.3.4. Free-living BNF

We measured free-living BNF on soil and litter using the ARA method calibrated with a $^{15}N_2$ tracer (Barron et al. 2009), conducted six and seven years after the last fires. In the dry season of October 2016 and the wet season of March 2017, we collected 30 samples of litter by hand and 30 samples of soil (0-2 cm) using a soil corer in each treatment, for a total of 180 incubations per season. We collected samples every 50 m along three transects 250 m apart across all three plots. Approximately 15 grams of litter or 25 grams of fresh surface soil were sealed in gas-tight jars described above. Litter samples were incubated overnight for 8-10 hours, and soil samples were incubated for 14-18 hours to accommodate lower expected rates of

acetylene reduction. Litter was dried at 65°C and soil was dried at 105°C for two days for dry weight and moisture measurements. We collected, stored and analyzed gas samples as described above.

Three replicates of ethylene production from litter were made per sampling day without exposure to acetylene, as litter is known to produce ethylene (Reed et al. 2007). Ethylene production rates from litter averaged 17% of the total ethylene concentrations, but varied widely, with a relative standard deviation of 107%. Ethylene production from soil without exposure to acetylene was insignificant. Ethylene blanks averaged 12% of the ethylene production in litter incubations but 50% in soil incubations, due to the low rates measured. We calculated ARA rates in units of nanomoles of ethylene produced per gram dry mass of sample per hour of incubation.

To convert acetylene reduction rates into BNF rates, we used a site specific-ratio of 2.3:1 (mol acetylene reduced):(mol N_2 fixed) by measuring the incorporation of ^{15}N-labeled N_2 in soil. We used gas-tight 40 mL screw-cap vials with septa (Wheaton 225310), weighed ~15 g of soil, and replaced a third of the remaining headspace with 98 atom % $^{15}N_2$ (Cambridge Isotope Laboratories). After incubating paired ARA samples with $^{15}N_2$ incubations, we terminated the $^{15}N_2$ incubations in an oven at 65°C, ground the samples, and analyzed changes in soil $\delta^{15}N$ at the Cornell University Stable Isotope Laboratory (COIL) on a continuous flow isotope ratio mass spectrometer (Finnigan MAT Delta Plus plumbed to a Carlo Erba NC2500 elemental analyzer). We present results using both the site-specific (2.3:1) and theoretical ratio (3:1) of (mol acetylene reduced):(mol N_2 fixed).

4.3.5. Inorganic soil N and pH

We composited the same 90 soils per season sampled for free-living BNF for laboratory analyses of soil moisture (gravimetric moisture), pH, and 2M KCl extractions to measure exchangeable ammonium (NH_4^+) and nitrate (NO_3^-) following the methods of Neill et al. (1995). KCl extracts were kept frozen and analyzed for NH_4^+ and NO_3^- via colorimetric analyses at the Woods Hole Research Center, using an Astoria Pacific 303A (cartridge base) and 305D (digital detector). We measured soil pH using a 1:2 soil to distilled water ratio, stirred and equilibrated for 30 minutes with a pH meter standardized at pH 7 and 4.

4.3.6. Litterfall collection and area-based BNF estimates

Annual litterfall production was measured to extrapolate free-living BNF rates in the litter layer from a mass basis to a per-area flux. Litterfall was estimated by collecting the production of dead organic material ≥ 2 cm diameter in 25 litter traps (50 × 50 cm) placed 1 m above the ground at 50 m intervals within each plot and collected every two weeks (Rocha et al. 2014) from 2010 to 2016. We used annual litterfall production rates to scale free-living BNF rates to annual rates with a decay constant (k = 1.5) from Sanches et al. (2008) applied to an exponential decay rate equation, $X = X_0 e^{-k/t}$, where X = mass, X_0 = original annual litterfall, and k = decay constant, calculating litterfall and decay for five years. To scale up free-living BNF rates in the soil, we assumed BNF was occurring in the top 10 cm of soil and applied a bulk density of 1.09 g cm^{-3} from Riskin et al. (2013). We calculated annual estimates assuming a 4.5 month dry season (Brando et al. 2014).

4.3.7. Forest inventory and wood N pool estimates

To estimate changes in aboveground N and thereby compare the amount of recovered N that was derived from BNF since the fires, in 2004 we tagged, mapped, measured diameter at breast height (dbh), and estimated the height of all trees ≥ 40 cm dbh (n ≅ 2300 individuals across all plots) within each 50 ha treatment plot. Trees and lianas (20–39.9 cm dbh) were sampled in belt transects (500 × 20 m) at 0, 30, 100, 250, 500, and 750 m from the forest edge (n ≅ 3400 individuals across all plots). Nested sub-sampling (500 × 4 m) was conducted within these belt transects to measure trees and lianas (10–19.9 cm) (n ≅ 3070 individuals across all plots). To sample 5.0–9.9 cm individuals, plots (500 × 2.5 m) were also nested within these belt transects (n ≅ 1500 individuals across all plots).

We calculated aboveground biomass with a best-fit pantropical model (Chave et al. 2014) using height, dbh measurements, and previously-measured site-specific wood density (see Balch et al. 2011). To estimate wood N, we grouped each of ten most dominant tree taxa (Balch et al. 2008) to the nearest genus or family in a published wood N inventory (Martin et al. 2014), and estimated a site-specific wood N of 0.22%, weighting the %N to dominance values of the specific tree taxa to which we applied to the summed aboveground biomass. The allometric aboveground biomass calculation (Chave et al. 2014) includes an estimate of leaf biomass, which is typically less than 5% of aboveground biomass (Delitti et al. 2006).

4.3.8. Leaf area index (LAI) and leaf N pool estimates

We separately calculated a leaf N pool (because leaves contain disproportionately more N than wood) by using LAI, specific leaf area, and a leaf %N

calculated from the ten most dominant species from 2004 to 2016. Seasonally, one LAI-2000 (LI-COR Instruments) was placed in an adjacent open field to measure incoming radiation with no canopy influence while below-canopy measurements were simultaneously taken (Balch et al. 2008). LAI was measured at 50 m intervals within each plot (n = 600) four times per year.

In the wet season of 2017 (March to April), we used a slingshot to sample canopy leaves; we collected three branches from three individual trees of the ten dominant species (Balch et al. 2008) in each plot, for a total of 90 individual trees. We weighed the leaves after drying for two days at 65°C and analyzed the surface area of the leaves using a LI-COR LI-3100C Area Meter to calculate a specific leaf area. Dried leaf samples were ground and measured for C, N, and $\delta^{15}N$ analysis on a Delta Plus, ThermoQuest-Finnigan analyzer at Centro de Energia Nuclear na Agricultura (CENA) at the University of São Paulo, Piracicaba. We calculated the mass of N (kg ha^{-1}) by combining LAI (m^2/m^2) with specific leaf area (g/m^2) and the %N of the leaves.

4.3.9. Soil analysis

In January 2016, six years after the last fires, we collected twelve soil cores to depths of 0-2 cm and 2-10 cm in each treatment plot. We ground the soil in an alumina ceramic ring and puck shatterbox. Samples were oven-dried at 105°C, ashed at 550°C for four hours, and digested in concentrated nitric acid (HNO_3) using the 3052 EPA microwave-assisted acid digestion of siliceous and organically based matrices. We centrifuged, filtered, and diluted digests prior to Mo and V analysis on a Finnigan Element 2 inductively coupled plasma mass spectrometer (ICP-MS) and P analysis on

a Spectroblue ICP-OES Inductively Coupled Plasma Optical Emission Spectroscopy (ICP-OES). We digested a certified natural sample (SDO-1, a Devonian Ohio shale from the USGS), run in parallel with the samples. The remaining subsamples were used to analyze bulk carbon (C), N, and the soil N isotopic signature ($\delta^{15}N$) at COIL. Based on analyses of duplicate samples and standards, we estimate that the precision on the ICP-MS analysis was ~5% relative standard deviation. While the concentrated nitric acid digestion is not a total digestion, we used this method to most consistently compare concentrations of Mo and P at our site to Mo and P concentrations measured in other BNF studies (Barron et al. 2009, Wurzburger et al. 2012, Jean et al. 2013).

4.3.10. Statistical analyses

We compared soil $\delta^{15}N$, Mo, and V using a two-way ANOVA with depth and treatment as factors, and foliar C, N, and $\delta^{15}N$ between burn treatments using a one-way ANOVA. We analyzed soil C, N, C/N, and P, and foliar C/N and specific leaf area (g/m^2) by ln-transforming the data and also using a two-way ANOVA for soil, and a one-way ANOVA for foliage. While soil pH was not transformed, NH_4^+ and NO_3^- were analyzed by ln-transforming (+0.1) the data and using a two-way ANOVA with season as a factor, including an interaction with the burn treatment. Post-hoc analysis was conducted with a Tukey test. Free-living BNF in soil and litter violated assumptions of parametric tests, so we used the Kruskal-Wallis test separately for each season with treatment as the predictor variable. Post-hoc analysis was conducted with the Dunn's test. We tested the relationship between BNF and moisture using a Theil–Sen estimator. We inspected residuals visually by examining QQ plots to check for

normal distribution and investigate heteroscedasticity. Statistical analyses were performed using R software v.3.0.3 (R Development Core Team).

4.4. Results

4.4.1 Symbiotic BNF

Symbiotic BNF was low or non-existent across the experimental area (Figure 4.1). We found no presence of symbiotic BNF in the Control and Burn 1yr treatment, and an average of 0.48 ± 0.45 kg N ha^{-1} yr^{-1} in the Burn 3yr treatment (Table 4.1). This annual rate was calculated based on two of four survey grids within the Burn 3yr plot that contained root nodules. Using metrics defined by Winbourne et al. (2018b), the proportion of cores within the four survey grids in the Burn 3yr treatment that contained nodules, *p*, was 0.0732, while the variation among nodule weights, *v*, was 0.731. In one survey grid, we found 0.031 g nodule m^{-2} and an average ARA rate of 7.61 µmol C_2H_4 g^{-1} h^{-1} and in the second, we found 0.097 g nodule m^{-2} and an average ARA rate of 46.0 µmol ethylene g^{-1} h^{-1}.

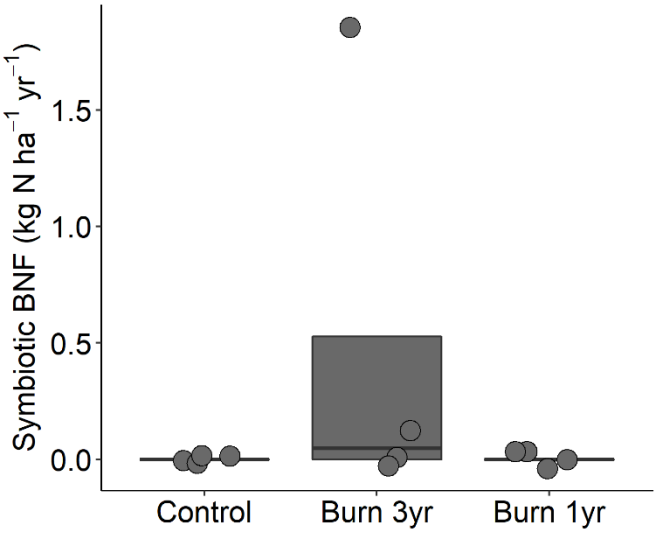

Figure 4.1. Annual average symbiotic nitrogen fixation rates (kg N ha^{-1} yr^{-1}) across the unburned (Control), triennially burned (Burn 3yr), and annually burned (Burn 1yr) forest treatments in the southeastern Amazon, measured seven years after the last fire; n = 4 survey plots per treatment, black line indicates median and grey shading indicates interquartile range.

Table 4.1. Mean nitrogen fixation acetylene reduction activity (ARA) in litter and soil on a mass basis during the dry and wet season, and mean nitrogen fixation fluxes on an area basis. Data are means ± 1 standard error; n = 30. Letters indicate significant differences ($p < 0.05$).

	Litter ARA (nmol C_2H_4 hr^{-1} g^{-1})		**Soil ARA** (nmol C_2H_4 hr^{-1} g^{-1})		**Annual free-living BNF** (kg N ha^{-1} yr^{-1})**	**Annual symbiotic BNF** (kg N ha^{-1} yr^{-1})	**Annual total BNF** (kg N ha^{-1} yr^{-1})
	Dry	Wet	Dry	Wet			
Control	0.062 (0.045)^{a}	0.288 (0.210)^{a}	0.0014 (0.0009)^{a}	0.00425 (0.0005)^{a}	0.27 - 0.33	0	0.27 – 0.33
Burn 3yr	0.014 (0.059)^{a}	0.064 (0.022)^{b}	0.000019 (0.00002)^{a}	0.00528 (0.001)^{a}	0.16 - 0.21	0.48*	0.64 – 0.69
Burn 1yr	0.038 (0.015)^{a}	0.022 (0.010)^{c}	0.00065 (0.0002)^{a}	0.00358 (0.0006)^{a}	0.12- 0.16	0	0.12- 0.16

*From (Winbourne et al. 2018b) error estimates for symbiotic BNF are: p = 0.0732, and v=0.731. p is the proportion of soil cores containing nodules, and v is the standard deviation of nodule biomass divided by the nodule biomass mean found in cores with nodules

** Using both the site specific (2.3:1) and theoretical ratio (3:1) (mol acetylene reduced:mol N_2 fixed)

4.4.2. Free-living BNF

Overall, BNF rates in the litter and soil were higher across the wet season, and BNF rates were generally higher in the Control relative to the Burn 3yr and Burn 1yr treatments (Figure 4.2). BNF rates in the litter layer on a mass basis were significantly higher in the Control relative to Burn 3yr ($p = 0.05$) and the Burn 1yr treatments ($p = 0.00016$), averaging five times of the rate in the Burn 3yr treatment and thirteen times the rates in the Burn 1yr treatment (Table 4.1). In the dry season, BNF rates in the litter layer were approximately four times higher in the Control relative to the Burn 3yr treatment and approximately two times higher than the Burn 1yr treatment, but the high variation precluded detection of significant differences ($p = 0.16$). In the wet season, rates of free-living BNF in surface soils in the Control averaged 50% higher than rates found in the Burn 3yr and the Burn 1yr treatments (Table 4.1). However, this difference was only marginally higher in the Burn 1yr treatment ($p = 0.052$), and there were no significant differences between the Control and the Burn 3yr treatment ($p = 0.29$). In the dry season, the rates of free-living BNF in surface soils in the Control treatment averaged seven times higher than the Burn 3yr treatment and two times higher than the Burn 1yr treatment, but again the high variation precluded detection of significant differences ($p = 0.12$ for Burn 3yr, $p = 0.086$ for Burn 1yr) (Table 4.1).

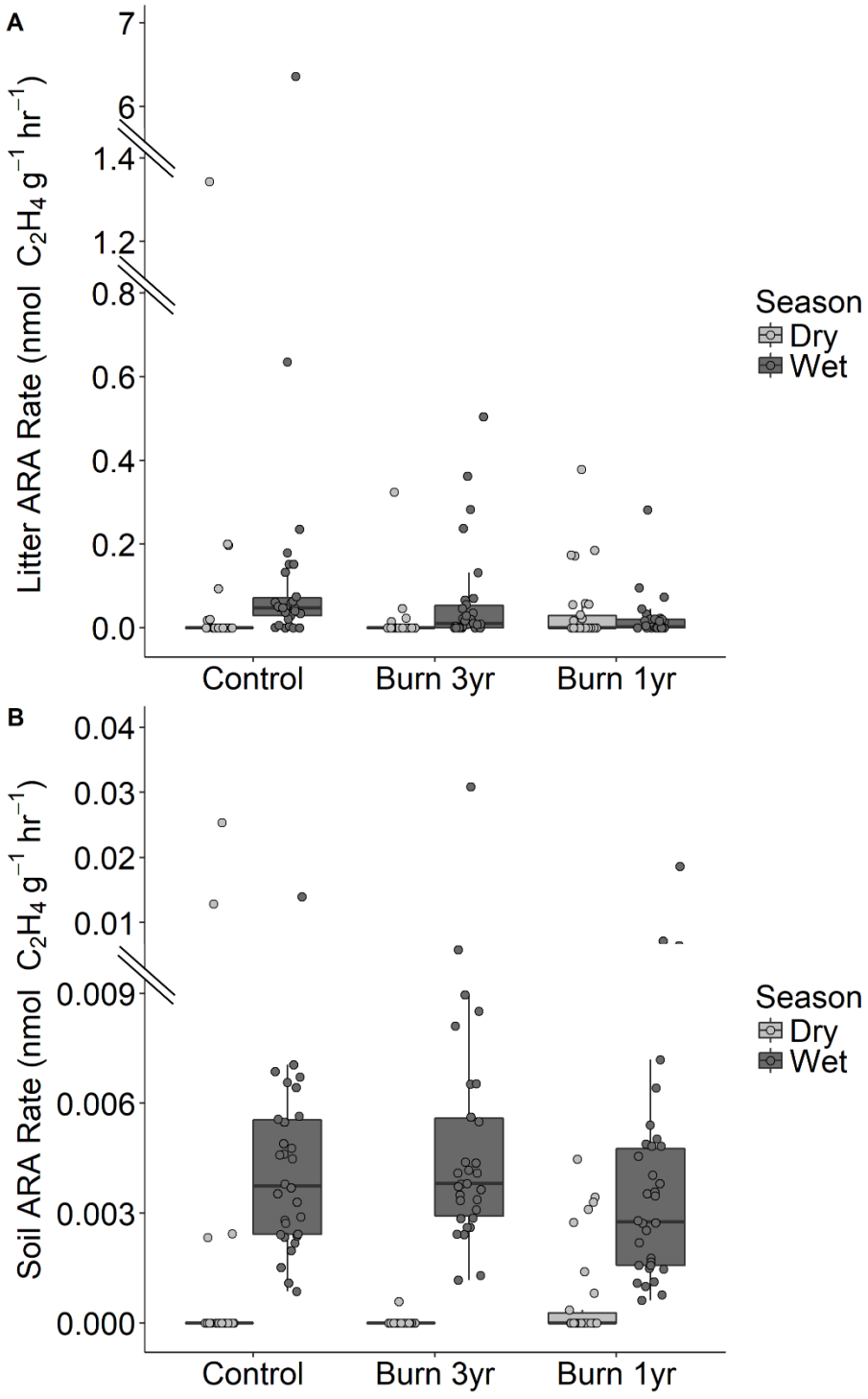

Figure 4.2. Free-living nitrogen fixation acetylene reduction activity (ARA) in the litter layer (A) and surface soil (B) across the unburned (Control), triennially burned (Burn 3yr), and annually burned (Burn 1yr) forest treatments in the southeastern Amazon measured six and seven years after the last fires; n = 30 per treatment, black line indicates median and grey shading indicates interquartile range.

When we grouped the treatments together by season, free-living BNF rates were significantly higher in the wet season compared to the dry season in the litter ($p < 0.0001$) and soil ($p < 0.0001$). Rate and moisture were significantly correlated in the soil ($p < 0.0001$) and in the litter ($p < 0.0001$).

Rates of free-living BNF in both litter and soils were highly variable across sampling locations and between seasons, with a small number of samples that represented disproportionately high rates. In the wet season litter layer, 1% of the measurements accounted for 57% of the free-living BNF in litter across all plots, and 4% accounted for 68%. In the dry season litter, 6% of the measurements accounted for 71% of the BNF. For soils in the dry season, 2% of the measurements accounted for 60% of the BNF, but this effect was less pronounced in the wet season, where 3% of the measurements accounted for 16% of the BNF (Figure 4.2).

Scaled to an annual, area basis, all free-living BNF rates were ≤ 0.33 kg ha^{-1} yr^{-1} (Table 4.1).

4.4.3. Inorganic soil N and pH

Soil surface nitrate and ammonium concentrations were higher in the Control plots than the burned treatments in both the wet and dry seasons, while soil pH was higher in the burned treatments (Figure 4.3). In the dry season, ammonium concentrations in the Burn 3yr and Burn 1yr treatments were both significantly lower than the Control ($p = 0.0061$ for Burn 3yr, $p = 0.0004$, for Burn 1yr), with concentrations about two times higher in the Control than the burned treatments (Figure 4.3, Appendix C Supplementary Table 3). In the wet season, ammonium concentrations were significantly lower in the Burn 1yr plot than in the Control ($p =$

0.0008), while the Burn 3yr and Control did not differ (p = 0.18), with concentrations about 1.5 times lower. Wet and dry season concentrations of ammonium were significantly different within all treatments (Control p < 0.0001 for Control, p = 0.0002 for Burn 3yr, p < 0.0001 for Burn 1yr) (Appendix C Supplementary Table 3).

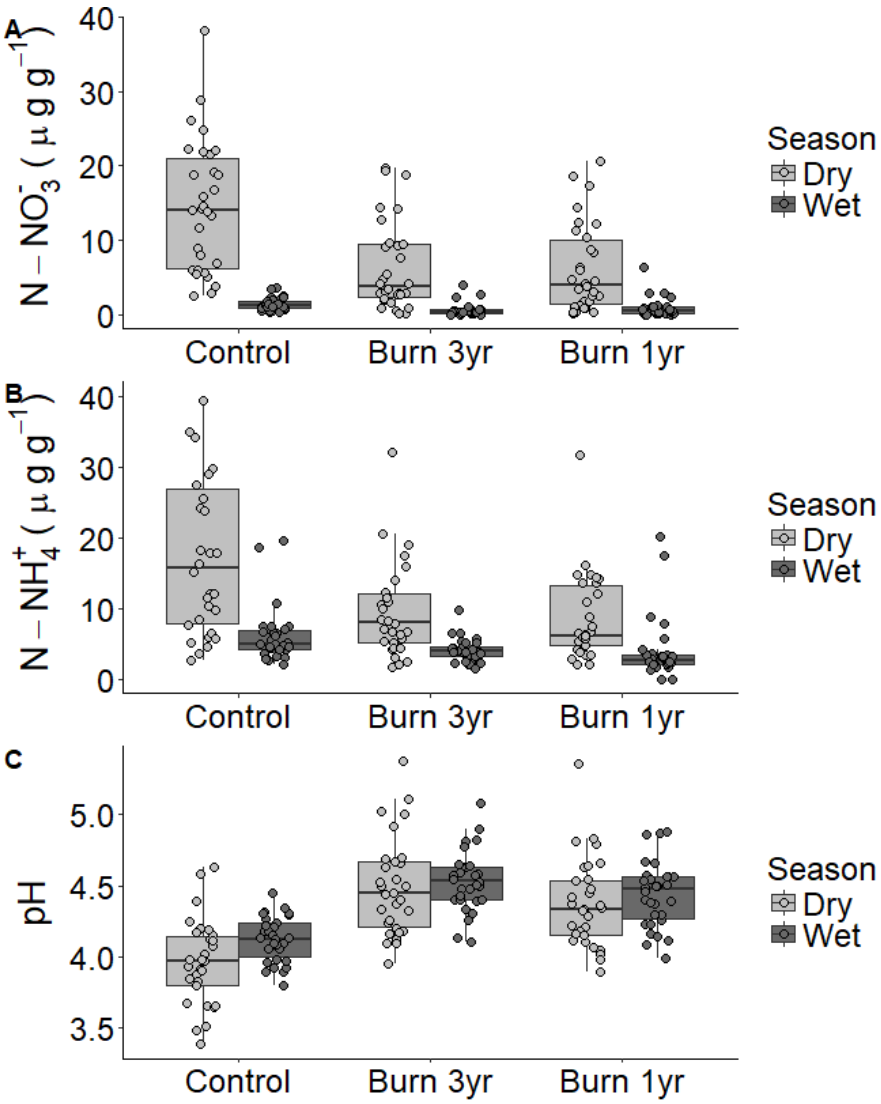

Figure 4.3. Nitrate (NO_3^-) (A), Ammonium (NH_4^+) (B), and pH (C) of surface soils (0-2 cm) across the wet and dry seasons and the unburned (Control), triennially (Burn 3yr), and annually burned (Burn 1yr) forest treatments in the southeastern Amazon; n = 30 per treatment, black line indicates median and grey shading indicates interquartile range.

Consistent with ammonium, nitrate concentrations in both the wet and dry season were significantly lower in the Burn 3yr and Burn 1yr treatments relative to the Control ($p = 0.0002$, $p = 0.0168$, respectively in the wet, and $p < 0.0001$, $p < 0.0001$ in the dry, respectively), with concentrations over two times higher in the Control than the burned treatments (Figure 4.3). Dry season concentrations of ammonium and nitrate were higher across all plots relative to the wet season ($p < 0.0001$ for all treatments). Ammonium dominated over nitrate across the wet and dry seasons in all treatments (Figure 4.3).

The prescribed fires raised surface soil pH in both burned treatments relative to the Control in both the dry and wet seasons (Figure 5). The soil pH of the Control (pH = 4.0) was significantly lower than in the Burn 3yr (pH = 4.5, $p < 0.0001$) and Burn 1yr treatments (pH = 4.4, $p < 0.0001$) (Figure 5). In the wet season, soil pH of the Control (pH = 4.1) was also significantly lower than the Burn 3yr (pH = 4.5, $p < 0.0001$) and Burn 1yr (pH = 4.4, $p < 0.0001$) treatments (Figure 4.3). Within each treatment, soil pH was generally higher during the wet season, but only significantly different in the Control ($p = 0.023$ for Control, $p = 0.52$ for Burn 3yr, $p = 0.39$ for Burn 1yr) (Appendix C Supplementary Table 3).

4.4.4. Aboveground N stocks

The fires depleted aboveground N stocks, leaving 49% of total aboveground N in the Burn 3yr treatment, and 57% of total aboveground N in the Burn 1yr treatment. Wood biomass N was at a minimum in 2016, averaging 200 kg N ha^{-1} in the Burn 3yr and 230 kg N ha^{-1} in the Burn 1yr treatments, or 55% and 62% of the Control. In contrast, wood N biomass ranged from 370 to 430 kg ha^{-1} in the Control (Figure 4.4).

Leaf N biomass stocks were at the minimum three years after the last fire (2013) when leaf N pools in the Burn 3yr (39 kg N ha^{-1}) and Burn 1yr (45 kg N ha^{-1}) treatments were compared with the Control (120-150 kg N ha^{-1}) (Figure 4.4), composing 30 and 34% of the Control. Six years after the last fire, leaf N biomass in the Burn 3yr and Burn 1yr treatments recovered to 74 and 67 kg N ha^{-1}, equivalent to 53 and 48% of the Control (Figure 4.4). The leaf area indices (LAI) recovered rapidly in Burn 3yr and Burn 1yr treatments, from 53% and 52% of the Control in 2011 to 83% and 74% of the Control LAI in 2016 (Appendix C Supplementary Figure 1). Specific leaf area was lower in the Burn 1yr treatment relative to the Control ($p = 0.0016$) but not significantly lower in the Burn 3yr treatment ($p = 0.12$) (Table 4.2).

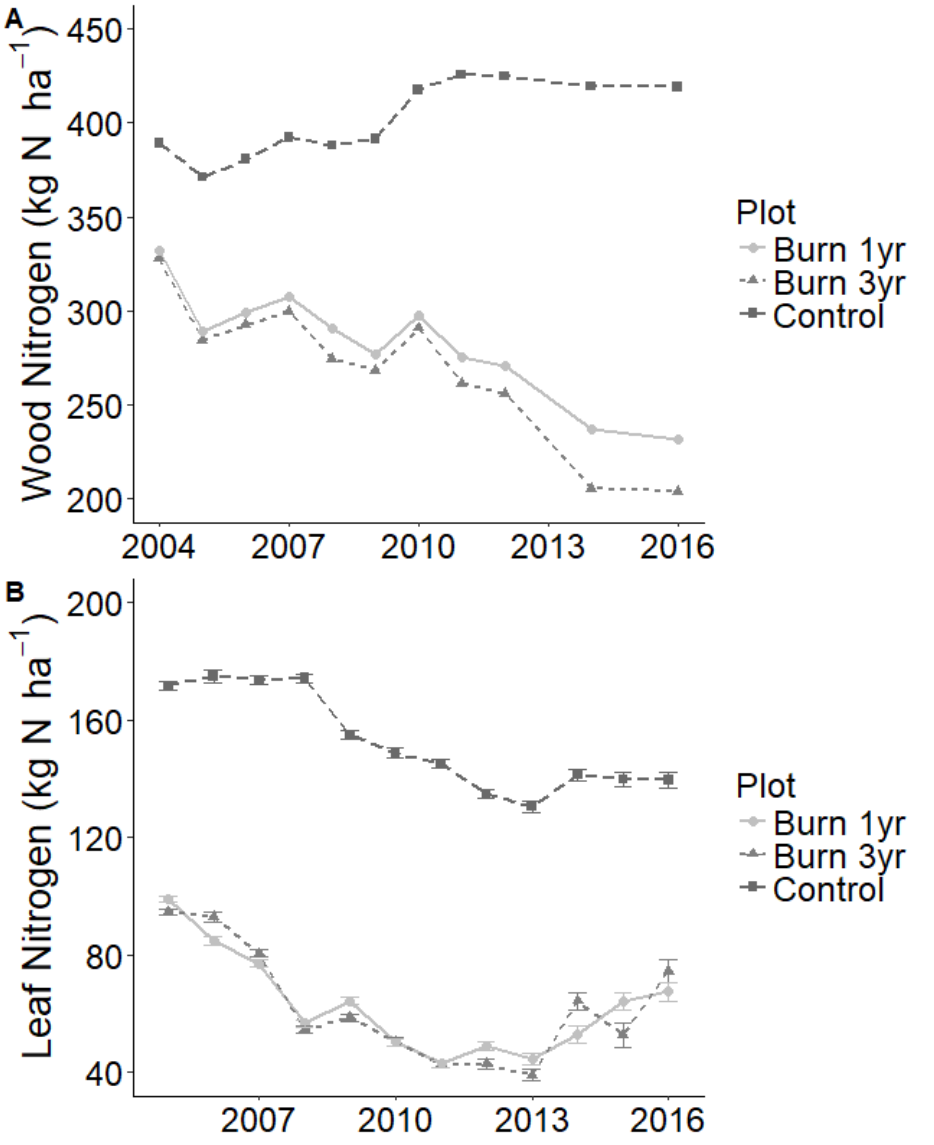

Figure 4.4. Annual wood (A) and leaf (B) N pools across the unburned (Control), triennially burned (Burn 3yr), and annually burned (Burn 1yr) forest treatments in the southeastern Amazon, with the last fires in 2010.

Table 4.2. Soil and foliar nitrogen and carbon across the experimental burn treatments. Data are means ± 1 standard error; n = 12 for soils and n = 30 for foliage. Lower-case letters indicate significant groupings in surface soils (0-2 cm) and foliage, capital letters indicate significant groups in deeper soils (2-10 cm), and daggers (†, ‡) indicate if there are differences between soil depths between each group ($p < 0.05$).

	Soil					**Foliage**				
Treatment	Depth	%N*	$\delta^{15}N$	%C*	C/N*	%N	$\delta^{15}N$	%C	C/N*	g/m^2*
Control	0-2 cm	0.28 (0.03) a, †	4.19 (0.20) a, †	4.77 (0.65) a, †	16.63 (0.53) b, †	2.11 (0.05) a	3.16 (0.16) a	50.19 (0.48) a	24.12 (0.58) b	145.9 (9.7) a
	2-10 cm	0.17 (0.01) A, ‡	5.30 (0.19) A, ‡	2.63 (0.22) A, ‡	15.28 (0.20) A, ‡					
Burn 3yr	0-2 cm	0.27 (0.04) a, †	3.88 (0.19) a, †	4.75 (0.84) a, †	17.04 (0.66) b, †	2.07 (0.07) a	3.33 (0.26) a	50.19 (0.47) a	24.96 (0.79) ab	110.9 (4.9) b
	2-10 cm	0.14 (0.02) AB, ‡	5.34 (0.26) A, ‡	2.12 (0.28) AB, ‡	15.17 (0.34) A, ‡					
Burn 1yr	0-2 cm	0.24 (0.02) a, †	4.15 (0.11) a, †	4.55 (0.43) a, †	19.01 (0.59) a, †	1.94 (0.06) a	3.07 (0.23) a	50.02 (0.53) a	26.26 (0.72) a	126.3 (5.0) ab
	2-10 cm	0.11 (0.01) B, ‡	5.73 (0.17) A, ‡	1.76 (0.15) B, ‡	15.52 (0.31) A, ‡					

*Indicates if group was ln-transformed prior to statistical tests

4.4.5. Foliar N and $\delta^{15}N$

The fire treatments did not affect foliar %N or the $\delta^{15}N$ in the burned treatments relative to the Control. The %N in leaves was similar in the Control and Burn 3yr and Burn 1yr treatments ($p = 0.11$, ANOVA) (Table 4.2, Appendix C Supplementary Table 2). Foliar $\delta^{15}N$ did not differ across treatments ($p = 0.70$, ANOVA) (Table 4.2). The C/N ratios were marginally lower in the Burn 1yr treatment compared to the Control ($p = 0.08$), but no differences were observed between the Control and the Burn 3yr treatment ($p = 0.73$).

4.4.6. Soil nutrients and characteristics

In the burned treatments, Mo and P generally increased by 50% in the top surface soil (0-2 cm), while V decreased by a third. The surface soil Mo concentration was significantly higher in the Burn 3yr treatment compared to the Control ($p = 0.0027$) but not in the Burn 1yr treatment ($p = 0.33$). The soil P concentration was significantly higher in the Burn 1yr treatment ($p = 0.034$) but not the Burn 3yr treatment ($p = 0.71$). The soil V concentrations were significantly lower in the Burn 3yr ($p = 0.0015$) and Burn 1yr treatments ($p = 0.0012$) relative to the Control. The soil P concentrations were higher in the surface soils (0-2 cm) compared to the deeper soils (2-10 cm) in both the Burn 3yr and Burn 1yr treatments ($p = 0.002$, $p = 0.0001$, respectively), but not in the Control ($p = 0.12$). The same pattern was found for Mo, where surface Mo concentrations were higher in the surface (0-2 cm) than the deeper soils (2-10 cm) for both the Burn 3yr and Burn 1yr treatments ($p = 0.028$, $p = 0.0004$) but not the Control ($p = 0.10$) (Figure 4.5, Appendix C Supplementary Table 2).

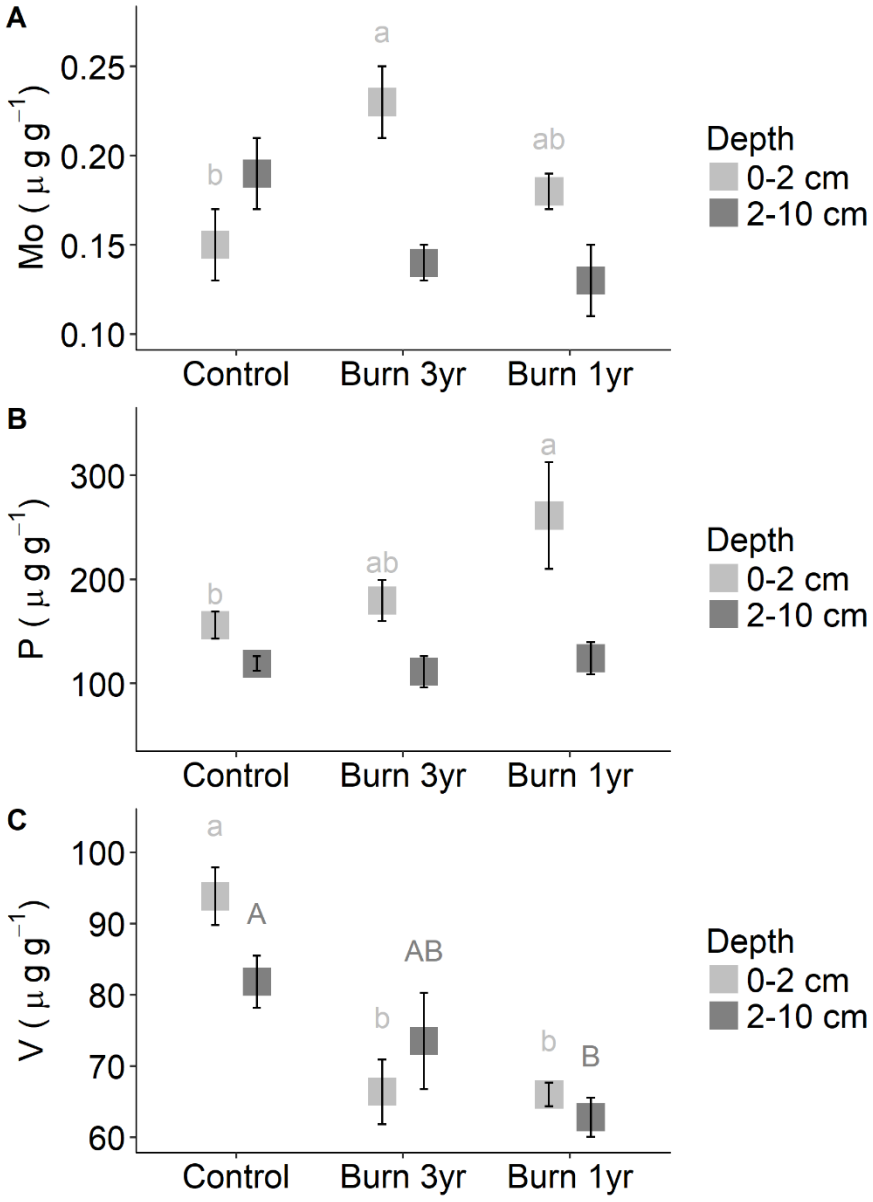

Figure 4.5. Total molybdenum (Mo) (A), phosphorus (P) (B), and vanadium (V) (C) soil concentrations (µg g^{-1} dry weight soil) across the unburned (Control), triennially burned (Burn 3yr), and annually burned (Burn 1yr) forest treatments in the southeastern Amazon; data are means ± 1 standard error; n = 12. Lower-case letters indicate significant groupings in surface soils (0-2 cm), capital letters indicate significant groupings in deeper soils (2-10 cm), and no letters indicate no significant differences ($p < 0.05$).

The fire treatments did not affect surface soil %C or %N. There were no differences in the surface soils between the Control and the Burn 3yr and Burn 1yr treatments in %C ($p = 0.99$, $p = 0.89$, respectively), %N ($p = 0.054$, $p = 0.79$, respectively), or soil $\delta^{15}N$ ($p = 0.98$, $p = 0.48$, respectively) (Table 4.2). However, the C/N ratio was significantly higher in the Burn 1yr treatment ($p = 0.0024$) compared to the Control (Table 4.2).

4.5. Discussion

4.5.1. Low rates of biological nitrogen fixation post-fire

Contrary to our hypothesis that both symbiotic and free-living BNF would ramp up post-fire to resupply the lost aboveground N, we did not find evidence of higher rates of BNF post-fire in the seasonally dry Amazon tropical forests. Though we found higher rates of symbiotic BNF in the forests burned every three years, or triennially-burned, the rates (0.48 kg N ha^{-1} yr^{-1}) were still low compared to rates found in other tropical forests. Surprisingly, rates of free-living BNF were generally higher in the unburned forest, likely because the litter and soil stay moist for a longer time, compared to the burned forests which dry out as a result of lower canopy coverage and more exposure to direct sunlight. This is consistent with the well-established observation that moisture is a key factor in supporting microbial activity and thus BNF (e.g. Koch and Oya 1974; Cusack et al. 2009). On an area basis, the higher free-living litter BNF fluxes in unburned forest plots correlated with higher litter mass (Table 4.1), suggesting that substrate availability may be an important control on free-living BNF in this system. Despite the low BNF rates in the burned treatments, recovery of the aboveground biomass N was apparent, as stocks of leaf N

in the burned forests increased from 30% to 50% of the unburned forest within three years (Figure 4). Although we did not observe recovery of the woody N pool after six years, this is likely a result of much longer recovery times for these pools—previous observations have suggested that it takes ~66 years to recover to 90% of the original mature forest cover (Poorter et al. 2016).

Our results contrasted with other studies that have found greater BNF rates in recovering secondary forests. In wet tropical forests in Panama and Costa Rica, for example, symbiotic BNF rates were higher in younger, recovering forests relative to mature forests (Batterman et al. 2013, Sullivan et al. 2014, Taylor et al. 2019). In contrast, across a land-use gradient in the Atlantic Forest of Brazil, Winbourne et al. (2018a) did not find significant differences in symbiotic BNF rates between recovering forests and mature forests, concluding that the aboveground N may have fully recovered within 20 years, equivalent to the age of the youngest forests sampled. Similarly, in a tropical dry forest chronosequence in Costa Rica, Gei (2014) concluded that BNF did not change throughout succession. The response of free-living BNF across a disturbance gradient has received less study than that of symbiotic BNF, but observations have demonstrated an increase after a disturbances in Costa Rica, where free-living BNF rates were generally higher in secondary forest compared with mature forest (Sullivan et al. 2014, Taylor et al. 2019). In contrast, Winbourne et al. (2018a) did not find a relationship between forest age and free-living BNF in the Atlantic Forest of Brazil. However, at a site most similar to ours in the Amazon, elevated inputs from symbiotic BNF during forest recovery were not detectable using foliar $\delta^{15}N$ as a proxy (Davidson et al. 2007), consistent with our findings.

Free-living and symbiotic BNF rates at our site in the southeastern Amazon were surprisingly low compared to other tropical forests. BNF rates (0.16-0.69 kg N ha^{-1} yr^{-1} across all treatments) were at least eight-fold lower than average estimates for tropical forests as a whole (5.7 kg N ha^{-1} y^{-1}) (Sullivan et al. 2014). Symbiotic BNF rates were, to our knowledge, substantially lower than all other previous estimates in wet and dry tropical forests (e.g. Batterman et al. 2013; Gei 2014; Winbourne et al. 2018a). Our estimates, however, fall closer to symbiotic BNF values estimated by Sylvester-Bradley et al. (1980) found for the central Amazon (2.5 kg N ha^{-1} yr^{-1}) and total BNF that Sullivan et al. (2014) measured in mature forest in Costa Rica (1.2 kg N ha^{-1} yr^{-1}). Free-living BNF in the soil and litter measured here ($\leq$ 0.33 kg N ha^{-1} yr^{-1}) were also substantially lower than reported values for rates in soil in another study in a lowland wet tropical forest in Costa Rica (3 kg N ha^{-1} yr^{-1} ; Reed et al. 2007) and the Venezuelan Amazon (7 kg N ha^{-1} yr^{-1}; Jordan et al. 1983), and rates in litter, ranging from <1 to 8 kg N ha^{-1} yr^{-1} (Jordan et al. 1983, Russell and Vitousek 1997, Ley and D'Antonio 1998).

The low rates of symbiotic BNF that we measured in the southeastern Amazon could in part be explained by the lower abundance of N-fixing trees compared to other tropical forests, and by the lower occurrence of nodules. In this southeastern Amazon forest, the proportion of soil cores containing nodules, *p*, ranged from 0 to 0.07, which is on the lower end compared to values found in Costa Rica where *p* ranged from 0.05 to 0.2 (Taylor et al. 2019), while the nodule fixation rates per gram of nodule measured here were well within the range found in Panama (Batterman et al. 2013). The percent stem density of the N-fixing family, *Fabaceae*, averaged 6% across all

treatments and percent basal area averaged 5% across all treatments, which was on the lower end compared to the basal area percentage range of 2.6 to 37% found in other secondary and mature forests across central America where symbiotic BNF rates were higher (Batterman et al. 2013, Sullivan et al. 2014, Winbourne et al. 2018a, Taylor et al. 2019). *Fabaceae* abundance in this region of the southeastern Amazon was also lower than in forests where symbiotic BNF has not yet been quantified, where stem percentages ranged from 3 to 13% (Ashton and CTFS Working Group 2004).

The fires consumed approximately half of the original aboveground N and likely lowered the N:P stoichiometry in this forest, but less total N was lost compared to clear-cut forests, which subsequently could not induce temporal N limitation and thus increased BNF. The fires consumed 51% of total aboveground N in the triennially burned forest, and 43% of total aboveground N in the annually burned forest relative to the unburned forest. The triennially burned forest lost more N than the annually burned forest due to increased fuel loads that accumulated during the non-burned years (Brando et al. 2014). The annually burned forest also had more grass invasion (Silvério et al. 2013) which reduced tree coverage and could perhaps explain the lower symbiotic BNF rate (0 kg N ha^{-1} yr^{-1}) compared to the triennially burned forest (0.48 kg N ha^{-1} yr^{-1}). Regardless of the differences between the burned forests, the decreased nitrate and ammonium in the burned plots (Figure 4.3) suggests a higher N demand in the burned treatments to support recovery, indicating that N availability is lower in the burned forests compared to the unburned forest.

The lower rates of BNF across the treatments could also be explained by suppression owing to high levels soil N richness here in the southeastern Amazon.

Many studies have demonstrated that BNF declines rapidly with N fertilization (e.g. Crews et al. 2000; Barron et al. 2008; Cusack et al. 2009; Winbourne et al. 2017). Crucially, substantial deep soil inorganic N pools have been found in these forests at Fazenda Tanguro. Jankowski et al. (2018) measured inorganic N accumulation of up to 230 kg N-NO_3^- + NH_4^+ ha^{-1} in the top 4 m of the soil profile, indicating a significant buildup of N in these soils that may provide an ongoing pool for biomass recovery, and precluding the need for high rates of energetically-expensive BNF. Large inorganic N pools have also been found in central Amazon (Schroth et al. 1999), making these forests across the Amazon relatively unique compared to other tropical forests where BNF has been quantified. The surface inorganic N concentrations in the unburned forest were also relatively high at our site in the southeastern Amazon, averaging a total of 37 µg and 7.5 µg NO_3^- + NH_4^+ g^{-1} (dry season and wet season, respectively). Concentrations were similarly high in the central Amazon (23 µg NO_3^- + NH_4^+ g^{-1}; Davidson et al. 2007). However, in forests with higher rates of BNF, nitrate and ammonium concentrations have been found to be both on the low end, ranging from 2 to 4 µg NO_3^- + NH_4^+ g^{-1} in mature forests in Costa Rica and the Atlantic Forest of Brazil (Sullivan et al. 2014, Winbourne et al. 2018a), or on the high end, such as found in another mature forest in Costa Rica (23 µg NO_3^- + NH_4^+ g^{-1}; Taylor et al. 2019). Regardless of the surface concentrations, the large pools of inorganic N stored in deep soils in the southeastern and central Amazon indicate a buildup of available N over time, likely suppressing the need for BNF, even after a disturbance.

Other N cycle indicators, such as foliar %N, foliar $\delta^{15}N$, and static soil N pools also indicate that N is relatively abundant in these forest soils. Martinelli et al. (1999)

found that tree species with higher N concentrations in their leaves tended to have higher $\delta^{15}N$ values, and the values measured in the southeastern Amazon fit that pattern relative to other tropical forest sites. The higher foliar %N and $\delta^{15}N$ across all treatments, ranging from 1.9 and 2.1 %N and 2.1 to 3.2‰ (Table 4.2), more closely resembled those of mature tropical forests (1.9 %N, and 3.7 ± 3.5‰, respectively; Martinelli et al. 1999) rather than those of younger forests (1.4 %N, and -0.5‰, respectively; Davidson et al. 2007). An enriched foliar $\delta^{15}N$ in mature forests has been thought to be indicative of a leaky N cycle, in which isotopically light N is lost from the ecosystem owing to fractionation during nitrification and denitrification, leaving isotopically enriched N behind (Amundson et al. 2003). In addition, although a static soil pool of N cannot indicate availability (Vitousek and Sanford 1986), Davidson et al. (2007) concluded that the top 10 cm of mineral soil contains enough organic-N stocks ($\geq$ 1000 kg N ha^{-1}) to supply the regrowing forest even if only a small fraction is gradually mineralized to a bioavailable form a site most similar to ours in the central Amazon. Although Winbourne et al. (2018a) found higher rates of BNF, they made the same conclusion, estimating that the top 10 cm of mineral soil contained approximately 1900 kg N ha^{-1} to support a majority of the forest recovery. In these southeastern Amazon forests, soils contained approximately 2100 kg N ha^{-1} in the top 10 cm, further supporting the conclusion that large stocks of soil N could support regrowing biomass after fire.

Patterns of BNF can be difficult to constrain due to BNF hotspots, defined as disproportionately high rates relative to the surrounding area (McClain et al. 2003) in space and time. First, characteristic of other biogeochemical and microbial processes,

we found hotspots of free-living BNF in the soil and litter across all plots. These may affect how this study and other studies have scaled up estimates, and future work is needed in the field to constrain error estimates and improve scaling accuracy. Free-living BNF hotspots are not unique our site and could account for a missing source of N inputs that we were unable to capture with our sampling strategy. Second, because our study only measured BNF at the 6 and 7 year mark post-fire, we do not have a complete temporal picture of BNF across time during forest recovery. Third, while most BNF occurs on the forest floor, there may have been free-living BNF in the canopy (Reed et al. 2008), and BNF associated with ants (Pinto-Tomás et al. 2009), bryophytes, lichens, and decaying wood (Matzek and Vitousek 2003) unaccounted for. Lastly, because symbiotic BNF is notoriously difficult to scale up, our survey may not have sampled enough cores to accurately represent the forest (Winbourne et al. 2018b).

4.5.2. Increases of soil molybdenum, phosphorus, and pH, and decreases in vanadium post-fire

Molybdenum (Mo) and P concentrations were relatively low across in the southeastern Amazon, which makes the lack of response in BNF to increased Mo and P post-fire more surprising. Due to non-existent parent material weathering and low atmospheric inputs in these southeastern Amazon forests, average Mo and P concentrations were low in the unburned surface soils, averaging 0.15 and 16 μg g^{-1}, respectively, and substantially depleted with respect to their average crustal abundance worldwide (Taylor and McLennan 1995). The scarcity of tropical soil Mo values generally make it difficult to assess these concentrations in a broader context, but we

note that the mineral soil Mo concentrations at this site are lower than concentrations found at other tropical sites (Reed et al. 2013, Winbourne et al. 2017), and that total P concentrations in these soils were also low compared to other tropical sites (e.g. Wurzburger et al. 2012; Sullivan et al. 2014). The P concentrations found in this study were consistent with ranges found here previously examining P dynamics (Riskin et al. 2013). While V is relatively abundant in these soils, very little is known about the soil V distributions in tropical soils. Even at higher soil Mo and P concentrations, Mo and P limitation have been demonstrated for free-living BNF (Wurzburger et al. 2012, Reed et al. 2013, Winbourne et al. 2017).

Despite generally low concentrations of both rock-derived nutrients compared to other tropical forests, Mo and P limitation are likely not the main reasons for low rates of BNF in the southeastern Amazon. The increased concentrations of soil Mo and P should have facilitated higher rates of BNF if BNF was limited by Mo or P. Our results of increased Mo post-fire add to growing evidence of increased rock-derived nutrients in surface soils following fire, as found by Kauffman et al. (1995) and Garcia-Montiel et al. (2000). Interestingly, given that accumulation from ash is the likely mechanism behind this observation, we found that V concentrations decreased post-fire, even though V has a relatively high temperature of volatilization compared with the other elements (Wang and Tomita 2003). Instead, this effect may be explained as a result of interactions between V and sulfur (S), since S is more easily lost during combustion (Kauffman et al. 1995).

Further, we also hypothesized that the increased soil pH in the burned plots also could theoretically reduce pH effects on Mo and P availability, making them

more available for microbial activity. The forest soils in the southeastern Amazon are highly acidic at pH 4, which affects Mo and P formation of chemical complexes and sorption to soils (Haynes 1982, Reddy and Gloss 1993). We found that burning did increase pH, consistent with previous observations in tropical forests and woodlands where burning tends to raise the soil pH as ash is deposited on the soil surface and more cations are released, which raises the base saturation and thus the soil pH (Kauffman et al. 1992, Nardoto and Bustamante 2003). Regardless, despite the increase in soil pH, as well as the increase in Mo and P concentrations, we still did not see an increase in free-living BNF seven years following the last fires.

4.5.3. Biological nitrogen fixation and nitrogen cycling in the southeastern Amazon

In the tropics, high rates of BNF are often associated with large ecosystem N losses, which support ongoing N demand BNF (Hedin et al. 2009). But compared to other tropical sites, measurements at our site in the southeastern Amazon indicate that hydrologic and gaseous N losses are generally very low. Previous work at this site found low N losses through leaching, and to the atmosphere through denitrification to nitrous oxide (N_2O) and dinitrogen (N_2) (Figure 4.6). Riskin et al. (2017) estimated N leaching losses from mature forest sites at Fazenda Tanguro to average 0.07 ± 0.02 kg NO_3^--N ha^{-1} yr^{-1} and 0.25 ± 0.10 kg NH_4^+-N ha^{-1} yr^{-1}, while gaseous N losses were estimated to be 0.75 kg N_2O-N ha^{-1} yr^{-1} (O'Connell 2015). Dinitrogen emissions are likely low because the soils are well-drained and because of the long dry season (Figueira et al. 2016), but nitric oxide (NO) emissions may be a more important loss, since NO emissions were found to exceed N_2O emissions in the nearby Cerrado region

on similar soils with a slightly drier climate (Varella et al. 2004, Figueira et al. 2016). Dissolved organic N (DON) can account for the majority of nitrogen losses from some tropical forests (Perakis and Hedin 2002), but while DON has not yet been measured, at a similar site in central Rondônia, Brazil, DON made up 54–65% of total N exports in forest streams (Neill et al. 2001). The gaseous and hydrologic losses of N in this region contrast with the high N losses found at other tropical sites: for example, losses of nitrate totaling 4-6 kg NO_3^--N ha^{-1} yr^{-1} in Costa Rica (Newbold et al. 1995) and denitrification losses ranging from 2-9 kg N ha^{-1} yr^{-1} across many other sites (Houlton et al. 2006). In addition, N deposition is likely low in this region, about < 1 kg N ha^{-1} yr^{-1} according to estimates found by Germer et al. (2009). In summary, the relatively low losses of N from this region indicate that aside from disturbance, relatively little excess N from BNF is required.

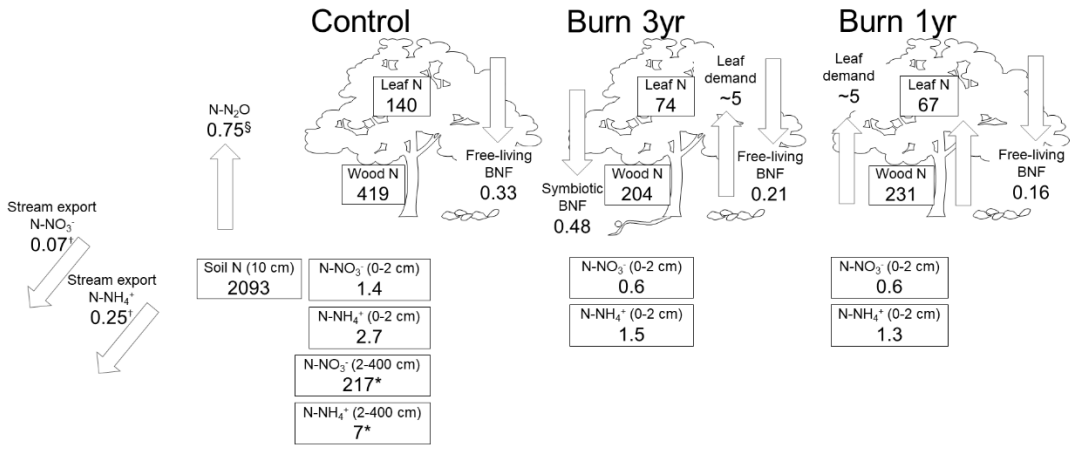

Figure 4.6. Diagram of the pools of N (outlined in black boxes) in 2016, six years after the last fires, and fluxes (grey arrows) in 2016 and 2017, six and seven years after the last fires across the unburned (Control), triennially burned (Burn 3yr), and annually burned (Burn 1yr) forest treatments in the southeastern Amazon. Components include leaf, wood, nitrate ($N\text{-}NO_3^-$), and ammonium ($N\text{-}NH_4^+$). Fluxes include inputs through free-living and symbiotic BNF, and average excess annual leaf demand compared to the unburned forest. On the left, soil stocks, inputs, and outputs measured at Tanguro are also presented for the unburned forest. All values are presented as kg N ha^{-1} for pools and kg N ha^{-1} yr^{-1} for fluxes. See discussion on estimated dinitrogen (N_2), nitric oxide (NO), and dissolved organic N (DON) fluxes, and ammonia (NH_3) deposition.

§ O'Connell 2015
† Riskin and others 2017
* Jankowski and others 2018

We conclude that this region of the southeastern Amazon is characterized by a relatively 'closed' N cycle with low inputs from BNF and low hydrologic and gaseous losses (Figure 4.6). Recent studies that have noted the heterogeneity of tropical forests (Townsend et al. 2008) where some forests do not follow the conventional N-rich paradigm of tropical N biogeochemistry (Soper et al. 2017). Within the Amazon, our results were consistent with the conclusion of Nardoto et al. (2014) that most *Fabaceae* species that are capable of nodulating do not fix N in Amazonia. They suggest that soil N stocks may have built up over the millennia, so while inputs and outputs are currently low, the mass of N stored in the soils remains high. Nardoto et al.

(2014) further suggest that *Fabaceae* proliferated in South America 50 Mya, and likely historically fixed N which led to an accrual of N stocks, which currently suppresses BNF. Perhaps the tectonic stability in this region and across the lower Amazon as a whole can reconcile why, for example, Panama, which has a relatively similar soil N percentage (Batterman et al. 2013), and Costa Rica, with high soil nitrate and ammonium concentrations (Taylor et al. 2019), are still characterized by high BNF rates.

The aboveground N recovery and relatively abundant soil inorganic N we observed highlight the potential resilience and lack of severe nutrient limitation following fire disturbance in some tropical forests. The relatively rapid recovery of nutrient cycling is consistent with findings by a recent meta-analysis looking at patterns of biogeochemical recuperation (Sullivan et al. 2019). However, this study raises new questions: are low BNF rates more common in some tropical forests than previously thought? What drives some systems to exhibit a more 'closed' N cycle, while others exhibit leakier cycling? What controls patterns of BNF that can reconcile the variation in rates measured across the tropics? Further studies will shed light on patterns of BNF, and the possible role of tectonic history as suggested by Nardoto et al. (2014) in explaining broader biogeochemical processes across ecosystems.

Acknowledgements

We thank Louis Derry and Greg McLwee (Cornell University, Earth and Atmospheric Sciences); and Melanie Hayn (Cornell University Ecology and Evolutionary Biology); Richard McHorney (Marine Biological Laboratory); Stephen Parry (Cornell Statistical Consulting Unit); Darlisson Nunes, Maria Lucia Nascimento,

Raimundo Mota Quintino, Leonardo Maracahipes dos Santos, and Sebastião Aviz do Nascimento for the field help (Instituto de Pesquisa Ambiental da Amazônia); Hillary Sullivan, Paul Lefebvre, and Lindsay Scott (Woods Hole Research Center); Kim Sparks (COIL); Joy Winbourne and Ben Sullivan for sampling method development, and Fiona Soper for comments on the manuscript. Access to field site was provided by Grupo André Maggi and IPAM. We also thank Luiz Martinelli for the foliar analysis. Funding was provided by Mario Einaudi and Cornell University travel grants, Sigma Xi (Cornell Chapter), Paul P. Feeny Fund, the Andrew W. Mellon Grant, and the Cornell University Program in Cross-Scale Biogeochemistry and Climate (NSF-IGERT, DGE-1069193) and the Atkinson Center for a Sustainable Future.

4.6. References

Aguiar, A. P. D., I. C. G. Vieira, T. O. Assis, E. L. Dalla-Nora, P. M. Toledo, R. A. Oliveira Santos-Junior, M. Batistella, A. S. Coelho, E. K. Savaget, L. E. O. C. Aragão, C. A. Nobre, and J. P. H. Ometto. 2016. Land use change emission scenarios: Anticipating a forest transition process in the Brazilian Amazon. Global Change Biology 22:1821–1840.

Amundson, R., A. T. Austin, E. A. G. Schuur, K. Yoo, V. Matzek, C. Kendall, A. Uebersax, D. Brenner, and W. T. Baisden. 2003. Global patterns of the isotopic composition of soil and plant nitrogen. Global Biogeochemical Cycles 17:1–5.

Andreae, M. O., and P. Merlet. 2001. Emission of trace gases and aerosols from biomass burning. Global Biogeochemical Cycles 15:955–966.

Aragão, L. E. O. C., L. O. Anderson, M. G. Fonseca, T. M. Rosan, L. B. Vedovato, F. H. Wagner, C. V. J. Silva, C. H. L. Silva Junior, E. Arai, A. P. Aguiar, J. Barlow, E. Berenguer, M. N. Deeter, L. G. Domingues, L. Gatti, M. Gloor, Y. Malhi, J. A. Marengo, J. B. Miller, O. L. Phillips, and S. Saatchi. 2018. 21st Century drought-related fires counteract the decline of Amazon deforestation carbon emissions. Nature Communications 9:1–12.

Aragão, L. E. O. C., B. Poulter, J. B. Barlow, L. O. Anderson, Y. Malhi, S. Saatchi, O. L. Phillips, and E. Gloor. 2014. Environmental change and the carbon balance of Amazonian forests. Biological Reviews 89:913–931.

Ashton, P. S., and CTFS Working Group. 2004. Floristics and Vegetation of the Forest Dynamics Plots. Pages 90–118 in E. C. Losos and E. F. Leigh, Jr., editors. Tropical Forest Diversity and Dynamics. University of Chicago Press, Chicago.

Balch, J. K., D. C. Nepstad, P. M. Brando, L. M. Curran, O. Portela, O. de Carvalho, and P. Lefebvre. 2008. Negative fire feedback in a transitional forest of southeastern Amazonia. Global Change Biology 14:2276–2287.

Balch, J. K., D. C. Nepstad, L. M. Curran, P. M. Brando, O. Portela, P. Guilherme, J. D. Reuning-Scherer, and O. de Carvalho Jr. 2011. Size, species, and fire behavior predict tree and liana mortality from experimental burns in the Brazilian Amazon. Forest Ecology and Management 261:68–77.

Barron, A. R., N. Wurzburger, J. P. Bellenger, S. J. Wright, A. M. L. Kraepiel, and L. O. Hedin. 2009. Molybdenum limitation of asymbiotic nitrogen fixation in tropical forest soils. Nature Geoscience 2:42–45.

Batterman, S. A., L. O. Hedin, M. Van Breugel, J. Ransijn, D. J. Craven, and J. S. Hall. 2013. Key role of symbiotic dinitrogen fixation in tropical forest secondary succession. Nature 502:224–227.

Bellenger, J.-P., Y. Xu, X. Zhang, F. M. M. Morel, and A. M. L. Kraepiel. 2014. Possible contribution of alternative nitrogenases to nitrogen fixation by asymbiotic N_2-fixing bacteria in soils. Soil Biology and Biochemistry 69:413–420.

Brando, P. M., J. K. Balch, D. C. Nepstad, D. C. Morton, F. E. Putz, M. T. Coe, D. Silvério, M. N. Macedo, E. A. Davidson, C. C. Nóbrega, A. Alencar, and B. S. Soares-Filho. 2014. Abrupt increases in Amazonian tree mortality due to drought-fire interactions. Proceedings of the National Academy of Sciences of the United States of America 111:6347–52.

Casals, P., J. Romanya, and V. R. Vallejo. 2005. Short-term nitrogen fixation by legume seedlings and resprouts after fire in Mediterranean old-fields. Biogeochemistry 76:477–501.

Chave, J., M. Réjou-Méchain, A. Búrquez, E. Chidumayo, M. S. Colgan, W. B. C. Delitti, A. Duque, T. Eid, P. M. Fearnside, R. C. Goodman, M. Henry, A. Martínez-Yrízar, W. A. Mugasha, H. C. Muller-Landau, M. Mencuccini, B. W. Nelson, A. Ngomanda, E. M. Nogueira, E. Ortiz-Malavassi, R. Pélissier, P. Ploton, C. M. Ryan, J. G. Saldarriaga, and G. Vieilledent. 2014. Improved allometric models to estimate the aboveground biomass of tropical trees. Global Change Biology 20:3177–3190.

Cochrane, M. A. 2001. Synergistic interactions between habitat fragmentation and fire in evergreen tropical forests. Conservation Biology 15:1515–1521.

Cochrane, M. A., and M. D. Schulze. 1999. Fire as a recurrent event in tropical forests of the Eastern Amazon: Effects on Forest Structure, Biomass, and Species Composition. Biotropica 31:2–16.

Cox, P. M., R. A. Betts, C. D. Jones, S. A. Spall, and I. J. Totterdell. 2000. Acceleration of global warming due to carbon-cycle feedbacks in a coupled climate model. Nature 408:184–187.

Crews, T. E., H. Farrington, and P. M. Vitousek. 2000. Changes in asymbiotic, heterotrophic nitrogen fixation on leaf litter of metrosideros polymorpha with long-term ecosystem development in Hawaii. Ecosystems 3:386–395.

Cusack, D., W. Silver, and W. McDowell. 2009. Biological nitrogen fixation in two tropical forests: ecosystem-level patterns and effects of nitrogen fertilization. Ecosystems 12:1299–1315.

Darnajoux, R., X. Zhang, D. L. McRose, J. Miadlikowska, F. Lutzoni, A. M. L. Kraepiel, and J. P. Bellenger. 2017. Biological nitrogen fixation by alternative nitrogenases in boreal cyanolichens: importance of molybdenum availability and implications for current biological nitrogen fixation estimates. New Phytologist 213:680–689.

Davidson, E. A., C. J. R. de Carvalho, A. M. Figueira, F. Y. Ishida, J. P. H. B. Ometto, G. B. Nardoto, R. T. Sába, S. N. Hayashi, E. C. Leal, I. C. G. Vieira, and L. A. Martinelli. 2007. Recuperation of nitrogen cycling in Amazonian forests following agricultural abandonment. Nature 447:995–998.

Davidson, E. A., D. Markewitz, R. de O. Figueiredo, and P. B. de Camargo. 2018. Nitrogen Fixation Inputs in Pasture and Early Successional Forest in the Brazilian Amazon Region: Evidence From a Claybox Mesocosm Study. Journal of Geophysical Research: Biogeosciences 123:712–721.

Delitti, W. B. C., M. Meguro, and J. G. Pausas. 2006. Biomass and mineralmass estimates in a "cerrado" ecosystem. Brazilian Journal of Botany 29:531–540.

Figueira, A. M. e. S., E. A. Davidson, R. C. Nagy, S. H. Riskin, and L. A. Martinelli. 2016. Isotopically constrained soil carbon and nitrogen budgets in a soybean field chronosequence in the Brazilian Amazon region. Journal of Geophysical Research: Biogeosciences 121:2520–2529.

Garcia-Montiel, D. C., C. Neill, J. Melillo, S. Thomas, P. A. Steudler, and C. C. Cerri. 2000. Soil Phosphorus Transformations Following Forest Clearing for Pasture in the Brazilian Amazon. Soil Science Society of America Journal 64:1792–1804.

Gehring, C., P. L. G. Vlek, L. A. G. De Souza, and M. Denich. 2005. Biological nitrogen fixation in secondary regrowth and mature rainforest of central Amazonia. Agriculture, Ecosystems and Environment 111:237–252.

Gei, M. G. 2014. Biological nitrogen fixation in tropical dry forests of Costa Rica: patterns and controls:1–221.

Gei, M., D. M. A. Rozendaal, L. Poorter, F. Bongers, J. I. Sprent, M. D. Garner, T. M. Aide, J. L. Andrade, P. Balvanera, J. M. Becknell, P. H. S. Brancalion, G. A. L. Cabral, R. G. César, R. L. Chazdon, R. J. Cole, G. D. Colletta, B. De Jong, J. S. Denslow, D. H. Dent, S. J. Dewalt, J. M. Dupuy, S. M. Durán, M. M. Do Espírito Santo, G. W. Fernandes, Y. R. F. Nunes, B. Finegan, V. G. Moser, J. S. Hall, J. L. Hernández-Stefanoni, A. B. Junqueira, D. Kennard, E. Lebrija-Trejos, S. G. Letcher, M. Lohbeck, E. Marín-Spiotta, M. Martínez-Ramos, J. A. Meave, D. N. L. Menge, F. Mora, R. Muñoz, R. Muscarella, S. Ochoa-Gaona, E. Orihuela-Belmonte, R. Ostertag, M. Peña-Claros, E. A. Pérez-García, D. Piotto, P. B. Reich, C. Reyes-García, J. Rodríguez-Velázquez, I. E. Romero-Pérez, L. Sanaphre-Villanueva, A. Sanchez-Azofeifa, N. B. Schwartz, A. S. De Almeida, J. S. Almeida-Cortez, W. Silver, V. De Souza Moreno, B. W. Sullivan, N. G. Swenson, M. Uriarte, M. Van Breugel, H. Van Der Wal, M. D. D. M. Veloso, H. F. M. Vester, I. C. G. Vieira, J. K. Zimmerman, and J. S. Powers. 2018. Legume abundance along successional and rainfall gradients in Neotropical forests. Nature Ecology and Evolution 2:1104–1111.

Germer, S., C. Neill, T. Vetter, J. Chaves, A. V. Krusche, and H. Elsenbeer. 2009.

Implications of long-term land-use change for the hydrology and solute budgets of small catchments in Amazonia. Journal of Hydrology 364:349–363.

Hardy, R. W. F., R. D. Holsten, E. K. Jackson, and R. C. Burns. 1968. The Acetylene - Ethylene Assay for N_2 Fixation: Laboratory and Field Evaluation. Plant Physiology 43:1185–1207.

Haynes, R. J. 1982. Effects of liming on phosphate availability in acid soils - A critical review. Plant and Soil 68:289–308.

Hedin, L. O., E. N. J. Brookshire, D. N. L. Menge, and A. R. Barron. 2009. The Nitrogen Paradox in Tropical Forest Ecosystems. Annual Review of Ecology, Evolution, and Systematics 40:613–635.

Hedin, L. O., P. M. Vitousek, and P. A. Matson. 2003. Nutrient losses over four million years of tropical forest development. Ecology 84:2231–2255.

Houlton, B. Z., D. M. Sigman, and L. O. Hedin. 2006. Isotopic evidence for large gaseous nitrogen losses from tropical rainforests. Proceedings of the National Academy of Sciences of the United States of America 103:8745–8750.

INPE. (n.d.). Taxas anuais de desmatamento na Amazônia Legal Brasileira (AMZ). http://www.obt.inpe.br/prodes/dashboard/prodes-rates.html.

Ivanauskas, N. M., R. Monteiro, and R. R. Rodrigues. 2003. Alterations following a fire in a forest community of Alto Rio Xingu. Forest Ecology and Management 184:239–250.

Jankowski, K. J., C. Neill, E. A. Davidson, M. N. Macedo, C. Costa, G. L. Galford, L. Maracahipes Santos, P. Lefebvre, D. Nunes, C. E. P. Cerri, R. McHorney, C. O'Connell, and M. T. Coe. 2018. Deep soils modify environmental consequences of increased nitrogen fertilizer use in intensifying Amazon agriculture. Scientific Reports 8:1–11.

Jean, M. E., K. Phalyvong, J. Forest-Drolet, and J. P. Bellenger. 2013. Molybdenum and phosphorus limitation of asymbiotic nitrogen fixation in forests of Eastern Canada: Influence of vegetative cover and seasonal variability. Soil Biology and Biochemistry 67:140–146.

Jordan, C., W. Caskey, G. Escalante, R. Herrera, F. Montagnini, R. Todd, and C. Uhl. 1983. Nitrogen Dynamics during Conversion of Primary Amazonian Rain Forest to Slash and Burn Agriculture. Oikos 40:131–139.

Kauffman, J. B., D. L. Cummings, D. E. Ward, and R. Babbitt. 1995. Fire in the Brazilian Amazon: 1. Biomass, nutrient pools, and losses in slashed primary forests. Oecologia 104:397–408.

Kauffman, J. B., K. M. Till, and R. W. Shea. 1992. Biogeochemistry of Deforestation

and Biomass Burning. Pages 428–456 in O'Brien and Dunnette, editors. The Science of Global Change. ACS Symposium Series, Washington D.C.

Koch, B. L., and J. Oya. 1974. Non-symbiotic nitrogen fixation in some Hawaiian pasture soils. Soil Biology and Biochemistry 6:363–367.

Ley, R. E., and C. M. D'Antonio. 1998. Exotic grass invasion alters potential rates of N fixation in Hawaiian woodlands. Oecologia 113:179–187.

Mahowald, N. M., P. Artaxo, A. R. Baker, T. D. Jickells, G. S. Okin, J. T. Randerson, and A. R. Townsend. 2005. Impacts of biomass burning emissions and land use change on Amazonian atmospheric phosphorus cycling and deposition. Global Biogeochemical Cycles 19:1–15.

Martin, A. R., D. L. Erickson, W. J. Kress, and S. C. Thomas. 2014. Wood nitrogen concentrations in tropical trees: phylogenetic patterns and ecological correlates. New Phytologist 204:484–495.

Martinelli, L. A., M. C. Piccolo, A. R. Townsend, P. M. Vitousek, E. Cuevas, W. McDowell, G. P. Robertson, O. C. Santos, and K. Treseder. 1999. Nitrogen stable isotopic composition of leaves and soil: Tropical versus temperate forests. Biogeochemistry 46:45–65.

Matzek, V., and P. Vitousek. 2003. Nitrogen fixation in bryophytes, lichens, and decaying wood along a soil-age gradient in Hawaiian montane rain forest. Biotropica 35:12–19.

McClain, M. E., E. W. Boyer, C. L. Dent, S. E. Gergel, N. B. Grimm, P. M. Groffman, S. C. Hart, J. W. Harvey, C. A. Johnston, E. Mayorga, W. H. McDowell, and G. Pinay. 2003. Biogeochemical Hot Spots and Hot Moments at the Interface of Terrestrial and Aquatic Ecosystems. Ecosystems 6:301–312.

McGrath, D. A., C. K. Smith, H. L. Gholz, and F. de Assis Oliveira. 2001. Effects of Land-Use Change on Soil Nutrient Dynamics in Amazônia. Ecosystems 4:625–645.

Nardoto, G. B., and M. M. D. C. Bustamante. 2003. Effects of fire on soil nitrogen dynamics and microbial biomass in savannas of Central Brazil. Pesquisa Agropecuaria Brasileira 38:955–962.

Nardoto, G. B., C. A. Quesada, S. Patiño, G. Saiz, T. R. Baker, M. Schwarz, F. Schrodt, T. R. Feldpausch, T. F. Domingues, B. S. Marimon, B.-H. Marimon Junior, I. C. G. Vieira, M. Silveira, M. I. Bird, O. L. Phillips, J. Lloyd, and L. A. Martinelli. 2014. Basin-wide variations in Amazon forest nitrogen-cycling characteristics as inferred from plant and soil 15N:14N measurements. Plant Ecology & Diversity 7:173–187.

Neary, D. G., C. C. Klopatek, L. F. DeBano, and P. F. Ffolliott. 1999. Fire effects on

belowground sustaibablity: a review and synthesis. Forest Ecology and Management 122:51–71.

Neill, C., L. A. Deegan, S. M. Thomas, and C. C. Cerri. 2001. Deforestation for pasture alters nitrogen and phosphorus in small Amazonian streams. Ecological Applications 11:1817–1828.

Neill, C., M. C. Piccolo, P. A. Steudler, J. M. Melillo, B. J. Feigl, and C. C. Cerri. 1995. Nitrogen dynamics in soils of forests and active pastures in the western Brazilian Amazon Basin. Soil Biol. Biochem. 27:1167–1175.

Newbold, J. D., B. W. Sweeney, J. K. Jackson, and L. A. Kaplan. 1995. Concentrations and export of solutes from six mountain streams in northwestern Costa Rica. Journal of the North American Benthological Society 14:21–37.

O'Connell, C. S. 2015. Ecological Tradeoffs to an Agricultural Amazonia: Investigating the effects of increased agricultural production on Amazonia's contribution to global climate and nitrogen. University of Minnesota, ProQuest Dissertations Publishing, 2015. 3746826.

Pan, Y., R. A. Birdsey, J. Fang, R. Houghton, P. E. Kauppi, W. A. Kurz, O. L. Phillips, A. Shvidenko, S. L. Lewis, J. G. Canadell, P. Ciais, R. B. Jackson, S. W. Pacala, A. D. McGuire, S. Piao, A. Rautiainen, S. Sitch, and D. Hayes. 2011. A large and persistent carbon sink in the world's forests. Science 333:988–993.

Perakis, S. S., and L. O. Hedin. 2002. Nitrogen loss from unpolluted South American forests mainly via dissolved organic compounds. Nature 415:416–419.

Pinto-Tomás, A. A., M. A. Anderson, G. Suen, D. M. Stevenson, F. S. T. Chu, W. W. Cleland, P. J. Weimer, and C. R. Currie. 2009. Symbiotic Nitrogen Fixation in the Fungus Gardens of Leaf-Cutter Ants. Science 326:1120–1123.

Poorter, L., F. Bongers, T. M. Aide, A. M. Almeyda Zambrano, P. Balvanera, J. M. Becknell, V. Boukili, P. H. S. Brancalion, E. N. Broadbent, R. L. Chazdon, D. Craven, J. S. De Almeida-Cortez, G. A. L. Cabral, B. H. J. De Jong, J. S. Denslow, D. H. Dent, S. J. DeWalt, J. M. Dupuy, S. M. Durán, M. M. Espírito-Santo, M. C. Fandino, R. G. César, J. S. Hall, J. L. Hernandez-Stefanoni, C. C. Jakovac, A. B. Junqueira, D. Kennard, S. G. Letcher, J. C. Licona, M. Lohbeck, E. Marín-Spiotta, M. Martínez-Ramos, P. Massoca, J. A. Meave, R. Mesquita, F. Mora, R. Munõz, R. Muscarella, Y. R. F. Nunes, S. Ochoa-Gaona, A. A. De Oliveira, E. Orihuela-Belmonte, M. Penã-Claros, E. A. Pérez-Garciá, D. Piotto, J. S. Powers, J. Rodríguez-Velázquez, I. E. Romero-Pérez, J. Ruíz, J. G. Saldarriaga, A. Sanchez-Azofeifa, N. B. Schwartz, M. K. Steininger, N. G. Swenson, M. Toledo, M. Uriarte, M. Van Breugel, H. Van Der Wal, M. D. M. Veloso, H. F. M. Vester, A. Vicentini, I. C. G. Vieira, T. V. Bentos, G. B. Williamson, and D. M. A. Rozendaal. 2016. Biomass resilience

of Neotropical secondary forests. Nature 530:211–214.

Projeto, R. 1981. Folha SD.22 Goiàs. Page Geologia, geomorphologia, pedologia, vegetaçao, uso potencial da terra. Rio de Janeiro: Ministério das Minas e Energia, Departamento Nacional de Mineral, Fundução, Rio de Janeiro, Brasil.

Quesada, C. A., J. Lloyd, L. O. Anderson, N. M. Fyllas, M. Schwarz, and C. I. Czimczik. 2011. Soils of Amazonia with particular reference to the RAINFOR sites. Biogeosciences 8:1415–1440.

Reddy, K. J., and S. P. Gloss. 1993. Geochemical speciation as related to the mobility of F , Mo and Se in soil leachates. Applied Geochemistry 8:159–163.

Reed, S. C., C. C. Cleveland, and A. R. Townsend. 2007. Controls Over Leaf Litter and Soil Nitrogen Fixation in Two Lowland Tropical Rain Forests. Biotropica 39:585–592.

Reed, S. C., C. C. Cleveland, and A. R. Townsend. 2008. Tree species control rates of free-living nitrogen fixation in a tropical rain forest. Ecology 89:2924–34.

Reed, S. C., C. C. Cleveland, and A. R. Townsend. 2013. Relationships among phosphorus, molybdenum and free-living nitrogen fixation in tropical rain forests: results from observational and experimental analyses. Biogeochemistry 114:135–147.

Riskin, S. H., C. Neill, K. Jankowski, A. V. Krusche, R. McHorney, H. Elsenbeer, M. N. Macedo, D. Nunes, and S. Porder. 2017. Solute and sediment export from Amazon forest and soybean headwater streams. Ecological Applications 27:193–207.

Riskin, S. H., S. Porder, C. Neill, A. M. e Silva Figueira, C. Tubbesing, and N. Mahowald. 2013. The fate of phosphorus fertilizer in Amazon soya bean fields. Philosophical Transactions of the Royal Society B: Biological Sciences 368:1–10.

Rocha, W., D. B. Metcalfe, C. E. Doughty, P. Brando, D. Silvério, K. Halladay, D. C. Nepstad, J. K. Balch, and Y. Malhi. 2014. Ecosystem productivity and carbon cycling in intact and annually burnt forest at the dry southern limit of the Amazon rainforest (Mato Grosso, Brazil). Plant Ecology and Diversity 7:25–40.

Russell, A. E., and P. M. Vitousek. 1997. Decomposition and potential nitrogen fixation in Dicranopteris linearis litter on Mauna Loa, Hawai'i. Journal of Tropical Ecology 13:579–594.

Sanches, L., C. M. A. Valentini, O. B. Pinto Júnior, J. de S. Nogueira, G. L. Vourlitis, M. S. Biudes, C. J. da Silva, P. Bambi, and F. de A. Lobo. 2008. Seasonal and interannual litter dynamics of a tropical semideciduous forest of the southern

Amazon Basin, Brazil. Journal of Geophysical Research: Biogeosciences 113:1–9.

Schroth, G., L. F. da Silva, R. Seixas, W. Geraldes, J. L. V. Macêdo, and W. Zech. 1999. Subsoil accumulation of mineral nitrogen under polyculture and monoculture plantations, fallow and primary forest in a ferralitic Amazonian upland soil. Agriculture, Ecosystems and Environment 75:109–120.

Silvério, D. V., P. M. Brando, J. K. Balch, F. E. Putz, D. C. Nepstad, C. Oliveira-Santos, and M. C. Bustamante. 2013. Testing the Amazon savannization hypothesis: fire effects on invasion of a neotropical forest by native cerrado and exotic pasture grasses. Philosophical Transactions of the Royal Society B: Biological Sciences 368:1–8.

Soper, F. M., P. G. Taylor, W. R. Wieder, S. R. Weintraub, C. C. Cleveland, S. Porder, and A. R. Townsend. 2017. Modest Gaseous Nitrogen Losses Point to Conservative Nitrogen Cycling in a Lowland Tropical Forest Watershed. Ecosystems 21:901–912.

ter Steege, H., N. C. A. Pitman, O. L. Phillips, J. Chave, D. Sabatier, A. Duque, J. F. Molino, M. F. Prévost, R. Spichiger, H. Castellanos, P. Von Hildebrand, and R. Vásquez. 2006. Continental-scale patterns of canopy tree composition and function across Amazonia. Nature 443:444–447.

Sullivan, B. W., R. L. Nifong, M. K. Nasto, S. Alvarez-Clare, C. Dencker, F. M. Soper, K. T. Shoemaker, F. Y. Ishida, J. Zaragoza-Castells, E. A. Davidson, and C. C. Cleveland. 2019. Biogeochemical recuperation of lowland tropical forest during succession. Ecology, in press:e02641.

Sullivan, B. W., W. K. Smith, A. R. Townsend, M. K. Nasto, S. C. Reed, R. L. Chazdon, and C. C. Cleveland. 2014. Spatially robust estimates of biological nitrogen (N) fixation imply substantial human alteration of the tropical N cycle. Proceedings of the National Academy of Sciences of the United States of America 111:8101–6.

Sylvester-Bradley, R., L. A. de Oliveira, J. A. de Podestá Filho, and T. V. St. John. 1980. Nodulation of legumes, nitrogenase activity of roots and occurrence of nitrogen-fixing Azospirillum ssp. in representative soils of central Amazonia. Agro-Ecosystems 6:249–266.

Taylor, B. N., R. L. Chazdon, and D. N. L. Menge. 2019. Successional dynamics of nitrogen fixation and forest growth in regenerating Costa Rican rainforests. Ecology, in press e02637.

Taylor, S. R., and S. M. McLennan. 1995. The geochemical evolution of the continental crust. Reviews of Geophysics 33: 241-256.

Townsend, A. R., G. P. Asner, and C. C. Cleveland. 2008. The biogeochemical

heterogeneity of tropical forests. Trends in Ecology and Evolution 23:424–431.

Uhl, C., and J. B. Kauffman. 1990. Deforestation, fire susceptibility, and potential tree responses to fire in the eastern Amazon. Ecology 71:437–449.

Varella, R. F., M. M. C. Bustamante, A. S. Pinto, K. W. Kisselle, R. V. Santos, R. A. Burke, R. G. Zepp, and L. T. Viana. 2004. Soil fluxes of CO2, CO, NO, and N2O from and old pasture and from native savanna in Brazil. Ecological Applications 14:S221–S231.

Vitousek, P. M. 1984. Litterfall, nutrient cycling, and nutrient fimitation in tropical forests. Ecology 65:285–298.

Vitousek, P. M., K. Cassman, C. Cleveland, T. Crews, C. B. Field, N. B. Grimm, R. W. Howarth, R. Marino, L. Martinelli, E. B. Rastetter, and J. I. Sprent. 2002. Towards an ecological understanding of biological nitrogen fixation. Biogeochemistry 57/58:1–45.

Vitousek, P. M., and R. W. Howarth. 1991. Nitrogen limitation on land and in the sea: how can it occur? Biogeochemistry 13:87–115.

Vitousek, P. M., and R. L. Sanford. 1986. Nutrient Cycling in Moist Tropical Forest. Annual Review of Ecology and Systematics 17:137–167.

Wang, J., and A. Tomita. 2003. A chemistry on the volatility of some trace elements during coal combustion and pyrolysis. Energy and Fuels 17:954–960.

Winbourne, J. B., S. W. Brewer, and B. Z. Houlton. 2017. Iron controls over di-nitrogen fixation in karst tropical forest. Ecology 98:773–781.

Winbourne, J. B., A. Feng, L. Reynolds, D. Piotto, M. G. Hastings, and S. Porder. 2018a. Nitrogen cycling during secondary succession in Atlantic Forest of Bahia, Brazil. Scientific Reports 8:1–9.

Winbourne, J. B., M. T. Harrison, B. W. Sullivan, S. Alvarez-Clare, S. R. Lins, L. Martinelli, M. Nasto, D. Piotto, S. Rolim, M. Wong, and S. Porder. 2018b. A New Framework for Evaluating Estimates of Symbiotic Nitrogen Fixation in Forests. The American Naturalist 192:618–629.

Wright, S. J., B. L. Turner, J. B. Yavitt, K. E. Harms, M. Kaspari, E. V. J. Tanner, J. Bujan, E. A. Griffin, J. R. Mayor, S. C. Pasquini, M. Sheldrake, and M. N. Garcia. 2018. Plant responses to fertilization experiments in lowland, species-rich, tropical forests. Ecology 99:1129–1138.

Wurzburger, N., J. P. Bellenger, A. M. L. Kraepiel, and L. O. Hedin. 2012. Molybdenum and phosphorus interact to constrain asymbiotic nitrogen fixation in tropical forests. PloS one 7:1–7.

Yelenik, S., S. Perakis, and D. Hibbs. 2013. Regional constraints to biological nitrogen fixation in post-fire forest communities. Ecology 94:739–750.

CHAPTER 5 . TREES CAPABLE OF SUPPORTING SYMBIOTIC NITROGEN FIXATION RECRUIT AND GROW FASTER AFTER FOREST FIRES IN THE SOUTHEASTERN AMAZON

Authors

Wong, Michelle Y.[1*], Christopher Neill[2], Divino V. Silvério[3], Paulo M. Brando[2,3], Roxanne Marino[1], Robert W. Howarth[1,2].

[1]Department of Ecology and Evolutionary Biology, Cornell University, Ithaca, NY 14853, U.S.A.
[2]Woods Hole Research Center, Falmouth, MA 02450, U.S.A.
[3]Instituto de Pesquisa Ambiental da Amazônia, Brasília-DF, Brazil

5.1. Summary

Recovering secondary tropical forests are an important part of terrestrial land carbon sink. Plant species in the *Fabaceae* family that are capable of supporting symbiotic nitrogen fixation, or potential N fixers, are abundant in tropical forests, and may play an important role early in forest recovery. However, the early demographic trends of recruitment, mortality, and growth of potential N-fixing species have not yet been investigated after tropical forest fires. We used a census from a large-scale fire experiment in the southeastern Amazon (2004-2016) to investigate the successional patterns of non-fixers and potential N fixers post-fire and test the hypothesis that potential N-fixing species are more competitive than non-fixers early in succession. We found that post-fire, potential N fixer abundance and basal area percentage increased relative to the mature control forest, particularly in the smaller size classes. This pattern was driven by a higher recruitment rate of potential N fixers in the burned forests and faster growth rates of potential N fixers relative to non-fixers, as well as lower mortality of N fixers in the burned relative to the mature forest. Most of the

demographic processes were driven by one potential N-fixing species, *Tachigali vulgaris*, which is common in the Cerrado and southern Amazon biomes. However, nodule surveys and indirect isotopic evidence suggest that *T. vulgaris* was not fixing N in our forest. Future studies examining the demographic processes of potential N-fixing species should determine if the species are actively fixing N before using the functional trait of N fixation. Potential N fixers could have a competitive advantage over non-fixers early in succession from a higher water-use efficiency and higher leaf N, rather than symbiotic N fixation alone.

5.2. Introduction

Secondary tropical forests are fast-growing, accumulate large amounts of carbon, and play an important role in regulating climate (Pan et al. 2011, Poorter et al. 2016). More than half the world's tropical forests are in secondary recovery (FAO 2015), and rates of forest recovery of may be linked to nitrogen (N) supply (Davidson et al. 2007, Wright et al. 2018). Tropical forests are thought to recover N stocks relatively rapidly in part because they are characterized by a high abundance of leguminous trees in the *Fabaceae* family, some of which can form symbiotic relationships with bacteria to fix atmospheric N (potential N fixers). Rates of symbiotic N fixation in wet tropical forests have been measured to be up to 50-150 kg N ha^{-1} yr^{-1} (Binkley and Giardina 1997), much higher than other biomes (Cleveland et al. 1999). In recovering wet tropical forests, higher abundances of potential N-fixing trees and higher rates of symbiotic N fixation relative to mature, intact forests indicate the important role that N-fixers may have in bringing in new N to the ecosystem during regrowth (Batterman et al. 2013, Sullivan et al. 2014). However, less is known

about the role of potential N fixers and associated symbiotic N fixation early in succession in seasonally dry tropical forests.

Tropical forest fires are occurring more often, particularly in the southern Amazon where interactions of deforestation, drought, and agriculture are increasing forest vulnerability to fires (Uhl and Kauffman 1990, Cochrane 2001). In seasonally dry tropical forests, potential N fixers are often found in even higher abundances than in wet tropical forests, perhaps due to their reduced leaflet size and thereby drought tolerance, as well as their ability to fix N (Gei et al. 2018). Aside from symbiotic N fixation, N fixers as a functional group may still have a competitive advantage over non-fixers, since plants in the *Fabaceae* family typically exhibit higher water use efficiencies and higher foliar N, which could lead to higher drought tolerance, seed N, and plant defenses (Adams et al. 2016). Frequent disturbance by fire may favor N fixers over non-fixers because of higher growth rates under N-limited conditions resulting from N losses via fire (Sheffer et al. 2015). For example, in savanna biomes, fire has been found to increase both N-fixing species richness and the abundance of N fixers relative to non-fixers (Högberg 1986, Da Silva and Batalha 2008, Cramer et al. 2010, Silva et al. 2013). However, there are limited data on successional trends of potential N-fixing trees in seasonally dry tropical forests, and no studies to our knowledge that examine how fire affects the growth, recruitment, and mortality of species capable of fixing N in comparison to non-fixers. Higher growth and recruitment, or lower mortality of potential N fixers could enhance their abundances later in succession and impact the trajectory of forest development.

The abundance of potential N-fixers early in succession can also impact the

growth of the neighboring non-fixers, either stimulating growth through provision of limiting N (Batterman et al. 2013) or depressing growth through competition for light, water and other resources (Taylor et al. 2019). The impact of potential N-fixers on the growth of neighbors was mixed in other wet tropical forests in Panama, perhaps because the potential N fixers were not all actively fixing N. Many N-fixing species are facultative, and only fix N when N is in low abundance (Barron et al. 2011) because symbiotic N fixation is an energetically-expensive process (Gutschick 1981). In the present study, we tested the relationship between the abundance of N fixers and the growth of neighboring non-fixers in a seasonally-dry tropical forest. Because the abundance of potential N fixers does not always reflect ecosystem N fixation rates (Hedin et al. 2009), we also sought to resolve the links between N fixer abundance and associated N fixation status.

Across Amazonia, indirect isotopic data from mature forests suggests that most N fixers usually do not fix N even though they have a capability to do so (Nardoto et al. 2014). Here we ask, after fire disturbance in a seasonally dry tropical forest in the southeastern Amazon, do trees capable fixing N grow faster, die more frequently, or recruit faster than trees without the capability of fixing N? And are there effects of potential N-fixing trees on the growth rates of neighboring plants, or the forest as a whole? We further examine the extent to which potential N-fixing species are actually fixing N, especially following fires. For example, do N losses during fires constrain soil N supply enough to stimulate facultative N fixers to fix N? Results will help us predict the successional trends across different tropical forests, and examine which patterns are generalizable across tropical forests. These results may improve our

ability to predict how secondary tropical forests will play a role in the global carbon sink, particularly in seasonally dry tropical forests like those in the southeastern Amazon that face disturbance by fire.

5.3. Methods

5.3.1. Study Area

The forest inventory used here was collected from a fire experiment at Fazenda Tanguro, an 800 km^2 working ranch in eastern Mato Grosso State, Brazil. Fazenda Tanguro contains 400 km^2 of predominantly primary evergreen tropical forest. It is 30 km north of the southern boundary of the Amazon forest (13°04' S, 52°23' W). The average annual air temperature is 27°C with < 5°C seasonal variation. Annual rainfall is 1700 mm (Appendix D Supplementary Table 1), with an intense dry season between May and September. Forest tree species composition represents a transition between the central Amazon forest and the more seasonal savannah of the Cerrado (Ivanauskas et al. 2003).

5.3.2. Fire treatments

To test tropical forest susceptibility to fire, a prescribed fire experiment was initiated at Fazenda Tanguro in 2004. Three 0.5 x 1 km (50 ha) plots were established with three treatments: (1) an unburned control, (2) a plot burned three times three years apart, in 2004, 2007, and 2010 (Burn 3yr), and a plot burned annually from 2004 to 2010 (except 2008) (Burn 1yr). Experimental fires were ignited at the end of the dry season when forests of the region are most susceptible to fire. Initial fires were of low-intensity and slow-moving (Balch et al. 2008) typical of tropical understory forest fires (Cochrane and Schulze 1999). For the initial fires, mean flame height was 31 (±1) cm,

with a mean initial temperature that ranged from 128°C belowground (2 cm) to 273°C at the surface to 87°C aboveground (100 cm). The fire in the Burn 3yr treatment during 2007 was more severe than the Burn 1yr treatment because of extreme dry conditions due to drought and increased fuel load from accumulated litterfall (Brando and others 2014). By 2009, the cumulative tree mortality (≥ 5 cm) was 63% in the Burn 3yr treatment and 50% in the Burn 1yr treatment (Brando et al. 2014). Balch and others (2008) provide a further description of the site, experimental design, and fire behavior.

5.3.3. Tree inventory

To compare potential N fixers to non-fixers in growth, recruitment, and mortality, in 2004 (pre-treatment) we identified, tagged, mapped species, and estimated the height of all overstory trees (≥ 40 cm dbh) within each 50 ha treatment plot. Intermediate sized trees and lianas (20–39.9 cm dbh) were tagged in belt transects (500 × 20 m) at 0, 30, 100, 250, 500, and 750 m from the forest edge (5.5 ha sampled per treatment). Nested sub-sampling (500 × 4 m) was conducted within these belt transects to measure smaller trees and lianas (10–19.9 cm) (1.2 ha sampled per treatment). To sample saplings (5.0–9.9 cm), plots (500 × 2.5 m) were also nested within these belt transects (Appendix D Supplementary Figure 1). Individuals (≥ 5 cm) were tagged and inventoried in 2004, 2006, and 2008. Those individuals and new recruits were monitored and measured for their diameter at breast height (1.3 m; dbh) of in 2008, 2010, 2011, 2012, 2014, and 2016. In addition, recruits were monitored in 2007. Stems were measured to the nearest 0.1 cm for dbh, and were recorded as dead if there was no visible aboveground live tissue, or if only basal sprouts were alive.

5.3.4. Potential N-fixing taxa classification

Because not all leguminous plants can form a symbiotic relationship with rhizobia, we used a three-tiered approach to assign tree species as either capable or incapable of supporting symbiotic N fixation, “potential N fixers” or “non-fixers”, respectively. First, species listed in the appendix of Sprent (2009) are confirmed as capable of symbiotic N fixation. Second, we compared our species list with Tedersoo *et al.* (2018), who list genera in the *Fabaceae* family that are capable of forming the symbiosis. Third, we searched individual papers for all the *Fabaceae* species in ourinventory to find presence of nodulation capability (Moreira, Fatima Maria de Souza, da Silva and de Faria 1992, Haddad et al. 2004, Batterman et al. 2013, Nasto et al. 2014, Silva et al. 2015) (Table 5.1). Note that hereafter we designate as “potential N-fixers” species that are capable of supporting N fixation even if they are not actively fixing N.

Table 5.1. *Fabaceae* and confirmed nitrogen (N)-fixing species at Fazenda Tanguro, Mato Grosso, Brazil, in the southeastern Amazon

Genus	**Species**	**% of *Fabaceae***	**N fixer classification** (Sprent 2009)	**N fixer classification by citation**	**N fixer classification** (Tedersoo et al. 2018)
Derris	*floribunda (Bth.) Ducke*	1	no	NA	Rhizobia
Enterolobium	*schomburgkii (Benth.) Benth.*	11	yes	(Moreira, Fatima Maria de Souza, da Silva and de Faria 1992)	likely Rhizobia
Hymenaea	*courbaril L.*	5	no	(Moreira, Fatima Maria de Souza, da Silva and de Faria 1992)	None
Inga	*alba (SW.) Willd.*	1	yes	(Nasto et al. 2014)	Rhizobia
Inga	*thibaudiana*	1	yes	(Batterman et al. 2013)	Rhizobia
Inga	*heterophylla Willd.*	9	yes	(Moreira, Fatima Maria de Souza, da Silva and de Faria 1992)	Rhizobia
Ormosia	*paraensis Ducke.*	10	yes	(Silva et al. 2015)	Rhizobia
Tachigali (Sclerolobium)	*vulgaris (paniculatum Vog.)*	61	yes	(Haddad et al. 2004)	likely Rhizobia
Diplotropis	*purpurea (Rich.) Am. Var.Leptophylla (kleinh) Am.*	2	yes	(Moreira, Fatima Maria de Souza, da Silva and de Faria 1992)	Rhizobia
Machaerium	*quinata (Aubl) Sndw.*	0.1	yes	(Moreira, Fatima Maria de Souza, da Silva and de Faria 1992)	Rhizobia

5.3.5. Calculations

To compare potential N fixers to non-fixers, we calculated relative potential N fixer abundance (stem percentage) over time, proportion of recruits as potential N fixers, recruitment rates of potential N fixers and non-fixers, and mortality rates of potential N fixers and non-fixers across all treatments. We calculated the relative potential N fixer abundance as the percentage of individual trees that were potential N fixers surviving for each inventory year, or time, *t*. The number of stems was

calculated from the total number of surviving individuals in the database at time *t*.

$$S_{fixer,}(\%) = \frac{N_{fixer,t}}{N_{total,t}}\ x\ 100$$

The basal area ($m^2\ ha^{-1}$) of potential N fixers and non-fixers was calculated by using the individual diameters of trees and aggregating all individuals per plot (m^2), for each size class, and dividing by the area sampled (ha). The basal area percentage of potential N fixers was calculated by dividing by the total forest basal area at each time *t*.

$$BA\ (m^2) = \frac{\pi(\frac{dbh}{2})^2}{10000}$$

The proportion of total recruits as potential N fixers for each year *t* was calculated by examining the proportion of new recruits as potential N fixers at time *t* added into the inventory after 2006.

$$R_{fixer,}(\%) = \frac{R_{fixer,t}}{R_{total,t}}\ x\ 100$$

Recruitment rate was calculated as an annual or biennial event following Menge & Chazdon (2016). The recruitment rate, presented as a percentage of the number of individuals $N_{p,f,t}$, from the previous census and with $R_{p,f,t+1}$ representing the number of individuals ≥5 cm of N fixer or non-fixer, *f*, in each plot, *p*, that appeared from *t* to *t* + 1. Here, we designate one plot as one transect within each treatment (Appendix D Supplementary Figure 1).

$$r_{p,f,t+1}(\%) = \frac{R_{p,f,t+1}}{N_{p,f,t}}\ x\ 100$$

The growth rate ($cm\ yr^{-1}$) was calculated following Taylor et al. (2017),

$$G_{i,c+1} = \frac{dbh_{i,t+1}\, dbh_{i,t}}{t}$$

where G*i,t* is the growth rate of individual, *i*, at time t, and dbh_{ic} is the dbh of individual *i* at time *t*, and *t* is number of years between surveys.

Mortality (% yr^{-1}) was calculated following Balch et al. (2011) and Sheil & May (1996),

$$m_f = 1 - \left(1 - \frac{D}{N}\right)^{\frac{1}{t}} x\ 100$$

where N is the initial number of live stems, D is the number of dead stems at the end of the measurement interval, *t* is the number of years between censuses, and the mortality is calculated for *f*, either potential N fixers or non-fixers.

5.3.6. Nodule sampling and NDFA

To confirm that the potential N-fixing species formed nodules and were actively fixing N, we conducted nodule surveys around the base of 42 potential N-fixing trees. During the 2017 wet season, we excavated soil within a 2 m diameter around the base of 16 potential N-fixing trees to search for nodules in the field, but we did not find nodules. In the 2018 wet season, we randomly sampled 12 cores (5.7 cm diameter and 10 cm deep) following (Barron et al. 2011, Wurzburger and Hedin 2016), around a total of 26 trees of potential N-fixers (Appendix D Supplementary Table 3). We brought soils back into the laboratory to sieve and examine for nodules. When we did find nodules, nodules were confirmed as active by conducting the acetylene reduction assay (Barron et al. 2011) and measuring ethylene production (Chapter 4). Gas samples were collected and returned to Cornell University where ethylene concentrations were measured using a Shimadzu 8-A gas chromatograph

equipped with a flame ionization detector (330°C) and a Porapak-N 80/100 column at 70°C.

We also quantified foliar N and $\delta^{15}N$ for 21 trees of potential N fixers to quantify the proportion of N derived from the atmosphere (NDFA), an indirect indicator of N fixation (Nardoto et al. 2014) (Appendix D Supplementary Table 4). Leaf samples were collected from a subset of the potential N-fixing species at Fazenda Tanguro in 2018 using a slingshot. We collected three individual branches at the top of the canopy from each individual tree. For reference non-fixers, we sampled three individual trees of each species of the ten most dominant species (Balch et al. 2008) across the three plots, for a total of 90 individual trees. Leaves were collected, weighed for dry weight after storage in an oven two days at 65°C, and analyzed for surface area using a LI-COR LI-3100C Area Meter. Dried leaf samples were ground and measured for N and $\delta^{15}N$ on a Delta Plus, ThermoQuest-Finnigan analyzer at the University of São Paulo, Piracicaba.

5.3.7. Statistical analyses

We compared the potential N fixer basal area percentage, percentage of potential N fixer recruits from 2008 to 2016, recruitment rates, and mortality rates using linear mixed-effects models with the transect, treated as a plot, added as a random effect for individuals ≤ 40 cm. We use random effects to account for the variability that occurs among transects within a forest plot. The percentage values were analyzed by log-transforming (+1) values. For potential N fixer basal area percent and percent of N fixer recruits, treatment and size class were analyzed as factors, including their interaction. Recruitment rate was also analyzed with treatment

and size class as factors, and a third factor indicating potential N fixer or non-fixer functional type. Mortality rate was analyzed with treatment and functional type as factors, including their interaction. To test whether potential N fixer abundance affected the growth of a forest as a whole, we analyzed the relationship between N fixer basal area percent and the change in total basal area and non-fixer basal area (net and percent change) using a linear mixed-effects model the regressions. Foliar %N, $\delta^{15}N$, and NDFA were analyzed using a one-way ANOVA with the potential N-fixing species as the factor. To test for species differences in formation of nodules, we treated nodule presence or absence as a categorical variable in a generalized linear model with binomial distribution and a maximum likelihood estimation. Post-hoc analyses were conducted with a Tukey test. We inspected residuals visually by examining QQ plots to check for normal distribution and investigate heteroscedasticity. Statistical analyses were performed using R software v.3.0.3 (R Development Core Team).

5.4. Results

5.4.1. Potential N-fixing species

Of the ~97 species at these sites in the southeastern Amazon, ten were classified as leguminous plants in the *Fabaceae* family; eight of these were classified as potential N fixers according to Sprent, (2009) and Tedersoo *et al.*, (2018) and seven of these ten were classified as potential N fixers according to the other literature sources we compiled (Table 5.1).

Tachigali vulgaris (formerly identified as *Sclerobium paniculatum Vog.*) accounted for 61% of all the *Fabaceae* individuals and 78% of the stems of potential

N-fixing individuals in the inventory. Fifty-eight percent of the *T. vulgaris* were recruited into the forest (≥ 5 cm) between 2014 and 2016, driving many of the demographic patterns post fire.

5.4.2. Potential N fixers recruited faster post-fire

Potential N fixer abundance (i.e. relative to total number of species) increased in the burned treatments from 2004 to 2016, driven by increases in the smaller size classes. In the Burn 3yr treatment, potential N fixers increased from 2% in 2004 to 10% in 2016, and in the Burn 1yr treatment, potential N fixers increased from 2% in 2004 to 8% in 2016. In contrast, potential N fixer abundance in the Control treatment decreased from 3% in 2004 to 1% in 2016 (Figure 5.1). In the 5-9.9 cm class in the Burn 3yr treatment, potential N fixer abundance increased from 0% in 2004 to 17% in 2016, and in the Burn 1yr treatment, potential N fixer abundance increased from 1% in 2004 to 17% in 2016. In the 10-19.9 cm class, potential N fixer abundance increased from 2% in 2004 to 20% in 2016 in the Burn 3yr treatment, and from 1% in 2004 to 15% in 2016 in the Burn 1yr treatment (Figure 5.2).

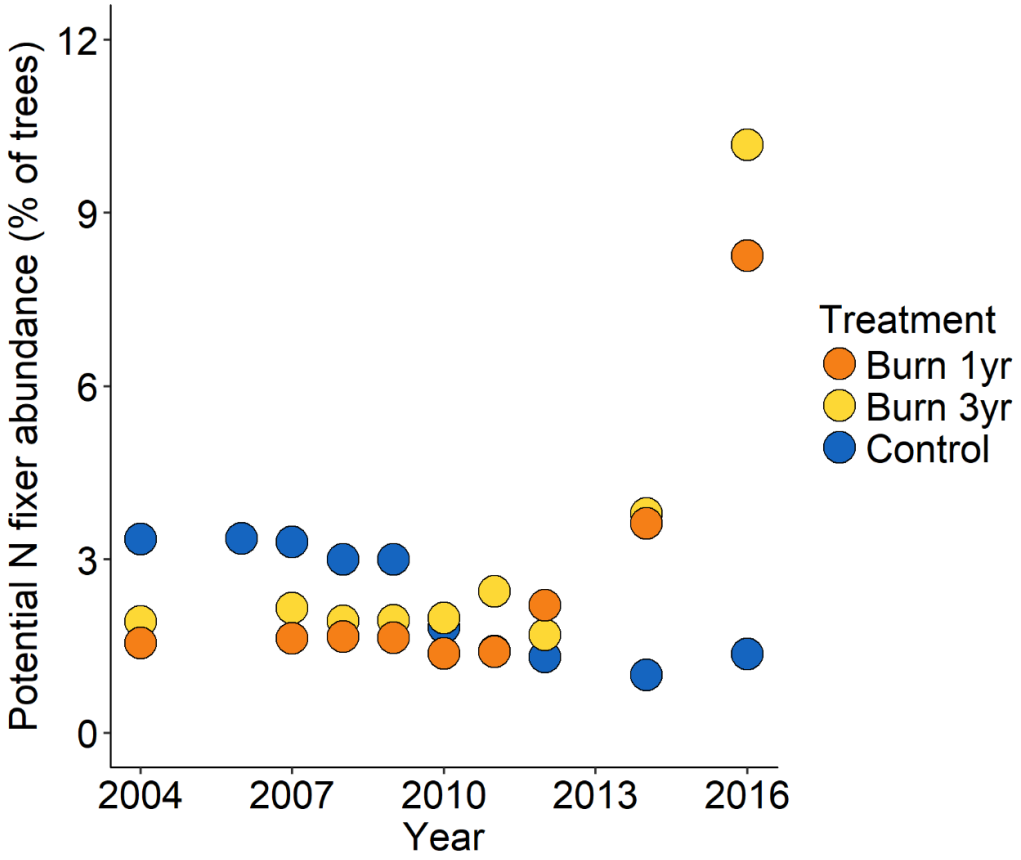

Figure 5.1. Potential nitrogen (N) fixer abundance (% of all trees) across the unburned (Control), triennially burned (Burn 3yr), and annually burned (Burn 1yr) forest treatments in the southeastern Amazon for all individuals in the tree inventory (non-fixer abundance would be 100% minus these values). The fires occurred between 2004 and 2010, except 2008 in the annually burned forest.

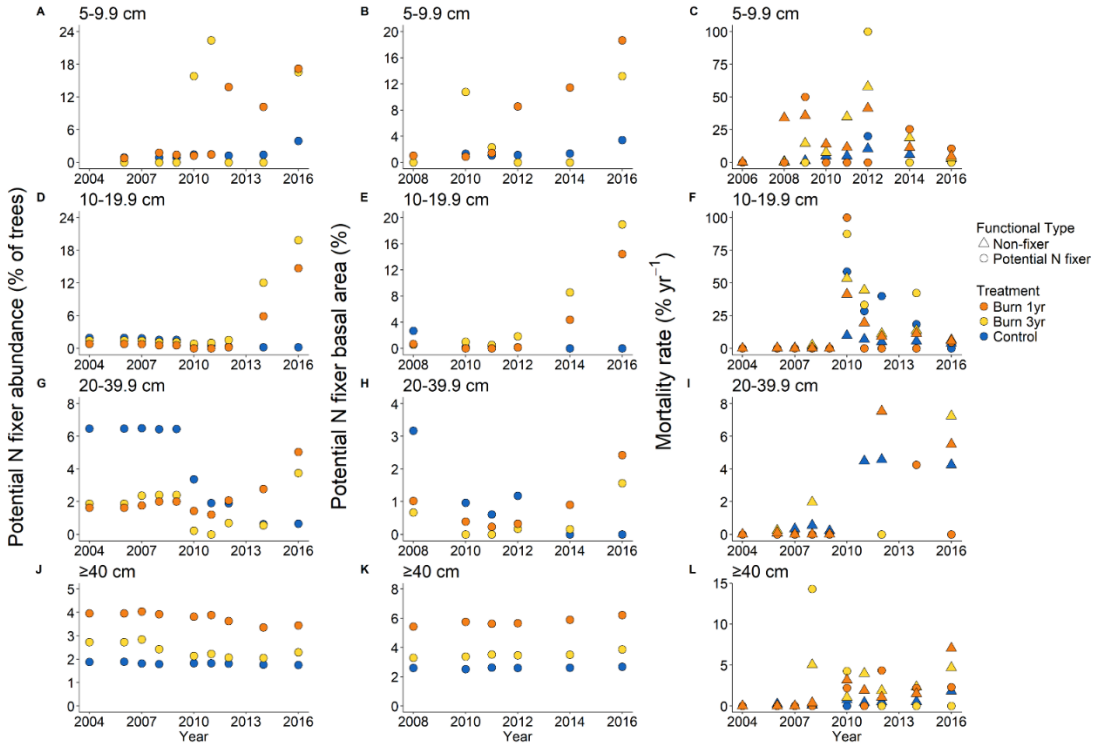

Figure 5.2. Potential nitrogen (N) fixer abundance (% of all trees) for all individuals in for the size classes 5-9.9 cm (A), 10-19.9 cm (D), 20-39.9 cm (G), and ≥ 40 cm (J) (non-fixer abundance would be 100% minus these values), potential N fixer basal area (%) 5-9.9 cm (B), 10-19.9 cm (E), 20-39.9 cm (H), and ≥ 40 cm (K), and mortality rate (% yr^{-1}) for the size classes 5-9.9 cm (C), 10-19.9 cm (F), 20-39.9 cm (I), and ≥ 40 cm (L) across the unburned (Control), triennially burned (Burn 3yr), and annually burned (Burn 1yr) forest treatments in the southeastern Amazon. The fires occurred between 2004 and 2010, except 2008 in the annually burned forest.

The increase in potential N fixer abundance in the burned treatments relative to the Control was driven both by a higher proportion of potential N fixers among recruits in the burned treatments and by higher total recruitment in the burned treatments. When aggregating across all transects, the proportion of potential N fixers as new recruits was about five times higher in the 5-9.9 cm class in the Burn 3yr treatment ($p = 0.035$) and seven times higher in the Burn 1yr treatment ($p = 0.0018$) relative to the Control. In the 10-19.9 cm class, the proportion of potential N fixers of the new recruits was approximately 20 times higher in the Burn 3yr treatment ($p = 0.015$) and in the Burn 1yr treatment ($p = 0.0035$) relative to the Control (Table 5.2).

Table 5.2. Mean proportion of potential N fixers as new recruits from 2006 to 2016 (n = 8), and mean potential N fixer basal area from 2004 to 2016 (n = 48) for all size classes across the unburned (Control), triennially burned (Burn 3yr), and annually burned (Burn 1yr) forest treatments in the southeastern Amazon. Data are means ± 1 standard error. Letters indicate significant differences ($p < 0.05$).

Treatment	Potential N fixer recruits (%)			Potential N fixer basal area (%)		
	5-9.9 cm	10-19.9 cm	20-39.9 cm	5-9.9 cm	10-19.9 cm	20-39.9 cm
Control	5.34 (2.13)[b]	0.62 (0.42)[b]	2.15 (1.36)[b]	1.28 (0.36)[b]	0.64 (0.35)[b]	1.91 (0.74)[a]
Burn 3yr	25.01 (8.77)[a]	14.05 (3.22)[a]	25.63 (13.11)[a]	12.70 (5.18)[a]	16.43 (4.49)[a]	3.35 (2.57)[a]
Burn 1yr	36.99 (7.15)[a]	11.94 (4.16)[a]	20.22 (5.81)[a]	8.34 (2.27)[a]	6.25 (2.04)[a]	1.82 (0.54)[a]

The recruitment rate was also higher for potential N fixers than non-fixers in the burned treatments. In the Control treatment, the recruitment rate of potential N fixers was not significantly different compared to non-fixers (5-9.9 cm, $p = 0.66$; 10-19.9 cm, $p = 0.10$; 20-39.9 cm, $p = 0.35$). In contrast, in the smallest size class (5-9.9 cm), the recruitment rate of potential N fixers was 9.1 times higher than non-fixers in the Burn 1yr treatment ($p = 0.0004$), with no differences in the Burn 3yr treatment ($p = 0.85$), likely due to the high variation in recruitment rates between transects for the potential N fixers. In the 10-19.9 cm size class, the recruitment rate of potential N fixers was 2.7 times higher than non-fixers in the Burn 3yr treatment ($p = 0.0028$) and 19 times higher for the Burn 1yr treatment ($p = 0.028$) (Table 5.3).

Table 5.3. Mean annual recruitment rate of potential N fixers and non-fixers from 2004 to 2016 for the size classes between 5 and 39.9 cm across the unburned (Control), triennially burned (Burn 3yr), and annually burned (Burn 1yr) forest treatments in the southeastern Amazon. Recruitment rate was calculated for each transect (plot) for each functional type for each time step only if there were individuals in transect at time t. Data are means ± 1 standard error. Letters indicate significant differences between N fixers and non-fixers within their respective size classes and treatments ($p < 0.05$).

Treatment	Functional Type	*n*	5-9.9 cm	*n*	10-19.9 cm	*n*	20-39.9 cm
Control	Potential N fixer	9	34.26 (13.8)[a]	10	12.83 (8.4)[a]	12	0.90 (0.6)[a]
	Non-fixer	31	67.21 (42.0)[a]	45	19.71 (4.9)[a]	46	2.23 (0.5)[a]
Burn 3yr	Potential N fixer	6	359.05 (348.2)[a]	14	140.97 (50.3)[a]	9	12.47 (8.6)[a]
	Non-fixer	28	156.22 (76.9)[a]	42	52.38 (30.6)[b]	40	3.79 (2.5)[a]
Burn 1yr	Potential N fixer	8	178.33 (61.1)[a]	8	238.96 (168.1)[a]	14	31.86 (10.5)[b]
	Non-fixer	32	19.60 (11.1)[b]	46	12.47 (5.0)[b]	43	108.09 (106.4)[a]

5.4.3. Potential N fixers increased in basal area post-fire

After 2008, potential N fixers increased in total basal area (m^2 ha^{-1}) and basal area percentage (%) relative to non-fixers in both burned treatments. In the Control treatment, the total basal area and basal area % decreased for potential N fixers from 0.76 m^2 ha^{-1} in 2008 to 0.26 m^2 ha^{-1} in 2016, or 2.9% in 2008 to 0.76% in 2016. In contrast, in the Burn 3yr treatment, the total basal area increased for potential N fixers from 0.18 m^2 ha^{-1} in 2008 to 1.18 m^2 ha^{-1} in 2016, or 1% in 2008 to 9.8% in 2016. Patterns were similar for the Burn 1yr treatment, as the potential N fixer basal area increased from 0.32 m^2 ha^{-1} in 2008 to 1.52 m^2 ha^{-1} in 2016, or from 1.4% in 2008 to 9% in 2016 (Appendix D Supplementary Figure 3).

Across transects, the basal area % of potential N fixers was significantly higher in the Burn 3yr treatment ($p = 0.0004$) and the Burn 1yr treatment ($p = 0.0008$) relative to the Control, but not between the burned treatments ($p = 0.99$). In the 5-9.9

cm size class, the basal area % was about 10 times higher in the Burn 3yr treatment ($p = 0.0971$) and 7 times higher in the Burn 1yr treatment ($p = 0.0076$) relative to the Control. In the 10-19.9 cm class, the basal area % was about 26 times higher in the Burn 3yr treatment ($p < 0.0001$) and 10 times higher than the Burn 1yr treatment ($p = 0.0074$) relative to the Control. There were no significant differences between treatments in the larger (20-39.9 cm) size class (Table 5.2).

A majority of the changes in potential N fixer basal area were driven by those in the smaller size classes because of high recruitment in the burned treatments. For example, in 2014 the 5-19.9 cm classes composed 69% and 57% of the total potential N fixer basal area in the Burn 3yr and Burn 1yr treatments, which increased in 2016 to 86% and 79% of the potential N fixer basal area in the Burn 3yr and Burn 1yr treatments. In contrast, the 5-9.9 cm class and the 10-19.9 cm class accounted for only 22% of the total basal area in 2014 and 44% of the total potential N fixer basal area in 2016 in the Control treatment (Figure 5.2).

5.4.4. Growth rates of potential N fixers were faster than non-fixers

Potential N fixers grew faster (diameter) than non-fixers overall, but this difference was observed only for the burned treatments. For example, between 2012 and 2014, potential N fixers did not grow significantly faster than non-fixers in the Control ($p = 0.12$), but grew 4.2 times faster in the Burn 3yr treatment ($p = 0.0004$), and 3.8 times faster in the Burn 1yr treatment ($p = 0.0001$); this pattern also persisted from 2014-2016. Diameter growth rates, represented by Δdbh (cm yr^{-1}), ranged between 0.32 to 0.48 cm yr^{-1} for non-fixers and between 0.73 to 2.76 cm yr^{-1} for potential N fixers (Table 5.4).

Table 5.4. Mean growth rate change in diameter at breast height Δdbh (cm yr^{-1}) of potential N fixers and non-fixers from 2012 to 2016, mean annual mortality rate (% yr^{-1}) calculated for 5-39.9 cm stems of potential N fixers and non-fixers from 2004 to 2016, and mean diameter of surviving trees ≥ 40 cm dbh (cm) across the unburned (Control), triennially burned (Burn 3yr), and annually burned (Burn 1yr) forest treatments in the southeastern Amazon. Data are means ± 1 standard error. Lower-case letters indicate significant differences between potential N fixers and non-fixers within treatments ($p < 0.05$).

Treatment	Functional Type	Mean growth rate Δdbh (cm yr^{-1})				Annual mortality rate (% yr^{-1})		Individuals ≥40 cm dbh (cm)	
		N	2012-2014	*n*	2014-2016	*n*	2004-2016	*n*	Mean dbh (cm)
Control	Potential N fixer	4	0.73 (0.11)[a]	4	0.48 (0.17)[a]	32	33.5 (6.8)[a]	19	61.29 (2.97)[a]
	Non-fixer	194	0.39 (0.02)[a]	197	0.32 (0.02)[b]	121	4.6 (0.4)[b]	1057	51.86 (0.37)[b]
Burn 3yr	Potential N fixer	3	2.76 (0.93)[a]	3	1.68 (0.56)[a]	24	45.7 (9.7)[a]	14	64.93 (5.39)[a]
	Non-fixer	95	0.66 (0.07)[b]	88	0.52 (0.07)[b]	107	23.0 (2.6)[a]	584	51.33 (0.53)[b]
Burn 1yr	Potential N fixer	4	2.74 (0.52)[a]	4	1.60 (0.27)[a]	29	28.5 (7.5)[a]	25	57.36 (2.73)[a]
	Non-fixer	127	0.73 (0.06)[b]	121	0.56 (0.05)[b]	117	15.3 (1.9)[a]	665	49.36 (0.43)[b]

5.4.5. Mortality was higher for potential N fixers than for non-fixers in the Control treatments, but not in the burned treatments

Mortality rates across all the size classes were generally higher for potential N fixers than for non-fixers, particularly in the years following the fires (Figure 5.2, Appendix D Supplementary Figure 4). When examining mortality rates across the transects and size classes, mortality was about 7.3 times higher for potential N fixers than non-fixers in the Control ($p = 0.0096$), but not statistically different in the Burn 3yr ($p = 0.71$) and Burn 1yr ($p = 0.54$) treatments (Table 5.4).

5.4.6. Potential N fixers were larger than non-fixers in older forests

Of the surviving trees greater than 40 cm, potential N fixers generally were larger than non-fixers across all treatments. N fixers ranged from 1.2 to 1.3 times larger than non-fixers, or about 10 cm on average greater in diameter (dbh). This

difference was significant between potential N fixers and non-fixers across all treatments (Control, p = 0.0005; Burn 3yr, p = 0.0001; and Burn 1yr, p = 0.0006) (Table 5.4).

5.4.7. Potential N fixer basal area (%) did not strongly affect changes in non-fixer basal area and total forest basal area (m^2 ha^{-1})

To test whether or not potential N fixers stimulate or depress the growth of non-fixers, and whether or not the whole forest grows faster when there are more N fixers, we present the effects of potential N fixer abundance on the net change in total forest and non-fixer basal area, as well as the % change. There was a slightly positive trend for total forest basal area change (m^2 ha^{-1}) (p = 0.025) with increasing N fixer basal area %. For percent change for total forest basal area, the effect of N fixer basal area % was not highly significant (p = 0.072). There was not a strong relationship between N fixer basal area % and non-fixer basal area change with (p = 0.084). This was also consistent for the effect of N fixer basal area % on the percent change for non-fixer basal area (p = 0.28) (Figure 5.3).

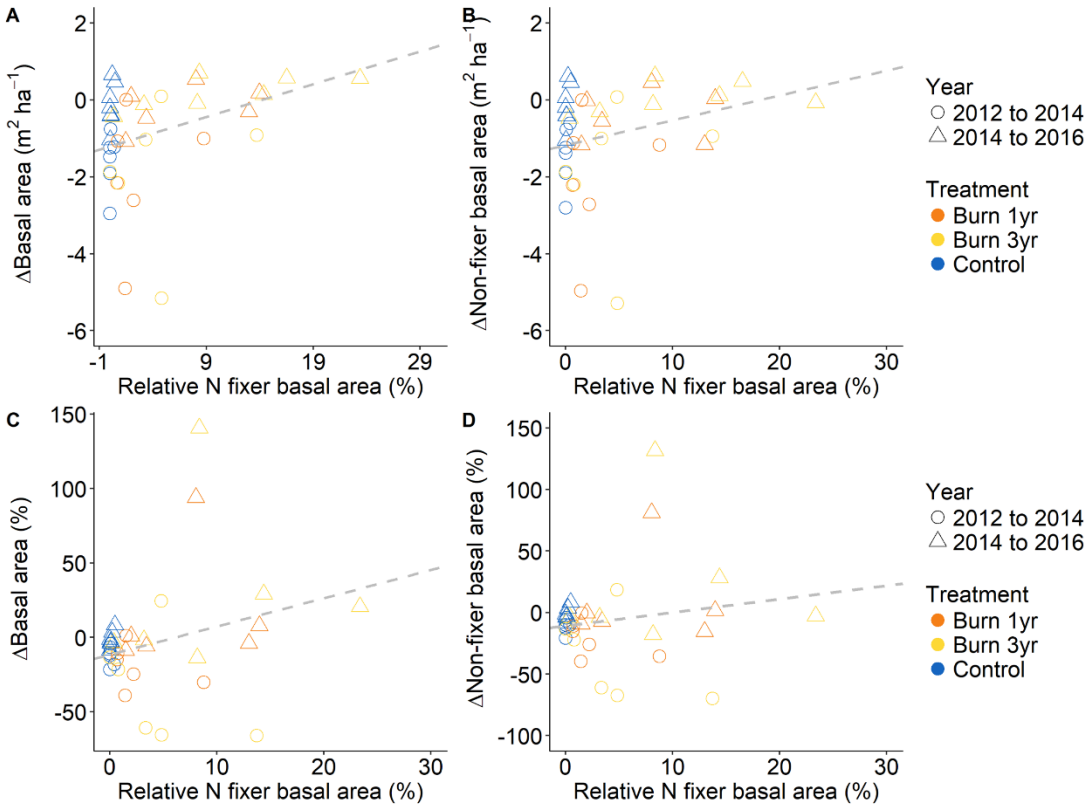

Figure 5.3. Effect of potential N fixer basal area (%) across all size classes on the change in total forest basal area (m^2 ha^{-1}) (A), non-fixer basal area (m^2 ha^{-1}) (B), total forest basal area (%) (C), and non-fixer basal area (%) (D). The dotted grey lines represent the regression.

5.4.8. Nodule sampling and NDFA

Most of the potential N-fixing trees were not nodulating at Fazenda Tanguro, and the foliar $\delta^{15}N$ was not significantly different between potential N-fixing species and reference non-fixers, also indicating a lack of symbiotic N fixation. Only two of 11 sampled *Inga thibaudiana* individuals yielded nodules in sampled soil cores and excavated soil. *Enterolobium schomburgkii (Benth.) Benth.* (n = 9), *Inga heterophylla Willd* (n = 10), and *Tachigali vulgaris* (n = 12) did not yield nodules within the soil cores or excavated soil. Thus, we were unable to detect a significant difference between species (p = 1.0 between all species) (Table 5.6).

The foliar %N was significantly higher for the potential N-fixing *Enterolobium schomburgkii (Benth.) Benth.* in comparison to all the reference species ($p < 0.0001$), as well as *Inga heterophylla Willd*. ($p < 0.0001$), and *Inga thibaudiana* ($p = 0.0002$), but not *Tachigali vulgaris* ($p = 0.91$). However, the foliar $\delta^{15}N$ was not significantly different for all the potential N fixers relative to the reference ($p > 0.97$ for all species). In addition, there were no significant differences in NDFA for all the potential N fixers relative to the reference ($p > 0.99$ for all species) (Table 5.6).

Table 5.5. Proportion of tree species capable of supporting symbiotic N fixation (N-fixing) with nodules and foliar properties of N-fixing trees at Fazenda Tanguro in the southeastern Amazon. Lower-case letters indicate significant differences between species ($p < 0.05$). References values were calculated from the top ten dominant species of confirmed non-fixers.

Species	***n***	**Proportion with nodules**	***n***	**$\delta^{15}N$ ‰**	**%N**	**NDFA**
Enterolobium schomburgkii (Benth.) Benth.	9	0	7	3.107 (0.615)[a]	3.500 (0.126)[a]	2.517 (19.319)[a]
Inga heterophylla Willd.	10	0	5	3.218 (0.479)[a]	3.378 (0.131)[a]	-0.911 (15.021)[a]
Inga thibaudiana	11	0.2	3	3.030 (0.860)[a]	2.890 (0.349)[ab]	4.878 (26.940)[a]
Tachigali vulgaris	12	0	6	3.238 (0.124)[a]	2.158 (0.075)[bc]	-1.581 (3.904)[a]
Reference			90	3.187 (0.124)[a]	2.041 (0.034)[c]	0.000 (3.886)[a]

5.5. Discussion

5.5.1. Patterns of potential N fixer growth, recruitment, and mortality in the southeastern Amazon are similar to other tropical forests after succession

We hypothesized that species capable of supporting symbiotic N fixation, or potential N fixers, would increase in relative abundance following experimental fires in the southeastern Amazon. During the first six years after the last experimental forest fires, we found that potential N fixers had higher growth and recruitment rates than

non-fixers, a pattern that was not observed in the mature control forest. In addition, we also found that potential N fixers post-fire had a lower mortality rate compared potential N fixers in the in the control forest. As a consequence, both the relative abundance and the basal area of potential N fixers increased relative to non-fixers in the burned forests. However, the success of the potential N fixers was not accompanied by an increase in symbiotic N fixation, as only one potential N-fixing species (*Inga thibaudiana*) yielded nodules in our soil surveys. Our results were similar to patterns in the Brazilian Atlantic forest, where potential N fixers increased in stem percentage after clear-cutting, but there was no associated increase in symbiotic N fixation (Winbourne et al. 2018a). However, our results contrasted with studies in wet tropical forests of Panama and Costa Rica, where higher nodulation and N fixation rates were associated increase in stem and basal area of N-fixers (Batterman et al. 2013, Sullivan et al. 2014).

In the southeastern Amazon, recruitment rates were significantly higher for the potential N fixers than the non-fixers, which contrasted with results from a wet tropical forest in Costa Rica (Menge and Chazdon 2016). Menge and Chazdon (2016) found that recruitment was the only demographic process where potential N fixers were not more competitive than non-fixers, likely due to the larger seed size of leguminous plants, which results in a lower abundance of seeds produced and lower disperal distances. However, the youngest forests in their analysis were 11 years, while our oldest forests were 6 years. The differences in recruitment rates could either be driven by the difference in time scales, or differences in rainfall, which drive successional differences between wet and dry tropical forests (Gei et al. 2018). Our

mortality results were consistent with (Lai et al. 2018) who found that in wet tropical forests in Panama, potential N fixers exhibited higher rates of mortality than non-fixers, but less so earlier in succession. Consistent with other studies in Costa Rica and Panama, in the younger forests, potential N fixers in the southeastern Amazon grew faster than non-fixers (Batterman et al. 2013, Menge and Chazdon 2016, Lai et al. 2018). These results converge on the widespread knowledge that many potential N-fixing species are pioneer species, and are more competitive in younger forests, particularly in seasonally dry tropical forests (Gei et al. 2018).

In the southeastern Amazon, N fixers were about 1.2 to 1.3 times larger than non-fixers. Similar to a secondary forest in Costa Rica (Menge and Chazdon 2016), as forests aged, potential N fixers were generally larger than non-fixers. In the ≥ 40 cm size class, *Enterolobium schomburgkii* dominated, making up about 68% and *Ormosia paraensis Ducke.* made up about 32% of potential N fixers by stem abundance. There was only one *T. vulgaris* individual that survived ≥40 cm. In contrast, patterns in Costa Rica were driven mainly by *Pentaclethra macroloba*. Despite the different dominant N-fixing species in Costa Rica, Panama, and in the southeastern Amazon, many of the demographic patterns are similar for N fixers, which could be due the evolutionary advantages that N fixers have over non-fixers early or late in succession.

The potential N fixer basal area at Tanguro in the southeastern Amazon averaged 0.26 m^2 ha^{-1} (0.75 % basal area) in the control forest, 1.18 m^2 ha^{-1} (11% basal area) in the triennially-burned forest, and 1.52 m^2 ha^{-1} (15% basal area) in the annually-burned forest (compared to 33.7 m^2 ha^{-1} of non-fixers); this abundance ranks between 16^{th} and 30^{th} percentile of legume (*Fabacaeae*) basal area in comparison to

other neotropical forests (Gei et al. 2018). While the forests in the southeastern Amazon exhibit a relatively lower basal area of potential N fixers compared to many other dry tropical forests, the success of these N-fixers early in succession is consistent with many other seasonally-dry tropical forests (Gei et al. 2018).

5.5.2. N fixation is not likely the trait driving the success of potential N fixers post-fire

Potential N fixers have also been hypothesized to promote the growth of non-fixers, especially early in succession by bring new N into younger forests Panama (Batterman et al. 2013). In contrast, N fixers have also been hypothesized to inhibit the growth of their non-fixing neighbors in Costa Rica (Taylor et al. 2017). In older forests in Panama, analogous results were inconclusive (Lai et al. 2018). We tested this hypothesis at our site, and did not find a strong relationship between N fixer basal area (%) and non-fixer growth (change in basal area). The trends towards a positive relationship between potential N fixer basal area and change in total and non-fixer basal area seemed to be driven by the high mortality rates in plots with little to no N fixers, even several years after the last fires. Lai et al., (2018) similarly concluded that they did not see a relationship because they did not evaluate which species were actually fixing N. We found similar results as Lai et al., (2018), but we would conclude that this is perhaps due to the fact that the species capable of fixing N are not nodulating and fixing N.

Six years after the last experiemental fire, N fixers made up 3% of the basal area in the smallest size class (5-9.9 cm) in the control forest, while in the burned forests, N-fixers comprised 13% in the triennially-burned forest and 19% in the

annually burned forest. Based on an extensive survey of nodules in this forest (Chapter 4), this level of N fixer abundance would correspond to a rate of 0.48 kg N ha^{-1} yr^{-1} in symbiotic N fixation rate (compared with 0 kg N ha^{-1} yr^{-1} in the control forest); this is a lower value than found in other tropical forests, where a global estimate of tropical N fixation estimated an average rate of 5.7 kg N ha^{-1} yr^{-1} (Sullivan et al. 2014), and much lower the maximum rates found in other forests >100 kg N ha^{-1} yr^{-1} (Sylvester-Bradley et al. 1980, Binkley and Giardina 1997). These results, along with our targeted nodule survey approach indicate that the success of N fixers, particularly *T. vulgaris*, in recruitment and growth are likely unrelated to symbiotic N fixation. From the nodule surveys, it appears that only one N-fixing species, *Inga thibaudiana*, was actually nodulating (and presumably fixing N) post-fire. At this site, most of the N-fixing trees do not appear to be fixing N, consistent with conclusions from a larger synthesis in the Amazon forest by Nardoto et al. (2014). As Gei et al., (2018) suggest, perhaps it is another trait, such as higher foliar N associated with N fixers, or higher water use efficiency that contribute to the success of the legumes post-fire. For example, a severe drought in 2015 may have driven some of the success of the N-fixing species (Appendix D Supplementary Table 2).

The strong presence of potential N fixers in this region in the southeastern Amazon could be more related to fire and interactions with water stress and tolerance. Legume abundance has been found to be negatively correlated with water availability, since species that can fix N also typically have bipinnate leaves (Gei et al. 2018). The smaller leaflet size allows for better temperature regulation and water conservation, and higher foliar N could contribute to higher rates of photosynthesis that allows for

higher water-efficiency (Adams et al. 2016, Gei et al. 2018).

The N fixation trait has commonly been used to predict the competitiveness of tree species and their impact on the broader forest community, but N fixation should be further investigated by examining for nodules in the field. As Barron et al. (2011) suggest, the presence of N-fixers does not imply that they are actively fixing N. Future studies that examine the role of N-fixers should quantify the trait of symbiotic N fixation and N dynamics to further connect the success of a particular trait with its function.

5.5.3. High recruitment of N fixers driven by one species, *Tachigali vulgaris*

After fire disturbances in the southeastern Amazon, *Tachigali vulgaris* (*Sclerolobium paniculatum Vogel*) clearly was the most successful potential N-fixing tree, recruiting and growing rapidly. In previous studies, *T. vulgaris* has been found to proliferate in the southern Amazon and Cerrado biomes (Felfili et al. 1999, Pires and Marcati 2005, Zhang et al. 2009, Melo and Durigan 2010, Freitas et al. 2012), particularly after fires, but its success was not attributed to the N fixation trait, even though *T. vulgaris* can produce nodules and fix N (Haddad et al. 2004). In studies conducted near our site in the Brazilian state of Mato Grosso, *T. vulgaris*' fast growth rates in secondary forests were attributed to the fact that this species is a native pioneer that responds positively to soil amendments, in particular to the addition of phosphorus (Martinotto et al. 2012, de Farias et al. 2016). In a nearby site in the Cerrado biome after fires, *T. vulgaris* also was the species that contributed most to the increase in forest basal area of individuals >10 cm in diameter (Reis et al. 2015, 2017). *T. vulgaris* is also thought to play an important role in the recovery of forest basal area

and carbon after fires (de Oliveira et al. 2017). Similar to our site, *T. vulgaris* played an important role in the forest recovery, but not necessarily by fixing N. We did not find the presence of nodules associated with *T. vulgaris* in a broader nodule survey, as well as targeted approaches even though *T. vulgaris* has a relatively shallow root system (Jackson et al. 1999, Scholz et al. 2007) that would make the presence of nodules easier to detect. The success of T. vulgaris likely has to do with other properties aside from N fixation, such as its ability to establish and persist well in a wide range of nutrient conditions (Castro et al. 1990, Carvalho 2005) with high nutrient efficiency (Morandi et al. 2015), particularly through rhizobial associations (de Castro et al. 1998). The drought tolerance and nodulation status of *T. vulgaris* should be further investigated to explain its success early in succession.

5.6. Conclusion

We found that potential N fixers are relatively competitive compared to non-fixers early in succession post-fire, and that this pattern is generally consistent with other seasonally dry tropical forests. However, N fixer success in the southeastern Amazon does not appear associated with increased rates of symbiotic N fixation. Future work should investigate the relationship between the abundance of N fixers with the forest-level inputs of N through symbiotic N fixation, since the success of N fixers may be driven by increased water use efficiency, or associated with the benefits of higher foliar N that may be unrelated to the ability to nodulate and fix N. Understanding when N-fixing species do fix N, and resolving the relationship between the presence of species and their function will help us better predict the role of the future tropical carbon sink.

Acknowledgements

We thank Stephen Parry (Cornell Statistical Consulting Unit); Darlisson Nunes, Raimundo Mota Quintino, Sebastião Aviz do Nascimento, and Sandro Rocha for the data collection, and Adilson Coelho (Instituto de Pesquisa Ambiental da Amazônia) for the data monitoring; and Paul Lefebvre (Woods Hole Research Center) for the map. Access to field site was provided by Grupo André Maggi and IPAM.

5.7. References

Adams, M. A., T. L. Turnbull, J. I. Sprent, and N. Buchmann. 2016. Legumes are different: Leaf nitrogen, photosynthesis, and water use efficiency. Proceedings of the National Academy of Sciences 113:4098–4103.

Balch, J. K., D. C. Nepstad, P. M. Brando, L. M. Curran, O. Portela, O. de Carvalho, and P. Lefebvre. 2008. Negative fire feedback in a transitional forest of southeastern Amazonia. Global Change Biology 14:2276–2287.

Balch, J. K., D. C. Nepstad, L. M. Curran, P. M. Brando, O. Portela, P. Guilherme, J. D. Reuning-Scherer, and O. de Carvalho Jr. 2011. Size, species, and fire behavior predict tree and liana mortality from experimental burns in the Brazilian Amazon. Forest Ecology and Management 261:68–77.

Barron, A. R., D. W. Purves, and L. O. Hedin. 2011. Facultative nitrogen fixation by canopy legumes in a lowland tropical forest. Oecologia 165:511–20.

Batterman, S. A., L. O. Hedin, M. Van Breugel, J. Ransijn, D. J. Craven, and J. S. Hall. 2013. Key role of symbiotic dinitrogen fixation in tropical forest secondary succession. Nature 502:224–227.

Binkley, D., and C. Giardina. 1997. Nitrogen fixation in tropical forest plantations. Pages 297–337 in E. K. S. Nambiar and A. G. Brown, editors. Management of soil, nutrients, and water in tropical forest plantations. Series: AC. ACIAR, Canberra, Australia.

Brando, P. M., J. K. Balch, D. C. Nepstad, D. C. Morton, F. E. Putz, M. T. Coe, D. Silvério, M. N. Macedo, E. A. Davidson, C. C. Nóbrega, A. Alencar, and B. S. Soares-Filho. 2014. Abrupt increases in Amazonian tree mortality due to drought-fire interactions. Proceedings of the National Academy of Sciences of the United States of America 111:6347–52.

Carvalho, P. E. R. 2005. Taxi-Branco. Circular Técnica - Empresa Brasleira de Pesquisa Agropecuária:1–11.

de Castro, A. W. V., J. T. de Farias Neto, and E. da S. Cavalcante. 1998. Efeito do espaçamento na produtividade de biomassa de Taxi-branco (Sclerolobium paniculatum vogel). Acta Amazonica 28:141–146.

Castro, A. W. V. de, J. A. G. Yared, R. N. B. Alves, L. S. Silva, and S. M. L. B. Meirelles. 1990. Comportamento Silvicultural de Sclerolobium paniculatum (Taxi-branco) no Cerrado Amapaense. EMBRAPA – Empres. Bras. Pesqui. Agropecuária 7:1–4.

Cleveland, C. C., A. R. Townsend, D. S. Schimel, H. Fisher, R. W. Howarth, L. O. Hedin, S. Perakis, E. F. Latty, C. Von Fischer, A. Elseroad, and M. F. Wasson.

1999. Global patterns of terrestrial biological nitrogen (N_2) fixation in natural ecosystems. Global Biogeochemical Cycles 13:623–645.

Cochrane, M. A. 2001. Synergistic interactions between habitat fragmentation and fire in evergreen tropical forests. Conservation Biology 15:1515–1521.

Cochrane, M. A., and M. D. Schulze. 1999. Fire as a recurrent event in tropical forests of the Eastern Amazon: Effects on Forest Structure, Biomass, and Species Composition. Biotropica 31:2–16.

Cramer, M. D., A. Van Cauter, and W. J. Bond. 2010. Growth of N_2-fixing African savanna Acacia species is constrained by below-ground competition with grass. Journal of Ecology 98:156–167.

Davidson, E. A., C. J. R. de Carvalho, A. M. Figueira, F. Y. Ishida, J. P. H. B. Ometto, G. B. Nardoto, R. T. Sába, S. N. Hayashi, E. C. Leal, I. C. G. Vieira, and L. A. Martinelli. 2007. Recuperation of nitrogen cycling in Amazonian forests following agricultural abandonment. Nature 447:995–998.

FAO. 2015. Global Forest Resources Assessment 2015: How are the World's Forests Changing? Page FAO Forestry Paper.

de Farias, J., B. S. Marimon, L. de Carvalho Ramos Silva, A. P. Fabiano, F. R. Andrade, P. S. Morandi, and B. H. Marimon-Junior. 2016. Survival and growth of native Tachigali vulgaris and exotic Eucalyptus urophylla×Eucalyptus grandis trees in degraded soils with biochar amendment in southern Amazonia. Forest Ecology and Management 368:173–182.

Felfili, J. M., L. F. Hilgbert, A. C. Franco, J. C. Sousa-Silva, A. V. Resende, and M. V. P. Nogueira. 1999. Comportamento de plântulas de Sclerolobium paniculatum Vog. var. rubiginosum (Tul.) Benth. sob diferentes níveis de sombreamento, em viveiro. Revista Brasileira de Botanica 22:297–301.

Freitas, G. A. De, A. Vaz-de-melo, M. A. B. Pereira, C. A. O. de Andrade, G. N. Lucena, and R. R. da Silva. 2012. Influência do sombreamento na qualidade de mudas de Sclerolobium paniculatum Vogel para recuperação de área degradada. Journal of Biotechnology and Biodiversity 3:5–12.

Gehring, C., and P. L. G. Vlek. 2004. Limitations of the ^{15}N natural abundance method for estimating biological nitrogen fixation in Amazonian forest legumes. Basic and Applied Ecology 5:567–580.

Gei, M., D. M. A. Rozendaal, L. Poorter, F. Bongers, J. I. Sprent, M. D. Garner, T. M. Aide, J. L. Andrade, P. Balvanera, J. M. Becknell, P. H. S. Brancalion, G. A. L. Cabral, R. G. César, R. L. Chazdon, R. J. Cole, G. D. Colletta, B. De Jong, J. S. Denslow, D. H. Dent, S. J. Dewalt, J. M. Dupuy, S. M. Durán, M. M. Do Espírito Santo, G. W. Fernandes, Y. R. F. Nunes, B. Finegan, V. G. Moser, J. S. Hall, J. L. Hernández-Stefanoni, A. B. Junqueira, D. Kennard, E. Lebrija-

Trejos, S. G. Letcher, M. Lohbeck, E. Marín-Spiotta, M. Martínez-Ramos, J. A. Meave, D. N. L. Menge, F. Mora, R. Muñoz, R. Muscarella, S. Ochoa-Gaona, E. Orihuela-Belmonte, R. Ostertag, M. Peña-Claros, E. A. Pérez-García, D. Piotto, P. B. Reich, C. Reyes-García, J. Rodríguez-Velázquez, I. E. Romero-Pérez, L. Sanaphre-Villanueva, A. Sanchez-Azofeifa, N. B. Schwartz, A. S. De Almeida, J. S. Almeida-Cortez, W. Silver, V. De Souza Moreno, B. W. Sullivan, N. G. Swenson, M. Uriarte, M. Van Breugel, H. Van Der Wal, M. D. D. M. Veloso, H. F. M. Vester, I. C. G. Vieira, J. K. Zimmerman, and J. S. Powers. 2018. Legume abundance along successional and rainfall gradients in Neotropical forests. Nature Ecology and Evolution 2:1104–1111.

Gutschick, V. 1981. Evolved strategies in nitrogen acquisition by plants. American Naturalist 118:607–637.

Haddad, C. R. B., D. P. Lemos, and P. Mazzafera. 2004. Leaf life span and nitrogen content in semideciduous forest tree species (Croton priscus and Hymenaea courbaril). Scientia Agricola (Piracicaba, Brazil) 51:462–465.

Hedin, L. O., E. N. J. Brookshire, D. N. L. Menge, and A. R. Barron. 2009. The Nitrogen Paradox in Tropical Forest Ecosystems. Annual Review of Ecology, Evolution, and Systematics 40:613–635.

Högberg, P. 1986. Nitrogen-Fixation and Nutrient Relations in Savanna Woodland Trees (Tanzania). Journal of Applied Ecology 23:675–688.

Ivanauskas, N. M., R. Monteiro, and R. R. Rodrigues. 2003. Alterations following a fire in a forest community of Alto Rio Xingu. Forest Ecology and Management 184:239–250.

Jackson, P. C., F. C. Meinzer, M. Bustamante, G. Goldstein, A. Franco, P. W. Rundel, L. Caldas, E. Igler, and F. Causin. 1999. Partitioning of soil water among tree species in a Brazilian Cerrado ecosystem. Tree Physiology 19:717–724.

Lai, H. R., J. S. Hall, S. A. Batterman, B. L. Turner, and M. van Breugel. 2018. Nitrogen fixer abundance has no effect on biomass recovery during tropical secondary forest succession. Journal of Ecology 106:1415–1427.

Martinotto, F., C. Martinotto, M. de F. B. Coelho, R. A. B. Azevedo, and M. C. de F. e Albuquerque. 2012. Sobrevivência e crescimento inicial de espécies arbóreas nativas implantadas em pastagem degradada. Pesquisa Agropecuária Brasileira 47:22–29.

Melo, A. C. G. de, and G. Durigan. 2010. Impacto do fogo e dinâmica da regeneração da comunidade vegetal em borda de Floresta Estacional Semidecidual (Gália, SP, Brasil). Revista Brasileira de Botânica 33:37–50.

Menge, D. N. L., and R. L. Chazdon. 2016. Higher survival drives the success of nitrogen-fixing trees through succession in Costa Rican rainforests. New

Phytologist 209:965–977.

Morandi, P. S., B. H. Marimon-Junior, E. A. de Oliveira, S. M. Reis, M. B. X. Valadão, M. Forsthofer, F. B. Passos, and B. S. Marimon. 2015. Vegetation succession in the Cerrado-Amazonian forest transition zone of Mato Grosso state, Brazil. Edinburgh Journal of Botany 73:83–93.

Moreira, Fatima Maria de Souza, da Silva, M. F., and S. M. de Faria. 1992. Occurrence of nodulation in legume species in the Amazon region of Brazil. New Phytologist 121:563–570.

Nardoto, G. B., C. A. Quesada, S. Patiño, G. Saiz, T. R. Baker, M. Schwarz, F. Schrodt, T. R. Feldpausch, T. F. Domingues, B. S. Marimon, B.-H. Marimon Junior, I. C. G. Vieira, M. Silveira, M. I. Bird, O. L. Phillips, J. Lloyd, and L. A. Martinelli. 2014. Basin-wide variations in Amazon forest nitrogen-cycling characteristics as inferred from plant and soil 15N:14N measurements. Plant Ecology & Diversity 7:173–187.

Nasto, M. K., S. Alvarez-Clare, Y. Lekberg, B. W. Sullivan, A. R. Townsend, and C. C. Cleveland. 2014. Interactions among nitrogen fixation and soil phosphorus acquisition strategies in lowland tropical rain forests. Ecology Letters 17:1282–1289.

de Oliveira, B., B. H. Marimon Junior, H. A. Mews, M. B. X. Valadão, and B. S. Marimon. 2017. Unraveling the ecosystem functions in the Amazonia–Cerrado transition: evidence of hyperdynamic nutrient cycling. Plant Ecology 218:225–239.

Pan, Y., R. A. Birdsey, J. Fang, R. Houghton, P. E. Kauppi, W. A. Kurz, O. L. Phillips, A. Shvidenko, S. L. Lewis, J. G. Canadell, P. Ciais, R. B. Jackson, S. W. Pacala, A. D. McGuire, S. Piao, A. Rautiainen, S. Sitch, and D. Hayes. 2011. A large and persistent carbon sink in the world's forests. Science 333:988–993.

Pires, I. P., and C. R. Marcati. 2005. Anatomia e uso da madeira de duas variedades de Sclerolobium paniculatum Vog. do sul do Maranhão, Brasil. Acta Botanica Brasilica 19:669–678.

Poorter, L., F. Bongers, T. M. Aide, A. M. Almeyda Zambrano, P. Balvanera, J. M. Becknell, V. Boukili, P. H. S. Brancalion, E. N. Broadbent, R. L. Chazdon, D. Craven, J. S. De Almeida-Cortez, G. A. L. Cabral, B. H. J. De Jong, J. S. Denslow, D. H. Dent, S. J. DeWalt, J. M. Dupuy, S. M. Durán, M. M. Espírito-Santo, M. C. Fandino, R. G. César, J. S. Hall, J. L. Hernandez-Stefanoni, C. C. Jakovac, A. B. Junqueira, D. Kennard, S. G. Letcher, J. C. Licona, M. Lohbeck, E. Marín-Spiotta, M. Martínez-Ramos, P. Massoca, J. A. Meave, R. Mesquita, F. Mora, R. Munõz, R. Muscarella, Y. R. F. Nunes, S. Ochoa-Gaona, A. A. De Oliveira, E. Orihuela-Belmonte, M. Penã-Claros, E. A. Pérez-Garciá, D. Piotto, J. S. Powers, J. Rodríguez-Velázquez, I. E. Romero-Pérez, J.

Ruíz, J. G. Saldarriaga, A. Sanchez-Azofeifa, N. B. Schwartz, M. K. Steininger, N. G. Swenson, M. Toledo, M. Uriarte, M. Van Breugel, H. Van Der Wal, M. D. M. Veloso, H. F. M. Vester, A. Vicentini, I. C. G. Vieira, T. V. Bentos, G. B. Williamson, and D. M. A. Rozendaal. 2016. Biomass resilience of Neotropical secondary forests. Nature 530:211–214.

Reis, S. M., E. Lenza, B. S. Marimon, L. Gomes, M. Forsthofer, P. S. Morandi, B. H. Marimon Junior, T. R. Feldpausch, and F. Elias. 2015. Post-fire dynamics of the woody vegetation of a savanna forest (Cerradão) in the Cerrado-Amazon transition zone. Acta Botanica Brasilica 29:408–416.

Reis, S. M., E. A. de Oliveira, F. Elias, L. Gomes, P. S. Morandi, B. S. Marimon, B. H. Marimon Junior, E. C. das Neves, B. de Oliveira, and E. Lenza. 2017. Resistance to fire and the resilience of the woody vegetation of the "Cerradão" in the "Cerrado"–Amazon transition zone. Revista Brasileira de Botanica 40:193–201.

Scholz, F. G., S. J. Bucci, G. Goldstein, F. C. Meinzer, A. C. Franco, and F. Miralles-Wilhelm. 2007. Biophysical properties and functional significance of stem water storage tissues in Neotropical savanna trees. Plant, Cell and Environment 30:236–248.

Shearer, G., and D. H. Kohl. 1988. Natural 15N abundance as a method of estimating the contribution of biologically fixed nitrogen to N_2-fixing systems: Potential for non-legumes. Plant and Soil 110:317–327.

Sheffer, E., S. A. Batterman, S. A. Levin, and L. O. Hedin. 2015. Biome-scale nitrogen fixation strategies selected by climatic constraints on nitrogen cycle. Nature Plants:1–6.

Sheil, D., and R. M. May. 1996. Mortality and Recruitment Rate Evaluations in Heterogeneous Tropical Forests. Journal of Ecology 84:91.

Silva, B. M. da S. e, C. de O. e Silva, F. V. Môro, and R. D. Vieira. 2015. Morphoanatomy of fruit, seed and seedling of Ormosia paraensis Ducke. Journal of Seed Science 37:192–198.

Silva, D. M., M. A. Batalha, and M. V. Cianciaruso. 2013. Influence of fire history and soil properties on plant species richness and functional diversity in a neotropical savanna. Acta Botanica Brasilica 27:490–497.

Da Silva, D. M., and M. A. Batalha. 2008. Soil-vegetation relationships in cerrados under different fire frequencies. Plant and Soil 311:87–96.

Sprent, J. I. 2009. Legume nodulation: a global perspective. John Wiley & Sons.

Sullivan, B. W., W. K. Smith, A. R. Townsend, M. K. Nasto, S. C. Reed, R. L. Chazdon, and C. C. Cleveland. 2014. Spatially robust estimates of biological

nitrogen (N) fixation imply substantial human alteration of the tropical N cycle. Proceedings of the National Academy of Sciences of the United States of America 111:8101–6.

Sylvester-Bradley, R., L. A. de Oliveira, J. A. de Podestá Filho, and T. V. St. John. 1980. Nodulation of legumes, nitrogenase activity of roots and occurrence of nitrogen-fixing Azospirillum ssp. in representative soils of central Amazonia. Agro-Ecosystems 6:249–266.

Taylor, B. N., R. L. Chazdon, B. Bachelot, and D. N. L. Menge. 2017. Nitrogen-fixing trees inhibit growth of regenerating Costa Rican rainforests. Proceedings of the National Academy of Sciences 114:201707094.

Taylor, B. N., R. L. Chazdon, and D. N. L. Menge. 2019. Successional dynamics of nitrogen fixation and forest growth in regenerating Costa Rican rainforests. Ecology, in press e02637.

Tedersoo, L., L. Laanisto, S. Rahimlou, A. Toussaint, T. Hallikma, and M. Pärtel. 2018. Global database of plants with root-symbiotic nitrogen fixation: NodDB. Journal of Vegetation Science 29:560–568.

Uhl, C., and J. B. Kauffman. 1990. Deforestation, fire susceptibility, and potential tree responses to fire in the eastern Amazon. Ecology 71:437–449.

Winbourne, J. B., A. Feng, L. Reynolds, D. Piotto, M. G. Hastings, and S. Porder. 2018. Nitrogen cycling during secondary succession in Atlantic Forest of Bahia, Brazil. Scientific Reports 8:1–9.

Wright, S. J., B. L. Turner, J. B. Yavitt, K. E. Harms, M. Kaspari, E. V. J. Tanner, J. Bujan, E. A. Griffin, J. R. Mayor, S. C. Pasquini, M. Sheldrake, and M. N. Garcia. 2018. Plant responses to fertilization experiments in lowland, species-rich, tropical forests. Ecology 99:1129–1138.

Wurzburger, N., and L. O. Hedin. 2016. Taxonomic identity determines N2 fixation by canopy trees across lowland tropical forests. Ecology Letters 19:62–70.

Zhang, Y. J., F. C. Meinzer, G. Y. Hao, F. G. Scholz, S. J. Bucci, F. S. C. Takahashi, R. Villalobos-Vega, J. P. Giraldo, K. F. Cao, W. A. Hoffmann, and G. Goldstein. 2009. Size-dependent mortality in a Neotropical savanna tree: The role of height-related adjustments in hydraulic architecture and carbon allocation. Plant, Cell and Environment 32:1456–1466.

APPENDIX A. SUPPLEMENTARY INFORMATION FOR CHAPTER 2.

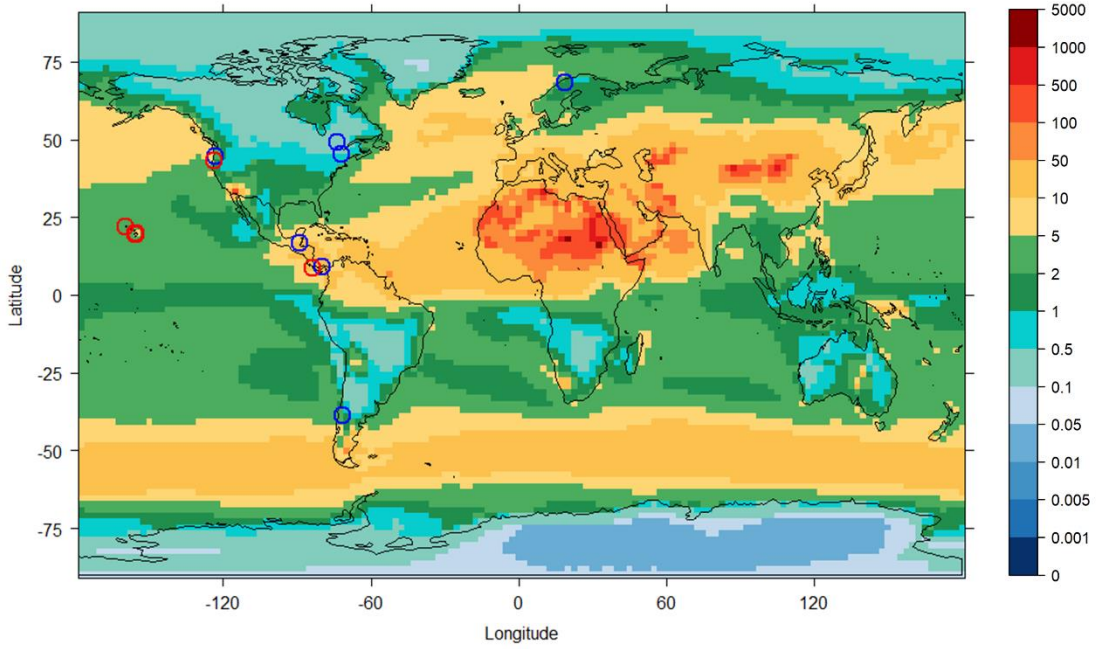

Figure S1. Locations of previous Mo addition experiments to free-living N fixation mapped with annual natural Mo deposition (μg m^{-2} yr^{-1}). Blue circles indicate a free-living BNF response to Mo, while red circles indicate no response of free-living BNF to Mo.

Isotopic Mo sample analysis

Molybdenum concentration and isotope data for the dust and sediment samples were measured at the W.M. Keck Foundation Laboratory for Environmental Biogeochemistry, School of Earth & Space Exploration, Arizona State University (ASU). The dust and sediment samples were oven-dried at 105°C, sieved at 2 mm and powdered, and ashed at 550°C overnight to remove organic matter. Samples were digested in HNO_3, HF, and HCl depending on sample solubility in a closed Savillex reactor on a hot plate. Samples were diluted in 2% HNO_3 and Mo and Al concentrations were determined by quadrupole ICP-MS (ThermoFisher Scientific iCAP Q, with CCT option). All samples were run in conjunction with SDO-1, a Devonian Ohio shale available from the USGS, and SCo-1, a grey shale low in Mo concentration available from the USGS.

To measure the Mo isotopic composition, the double spike procedure was used to allow for correction of both laboratory and instrument mass fractionation. Following digestion and Mo concentration measurements, samples were spiked with ^{97}Mo and ^{100}Mo, dried down and eluted in 6M HCL for column chemistry. Samples were purified with standard anion (Biorad AG1X-8 anion exchange resin, 100-200 mesh) and cation exchange (Biorad AG50WX-8 cation exchange resin, 200-400 mesh) columns. If samples sat more for a day, HF was added to stabilize the sample. Total sample concentrations were rechecked by quadruple ICP-MS.

Molybdenum isotopic concentrations were determined by MC-ICP-MS (Thermo Neptune using an Elemental Scientific, Inc. Apex-Q with a 50 or 100 µL/min nebulizer and 100 cycles of 4.2 seconds. Measured ion beams included ^{91}Zr, ^{92}Mo,

^{94}Mo, ^{95}Mo, ^{96}Mo, ^{97}Mo, ^{98}Mo, ^{99}Ru and ^{100}Mo). Sample δ^{98}Mo was recalculated as per mil deviations from the international standard NIST 3134:

$$\delta Mo^{98} = \left[\frac{^{98/95}Mo_{sample}}{^{98/95}Mo_{NIST\ 3134}} - 1 \right] * 1000$$

Standards were run every two samples or more frequently. The reproducibility are as follows: SDO-1 (USGS Devonian Ohio Shale; δ^{98}Mo = 0.81 ± 0.07‰, (2 sd, n = 7), NIST Mo (NIST 3134, Lot #891307; δ^{98}Mo = 0.00 ± 0.07‰ (2 sd, n = 8), UMd Mo (Johnson Matthey Chemical, Lot #013186S) δ^{98}Mo = -0.14 ± 0.06‰ (2 sd, n = 9) and KyotoMo (Johnson Matthey Chemical, Specpure Stock #38719, Lot #012793) δ^{98}Mo = -0.36 ± 0.08‰ (2 sd, n = 9). These values compare well with the inter-laboratory calibrated values of (Goldberg et al. 2013).

Results

Using Mo isotopes, we can discriminate Mo sources between dust and sea-salt spray. Mo isotopes are useful tracers because Mo has seven isotopes which are relatively equal in abundance, with a percent mass spread of ~10%. In addition, Mo chemistry is affected by large changes in redox state and coordination, leading to significant variations in the isotopic composition of Mo in nature (Baring et al 2001). We measured the isotopic composition of sediment and dust samples from the Bodélé Depression and found values that fall close to soils and rocks, which contrast strongly from the published signature of seawater (Figure 2). The Bodélé Depression dust samples average an a δ^{98}Mo value of 0.047 ± 0.014 ‰ while the sediment samples average a δ^{98}Mo value of δ^{98} 0.056 ± 0.034 ‰. Because of the long residence time of Mo, Mo isotopes are likely homogeneously distributed in the ocean (Nakagawa et al 2012). Seawater Mo has a heavy isotopic signature, averaging δ^{98}Mo = 2.34 ± 0.10‰

(Nakagawa et al. 2012) because in oxic conditions, Mo absorbs to iron- and manganese-(oxyhydr)oxides which preferentially scavenge light Mo (δ^{98}Mo ~ -0.7‰) (Siebert et al. 2003).

The Bodélé Depression dust samples were much more homogenous than the sediment samples, indicating that dust could be a potentially useful tracers. We assume that dust isotopic composition tends to be uniform, reflecting how the mobilized fraction of the soil has been highly weathered through repeated cycles of mobilization, deposition, and mixing (Prospero 1999), which explains why the dust samples exhibited a smaller range than the sediment samples (Figure 2, Table 1). Abouchami et al. 2013 also found that the dust and sediment samples were also not identical. With the Pb isotopes, the sediments exhibited a more restricted range from δ^{206}Pb/^{204}Pb = 18.9 to 19.2 ‰, while the dust samples were as low as 18.2‰. The Sr isotopic composition followed a similar pattern as well. The wind-borne dust exhibited slightly lighter values than the original sediment, indicating possible fractionation in the mobilization process.

The isotopic values in the sediment and dust samples from the Bodélé Depression were slightly heavier than average values found in bedrock, which fall closer to zero (Figure 2). In addition to Mo-organic matter interactions (King et al. 2016), Mo from dust and sea-salt aerosols could help explain the discrepancy between heavier river Mo isotopic composition and lighter bedrock Mo isotopic composition, assuming that the dust Mo isotopic composition has been consistent over time. In marine sediments, Mo concentrations and isotopic compositions are used to quantify redox conditions throughout Earth's history (Arnold et al. 2004, Poulson et al. 2006,

Siebert et al. 2006, Pearce et al. 2008), such as Great Oxidation Event (Anbar et al. 2007). These paleoredox studies have relied on the assumption that the riverine input of Mo has remained constant and reflects the isotopic composition of continental rocks, but because this is not supported by river concentrations (Archer and Vance 2008, Pearce et al. 2010, Neubert et al. 2011). The discrepancy could be due to the lack of incorporating weathering processes on Mo isotopic fractionation and atmospheric transport (King et al. 2016).

We aimed to constrain in this study by measuring the isotopic signature of Bodéle Depression dust to serve as a potential end-member for mixing models (King et al. 2014, 2016, Siebert et al. 2015). The lighter Mo isotopic signature of dust is promising in contrast to sea-water composition, and could help discern and quantify sources of dust compared to sea-salt. The heavy isotopic signature of marine-derived Mo (δ^{98}Mo = 2.34) was demonstrated in Iceland, where Siebert et al. 2015 found a heavier Mo isotope composition in soils (δ^{98}Mo= 0.31‰ and 0.38‰) relative to the bedrock (δ^{98}Mo = 0.18‰ and 0.09‰), which they attributed to the influence of sea-salt Mo. They confirmed the influence of sea-salt spray with supplemental evidence from the soil porewater Na/Cl ratios that matched seawater ratio, and estimated a Mo concentration in rain of 1.9–9.1 pg ml^{-1}, or 0.02–0.09 g ha^{-1} yr^{-1} Mo from sea-salt.

Table S1. Bodélé Depression Dust and Sediment Mo concentrations and isotopic composition

Sample	Latitude	Longitude	Mo (µg g-1)	d98Mo ‰	2 sd ‰	n
Dust						
#1 Faya Largeau (Chad)	17° 56.113’ N	19° 06.743’E	1.1	0.43	0.06	3
#1 Harmattan (Niamey, Niger)	13° 29.492’ N	2° 10.189’ E	1.2	0.09	0.03	3
#1 Radome (Niamey, Niger)	13° 29.492’ N	2° 10.189’ E	1.2	0.07	0.04	3
#2 Mao (rafters, Chad)	14° 07.704’ N	15° 18.753’ E	1.3	0.32	0.05	3
#2 Nguimi (police station, Chad)	14° 15.175’ N	13° 06.878’ E	1.0	0.20	0.06	3
Bodéle Sediment						
Bodéle soil 43.5 (Chad)	16° 06.12'N	18° 33.00 E	0.9	-0.39	0.07	3
Bodéle soil 44 (Chad)	16 °08.139'N	18 °35.930'E	1.1	0.74	0.01	2
Bodéle soil 44B (Chad)	16 °08.139'N	18 °35.930'E	2.4	1.70	0.08	2
Bodéle soil 44C (Chad)	16 °12.273'N	18 °36.397'E	0.7	-0.50	0.03	2
Bodéle soil 44D (Chad)	16 °12.273'N	18 °36.397'E	0.7	0.57	0.10	2
Bodéle soil 51 (Chad)	17 °13.777'N	19 °02.149'E	3.6	-1.00	0.03	3
Bodéle soil 54A (Chad)	16 °09.190'N	18 °35.464'E	0.7	-0.46	0.02	2
Bodéle soil 54B (Chad)	16 °09.190'N	18 °35.464'E	1.3	-0.52	0.09	4

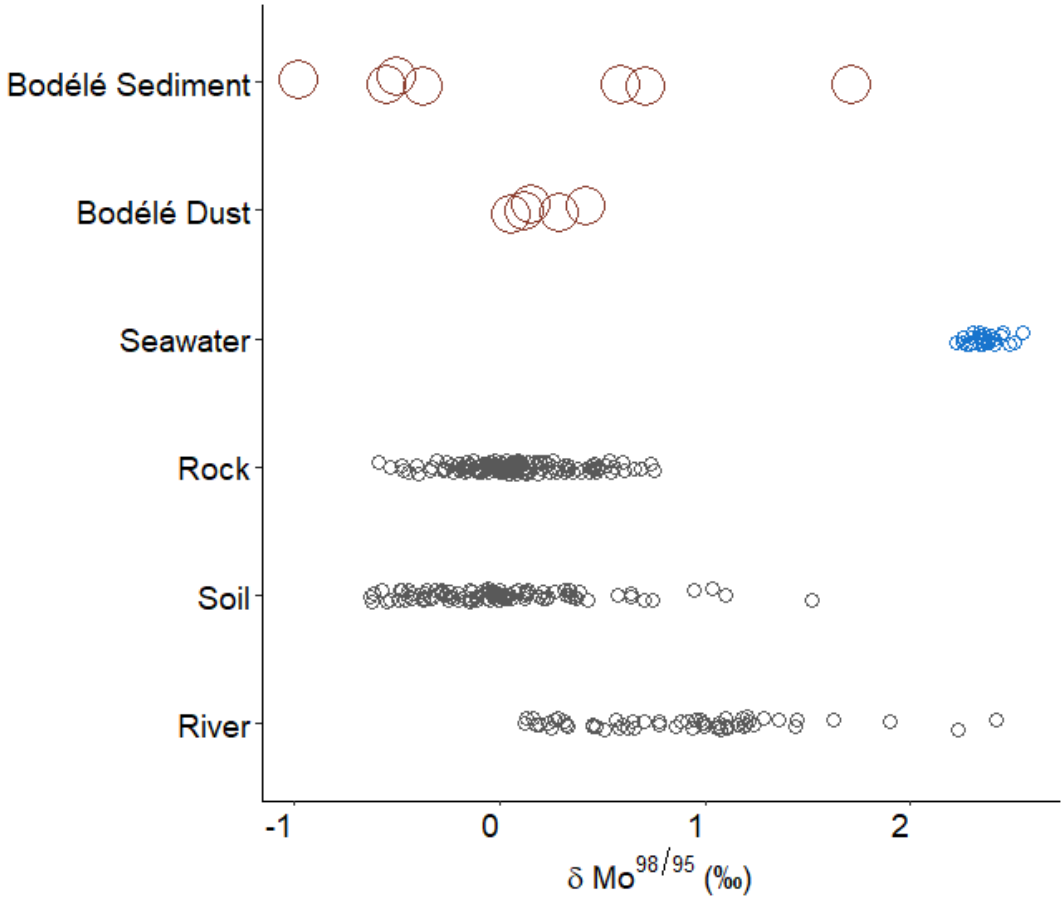

Figure S2. Summary of existing Mo isotope data from natural samples. Brown circles are data from this study, while blue represents seawater Mo values (Siebert et al. 2015, King et al. 2016), and grey represents rock (Siebert et al. 2003, 2015, Voegelin et al. 2012, 2014, Greber et al. 2014, 2015, King et al. 2016), soil (Siebert et al. 2015, King et al. 2016), and river (Archer and Vance 2008, Neubert et al. 2011) Mo values.

References

Anbar, A. D., Y. Duan, T. W. Lyons, G. L. Arnold, B. Kendall, J. Garvin, and R. Buick. 2007. A Whiff of Oxygen Before the Great Oxidation Event? Science 317:1903–1907.

Archer, C., and D. Vance. 2008. The isotopic signature of the global riverine molybdenum flux and anoxia in the ancient oceans. Nature Geoscience 1:597–600.

Arnold, G. L., A.D. Anbar, J. Barling, and T. W. Lyons. 2004. Molybdenum isotope evidence for widespread anoxia in mid-Proterozoic oceans. Science 304:87–90.

Goldberg, T., G. Gordon, G. Izon, C. Archer, C. R. Pearce, J. McManus, A. D. Anbar, and M. Rehkämper. 2013. Resolution of inter-laboratory discrepancies in Mo isotope data: an intercalibration. Journal of Analytical Atomic Spectrometry 28:724.

King, E. K., A. Thompson, O. A. Chadwick, and J. C. Pett-Ridge. 2016. Molybdenum sources and isotopic composition during early stages of pedogenesis along a basaltic climate transect. Chemical Geology 445:54–67.

King, E. K., A. Thompson, C. Hodges, and J. C. Pett-Ridge. 2014. Towards Understanding Temporal and Spatial Patterns of Molybdenum in the Critical Zone. Procedia Earth and Planetary Science 10:56–62.

Nakagawa, Y., S. Takano, and M. Firdaus. 2012. The molybdenum isotopic composition of the modern ocean. Geochemical Journal 46:131–141.

Neubert, N., A. R. Heri, A. R. Voegelin, T. F. Nägler, F. Schlunegger, and I. M. Villa. 2011. The molybdenum isotopic composition in river water: Constraints from small catchments. Earth and Planetary Science Letters 304:180–190.

Pearce, C. R., K. W. Burton, P. A. . P. von Strandmann, R. H. James, and S. R. Gíslason. 2010. Molybdenum isotope behaviour accompanying weathering and riverine transport in a basaltic terrain. Earth and Planetary Science Letters 295:104–114.

Pearce, C. R., A. S. Cohen, A. L. Coe, and K. W. Burton. 2008. Molybdenum isotope evidence for global ocean anoxia coupled with perturbations to the carbon cycle during the Early Jurassic. Geology 36:231.

Poulson, R. L., C. Siebert, J. McManus, and W. M. Berelson. 2006. Authigenic molybdenum isotope signatures in marine sediments. Geology 34:617.

Prospero, J. M. 1999. Long-range transport of mineral dust in the global atmosphere: Impact of African dust on the environment of the southeastern United States.

Proceedings of the National Academy of Sciences 96:3396–3403.

Scheiderich, K., G. R. Helz, and R. J. Walker. 2010. Century-long record of Mo isotopic composition in sediments of a seasonally anoxic estuary (Chesapeake Bay). Earth and Planetary Science Letters 289:189–197.

Siebert, C., J. McManus, A. Bice, R. Poulson, and W. M. Berelson. 2006. Molybdenum isotope signatures in continental margin marine sediments. Earth and Planetary Science Letters 241:723–733.

Siebert, C., T. F. Nägler, F. von Blanckenburg, and J. D. Kramers. 2003. Molybdenum isotope records as a potential new proxy for paleoceanography. Earth and Planetary Science Letters 211:159–171.

Siebert, C., J. C. Pett-Ridge, S. Opfergelt, R. A. Guicharnaud, A. N. Halliday, and K. W. Burton. 2015. Molybdenum isotope fractionation in soils: Influence of redox conditions, organic matter, and atmospheric inputs. Geochimica et Cosmochimica Acta 162:1–24.

Voegelin, A. R., T. F. Nägler, T. Pettke, N. Neubert, M. Steinmann, O. Pourret, and I. M. Villa. 2012. The impact of igneous bedrock weathering on the Mo isotopic composition of stream waters: Natural samples and laboratory experiments. Geochimica et Cosmochimica Acta 86:150–165.

Voegelin, A. R., T. Pettke, N. D. Greber, B. von Niederhäusern, and T. F. Nägler. 2014. Magma differentiation fractionates Mo isotope ratios: Evidence from the Kos Plateau Tuff (Aegean Arc). Lithos 190–191:440–448.

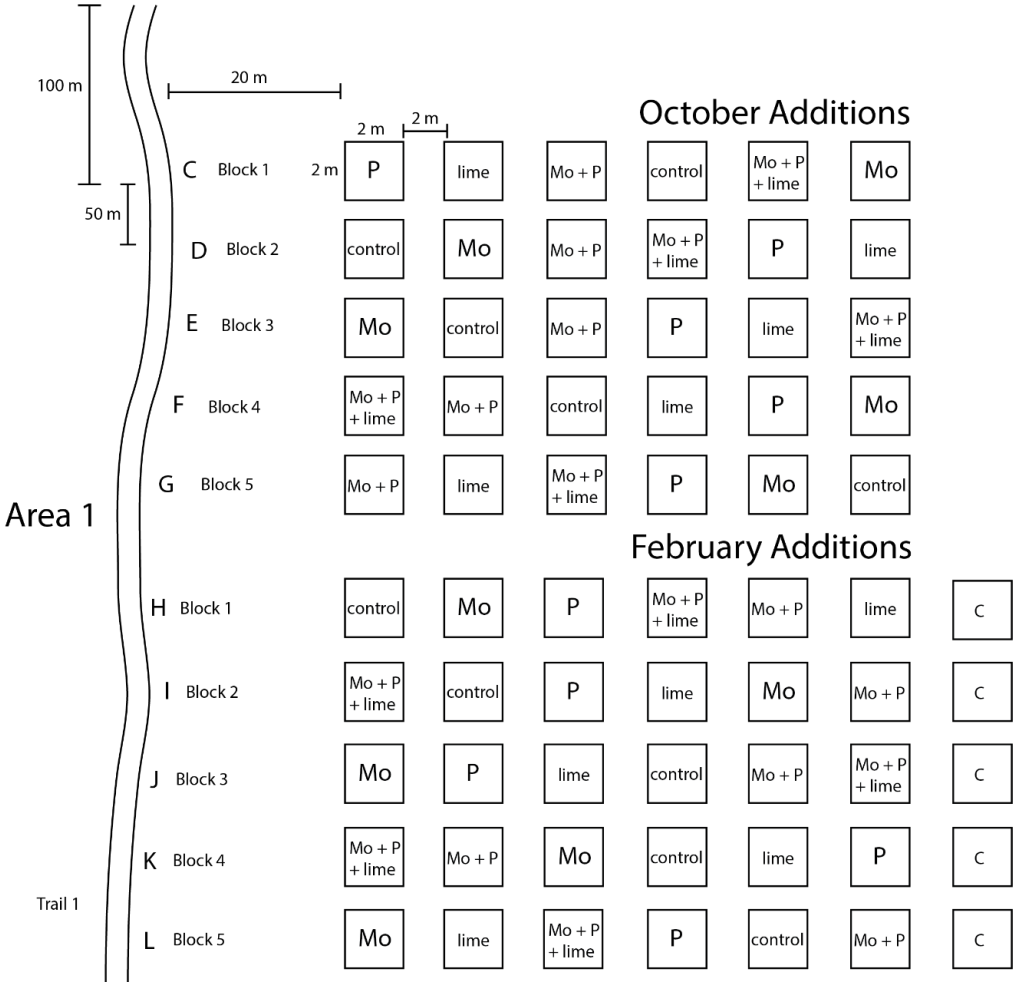

Figure S1. Plot setup of the randomized block field addition experiment. The October addition plots represent fertilizations that began during the dry season of October 2016, and the February addition plots represent fertilizations that began during the wet season of February 2017. The plots were laid 100 m away from the forest edge, and 50 m away from the nearest trail.

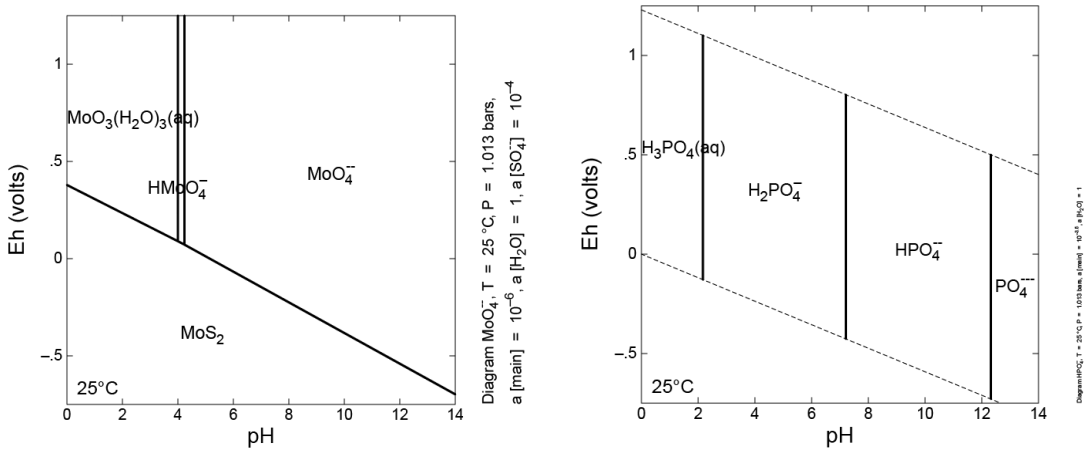

Figure S2. Pourbaix diagram, or EH-pH diagram of possible stable (equilibrium) phases of an aqueous electrochemical system of Mo (left) and P (right), generated from Geochemist's Workbench from soil properties (soil pH) and soil porewater concentrations of Na, Mg, Al, Si, K, and Ca from surface soils at Fazenda Tanguro.

Table S1. Field-based resin-extractable available molybdenum (Mo), phosphorus (P), and total Mo and P one day and one month after applications in the wet season (February additions) in the southeastern Amazon. Means are presented ± standard error. Letters signify statistically significant differences ($p < 0.05$) (Tukey post-hoc test).

	One Day				One Month			
	Mo (ng g^{-1})		P (µg g^{-1})		Mo (ng g^{-1})		P (µg g^{-1})	
	Resin*	Total	Resin	Total	Resin*	Total	Resin	Total
Control	2.25 (0.90)^{bc}	88.7 (14.4)^{b}	1.12 (0.44)^{a}	88.00 (18.5)^{b}	0.39 (0.19)^{b}	89.0 (14.8)^{b}	0.82 (0.16)^{b}	80.5 (8.17)^{b}
Lime	0.76 (0.18)^{c}	81.4 (13.7)^{b}	1.01 (0.26)^{a}	108.0 (8.31)^{ab}	0.88 (0.46)^{b}	94.5 (8.44)^{b}	1.14 (0.12)^{b}	93.9 (3.12)^{ab}
Mo	12.9 (3.10)^{ab}	167.0 (30.9)^{ab}	1.09 (0.17)^{a}	111.0 (6.78)^{ab}	14.2 (3.71)^{a}	155.0 (24.2)^{b}	1.25 (0.22)^{ab}	89.0 (5.19)^{b}
P	1.16 (0.45)^{c}	108.0 (19.9)^{ab}	2.10 (0.53)^{a}	164.0 (27.1)^{a}	0.50 (0.21)^{b}	109.0 (11.2)^{b}	1.70 (0.14)^{ab}	116.0 (7.45)^{a}
Mo + P	27.0 (10.9)^{a}	253.0 (67.0)^{ab}	2.29 (0.41)^{a}	166.0 (16.1)^{a}	21.3 (5.75)^{a}	285.0 (52.7)^{a}	1.58 (0.37)^{ab}	117.0 (14.1)^{a}
Mo + P + Lime	32.9 (12.1)^{a}	282.0 (62.4)^{a}	2.04 (0.21)^{a}	138.0 (11.0)^{ab}	18.5 (5.44)^{a}	181.0 (25.2)^{ab}	2.62 (0.59)^{a}	120.0 (8.11)^{a}

*Indicates if group was ln-transformed (+0.01) prior to statistical tests

Table S2. Field-based free-living BNF by acetylene reduction (nmol C_2H_4 g^{-1} hr^{-1}) in surface soils in response to fertilizations before applications, one day after, ten days after, and four months after applications that began during the dry season in October; and before additions, one day after, one week after, one month after, and eleven months after applications that began during the wet season in February in the southeastern Amazon.

Plots	October addition				February additions				
Season	Dry Season			Wet Season					
Dates	10/17/2016	10/20/2016	10/31/2016	2/13/2017	2/07/2017	2/15/2017	2/21/2017	3/20/2017	1/30/2018
	Pre-addition	One day	Ten day	3 month	Pre-addition	One day	One week	One month	Eleven months
Control	0.0010 (0.0008)	0.0028 (0.0016)	0.0017 (0.0006)	0.0226 (0.0128)	0.0043 (0.0011)	0.0058 (0.0012)	0.0031 (0.0005)	0.0023 (0.0006)	0.0192 (0.0105)
Lime	0.0026 (0.0013)	0.0060 (0.0021)	0.0040 (0.0017)	0.0039 (0.0009)	0.0066 (0.0009)	0.0068 (0.0012)	0.0027 (0.0003)	0.0035 (0.0010)	0.0119 (0.0015)
Mo	0.0040 (0.0017)	0.0043 (0.0017)	0.0026 (0.0011)	0.0021 (0.0006)	0.0060 (0.0011)	0.0065 (0.0007)	0.0035 (0.0005)	0.0035 (0.0008)	0.0094 (0.0009)
P	0.0033 (0.0013)	0.0049 (0.0020)	0.0469 (0.0444)	0.0043 (0.0014)	0.0047 (0.0008)	0.0077 (0.0013)	0.0038 (0.0007)	0.0038 (0.0004)	0.0735 (0.0598)
Mo + P	0.0021 (0.0014)	0.0478 (0.0390)	0.0053 (0.0043)	0.0155 (0.0098)	0.0051 (0.0006)	0.0074 (0.0006)	0.0038 (0.0008)	0.0047 (0.0010)	0.0100 (0.0016)
Mo + P + Lime	0.0025 (0.0014)	0.0106 (0.0029)	0.0022 (0.0006)	0.0043 (0.0011)	0.0044 (0.0007)	0.0081 (0.0010)	0.0038 (0.0009)	0.0124 (0.0057)	0.0126 (0.0026)

Table S3. Field-based free-living BNF by acetylene reduction (nmol C_2H_4 g^{-1} hr^{-1}) in the litter layer in response to fertilizations before applications, one day after, ten days after, and four months after applications that began during the dry season in October; and before additions, one day after, one week after, one month after, and eleven months after applications that began during the wet season in February in the southeastern Amazon.

	October addition				February additions				
	Dry Season			Wet Season					
	10/18/2016	10/21/2016	11/1/2016	2/14/2017	2/8/2017	2/16/2017	2/22/2017	3/21/2017	1/31/2018
	Pre-addition	One day	Ten day	3 month	Pre-addition	One day	One week	One month	Eleven months
Control	0.0095 (0.0044)	0.0628 (0.0115)	0.0095 (0.0095)	0.1479 (0.0531)	0.1116 (0.0785)	0.0769 (0.0373)	0.0117 (0.0079)	0.0511 (0.0278)	0.2003 (0.0512)
Lime	0.0120 (0.0086)	0.0811 (0.0229)	0.0000 (0.0000)	0.3880 (0.1123)	0.2237 (0.1044)	0.0717 (0.0496)	0.0187 (0.0094)	0.0483 (0.0282)	0.5090 (0.0990)
Mo	0.0178 (0.0127)	0.0858 (0.0205)	0.0337 (0.0337)	0.2078 (0.0923)	0.0687 (0.0319)	0.0650 (0.0385)	0.0798 (0.0512)	0.0921 (0.0612)	0.4196 (0.1951)
P	0.0321 (0.0132)	0.0626 (0.0144)	0.0053 (0.0048)	0.5311 (0.1718)	0.1282 (0.0519)	0.0876 (0.0548)	0.0733 (0.0394)	0.0805 (0.0359)	0.1540 (0.0256)
Mo + P	0.0231 (0.0138)	0.0810 (0.0237)	0.0004 (0.0004)	0.1175 (0.0502)	0.1335 (0.0920)	0.1718 (0.0899)	0.0968 (0.0644)	0.0440 (0.0375)	0.2378 (0.0640)
Mo + P + Lime	0.0313 (0.0098)	0.0744 (0.0287)	0.0006 (0.0006)	0.6244 (0.2016)	0.3343 (0.2461)	0.0893 (0.0556)	0.1469 (0.1008)	0.3602 (0.2416)	0.4094 (0.1272)

Table S4. Linear mixed-effects models for BNF.

Group	Model		Sum Sq	Mean Sq	Num DF	DenDF	F value	Pr(>F)	Groups	Variance	Std.Dev.
October Additions Soil	Timepoint x Plot + Block x Timepoint + Block x Plot x Timepoint	factor(Timepoint)	10.446	5.2228	2	12.011	1.9769	0.1811			
		Plot	13.572	2.7145	5	59.096	1.0274	0.4099			
		factor(Timepoint): Plot	39.141	3.9141	10	59.091	1.4815	0.1692			
									Block:Plot:Timepoint	0.4378	0.6616
									Block:Timepoint	0.8371	0.9149
									Residual	2.642	1.6254
April Additions Soil	Timepoint x Plot + Block x Timepoint + Block x Plot x Timepoint	factor(Timepoint)	24.2861	8.0954	3	15.715	11.5088	0.000304			
		Plot	6.5578	1.3116	5	75.995	1.8646	0.110487			
		factor(Timepoint): Plot	7.731	0.5154	15	75.979	0.7327	0.74417			
									Block:Plot:Timepoint	0.189	0.4347
									Block:Timepoint	0.1552	0.394
									Residual	0.7034	0.8387
October Additions Litter	Timepoint x Plot + Block x Timepoint + Block x Plot x Timepoint	factor(Timepoint)	105.008	52.504	2	11.983	45.1843	2.62E-06	***		
		Plot	5.656	1.131	5	59.403	0.9735	0.4414			
		factor(Timepoint): Plot	17.324	1.732	10	59.393	1.4909	0.1655			
									Block:Plot:Timepoint	0.8996	0.9485
									Block:Timepoint	0.3556	0.5963
									Residual	1.162	1.078
April Litter	Timepoint x Plot + Block x Timepoint + Block x Plot x Timepoint	factor(Timepoint)	47.575	15.8584	3	15.904	7.4806	0.002415	**		
		Plot	2.888	0.5776	5	73.922	0.2724	0.926816			
		factor(Timepoint): Plot	20.425	1.3617	15	73.213	0.6423	0.830145			
									Block:Plot:Timepoint	1.474	1.214
									Block:Timepoint	1.112	1.055
									Residual	2.12	1.456

Hotspots

Hotspots have been described as areas that have high activity relative to the surrounding matrix. Since there is no operating statistical definition, Reed et al. (2010) defined hotspots as deviating 3 standard errors from the median, which resulted in 20% of samples being defined as a hotspot. When we used this definition, 17.4% of our samples were deemed as hotspots, and when we counted hotspots as samples that were 3 times the mean, then 5.4% of our samples were hotspots.

Table S5. Frequency of hotspots per treatment.

Substrate	Treatment	Hotspot	Frequency
Litter	Control	No hotspot	82
Litter	Control	Hotspot	2
Litter	Lime	No hotspot	88
Litter	Lime	Hotspot	6
Litter	Mo	No hotspot	88
Litter	Mo	Hotspot	6
Litter	P	No hotspot	89
Litter	P	Hotspot	6
Litter	Mo+P	No hotspot	88
Litter	Mo+P	Hotspot	10
Litter	Mo+P+Lime	No hotspot	78
Litter	Mo+P+Lime	Hotspot	13
Soil	Control	No hotspot	114
Soil	Control	Hotspot	5
Soil	Lime	No hotspot	132
Soil	Lime	Hotspot	3
Soil	Mo	No hotspot	132
Soil	Mo	Hotspot	3
Soil	P	No hotspot	128
Soil	P	Hotspot	6
Soil	Mo+P	No hotspot	129
Soil	Mo+P	Hotspot	5
Soil	Mo+P+Lime	No hotspot	129
Soil	Mo+P+Lime	Hotspot	5

Table S6. Response ratios of ARA to additions in soil.

	October				April				
	Dry Season			Wet Season					
	Pre-Addition	One Day	Ten Day	3 Month	Pre-Addition	1 Day	1 Week	1 Month	11 Month
Control	0.40 (0.27)	0.61 (0.24)	5.02 (3.31)	1.00 (0.17)	1.00 (0.18)	1.00 (0.07)	1.00 (0.15)	1.00 (0.20)	1.08 (0.19)
Lime	1.76 (0.85)	6.79 (4.32)	13.03 (10.77)	0.52 (0.14)	1.71 (0.26)	1.35 (0.18)	1.03 (0.16)	1.75 (0.55)	0.93 (0.15)
Mo	1.59 (0.56)	11.71 (9.97)	2.97 (1.69)	0.56 (0.19)	1.59 (0.35)	1.43 (0.20)	1.36 (0.21)	2.02 (0.69)	0.74 (0.10)
P	2.02 (0.84)	2.02 (1.16)	23.18 (21.04)	0.60 (0.19)	1.31 (0.28)	1.89 (0.40)	1.65 (0.44)	2.01 (0.43)	4.12 (3.10)
Mo + P	0.87 (0.41)	34.72 (17.25)	16.73 (15.08)	1.43 (0.32)	1.42 (0.24)	1.74 (0.27)	1.46 (0.28)	2.38 (0.61)	0.79 (0.11)
Mo + P + Lime	0.88 (0.39)	31.62 (20.82)	2.69 (1.00)	0.65 (0.18)	1.26 (0.29)	1.79 (0.32)	2.03 (0.95)	9.82 (5.59)	1.07 (0.29)

Table S7. Response ratios of ARA to additions in litter.

	October				April				
	Dry Season			Wet Season					
	Pre-Addition	One Day	Ten Day	3 Month	Pre-Addition	1 Day	1 Week	1 Month	11 Month
Control	1.01 (0.46)	1.00 (0.18)	0.20 (0.20)	1.00 (0.20)	0.75 (0.26)	1.00 (0.30)	0.50 (0.33)	1.00 (0.31)	0.27 (0.07)
Lime	1.36 (0.93)	1.50 (0.55)	0.00 (0.00)	285.28 (216.57)	2.01 (0.83)	0.63 (0.42)	6.08 (4.91)	0.78 (0.53)	0.69 (0.13)
Mo	1.89 (1.27)	1.50 (0.39)	0.71 (0.71)	156.05 (105.07)	1.16 (0.71)	0.52 (0.29)	5.58 (2.55)	1.37 (0.79)	0.57 (0.27)
P	3.44 (1.34)	1.14 (0.31)	0.36 (0.36)	122.92 (81.34)	2.31 (1.21)	3.10 (1.90)	4.48 (2.12)	2.76 (1.88)	0.21 (0.03)
Mo + P	3.03 (1.92)	1.43 (0.39)	0.58 (0.58)	19.09 (11.93)	0.73 (0.31)	1.95 (0.96)	11.43 (6.44)	0.36 (0.28)	0.32 (0.09)
Mo + P + Lime	3.13 (0.98)	1.12 (0.32)	5.33 (4.79)	419.36 (293.39)	1.31 (0.70)	0.37 (0.23)	26.16 (15.19)	2.76 (1.83)	0.56 (0.17)

Table S8. Linear mixed-effects models analyzing response ratios.

Group	Model		Sum Sq	Mean Sq	Num DF	Den DF	F value	Pr(>F)	Groups	Variance	Std.Dev.
October Soil Response Ratio	Timepoint x Plot + Block x Timepoint + Block x Plot x Timepoint	factor(Timepoint)	2.6453	1.3227	2	12.016	0.5176	0.6087			
		Plot	10.3766	2.0753	5	59.072	0.8121	0.5458			
		factor(Timepoint): Plot	26.9488	2.6949	10	59.068	1.0546	0.4111			
									Block:Plot: Timepoint	0.5863	0.7657
									Block:Timepoint	0.3566	0.5972
									Residual	2.5554	1.5986
April Soil Response Ratio	Timepoint x Plot + Block x Timepoint + Block x Plot x Timepoint	factor(Timepoint)	0.5553	0.18511	3	16.12	0.3847	0.76547	.		
		Plot	4.6421	0.92842	5	76.134	1.9294	0.09918			
		factor(Timepoint): Plot	5.4379	0.36253	15	76.118	0.7534	0.72298			
									Block:Plot: Timepoint	0.1456	0.3816
									Block:Timepoint	0.3549	0.5958
									Residual	0.4812	0.6937
October Litter Response Ratio	Timepoint x Plot + Block x Timepoint + Block x Plot x Timepoint	factor(Timepoint)	13.9145	6.9573	2	12.005	6.3742	0.012999			
		Plot	7.6549	1.531	5	59.447	1.4027	0.23644			
		factor(Timepoint): Plot	15.6383	1.5638	10	59.436	1.4328	0.18854			
									Block:Plot: Timepoint	0.7733	0.8794
									Block:Timepoint	1.7557	1.325
									Residual	1.0915	1.0447
April Litter Response Ratio	Timepoint x Plot + Block x Timepoint + Block x Plot x Timepoint	factor(Timepoint)	7.4646	2.4882	3	15.975	1.4434	0.2673			
		Plot	2.3765	0.4753	5	72.67	0.2757	0.925			
		factor(Timepoint): Plot	26.2455	1.7497	15	71.341	1.015	0.4504			
									Block:Plot: Timepoint	0.6592	0.8119
									Block:Timepoint	0.2998	0.5475
									Residual	1.7239	1.313

Carbon additions

Introduction

Proximally, free-living BNF can be controlled by carbon (C) availability, moisture, and oxygen. The process of free-living BNF is energically expensive in an oxic environment, costing about 28-400 g glucose per gram of N fixed (Gutschick 1981). The nitrogenase enzyme is sensitive to oxygen (Hill 1988), and protecting nitrogenase from oxygen is probably the major reason why BNF is energetically costly. Thus heterotrophic BNF, which dominates in the tropics and heavily relies on plant litter C to fuel BNF (Vitousek et al. 2002a, Dynarski and Houlton 2018) may be controlled by largely by C availability. Temporally, free-living BNF may also be affected by moisture and oxygen, as oxygen affects the nitrogenase enzyme and thus can suppress BNF (Hill 1988), and rates are strongly affected by moisture (Hofmockel and Schlesinger 2007, Reed et al. 2007), as rates generally increase with increasing water availability because 1) microbial decomposition of organic matter can be water limited; and 2) oxygen is less of a problem as more of the pore spaces in a soil become filled with water, as this slows oxygen diffusion.

Because previous studies have demonstrated responses of free-living BNF to labile C additions (Hofmockel and Schlesinger 2007, Pérez et al. 2017) and have suggested C to play an important role in free-living BNF in the tropics, we tested C effects on free-living BNF in combination with Mo and P in the laboratory, effects of C additions in the field, and differences in response to C additions compared to oxygen-free conditions, because adding labile C can induce respiration and reduce the oxygen atmosphere much more rapidly than without labile C (Jia et al. 2014).

Methods

Bottle addition with carbon addition

To conduct the same experiment in a controlled laboratory study similar to previous Mo and P fertilization experiments, we conducted a bottle addition experiment with carbon (C) additions. At the same rates as the field experiment described in Chapter 3, we conducted a separate lab experiment with ten replicates of soil and litter each for the following treatments: control, lime (~0.2 g), Mo, P, Mo + P, Mo + P + lime, as well as C, Mo + C, P + C, and Mo + P + C, for a total of 220 incubations. Additions were added and incubated for 12 hours before ARA incubations were initiated, the time expected for microbes to respond to Mo in previous studies (Bellenger et al. 2011). Treatments were added in 5 mL solutions (control = distilled water, Mo = 0.83 µg Mo mL^{-1}; high Mo = 1.65 µg Mo mL^{-1}; +P = 80.3 µg P mL^{-1}, +C = 0.012 g C mL^{-1}) to about 15 grams of litter or 25 grams of fresh surface soil as Mo ($Na_2MoO_4 \cdot 2H_2O$) and P (trace metal grade NaH_2PO_4), and table sugar (fructose). Carbon was added at a rate of ~4.5 g C for every kg of soil, which was lower than another C bottle N fixation study (Pérez et al. 2017), equivalent to 6.3 g C kg^{-1} soil. While much more labile, for context, the C concentration added here was equivalent to one tenth of the amount of carbon added to the top 10 cm soil added by the annual litterfall (Rocha et al. 2014).

Lab experiment on water, carbon, and anaerobic controls

To confirm that the bottle additions conducted with nutrient additions were a direct result of the C added rather than a shift to anoxia, and to test the effect of moisture on BNF, we conducted a separate lab experiment. Ten replicates of each

were added in 5 mL solution volumes. For the water and C additions, 5 mL solutions were added to each incubation. Carbon was added at the same rate as described above. For the N_2 flush, jars were capped and flushed with N_2 at 90 psi for a minute, and incubated for three hours prior to adding acetylene to start the ARA. Soils were treated as controls, or with water additions, glucose additions, and an N_2 flush while litter was treated as either control or water additions with ten replicates each. After the acetylene reduction assay was terminated, litter was dried at 65°C for two days for dry weight measurements. Soil samples were weighed for field and dry moisture after drying in the oven for two nights at 105°C.

Carbon field addition

To test if C additions in the field would reflect the results in the lab, we conducted a short-term field carbon addition experiment by adding labile C to see if we could induce free-living BNF. A field addition with C additions was conducted next to the February (wet season) addition plots in February 2018 for a total of five C addition plots (Appendix B Figure S1). Fructose was added to the plots at the same rates as Garcia-Montiel *et al.*, (2003), or one fourth the rates as in the bottle rates added here, 1.1 g C kg^{-1} soil and one sixth the ratio of 6.3 g C kg^{-1} (Pérez et al. 2017). For logistical regions (dissolving the C in DI in amounts that could be carried to the forest sites), we used lower rates than we did in the lab experiment. Fructose was added and dissolved to distilled water, and sprayed over the litter layer using a broadcast sprayer, while distilled water was sprayed onto the control plots. ARA rates in the soil and litter were tracked the day of the applications four hours after the

applications and one day after because respiration responses to labile C occur instantaneously (Jones and Murphy 2007).

Statistical analyses

The field experiment with carbon additions was analyzed using a LLM with random effects for the block and plot with interactions with the time point and treatment as factors for an ln-transformed rate (ln for soils and ln(+0.001) for litter).

Results

Lab experiment

In the lab experiment, the C additions (C alone, C + Mo, C + P, C + P + Mo) significantly increased the BNF rates (Figure S3). All the C treatments were significantly higher than treatments without C ($F_{10,98}$=30.95, p < 0.0001, ANOVA). There were no significant differences in the litter when C was accounted for (F_{10}=1.17, p = 0.320, ANOVA) and when C was not accounted for (F_6=0.87, p = 0.522, ANOVA).

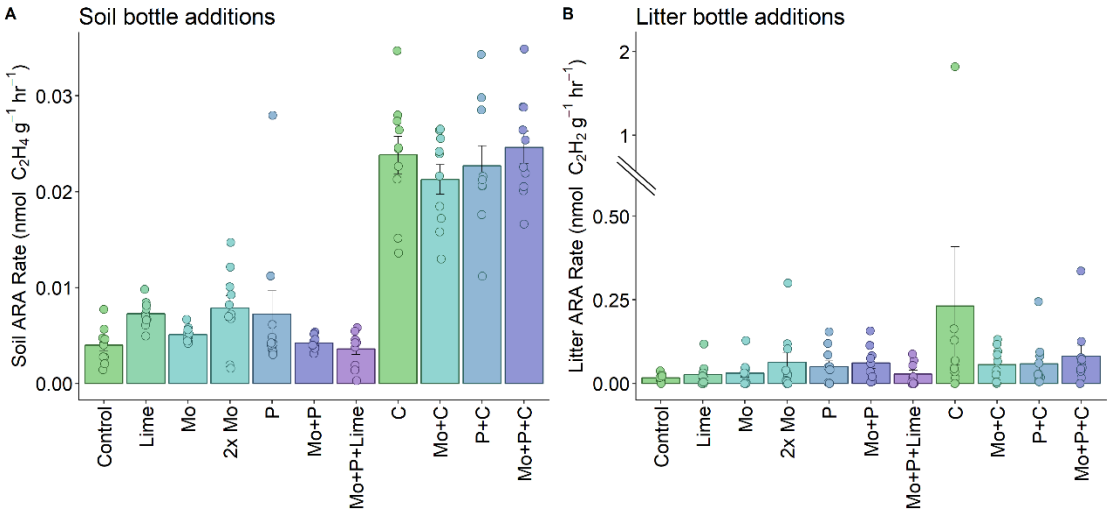

Figure S3. Free-living BNF by acetylene reduction in a lab-based addition experiment (nmol C_2H_4 g^{-1} hr^{-1}) in surface soil (A) and the litter layer (B) (n = 10). The control represents distilled water added alone. The boxes represent the mean and the error bars represent ± standard error.

In a separate lab experiment during the wet season testing moisture, C, and oxygen content, the manipulations significantly increased the BNF rates in the soil ($F_{3,36}$=42.19, p < 0.0001, ANOVA) (Figure S4). The C additions to the soil and the anaerobic N_2 flush both significantly increased BNF rates (p < 0.001, ANOVA, ln-transformed). The rates from the N_2 flush were significantly higher than the carbon additions (p < 0.001, Tukey post-hoc, ANOVA), while the water addition did not affect the rate (p > 0.05, Tukey post-hoc, ANOVA). The water addition also did not affect litter BNF rates during the wet season ($F_{1,18}$=3.798, p = 0.0671, ANOVA).

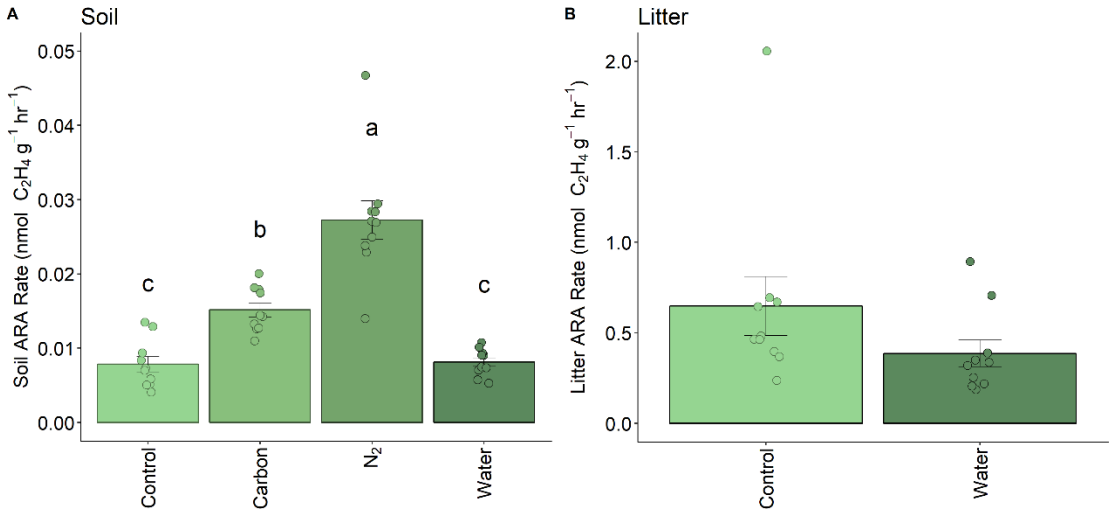

Figure S4. Lab-based free-living BNF by acetylene reduction (nmol C_2H_4 g^{-1} hr^{-1}) in surface soil with a carbon, moisture, and an oxygen treatment (A) and litter layer with a water treatment (B). The boxes represent the mean and the error bars represent ± standard error. Letters signify statistically significant differences (p < 0.05) (Tukey post-hoc test).

Carbon field additions. Carbon additions in the field did not exhibit anywhere near as strong of responses in the field as in the lab, but the C additions did very slightly increase BNF in the soil (Figure S5). In the field experiment, the C additions increased BNF slightly in the surface soil (p = 0.10, Tukey post-hoc, LMM) one day after the

applications, but not days after (p = 0.35, Tukey post-hoc, LMM). The C additions did not affect BNF in the litter either one day after the applications (p = 0.5059, Tukey post-hoc, LMM), or two days after (p = 1.0, Tukey post-hoc, LMM).

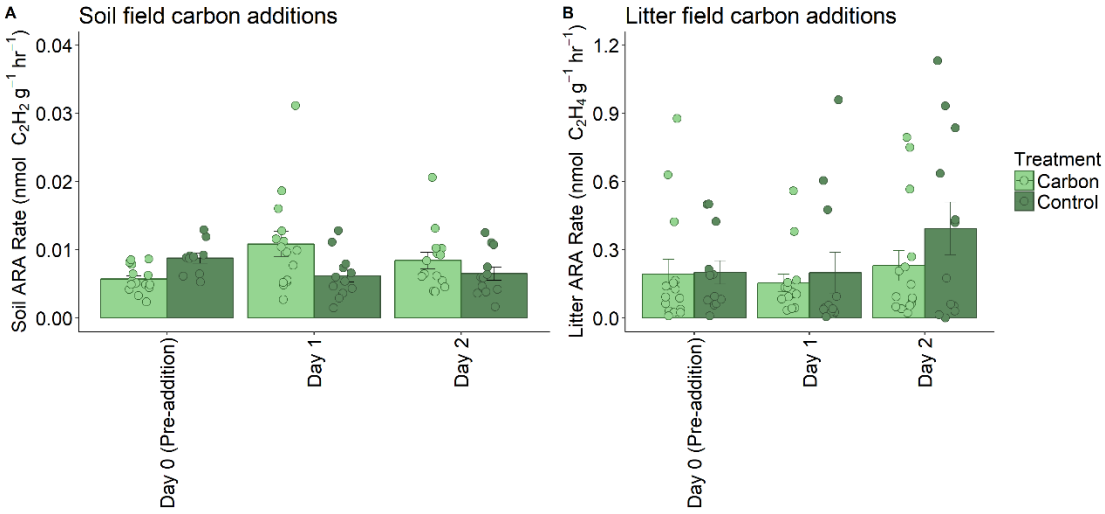

Figure S5. Field-based free-living BNF by acetylene reduction (nmol C_2H_4 g^{-1} hr^{-1}) in surface soil (A) and litter layer (B) in carbon additions in the field before additions, one day after, and two days after additions in the southeastern Amazon. The boxes represent the mean and the error bars represent ± standard error.

Discussion

The strong response of the soil to the carbon in the lab experiments, and to a much lesser extent in the field experiment, indicate that it is not for a lack of an N-fixing community to fix N that explains the low free-living BNF rates in this region. We found strong responses to labile C additions in the laboratory, while not in the field. While the C addition rates were lower in the field than in the lab (one fourth the application rates), the rates alone were not enough to explain the marked responses to C in the lab. The higher rates of BNF after flushing to anoxic environment with N_2 compared to the C additions alone in the lab indicate that anoxia may have played a more important role than C substrates alone in controlling BNF. While we are unable

to make conclusive results to whether or not anoxia alone that increased BNF in the soil because we did not test anoxia and labile C together, previous work has demonstrated that there are additive effects when anoxia and labile C are combined (Brouzes et al. 1969).

In previous studies, results have pointed out the results of labile C as a limitation on BNF, but did not discuss the potential co-variate of anoxia induced by respiration of labile C. While our results of strong responses of BNF to C are consistent with other studies, we suggest that future studies test both anoxia and labile C together and alone when testing for C limitation on free-living BNF.

References

Bellenger, J.-P., T. Wichard, Y. Xu, and A. M. L. Kraepiel. 2011. Essential metals for nitrogen fixation in a free-living N-fixing bacterium: chelation, homeostasis and high use efficiency. Environmental Microbiology 13:1395–1411.

Brouzes, R., J. Lasik, and R. Knowles. 1969. The effect of organic amendment, water content, and oxygen on the incorporation of 15N2 by some agricultural and forest soils. Canadian Journal of Microbiology 15:899–905.

Dynarski, K. A., and B. Z. Houlton. 2018. Nutrient limitation of terrestrial free-living nitrogen fixation. New Phytologist 217:1050–1061.

Garcia-Montiel, D. C., J. M. Melillo, P. A. Steudler, C. C. Cerri, and M. C. Piccolo. 2003. Carbon limitations to nitrous oxide emissions in a humid tropical forest of the Brazilian Amazon. Biology and Fertility of Soils 38:267–272.

Gutschick, V. 1981. Evolved strategies in nitrogen acquisition by plants. American Naturalist 118:607–637.

Hill, S. 1988. How is nitrogenase regulated by oxygen? FEMS microbiology reviews 4:111–29.

Hofmockel, K. S., and W. H. Schlesinger. 2007. Carbon Dioxide Effects on Heterotrophic Dinitrogen Fixation in a Temperate Pine Forest. Soil Science Society of America Journal 71:140.

Jia, X., X. Zhou, Y. Luo, K. Xue, X. Xue, X. Xu, Y. Yang, L. Wu, and J. Zhou. 2014. Effects of substrate addition on soil respiratory carbon release under long-term warming and clipping in a tallgrass prairie. PLoS ONE 9:1–16.

Jones, D. L., and D. V. Murphy. 2007. Microbial response time to sugar and amino acid additions to soil. Soil Biology and Biochemistry 39:2178–2182.

Pérez, C. A., F. M. Thomas, W. A. Silva, R. Aguilera, and J. J. Armesto. 2017. Biological nitrogen fixation in a post-volcanic chronosequence from south-central Chile. Biogeochemistry 132:23–36.

Reed, S. C., C. C. Cleveland, and A. R. Townsend. 2007. Controls Over Leaf Litter and Soil Nitrogen Fixation in Two Lowland Tropical Rain Forests. Biotropica 39:585–592.

Rocha, W., D. B. Metcalfe, C. E. Doughty, P. Brando, D. Silvério, K. Halladay, D. C. Nepstad, J. K. Balch, and Y. Malhi. 2014. Ecosystem productivity and carbon cycling in intact and annually burnt forest at the dry southern limit of the Amazon rainforest (Mato Grosso, Brazil). Plant Ecology and Diversity 7:25–40.

Vitousek, P. M., K. Cassman, C. Cleveland, T. Crews, C. B. Field, N. B. Grimm, R. W. Howarth, R. Marino, L. Martinelli, E. B. Rastetter, and J. I. Sprent. 2002. Towards an ecological understanding of biological nitrogen fixation. Biogeochemistry 57/58:1–45.

APPENDIX C. SUPPLEMENTARY INFORMATION FOR CHAPTER 4.

Table S1. Soil element concentrations using a concentrated nitric acid digestion. Data are means ± 1 standard error; n = 12. Lower-case letters indicate significant groupings in surface soils (0-2 cm), capital letters indicate significant groupings in deeper soils (2-10 cm), and daggers (†, ‡) indicate if there are differences between soil depths between each group ($p < 0.05$). No daggers indicate no significant differences between depths.

Treatment	**Burn 1yr**		**Burn 3yr**		**Control**	
Depth	0-2 cm	2-10 cm	0-2 cm	2-10 cm	0-2 cm	2-10 cm
P (µg/g)*	261.36 (51.24)$^{a, \dagger}$	111.25 (14.77)$^{A, \ddagger}$	179.77 (19.85)$^{ab, \dagger}$	119.00 (6.98)^{A}	156.02 (14.05)^{b}	124.10 (15.35)$^{A, \ddagger}$
Mo (ng/g)	181.02 (7.65)$^{ab, \dagger}$	139.67 (14.77)$^{A, \ddagger}$	231.03 (18.33)$^{a, \dagger}$	186.34 (24.18)^{A}	145.72 (19.09)^{b}	125.51 (16.08)$^{A, \ddagger}$
Na (µg/g)*	8.79 (1.41)^{b}	13.07 (1.99)^{A}	9.79 (1.19)^{b}	11.42 (2.04)$^{A, \ddagger}$	21.67 (6.44)$^{a, \dagger}$	4.69 (0.89)^{A}
Mg (µg/g)*	103.60 (17.26)$^{a, \dagger}$	47.64 (5.65)$^{A, \ddagger}$	92.88 (10.89)$^{a, \dagger}$	50.20 (3.11)$^{A, \ddagger}$	77.24 (8.31)$^{a, \dagger}$	47.09 (3.56)$^{A, \ddagger}$
Al (mg/g)*	65.87 (3.26)^{ab}	52.78 (8.26)^{B}	55.58 (7.54)^{b}	77.17 (5.34)^{A}	81.89 (9.04)^{a}	52.30 (4.73)^{B}
K (µg/g)	169.44 (9.99)$^{b, \dagger}$	144.83 (13.39)$^{B, \ddagger}$	182.86 (12.61)$^{b, \dagger}$	175.90 (9.55)$^{A, \ddagger}$	230.52 (11.08)$^{a, \dagger}$	138.99 (6.08)$^{B, \ddagger}$
Ca (µg/g)*	363.44 (112.37)$^{a, \dagger}$	113.07 (18.47)$^{A, \ddagger}$	270.51 (40.88)$^{a, \dagger}$	136.81 (33.72)^{A}	185.15 (38.25)^{a}	110.31 (18.83)$^{A, \ddagger}$
Ti (µg/g)	61.18 (3.14)^{a}	75.98 (7.66)^{A}	66.76 (6.20)^{a}	54.40 (5.43)^{B}	52.56 (6.22)^{a}	62.78 (4.82)^{AB}
V (µg/g)	66.00 (1.65)^{b}	73.49 (6.78)^{AB}	66.37 (4.56)^{b}	81.82 (3.68)^{A}	88.14 (3.99)^{a}	62.78 (2.73)^{B}
Cr (µg/g)	64.22 (2.16)^{b}	57.82 (5.03)^{B}	60.35 (4.61)^{b}	75.78 (3.61)^{A}	81.92 (5.24)^{a}	58.66 (3.12)^{B}
Mn (µg/g)*	47.34 (14.58)$^{a, \dagger}$	20.21 (2.75)$^{A, \ddagger}$	50.73 (9.81)$^{a, \dagger}$	13.81 (1.00)^{A}	20.36 (1.98)^{b}	18.93 (2.48)$^{A, \ddagger}$
Fe (mg/g)*	16.59 (0.49)^{a}	18.82 (1.78)^{A}	19.16 (1.48)^{a}	18.10 (1.54)^{A}	19.70 (1.86)^{a}	16.03 (0.58)^{A}
Zn (µg/g)	17.40 (1.07)^{a}	14.55 (1.50)^{A}	16.47 (1.25)^{a}	13.90 (0.68)^{A}	15.73 (1.32)^{a}	14.83 (1.15)^{A}
Sr (µg/g)*	7.70 (1.62)$^{a, \dagger}$	2.90 (0.34)$^{A, \ddagger}$	4.92 (0.70)$^{a, \dagger}$	2.63 (0.26)^{A}	2.79 (0.33)^{b}	2.99 (0.26)$^{A, \ddagger}$
Ba (µg/g)	14.04 (5.13)$^{a, \dagger}$	5.60 (0.46)^{A}	8.18 (0.98)^{a}	3.97 (0.18)^{A}	4.31 (0.33)^{b}	5.10 (0.71)$^{A, \ddagger}$
S (µg/g)*	154.31 (8.73)$^{b, \dagger}$	111.78 (16.85)^{A}	151.53 (11.39)^{b}	144.03 (9.60)$^{A, \ddagger}$	285.62 (44.03)$^{a, \dagger}$	94.87 (5.44)$^{A, \ddagger}$

*Indicates if group was ln-transformed prior to statistical tests

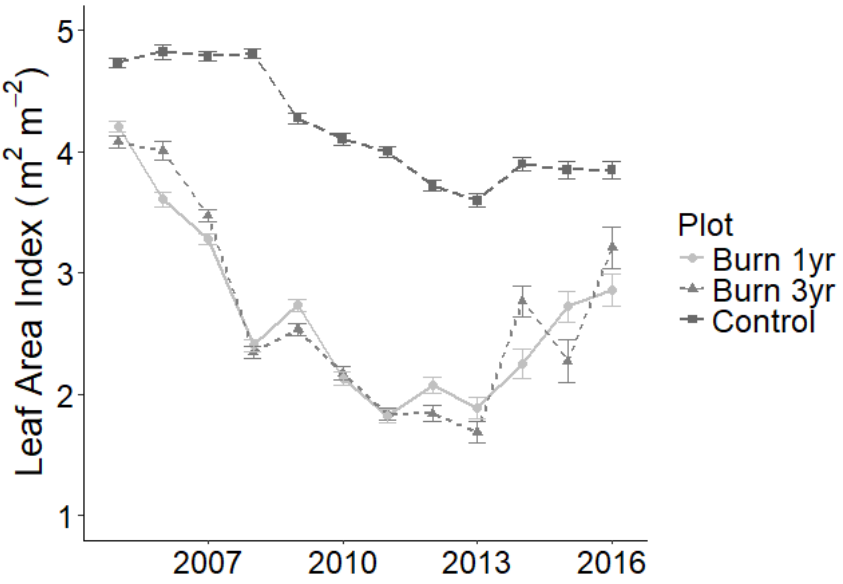

Figure S1. Annual average leaf area index (LAI) across the unburned (Control), triennially burned (Burn 3yr), and annually burned (Burn 1yr) forest treatments in the southeastern Amazon, with the last fires in 2010.

Table S2. Foliage information for dominant trees. Data are means ± 1 standard error, n = 3.

	Treatment	Importance Value Index (IVI)*	$\delta^{15}N$	%N	%C	C/N	g/m^2
Rubiaceae *Amaioua guianensis* Aubl.	Control	5.36	3.63 (0.11)	2.29 (0.06)	51.00 (0.33)	22.34 (0.67)	142.6 (29.7)
	Burn 3yr	8.25	4.20 (0.14)	2.28 (0.12)	52.43 (0.20)	23.40 (1.40)	98.2 (4.03)
	Burn 1yr	9.57	3.07 (0.05)	2.18 (0.08)	51.19 (0.30)	23.63 (0.82)	88.9 (6.48)
Lauraceae *Ocotea acutangula* Mez.	Control	5.85	2.32 (0.05)	2.55 (0.02)	53.89 (0.28)	21.18 (0.21)	152.5 (52.5)
	Burn 3yr	7.19	2.18 (0.22)	2.63 (0.07)	52.85 (0.36)	20.16 (0.41)	106.2 (11.0)
	Burn 1yr	9.51	2.42 (0.11)	2.34 (0.17)	52.41 (0.19)	23.17 (1.92)	121.9 (13.8)
Apocynaceae *Aspidosperma excelsum* Benth.	Control	10.32	3.20 (0.08)	2.19 (0.08)	52.26 (0.54)	24.08 (1.12)	99.2 (9.05)
	Burn 3yr	4.69	4.11 (0.12)	2.13 (0.04)	53.62 (0.50)	25.31 (0.76)	145.3 (15.4)
	Burn 1yr	4.46	3.29 (0.07)	2.12 (0.04)	54.77 (0.85)	25.90 (0.11)	128.1 (6.84)
Lauraceae *Ocotea guianensis* Aubl.	Control	5.38	1.76 (0.21)	2.24 (0.04)	49.19 (0.21)	22.00 (0.37)	184.0 (47.8)
	Burn 3yr	6.84	0.75 (0.39)	2.16 (0.03)	49.80 (0.44)	23.14 (0.43)	124.5 (12.6)
	Burn 1yr	6.25	0.84 (0.48)	1.80 (0.05)	48.30 (0.23)	26.93 (0.61)	135.5 (4.51)
Anacardiaceae *Tapirira guianensis* Aubl.	Control	7.22	3.42 (0.12)	1.97 (0.07)	48.98 (0.37)	24.99 (0.90)	162.8 (53.9)
	Burn 3yr	6.37	3.72 (0.24)	2.24 (0.11)	48.32 (0.09)	21.96 (1.16)	105.1 (24.8)
	Burn 1yr	4.07	4.29 (0.18)	1.89 (0.05)	49.73 (0.50)	26.47 (0.87)	123.2 (3.48)
Sapotaceae *Micropholis egensis* (A. DC.) Pierre	Control	2.89	3.91 (0.35)	2.09 (0.06)	49.02 (0.71)	23.61 (0.69)	133.6 (19.2)
	Burn 3yr	4.69	4.13 (0.10)	1.97 (0.09)	50.09 (0.56)	25.69 (0.94)	83.4 (4.44)
	Burn 1yr	5.61	3.75 (0.06)	1.72 (0.14)	50.65 (0.16)	30.84 (2.78)	115.3 (17.6)
Burseraceae *Trattinnickia burserafolia* Mart.	Control	5.10	3.90 (0.28)	2.07 (0.13)	46.35 (0.58)	22.88 (1.43)	137.33 (36.0)
	Burn 3yr	5.18	4.41 (0.52)	1.90 (0.13)	47.76 (0.22)	25.99 (2.07)	124.7 (9.26)
Burseraceae *Trattinnickia burserafolia* Mart.	Burn 1yr	2.16	4.07 (0.51)	1.87 (0.07)	46.66 (0.12)	25.12 (0.73)	172.3 (6.09)
Elaeocarpaceae *Sloanea eichleri* Schum.	Control	3.29	2.48 (0.08)	1.84 (0.06)	49.08 (0.68)	26.94 (1.24)	170.4 (14.5)
	Burn 3yr	4.09	2.14 (0.42)	1.60 (0.08)	46.59 (0.78)	29.43 (1.17)	93.5 (11.9)
	Burn 1yr	4.55	1.73 (0.26)	1.79 (0.07)	47.03 (0.38)	26.67 (1.24)	97.7 (10.4)

	Treatment	Importance Value Index (IVI)*	$\delta^{15}N$	%N	%C	C/N	g/m^2
Burseraceae *Trattinnickia rhoifolia* Willd.	Control	5.33	3.97 (0.08)	2.01 (0.02)	48.48 (0.38)	24.10 (0.35)	149.2 (14.9)
	Burn 3yr	4.11	4.24 (0.15)	1.75 (0.14)	48.90 (0.39)	29.12 (2.55)	115.2 (15.6)
	Burn 1yr	1.94	3.75 (0.18)	1.83 (0.06)	47.38 (0.30)	25.98 (0.86)	148.6 (15.4)
Sapotaceae *Pouteria ramiflora* (Mart.) Radlk	Control	2.50	3.04 (0.08)	1.85 (0.06)	53.67 (0.38)	29.11 (0.79)	127.7 (9.79)
	Burn 3yr	4.61	3.37 (0.35)	2.03 (0.02)	51.53 (0.84)	25.37 (0.20)	113.3 (19.8)
	Burn 1yr	3.74	3.52 (0.09)	1.91 (0.13)	52.10 (0.54)	27.91 (1.52)	131.3 (8.73)

*IVI values from Balch and others (2008)

Table S3. Surface soil (0-2 cm) nitrate (NO_3^-), ammonium (NH_4^+), and pH averages of soils during the wet and dry seasons in the unburned (Control), triennially burned (Burn 3yr), and annually burned (Burn 1yr) forest treatments in the southeastern Amazon; n = 30. Data are mean ± 1 standard error. Lower-case letters indicate significant groupings in treatments within the season, and daggers (†, ‡) indicate if there are differences between seasons within the treatment ($p < 0.05$).

Treatment	**NO_3^- (µg g^{-1})***		**NH_4^+ (µg g^{-1})***		**pH**	
	Dry	Wet	Dry	Wet	Dry	Wet
Control	14.6 (1.60)$^{a, \dagger}$	1.35 (0.15)$^{a, \ddagger}$	23.0 (5.46)$^{a, \dagger}$	6.17 (0.73)$^{a, \ddagger}$	4.0 (0.05)$^{b, \dagger}$	4.1 (0.03)$^{b, \ddagger}$
Burn 3yr	6.35 (1.09)$^{b, \dagger}$	0.59 (0.16)$^{b, \ddagger}$	10.9 (1.85)$^{b, \dagger}$	4.09 (0.30)$^{ab, \ddagger}$	4.5 (0.06)$^{a, \dagger}$	4.5 (0.04)$^{a, \dagger}$
Burn 1yr	6.12 (1.09)$^{b, \dagger}$	0.96 (0.24)$^{b, \ddagger}$	8.58 (1.13)$^{b, \dagger}$	4.01 (0.81)$^{b, \ddagger}$	4.4 (0.06)$^{a, \dagger}$	4.4 (0.04)$^{a, \dagger}$

*indicates if group was ln-transformed (+0.1) prior to statistical tests

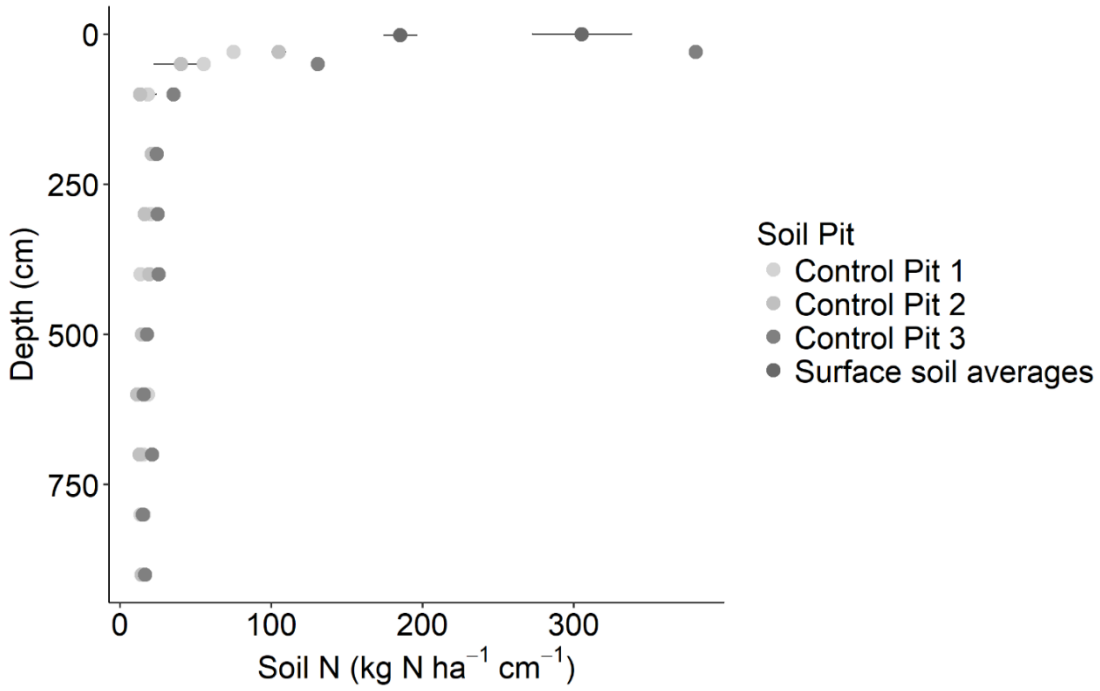

Figure S2. Total soil nitrogen (kg N ha^{-1} cm^{-1}) sampled in three soil pits dug to 10 m and in surface soils; n = 12.

APPENDIX D. SUPPLEMENTARY INFORMATION FOR CHAPTER 5.

Figure S1. Sampling design for plant stems (>5cm dbh). Experimental block (150 ha) is located on Fazenda Tanguro, adjacent to a pasture edge. Inset map shows study site located in Mato Grosso, Brazil, in the Amazon Basin.

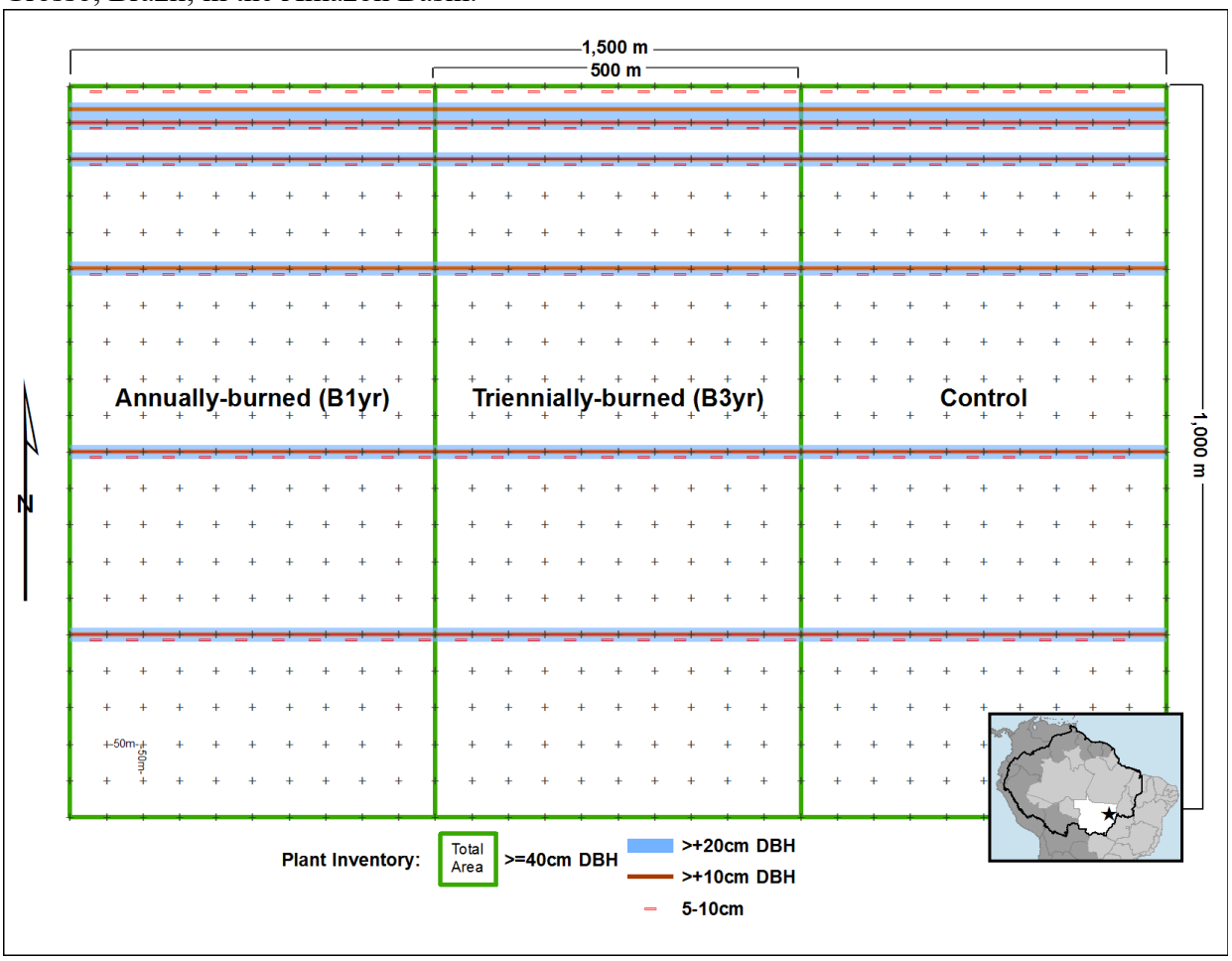

Table S1. Annual precipitation at Fazenda Tanguro, Mato Grosso, Brazil, in the Amazon Basin measured by rain gauges on site.

Year	Precipitation (mm)
2008	1236
2009	1332
2010	1610
2011	1865
2012	1565
2013	2309
2014	1539
2015	863
2016	1552

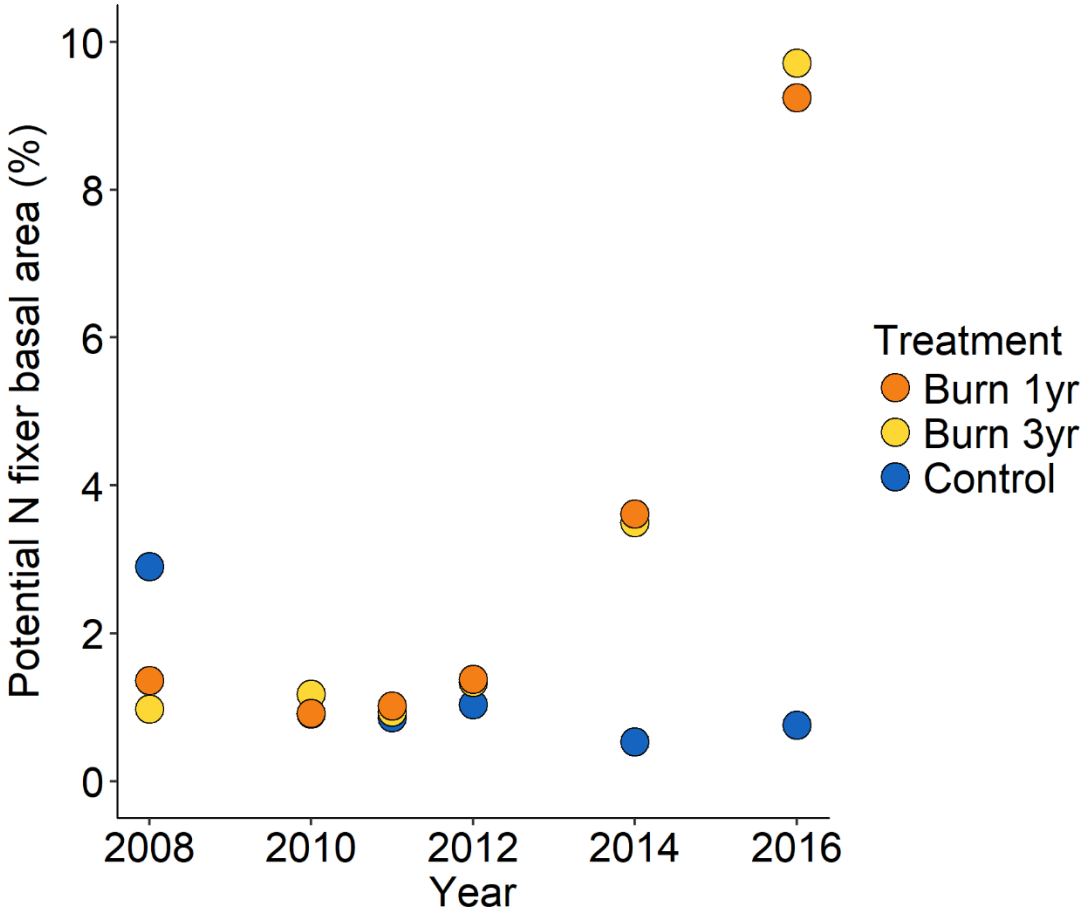

Figure S2. Potential N fixer basal area (%) across the unburned (Control), triennially burned (Burn 3yr), and annually burned (Burn 1yr) forest treatments in the southeastern Amazon for all individuals in the tree inventory. The fires occurred between 2004 and 2010, except 2008 in the annually burned forest.

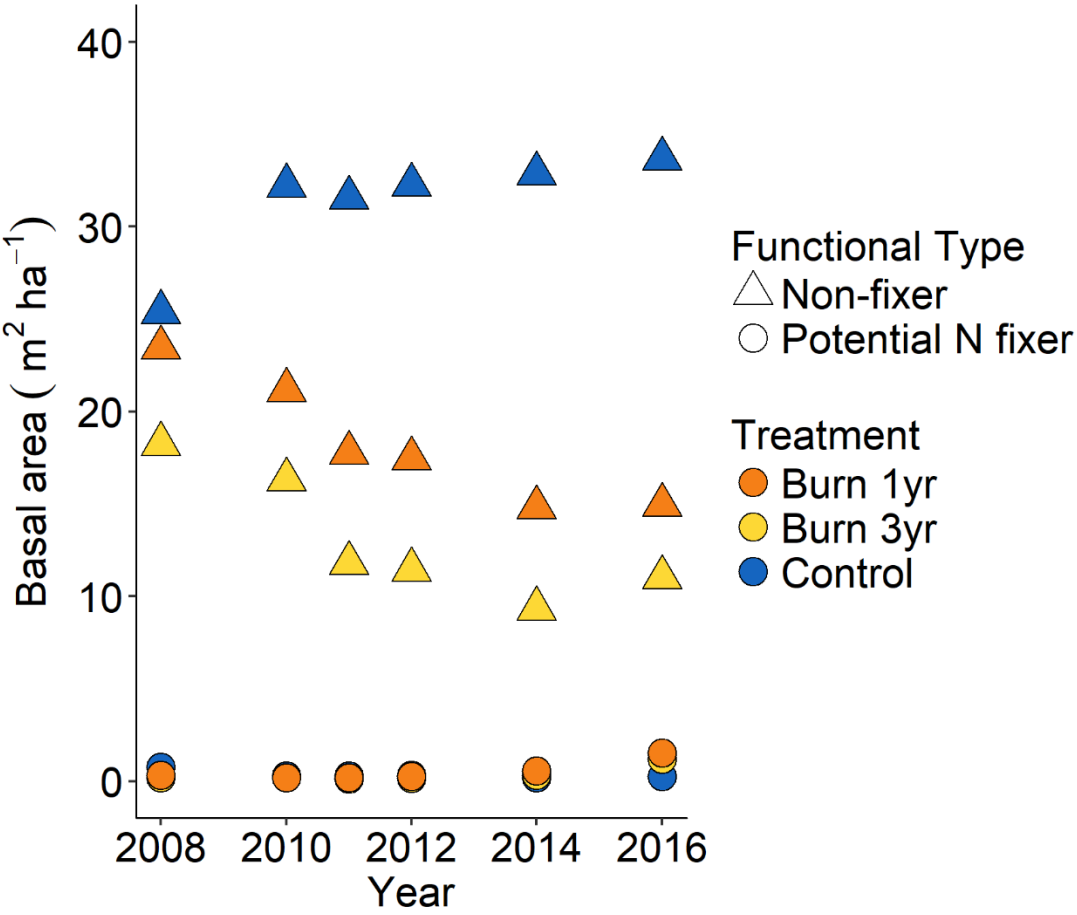

Figure S3. Non-fixer and potential N fixer basal area (m^2 ha^{-1}) across the unburned (Control), triennially burned (Burn 3yr), and annually burned (Burn 1yr) forest treatments in the southeastern Amazon for all individuals in the tree inventory. The fires occurred between 2004 and 2010, except 2008 in the annually burned forest

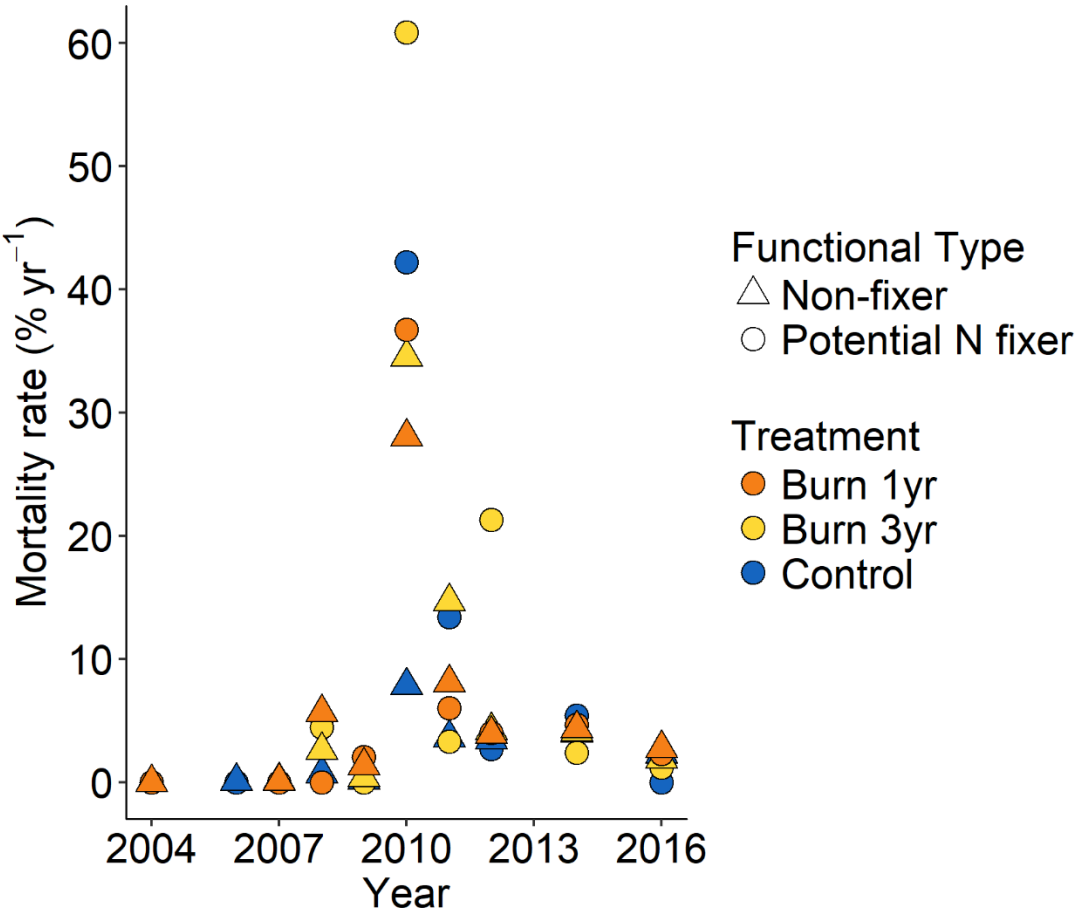

Figure S4. Mortality rate calculated for all size classes together for potential N fixers and non-fixers across the unburned (Control), triennially burned (Burn 3yr), and annually burned (Burn 1yr) forest treatments in the southeastern Amazon for all individuals in the tree inventory. The fires occurred between 2004 and 2010, except 2008 in the annually burned forest.

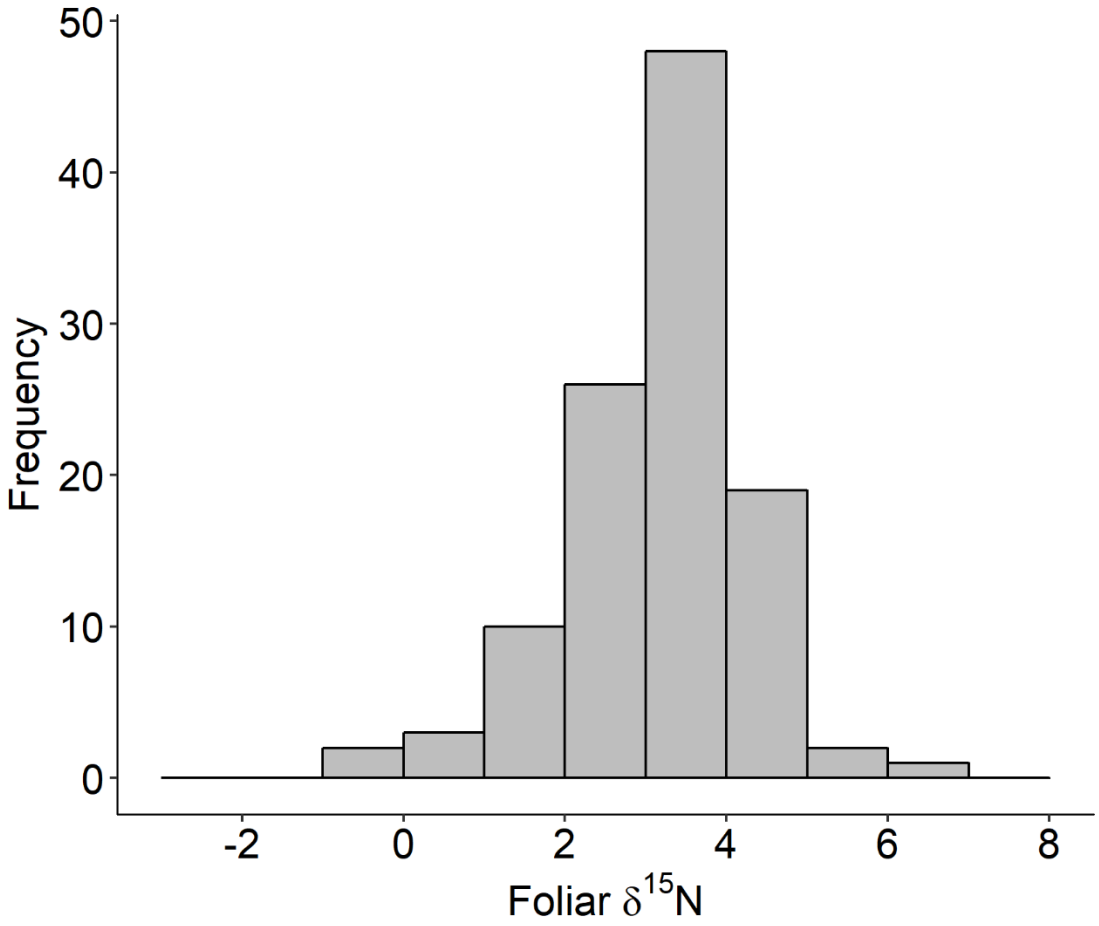

Figure S5. Frequency distribution of foliar nitrogen natural abundance for 112 trees sampled across burn treatments at Tanguro.

Nodulation and foliar δ^{15}N

We further attempted to quantify nodulation by individual trees using two approaches: first, we cored 12 soil cores around known N fixers. Then we excavated around the roots of the trees to further examine if nodulation was not captured by the 12 soil cores.

We also attempted the more indirect technique of using natural abundance of N isotopes to infer fixation (Gehring and Vlek 2004, Nardoto et al. 2014).

$$\delta\,^{15}\mathbf{N} = \frac{(\boldsymbol{atom\%\ 15N})_{\boldsymbol{sample}} - (\boldsymbol{atom\%\ 15N})_{\boldsymbol{standard}})}{(\boldsymbol{atom\%\ 15N})_{\boldsymbol{standard}})}\ \boldsymbol{x\ 1000}$$

%Ndfa was calculated according to (Shearer and Kohl 1988)

$$\%\boldsymbol{Ndfa} = \frac{\delta\,^{15}N_{reference} - \delta\,^{15}N_{fixing}}{\delta\,^{15}N_{reference} - \delta\,^{15}N_{fixed\ N}}$$

Table S2. Nodule survey for potential N fixers at Fazenda Tanguro, Mato Grosso, Brazil.

Species	dbh	Nodulation	Method
Enterolobium schomburgkii (Benth.) Benth.	16.8	-	12 cores
Enterolobium schomburgkii (Benth.) Benth.	121	-	12 cores
Enterolobium schomburgkii (Benth.) Benth.	3.5	-	12 cores
Inga heterophylla Willd.	5	-	12 cores
Inga heterophylla Willd.	27	-	12 cores
Inga heterophylla Willd.	4.8	-	12 cores
Inga heterophylla Willd.	14.6	-	12 cores
Inga heterophylla Willd.	11	-	12 cores
Inga heterophylla Willd.	7	-	12 cores
Inga heterophylla Willd.	32	-	12 cores
Inga heterophylla Willd.	19	-	12 cores
Inga heterophylla Willd.	25	-	12 cores
Inga heterophylla Willd.	21	-	12 cores
Inga thibaudiana	2.1	-	12 cores
Inga thibaudiana	7.8	-	12 cores
Inga thibaudiana	9.5	-	12 cores
Inga thibaudiana	20	+	12 cores
Inga thibaudiana	27	-	12 cores
Inga thibaudiana	18	-	12 cores
Inga thibaudiana	10	-	12 cores
Inga thibaudiana	23	+	12 cores
Tachigali vulgaris	7.9	-	12 cores
Tachigali vulgaris	61.8	-	12 cores
Tachigali vulgaris	88	-	12 cores
Tachigali vulgaris	59.4	-	12 cores
Tachigali vulgaris	48.6	-	12 cores
Enterolobium schomburgkii (Benth.) Benth.	8.917197	-	excavating around rooting zone
Enterolobium schomburgkii (Benth.) Benth.	7	-	excavating around rooting zone
Enterolobium schomburgkii (Benth.) Benth.	18	-	excavating around rooting zone
Enterolobium schomburgkii (Benth.) Benth.	NA	-	excavating around rooting zone
Enterolobium schomburgkii (Benth.) Benth.	NA	-	excavating around rooting zone
Enterolobium schomburgkii (Benth.) Benth.	NA	-	excavating around rooting zone
Inga thibaudiana		+	excavating around rooting zone

Species	dbh	Nodulation	Method
Inga thibaudiana	8	-	excavating around rooting zone
Inga thibaudiana	NA	-	excavating around rooting zone
Tachigali vulgaris	9.55414	-	excavating around rooting zone
Tachigali vulgaris	21.01911	-	excavating around rooting zone
Tachigali vulgaris	8	-	excavating around rooting zone
Tachigali vulgaris	7	-	excavating around rooting zone
Tachigali vulgaris	NA	-	excavating around rooting zone
Tachigali vulgaris	NA	-	excavating around rooting zone
Tachigali vulgaris	NA	-	excavating around rooting zone

Table S3. NDFA and foliar %N for potential N fixers at Fazenda Tanguro, Mato Grosso, Brazil.

Species	**δ^{15}N**	**%N**	**NDFA**	**Mean NDFA**
Tachigali vulgaris	3.80	2.06	-19.3	
Tachigali vulgaris	3.09	2.07	3.1	
Tachigali vulgaris	2.96	2.52	7.2	
Tachigali vulgaris	3.05	2.11	4.4	
Tachigali vulgaris	3.20	2.17	-0.4	
Tachigali vulgaris	3.33	2.02	-4.5	-1.58
Enterolobium schomburgkii (Benth.) Benth.	5.69	3.69	-78.6	
Enterolobium schomburgkii (Benth.) Benth.	4.44	3.55	-39.3	
Enterolobium schomburgkii (Benth.) Benth.	2.59	3.20	18.8	
Enterolobium schomburgkii (Benth.) Benth.	1.30	3.04	59.2	
Enterolobium schomburgkii (Benth.) Benth.	3.94	3.32	-23.6	
Enterolobium schomburgkii (Benth.) Benth.	1.52	4.01	52.4	
Enterolobium schomburgkii (Benth.) Benth.	2.27	3.69	28.8	16.04
Inga thibaudiana	4.19	2.45	-31.4	
Inga thibaudiana	3.55	3.58	-11.5	
Inga thibaudiana	1.35	2.64	57.5	4.88
Inga heterophylla Willd.	3.52	3.48	-10.5	
Inga heterophylla Willd.	4.60	3.23	-44.2	
Inga heterophylla Willd.	3.56	3.61	-11.6	
Inga heterophylla Willd.	1.75	2.94	45.2	
Inga heterophylla Willd.	2.66	3.63	16.5	-0.91
Non-fixer average	3.2	2.04		